ULTRASONIC EXAMINATION OF SPINE IN BEEF CATTLE FOR DETERMINATION OF A RELATIONSHIP WITH SKELETAL MATURITY

BY

MARIA EZZATKHAH

B.S., University of Massachusettes at Lowell, 1988

THESIS

Submitted in partial fulfillment of the requirements
for the degree of Master of Science in Nutritional Sciences
in the Graduate College of the
University of Illinois at Urbana-Champaign, 1999

Urbana, Illinois

TABLE OF CONTENTS

LIST OF TABLES

TABLE **PAGE**

LIST OF FIGURES

FIGURE **PAGE**

CHAPTER 1
INTRODUCTION

The U.S. Department of Agriculture (USDA) has long been interested in a uniform and objective method of grading slaughter beef in order to facilitate the industry's marketing system from producer to retailer and consumer. A beef carcass's quality grade is based on two major factors: degree of marbling and degree of maturity. Its yield grade is based on the amount of external fat, area of rib-eye muscle, carcass weight, and the amount of kidney, pelvic and heart fat. Current quality grades for beef carcasses is done by human estimation of quality and cutability. In order to determine the quality grade and the yield grade, a beef carcass is split into two sides. One side is then separated into a hindquarter and a forequarter by cutting it at the 12^{th} thoracic vertebra. The yield grade predictions are independent from the quality grade measurements [Official United States Grading Standards for Beef, 1997].

Estimation of both quality and yield grade on a production line is a subjective process. Graders do not have enough time to do any actual measurements on the carcasses, and must estimate parameters only visually. Therefore, there has been an interest in a more objective method to estimate quality and yield. Ultrasound has been investigated as a potential method to enhance accuracy and objectivity in beef carcass grading because ultrasound propagation through a tissue is affected by physical characteristics of a carcass that are directly relevant to existing quality and yield indicators.

Ultrasound has become one of the major diagnostic tools in the medical industry. Medical ultrasound devices utilize the backscatter information from acoustic signals to produce images based on reflections from within the irradiated tissue. This research project investigates the use of backscatter information from acoustic signals reflected by beef carcass spinous processes in determining the degree of maturity of the animal, which is an important variable in estimating the quality grade in beef carcasses.

Literature Summary

Beef quality and yield grade evaluations by USDA trained observers have been regarded as a subjective process. In 1978 the US General Accounting Office reported to the US Congress that the USDA needed to "increase research efforts to develop instruments to accurately measure beef carcass characteristics". As a result, in 1979 the USDA Agricultural Marketing Service, the USDA Food Safety and Inspection Service and NASA's Office of Technology jointly funded a study to determine the feasibility of applying NASA technology to beef grading. Two technologies were identified as potential methods to accomplish USDA goals to enhance accuracy in carcass grading and providing a more objective means of beef carcass grading. These two technologies were ultrasound and video image analysis. In 1989 at an Australian symposium on "Automated Measurement of Beef" ultrasound was identified as having the greatest potential for use in beef evaluation (Cross et al., 1994).

Ultrasound was first studied in measuring carcass characteristics of meat animals by Hazel and Kline (1959) and by Stouffer et al. (1959). Ultrasound has been identified as an objective way of measuring the attributes such as marbling for quality grade and area of longissimus muscle for yield grade.

Two of the important characteristics in determining the quality grade for beef carcasses are marbling and skeletal maturity. Quality is defined as "characteristics of lean, fat and bones associated with palatability". These characteristics are bone (skeletal) maturity, marbling, color (lean maturity), texture and firmness. Quality grades predict "palatability characteristics of the meat". These are based on stage of maturity and degree of marbling. Maturity is defined as the "chronological age of the carcass or cut as determined by the physiological appearance of bone and cartilage". For general maturity group classifications are:

1) Very young, characterized by very red and porous bone (redness displayed on entire rib). Buttons (soft cartilage tips on chine bones which ossify as an animal matures) are very soft and easily dented.
2) Young, characterized by red and porous bone (slight disappearance of the redness in the ribs). Buttons are soft and easily dented.

3) Intermediate, characterized by slight redness in the rib. Buttons show slight evidence of ossification and are not easily dented.
4) Mature, characterized by ribs lacking redness. Buttons are not easily distinguished and appear as ossified tips of chine bones.

Skeletal (bone) maturity is determined by visually observing the physiological appearance of bone in the vertebral column and rib cage of a carcass. Skeletal maturity is classified as A, B, C, D and E (youngest to oldest). These are discussed in more detail in beef quality grading section of this thesis. Figure 1 shows the relationship between maturity, marbling and quality grade. In determining this relationship, maturity of a carcass is determined by observing the bone and lean maturity. Lean maturity is based on color of lean which, is a bright red color in carcasses of A-maturity and it naturally becomes darker as a beef animal matures. In this thesis we will not be discussing the lean maturity since the data under study has been collected from the spine which, is directly related to skeletal maturity. Next, the amount (degree) of marbling is determined. For example, if a carcass is determined to be A50 (about 14-16 months) and has a small degree of marbling, the USDA quality grade would be a "low choice" (Parrish, 1994).

Much ultrasound research has been performed in determining the marbling of beef cattle. Speckle scores and attenuation have been used to estimate marbling within the ribeyes of meat animals (Perry et al., 1990; Brethour, 1990; Wittaker et al., 1992). Discriminant analysis techniques were performed to classify beef quality grading based on degree of marbling (Green et al., 1991; Amin et al., 1993; Brethour et al., 1994). A-mode and B-mode ultrasound systems have been used to evaluate content and distribution of intramuscular fat (marbling)(Patel et al, 1994; Chang et al.,1991).

Skeletal Maturity, which is another attribute of quality grade, has not been studied by ultrasound techniques. Degree of ossification at the spinous processes is considered in the determination of quality grade for beef carcasses. Beef cattle become maturer as they increase in size and age. Carcass skeletal maturity scores and chronological age were compared for heifers and cows ranging in age from 1.7 to 13.9 year by Shackelford et al, (1995). Skeletal, lean and overall maturity scores indicated that yearling heifers were less physiologically mature than two-year-old cows ($p< 0.01$). They concluded that carcass

skeletal maturity scores increase with increasing chronological age. Fitzhugh et al, (1971) defined the mature size as the final size eventually reached and expressed the size of the animal at an immature stage as a percentage of its mature size. They studied groups of bulls at birth, 6, 12, and 18 months. They reported a positive correlation between degree of maturity and body weight at the same age. This correlation showed that the genetically heavier animals at any given age tend to be maturer. Hamlin et al, (1995) used real time ultrasound to measure the fat thickness and longissimus muscle area among 180 feedlot steers representing 11 sire-breed groups. They attempted to describe the age and weight effects at two 60-day intervals when they made the above two measurements. They reported a positive correlation between age and weight of the beef cattle. This all supports the fact that maturity increases as animals gets older and heavier.

In maturer animals, the degree of ossification increases in all bones as well as the spinous processes located at the spine. Mello et al, (1978) removed cervical, thoracic, lumbar and sacral vertebral bones from 13 bovine of a wide age range and studied the changes in bone composition as a function of age and anatomical location. They reported that an increase in age leads to an increase in ossification. Ossification starts at the anterior and proceeds to the posterior of vertebral column. The result of their study showed that with increase in age there was an increase in specific gravity of bone which means a higher density due to high deposition of calcium and phosphorus (increase in mineral concentration). Cartilage acts as a template for the osseous skeleton and regulates skeletal growth. Cartilage contains considerable amount of keratin and chondroitin sulfate. Mello et al., reported a decrease in concentration of sulfur with an increase in age which serves as a measurement of bone maturity due to displacement of cartilage by bone.

Based on the results produced from different research groups we are able to assume that as animals mature the skeletal maturity increases which yields higher ossification at the spinous processes. The purpose of this research is to determine whether pulse-echo ultrasound reflected off of the spine contains information about the degree of ossification.

CHAPTER 2
THEORETICAL DEVELOPMENT

This chapter begins with an overview of the anatomy of the ruminant spinal column. The acoustical properties of different tissues such as bone and cartilage are discussed. USDA standards for beef classification and grading are described. The chapter concludes with the theory behind the use of ultrasound reflection coefficients to characterize tissue.

Anatomy of Ruminant Spinal Column

The vertebral column, also called the spine, is formed from irregular bones that consist mainly of spongy bone enclosed by thin layers of compact bone. Compact bone is dense and looks homogeneous whereas, spongy or cancellous bone is composed of needle like or flat pieces of bone called trabeculae separated by a good deal of open space. In ruminants, the vertebral axis runs parallel to the skin line in the loins and caudal part of the back. The vertebral column provides attachment points for the ribs and the muscle of the back. The individual vertebrae are separated by connective tissue discs. Each intervertebral disc is composed of an inner semifluid nucleus pulposus which provides elasticity and compressibility to the discs, and an outer ring of fibrocartilage which limits the expansion of the discs and holds the successive vertebrae together [Mariweb, 1989]. In cattle, the intervertebral discs are short and constitute only 10 per cent of the length of the column [Dyce et al., 1987].

Two major connecting ligaments, called the anterior and posterior longitudinal ligaments, run as continuous bands down the front and back surface of the spine [Mariweb, 1989]. In ruminants, these two major ligaments run along the vertebral column (spine) as it extends from the skull to the tip of the tail [Dyce et al., 1987]. In addition, short ligaments connect each vertebra to those immediately above and below it.

There are five regions of the ruminant vertebrae each with common features: cervical (neck), C; thoracic (back), T; lumbar (loins), L; sacral (croup), S; and caudal (tail), CD. The numbers of vertebrae composing those regions in cattle are represented by the following formula: C7, T13, L6, S5, CD 18-20.

Topographically, a typical vertebra consists of a massive body surrounded by an arch that completes the enclosure of a vertebral foramen. It is the summation of these foramina that constitutes the vertebral column. Each vertebra carries a number of processes. The dorsal or spinous process springs from the union of laminae and is generally prominent although its form, length and inclination vary with the region and with the species. The spinous processes of the thoracic region are very prominent and sloping whereas in the lumbar region they are shorter and perpendicular to the vertebrae. Figure 2.a. shows both the thoracic and lumbar region. It is evident from this figure that the spinous processes in the thoracic region are longer in length and are inclined in one direction whereas the spinous processes in lumbar region are shorter in length and assume a normal position with respect to the spine. The orientation of these processes is of importance since an incident ultrasonic beam normal to a surface will be reflected with a higher amplitude than if the beam and reflecting surface are not perpendicular to each other. Figure 2.b. shows location of cartilage and vertebrae for determination of skeletal maturity. The tips of these processes are cartilaginous in young cattle. They gradually ossify with age. In beef carcass evaluation, ossification changes in the cartilage and bones are used as key indicators of maturity at the time of slaughter. Ossification changes are best noticed in the split dorsal processes of the vertebrae of the backbones. Such changes are noticeable first in the sacral vertebrae. As animals mature these changes become evident in the lumbar and finally in the thoracic vertebrae.

Beef Grading

The importance of a uniform method and system of grading slaughter beef has been apparent to the U.S. Department of Agriculture (USDA) for many years. Grading simply is a process of classifying units of a commodity into categories that have different

characteristics or values. For beef, the grades are intended to segregate the beef supply into groups of carcasses with similar attributes of palatability and yields of marketable cuts [Official United States Grading Standards for Beef, 1997].

In 1916, the USDA formulated tentative standards that were promulgated as the official United States standards for grades of carcass beef on June 3, 1926 [Official United States Grading Standards for Beef, 1997].

USDA carcass beef grades fall into two mutually exclusive categories: "yield grade" that indicates yield of closely trimmed, boneless retail cuts derived from round, sirloin, short loin, rib and square-cut chunks of a carcass and "quality grade" which reflects the characteristics of the meat that predict palatability of the lean cuts [Parrish, 1994]. In this thesis we restrict our attention to issues of quality grading.

The USDA beef quality grades are prime, choice, select, standard, commercial, utility, cutter, and canner. A beef carcass quality grade is based on two major factors: 1) degree of marbling and 2) degree of maturity. Marbling is the intermingling or dispersion of fat within the lean which is an indicator of eating quality. Marbling is estimated on the lean cut surface of the ribeye muscle on the 12th rib interface. The amount of marbling in the eye muscle is divided into ten degrees, which are, from highest to lowest: abundant, moderately abundant, slightly abundant, moderate, modest, small, slight, trace, practically devoid and devoid. Each degree of marbling is divided in to 11 subcategories, which are numbered as multiples of 10 from 0 to 100. These numbers appear as subscripts to the degree of marbling. The lowest amount of marbling within each degree is designated as 0, and the highest is 100 [Meat Evaluation Handbook, 1988].

The maturity of a carcass is determined primarily by visually observing bone in the vertebral column and rib cage. Physiological indicators of maturity are bone characteristics, degree of ossification of cartilage at various carcass locations, dark color of lean due to myoglobin accumulation, and the coarse texture of muscle due to increase in size [Official United States Standards for Grades of Carcass Beef, 1997].

There are five maturity groups designated by the letters A, B, C, D, and E. The A and B maturities are from young carcasses whereas C, D and E are from mature cattle. Just as for the degree of marbling, the maturity groups are subdivided into 11 categories

from 0 to 100 (also multiples of 10). Within each maturity group the youngest carcass is designated as 0 and the oldest is designated as 100 [Meat Evaluation Handbook, 1988].

In the youngest of A maturity carcasses the sacral and lumbar cartilage are least ossified. As maturity proceeds from A to E, progressively more and more ossification becomes evident.

Table 1 (adapted from Burson, University of Nebraska Extension Meat Specialist, Extension Publication #357) summarizes the relationships among degree of maturity, age, and specific skeletal ossification measures. As the animal advances from A to E maturity there is more ossification of the cartilage tips of the lumbar and thoracic vertebrae.

Beef at 30 months of age or younger is usually acceptably tender and is called A maturity group. As the animal increases in age from 30 months to about 42 months, ossification of cartilage increases and tenderness decreases. At approximately 42 months of age ossification of cartilage in the sacral and lumbar region is completed and thereafter, the buttons of thoracic region begin to ossify extensively. In addition, the collagenous connective tissue associated with the muscles also undergo extensive cross-linkages resulting in dramatic increase in toughness of the meat. Thus, the age break between young and old cattle is at 42 months of age, between the B and C maturity groups [Official United States Grading Standards for Beef, 1997].

Figure 2 (adapted from the Official United States Grading Standards for Beef, 1989) shows the relationship between marbling, maturity, and the beef carcass quality grading. Carcasses of A and B maturity are eligible for prime, choice, select, standard and utility quality grades. Carcasses of C, D and E maturity qualify only for commercial, utility, cutter and canner grades.

A carcass's maturity and marbling scores are used to arrive at a final quality grade. Table 2 is an example of final quality grading for different maturity groups.

Acoustical Properties of Tissue

Assignment of USDA grade to an animal carcass is essentially an ultrasound tissue characterization problem. In the past few decades many ultrasonic tissue characterization

techniques have been developed to determine the composition of tissues and organs in the medical field. Much of this research can potentially be applied to beef grading.

Scientists have for some time sought to correlate ultrasonic acoustic parameters (such as scattering, attenuation, and acoustic impedance) to the molecular composition of various biological tissues [Greenleaf, 1986].

The use of ultrasound in beef grading requires an understanding of the tissue properties responsible for or associated with the propagation of sound in tissue. As an acoustic wave propagates through a heterogeneous medium such as biological tissues, part of its energy will be lost due to absorption and scattering, and part of its energy will be lost due to specular reflection at the boundary of two adjacent layers of tissues. Both scattering and reflection depend on the elastic properties of the tissues, which determine the acoustic impedance of the tissue [Shung, 1992]. The acoustic impedance of a medium is directly dependent on the speed of propagation in that medium and the density of the medium. Echogenicity of tissues is determined mostly by their connective tissue content [Fields and Dunn, 1973].

Connective tissue is found everywhere in the body. It is the most abundant and widely distributed of the primary tissues, but its amount in particular organs varies greatly. For example, bone is made up primarily of connective tissue, whereas the brain contains very little [Mariweb, 1989]. Connective tissue is very abundant in cartilage as well. The acoustic impedance of connective tissue has been shown to be much higher than that of other types of tissue.

Attenuation of ultrasound in connective tissues is quite high [Goss and O'Brien, 1980]. Attenuation is a process by which energy is lost from an ultrasound beam as it travels through a material such as biological tissue. This energy loss is due to absorption where acoustic energy is converted to heat, and to scattering, where energy is deflected away from the ultrasound beam axis [Guittet et al., 1996].

The backscatter coefficient is commonly used to quantify the scattering properties of biological tissue [Sigelmann et al., 1973]. When a wave is incident on an object, part of the wave is scattered and part is absorbed by the object. The scattering characteristics of an object is expressed by the term "scattering cross section". Experimental investigations

in-vitro have shown that different tissues exhibit different angular scattering patterns and frequency dependence [Linzer, 1979]. The backscattering coefficient, defined as backscattering cross section per unit volume of scatterers, for five different types of beef tissues as a function of frequency has been investigated [Fei & Shuns, 1985]. The results support the hypothesis that scattering from a tissue is dependent on the dimensions of the cellular elements in the tissue.

Considerable work has been done to develop ultrasonic tools for use in objective methods of evaluating tissue composition. Ultrasonic parameters such as speed, attenuation coefficient, and backscatter amplitude have been used to assess properties of tissue. Measurements of these parameters yield information regarding tissue composition and structure. Tissue properties, such as degree of inhomogeneity and scatterer type (e.g., fat or collagen), as well as scatter size, density, and distribution, all affect the nature of the ultrasonic backscattered signal. For example, studies on backscatter amplitude and attenuation coefficient in various tissues show a substantial decrease as a function of time for the mean backscatter amplitude and no significant change for the attenuation coefficient [Bamber et al., 1977].

Agemura's literature review led her to conclude that studies conducted since the 1950s support the idea that ultrasonic absorption occurs at the macromolecular level in biological tissues. Four tissue constituents that have acoustical importance are water, collagen, other proteins, and fat [O'Brien et al., 1988]. Comparison of data on ultrasound speed and attenuation coefficient [Dunn, 1978] versus water and protein concentration [Agemura, 1986] in various tissues indicates that the speed and attenuation coefficient in tissue increases as the water concentration decreases and protein concentration increases. For example, Agemura reports that tendon has a typical water concentration of 68% and a protein content of 33-40%. Both the speed and attenuation coefficient of ultrasound in tendon are among the highest for any tissue except bone [Dunn, 1978]. On the other hand, testis tissue, with 80 percent water and 12 percent protein, shows the lowest absorption of all tissues investigated [Dunn, 1978].

Two types of protein, one providing structural features and the other providing necessary metabolic functions are found in mammalian tissues. Collagen is the structural

protein which plays an important role in the acoustical properties of tissues. It is also the most abundant protein in the human body, exhibiting acoustic properties widely different from those of other tissue constituents. Ultrasonic speed is greater in collagen than in other tissue components because collagenous fibers exhibit 1000 times greater Young's modulus than that of the other soft tissues [Fields et al., 1973]. The higher speed in collagen implies higher characteristic acoustic impedance for collagen. The large impedance mismatch between collagen-containing tissue such as bone (with characteristic acoustic impedance of 7.8 Mrayl) and average soft tissue (with characteristic acoustic impedance of 1.62 Mrayl for any average soft tissue) results in a strong ultrasonic reflection at their interface [O'Brien, 1977b]. This trend is clearly demonstrated in the comprehensive compilation of empirical ultrasonic properties of mammalian tissues. Table 3 is a selected summary of different tissue categories and acoustic parameters such as velocity and attenuation [Dunn, 1978]. Thus, as the collagen content of different tissues increase ultrasound attenuation and speed of propagation also increase.

Since bone maturity is a key factor in determining the USDA quality grade of a carcass, ultrasound investigations of bone tissue are especially relevant to results presented in this thesis.

Ultrasonic bone status assessment is based upon the measurement in transmission of acoustic properties such as the slope of frequency-dependent attenuation and speed of sound. Roberjot et al. reported that this approach applied to heel bone (cancellous) has been shown useful in assessing fracture risk in elderly women and is recommended for osteoporosis diagnostic.

In another study integrated backscatter coefficient (IBC) was measured in 15 human calcaneal (heel bone) specimens, using X-ray quantitative computed tomography. The results indicate that IBC is sensitive to bone properties and can provide structural information on bone tissue [Roberjot et al., 1996]. Kitamura et al. (1996) characterized bone tissue by analysis of ultrasonic waves scattered around cancellous bone. The experimentally estimated values of the thickness and interval of trabecular bone in human heel (in vitro) are approximately equal to the values measured with a mechanical scale.

Reflection Coefficient

The ultrasonic method used for this project is called the pulse-echo method. Pulse-echo ultrasonic imaging is used routinely in the diagnosis of conditions involving soft tissue. Ultrasound echoes provide information on the shape, size, and position of tissue structures, since different tissue structures and inhomogeneities within organs are indicated by regions of increased or decreased ultrasound reflectivity.

In the pulse-echo method, a transducer is excited briefly by a pulse generator. Ultrasound energy from the transducer is transmitted into the object under investigation. The ultrasound pulse may be coupled to the object through an aqueous gel or water. As the pulse travels into the object it encounters scatterers. Echoes from scatterers travel back to and are detected by the transducer, are processed appropriately, and are displayed. The distance, d, from the transducer to a reflector known as the "range" can be determined from the time interval between when a pulse is sent out and when the echo signal from the reflector is picked up back at the transducer (Figure 3). Let t be the time interval. The distance, d, is then given by

$$d = ct / 2 \qquad (1)$$

where, c is the speed of sound in the medium. The average speed of sound in soft tissue is 1540 meters per second. Using equation (1) it can be determined that a time interval of 13 microseconds corresponds to a reflector depth of one cm [Zagzebski, 1994]. Equation (1) is sometimes referred to as the "range equation" in ultrasonography.

A-mode or amplitude mode is a commonly used echo signal display mode in pulse-echo ultrasonography. The A-mode displays the echo amplitude as a function of time, which converts directly to depth of penetration.

When an acoustic wave meets the boundary between one medium and another, some energy is reflected and some is transmitted [Kinsler, 1982]. In the back of the beef from outside to inside there are different types of tissues: skin, fat, ligament, cartilage, and bone. Besides creating interface boundaries in the beef, these tissues have different

densities and transmit sound at different speeds. In Figure 4, let the plane X = 0 be the boundary between medium I of characteristic acoustic impedance Z_1 and medium II of characteristic acoustic impedance of Z_2. Acoustic impedance is defined as:

$$Z = \rho\, c \tag{2}$$

where, ρ is the density of a substance and c is the propagation speed of ultrasound in that substance.

For an oblique incident (Figure 4), assuming that the separating boundary is at x = 0 and that the incident, transmitted, and reflected beams make the angles θi, θt, and θr with the x axis, the pressures for incident, reflected and transmitted waves are:

$$P_i = \overline{A_1}\, e^{\,j\,(\omega t - k_1 x\cos\theta_i - k_1 y\sin\theta_i)} \tag{3}$$

$$P_r = \overline{B_1}\, e^{\,j\,(\omega t + k_1 x\cos\theta_r - k_1 y\sin\theta_r)} \tag{4}$$

$$P_t = \overline{A_2} e^{\,j\,(\omega t - k_2 x\cos\theta_t - k_2 y\sin\theta_t)} \tag{5}$$

Note that the transmitted and incident beams have the same frequency in each medium but due to different phase speeds, c_1 and c_2, the wave numbers are different for different mediums:

$$k_1 = \frac{\omega}{c_1} \tag{6}$$

$$k_2 = \frac{\omega}{c_2} \tag{7}$$

The pressure reflection coefficient is defined as:

$$R = \frac{reflected\ amplitude}{incident\ amplitude} = \frac{\overline{B_1}}{\overline{A_1}} \tag{8}$$

Applying the first boundary condition gives the continuity of acoustic pressure across the boundary,

$$\overline{A_1}\, e^{j\,(\omega t - k_1 x\cos\theta_i - k_1 y\sin\theta_i)} + \overline{B_1}\, e^{j\,(\omega t + k_1 x\cos\theta_r - k_1 y\sin\theta_r)} =$$

$$\overline{A_2} e^{j\,(\omega t - k_2 x\cos\theta_t - k_2 y\sin\theta_t)} \tag{9}$$

The following are deduced from equation (9):

$$\omega\, t - k_1 y\sin\theta_i = \omega\, t - k_1 y\sin\theta_r \tag{10}$$

$$\omega\, t - k_1 y\sin\theta_i = \omega\, t - k_2 y\sin\theta_t \tag{11}$$

$$\frac{\sin\theta_i}{\sin\theta_t} = \frac{k_2}{k_1} = \frac{c_1}{c_2} \tag{12}$$

Substituting back in equation (9) yields

$$\overline{A_1} + \overline{B_1} = \overline{A_2} \tag{13}$$

Applying the second boundary condition, continuity of normal component of particle velocity, gives:

$$(\overline{A_1} - \overline{B_1})\frac{\cos\theta_i}{\rho_1 c_1} = \frac{\overline{A_2}}{\rho_2 c_2}\cos\theta_t \tag{14}$$

The results from the two boundary conditions determine the reflection coefficient:

$$R = \frac{\overline{B_1}}{\overline{A_1}} = \frac{Z_2\cos\theta_i - Z_1\cos\theta_t}{Z_2\cos\theta_i + Z_1\cos\theta_t} \tag{15}$$

Normal incidence is a special case where the ultrasound beam is incident on a boundary with an angle of zero degrees. Thus, θi, θt, and θr will be zero and equation 15 will become:

$$R = \frac{Z_2 - Z_1}{Z_2 + Z_1} \tag{16}$$

Figure 5 shows the normal incidence at a boundary of X = 0 between two mediums Z_1 and Z_2.

Let us consider the oblique incidence and give an example of different mediums involved. For example, considering different tissue types, when the ultrasound energy is travelling from bone (Z = 7.8) to soft tissue (Z = 1.62) medium, then the ratio of the characteristic impedance would be as following:

$$\frac{z_2}{z_1} \cong \frac{7.8}{1.62} \cong 4.82$$

Pressure reflection coefficient is shown in equation 17 where, reflected and transmitted waves are in phase and both have the same magnitude.

$$R = \frac{\overline{B_1}}{\overline{A_1}} = \frac{Z_2 \cos\theta_i - Z_1 \cos\theta_t}{Z_2 \cos\theta_i + Z_1 \cos\theta_t} = \frac{\left(Z_2 / Z_1\right) \cos\theta_i - \cos\theta_t}{\left(Z_2 / Z_1\right) \cos\theta_i + \cos\theta} \rightarrow 1 \qquad (17)$$

Pressure reflection coefficient where, reflected and transmitted waves are out of phase but have the same magnitude is shown in equation 18:

$$R = \frac{\overline{B_1}}{\overline{A_1}} = \frac{Z_2 \cos\theta_i - Z_1 \cos\theta_t}{Z_2 \cos\theta_i + Z_1 \cos\theta_t} = \frac{\left(Z_2 / Z_1\right) \cos\theta_i - \cos\theta_t}{\left(Z_2 / Z_1\right) \cos\theta_i + \cos\theta} \rightarrow -1 \qquad (18)$$

CHAPTER 3
VALIDATION STUDIES

Validation studies are both important and necessary for this research study. The composition of the spine tissue varies among animals. The heterogeneous and unknown composition of the tissue under research calls for an experiment with a known object that has defined acoustic properties as well as an apparent structure, so we can confirm the validity of the analysis procedure. Therefore this study has been conducted to validate the process of data analysis on the spine data.

This chapter begins with an explanation of the experimental procedure. Then, our data acquisition system as well as the data processing are discussed. Finally, there is a discussion of results.

Comb Experiment

Quality grading of beef cattle is done considering many factors, one of which is the degree of skeletal maturity at the spine. Skeletal maturity is estimated by visually observing the amount of ossification on the spinous processes. The tissue composition between the skin and the spine is quite variable among animals and depends on factors such as age, genetics, and the feed type. The reflected ultrasound signal from any object varies depending on the acoustic properties of that object. For example, the amplitude of the reflected signal from bone is much larger than the amplitude of the reflected signal from soft tissue. Due to this variability we need a well characterized model on which we could perform the same analysis that was performed on the spine data.

The test object in Figure 6 is a plastic comb of about 5 cm. The comb has 12 solid teeth. The center to center distance between the comb teeth is 4 mm. Figure 7.a. shows a cross section of a comb tooth with dimensions 2 mm $\times$ 1.5 mm. The comb teeth are not in perfect alignment with respect to each other. The comb has a concave shape with the middle teeth falling below the plane of the comb and the two ends bent above that plane.

Figure 7.b. shows the comb teeth as if looking at the tip of the teeth, and demonstrates the non-planar alignment of the comb teeth.

Figure 8.a. shows a block diagram of the main system components. Figure 8.b. is a photograph of the position of the comb with respect to the transducer in actual experimental set up. The host PC (ZEOS, 66 MHz) controls both the positioning system and the digital oscilloscope; it also stores acquired data for off-line processing. The pulser-receiver operates in pulse-echo mode and generates the shock pulses that excite the transducer. The plastic comb is placed in a tank of degassed water connected to the Daedal positioning system. The Daedal system is used to control the location of the comb. The system is manufactured by Daedal, Inc. (Harrison city, PA) and contains a MC2000 controller and a MD23/M34 motor drive system. The motor assembly controls test object movement along five axes, three translational and two rotational axes, with a linear accuracy of about 5 μm and a rotational accuracy of about 0.02 degrees. On the Daedal MC2000 controller the X, Y and Z axes are labeled as "AXIS 1", "AXIS 2" and "AXIS 3". Upon manual positioning of the transducer which sets the origin for the time of flight for the sound wave, generally one or two translational axes are used for the scan. Figure 9 shows a photograph of the Daedal system.

A Panametrics V309, 5 MHz focused transducer was used to scan the plastic comb. This transducer was characterized at the Bioacoustic Research Laboratory and has a center frequency of 5.9 MHz, wavelength of 253.5 μm , bandwidth of 2.7 MHz, beam width of 0.13 cm at the focus, and a focal length of 6 cm with depth of focus of 4.2 cm. One set of data was collected in the tank of degassed water using the plastic comb as target. The comb was placed in the tank with its flat face oriented approximately normal to the incident beam direction. The transducer was excited via Panametrics model 5800 pulser-receiver in pulse-echo mode and the received echo signal was amplified by 20 dB, band pass filtered 1-35 MHz, and displayed on the oscilloscope with 10-bit resolution. The sampling frequency was set at 50 MHz. The host PC retrieves the waveforms from the oscilloscope and stores them. The waveforms are then transferred via FTP to a Sun Sparc 20 for processing.

The direction of the beam axis perpendicular to the flat surface of the comb was found by adjusting the transducer to an angle and a depth at which the reflected signal was maximum. In order to get the best reflected signal the comb should be positioned at the transducer's focal length which in this case is 6 cm. At the time of this experiment the focal length was taken from the transducer specification sheet which had a value of 5 cm for the focal length. Therefore the plastic comb was placed at a distance of 5 cm from the transducer. This distance corresponds to a time of 67 microseconds on the digital oscilloscope. This time was determined using the range equation:

$$d = \frac{ct}{2} \tag{19}$$

where, c is the speed of sound in the medium, t is the time interval between when the pulse is sent out and when the echo signal is picked up, and d is the distance from the transducer to the reflector. Distance, d, was set to the focal zone of the transducer at 5 cm and c, the speed of sound in water, was at 1480 m/s.

The program used for data acquisition is called "rowscan.m" (Appendix E). This program acquires a set of RF echo data along one axis. The distance between two RF acquisitions (step size) and the total length of a scan row is selected. The scan direction is perpendicular to the axis of the comb tooth. Two files are created: the binary file with the extension bin which contains the unscaled integer signal points (1024 for each scan), and an ASCII file, which contains waveform and scan information. For this experiment there are 1024 data points for each RF signal and 51 RF signals with 1-mm step size. This corresponds to a scanning length of 5 cm.

Data Analysis

Data analysis was done in MATLAB. MATLAB is a computational software package that is used for the data analysis purposes. The program "File.m" (See Appendix E) loads the acquired binary and ASCII files into MATLAB. The program "Sanity.m" (See Appendix) squares the reflected amplitude, finds the maximum reflection for each RF

signal (called maximum power) and the location where the maximum reflected signal has occurred. This program also integrates the area under the squared reflected signal (called power signal).

Theoretically, when the sound beam is incident perpendicular to the comb tooth there will be a strong reflection, whereas if the sound wave is incident on the water between the comb tooth there will be no reflection. The program "Puscan.m" (See Appendix E) takes the data from the Sanity.m program as input and generates five graphs, as shown in Figure 10:

a) All 51 RF signals versus the distance from the transducer to the comb
b) One typical RF signal versus the distance from the transducer to the comb
c) Maximum power for 51 RF signals
d) The location of maximum power for all RF signals
e) The integral of area under the power signal

Figure 10.a. is a plot of superimposition of 51 RF signals. Each RF signal is a plot of received voltage as a function of time. The significance of this figure is that major echoes are relatively coincident as a function of distance. The plot was acquired by taking the voltage data from the transducer as a function of time. The time axis was transformed into distance using the range equation. In this plot the relative values of amplitudes are important because the voltage data were taken directly from the transducer, which means that they are proportional to pressure variation of the reflected sound wave. Figure 10.b. shows a typical RF signal. The amplitudes of RF echo signals differ according to distance from the transducer. Figure 10.c. is a plot of maximum power of each of the 51 RF signals. The plot is obtained as follows: First, all 51 RF signals were squared to obtain a plot of the relative power versus time. For each of these power plots the maximum value was found and plotted versus the corresponding RF signal. The maximum and minimum points of this plot correspond to instances where the ultrasonic beam is reflected from a mismatched or a well-matched boundary, respectively. Therefore, this plot indicates the profile of the object under experiment. The maximum power point in Figure 10.c.

corresponds to a distance by the range equation. This distance is plotted as a function of index of RF signals. Figure 10.d. is an indication of fine alignment of the comb teeth. Figure 10.e. is a plot of relative reflected power (energy signal) as a function of transducer position. This plot was acquired by taking the integral of the area of each RF signal after it has been squared.

Discussion

Figure 10.a. shows all 51 RF signals plotted in one graph. The first reflected signals appear occur between 4.8 and 4.9 cm from the transducer. The plastic comb was placed at 5 cm from the transducer. When sound waves traveling through water reach an interface, part of the sound energy gets reflected and the other part is scattered. The amplitude of the reflected signal varies based on the acoustic properties of the object at the interface. Thus the first reflection in our validation experiment was expected to occur at a distance of 5 cm from the transducer, where the incident beam first reached the front face of the comb tooth. If all the comb teeth were in perfect alignment, then the first reflection for all RF signals should happen at the same distance. This however, is not the case. Figure 9.b. clearly shows that the comb teeth are not perfectly aligned across the comb face. Each tooth is detected at a different distance from the transducer (such as 4.9, 5.0 and 5.1 cm). That is why in Figure 10.a. the first reflection from the comb falls in a range between 4.8 to 4.9 cm. The second reflected signal is at 5.0 cm. This is the same distance as from the transducer to the back surface of the comb tooth. The thickness of each comb tooth has been determined by direct measurement to be 2mm. The part of the incident wave that is transmitted into the comb tooth will encounter a second interface as it reaches the back surface of the tooth. By this time the sound wave has lost part of its energy at the first interface. The reflected signal at the second interface will have a smaller amplitude due to the energy loss mentioned above. The difference between the location of the first reflected signal and the second reflected signal was found to be 2 mm. This is in agreement with the directly measured thickness of the comb teeth. Figure 10.b. is a typical RF signal. Depending on which RF signal the figure represents, the reflected

amplitude will be different. Figure 10.c. is a graph of the maximum power signal. Each circle is representative of the maximum power for an RF signal. The maximum power is smaller when the sound wave is traveling between comb teeth and is at its maximum when it is at a normal incident to the comb tooth. When the beam is incident in between the comb teeth or close to one of the comb teeth, part of the reflection will be from the comb tooth surface if it falls in the beam width region of the transducer, which is 0.13 mm in this case. In this case the maximum power varies between the highest reflection (normal incidence on the comb) and the lowest reflection (normal incidence between comb teeth, water mainly) depending on whether and how much of the reflection from the comb tooth is in the transducer beam width region. Figure 10.d. shows at what distance from the transducer the maximum power for each RF signal has occurred. The location at which the maximum reflected signal has occurred varies from 4.78 to 4.9 cm. This figure demonstrates the unequal distance of the comb teeth from the transducer, which is due to uneven alignment of the comb teeth with respect to each other. The concave shape alignment of the comb teeth is apparent in this figure. Figure 10.e. is the integral of the power signal (energy signal). Each peak is representative of a comb tooth in this figure. The amplitude (y-axis) would be the same for all comb teeth if we had a perfect comb (a perfect comb has the same composition for all comb teeth)

We can conclude that the reflected power is at its maximum for the comb experiment if 1) the tooth is placed at or very near to focal length of the transducer, 2) all of the reflected signal falls in the beam width region of the transducer, 3) the beam is normally incident at the object.

The analysis deduced from Figure 10 agrees with the fact that the amplitude of the reflected signal from any object depends on the acoustical properties of that object. As ultrasound travels through an inhomogeneous medium such as tissue it loses energy and becomes reflected both by discrete internal scatterers and interfaces between two mismatched media. The inhomogeneity of the tissue in the spinous processes, which are more cartilaginous at the tip in younger animals and more ossified as the animal matures, allows us to study the characteristics of the reflected signals at the interface of bone and cartilage. We can also look at the reflected energy at the spinous processes. From the

comb experiment we know that the reflected energy is higher if the sound wave travels from a medium with smaller characteristic impedance to a medium with larger impedance.

Characteristic impedance is defined in equation 2 (Chapter 2, Reflection Coefficient) and, is a function of both density of the medium and the speed of sound in the medium:

Studying the reflected energy in the spine data will give us an idea of the tissue profile under the experiment. Theoretically, the area under the squared RF signals, which are proportional to the energy, should be smaller if the animal is younger, since the reflected amplitude would be smaller due to the less ossified cartilaginous tips of the spinous processes.

CHAPTER 4
DATA COLLECTION AND ANALYSIS

Chapter 4 contains three sections: the equipment used to perform the experiment is described; the spine scan protocol is explained; and the procedure for data analysis is discussed.

Equipment

Data processed for this research project were collected using the Beef Ultrasound Grading System (BUGS) equipment. BUGS is an experimental data collection system built for the purpose of obtaining a data base for the development of an ultrasound grading system for beef [Hein et al., 1992].

Five main components of the BUGS system are: 1) a 486 PC; 2) a superstructure, mounting to the back of the carcass, that controls the mechanical motion of the transducers; 3) motion control electronics which drive the mechanics of the system; 4) a two-channel pulser/receiver, which can multiplex between two transducers both transmitting and receiving; and 5) analog/digital conversion electronics that digitize the RF signals up to 50 MHz. Figure 11 illustrates the overall design of the ultrasound data acquisition system.

Figure 12 displays details of the electronics component of the system. The system controller is an Insight 486/33 PC equipped with a 550-MB hard drive and a 250-MB tape backup. Since massive amounts of data are collected and the system requires a large number of plug-in cards to interface to the PC, a Cubix Lan Central Station expansion chassis (Cubix Corp., Carson City, Nevada) is incorporated to accommodate all of the required PC interface cards. The pulser / receiver for this system is a RITEC RAM 10000 (RITEC Inc., Warwick, RI). This unit can generate output pulses of up to 1.3 kW at 5 MHz. It contains two receiver inputs and can be equipped with a multiplexer to switch between two separate transmitting transducers. Furthermore, it can be entirely computer

controlled for functions such as the output power, receiver gain, transmitted pulse frequency and number of cycles in the pulse, and transmitted pulse repetition frequency. The output from the RITEC receiver is digitized at 50 MHz with a Gage CS250 analog/digital card (Gage Applied Science, Inc., Montreal, Quebec, Canada). A Targa 16+ frame grabber board (Truevision, Inc., Indianapolis, IN) to generate the video images uses the captured RF data. A Panasonic LF5010 WORM drive is the primary data storage device for the system; it can permanently store 940 MB of data on a single cartridge. Transducers incorporated into the system were chosen for their large diameter apertures, required to obtain good quality signals from deep within the carcass. They are 1-inch diameter 3.5 MHz, 5.0 MHz, and 7.5 MHz transducers (Panametrics, Waltham, MA). They have foci ranging from 4.0 to 6.5 inches, focal zones ranging from 1 to 4 inches, and beam width of approximately 1 mm.

The superstructure weighing approximately 300-400 lb. consists of three main components: the carcass mounting structure, the transducer substructure, and the main superstructure housing. The main housing and transducer substructure are coupled to the carcass via the carcass mounting structure, which is the only part of the superstructure to come into contact with the carcass. The carcass mounting structure is constructed of aluminum in order to satisfy USDA regulations, which require thorough washing and cleaning. The main superstructure contains seven motors and position actuators. The positioning system is fully automated and allows for three-dimensional positioning of the transducers. The system rotates the angle of contact between the carcass and the transducer up to 25 degrees. The equipment rack contains seven Compumotor S57-83-E motor driver units as well as the 486/33 MHz PC with 550-MB hard drive and the Panasonic LF5010 WORM drive for data storage. Figure 13 shows the BUGS scanning table superstructure.

Spine Scan Protocol

RF echo data were collected at two orientations of the transducer: one with the plane of the sector scan parallel to the cross section of the animal (perpendicular to the long axis of the animal; denoted the horizontal scan) and the other with the plane of the

sector scan parallel to the long axis of the animal (vertical relative to the hanging animal; denoted the vertical scan.) For the vertical section orientation, three regions were evaluated, one centered over the spine, called the spine cartilage scan, and the other two centered over the longissimus muscles. This research project analyzes data from the spine cartilage scan protocol exclusively.

Placing the transducer directly over the animal's spine at the 13th rib centers the spine cartilage scan protocol. The direction of scanning is from the head to tail -35 mm to +35 mm relative to the center of the vertebra at the 13th rib. Data are collected at vertical increments of 1 mm. Figure 14 is a schematic of the spine cartilage scan.

Scanning was performed at three different times: the hide-on scan was started within 20 minutes after animal had been killed, with the animal's hide still on the carcass. (The animal's hair had been removed, exposing bare hide to the transducer.) The hide-off scan was accomplished immediately after the animal had been skinned and disemboweled. The cold scan was conducted after the carcass had been refrigerated for a minimum of 12 hours. Hide-on and hide-off scans were completed the day of slaughter, while cold scans were performed within 36 hours of the time the animal was killed.

Data Acquisition

Data were collected from hide-on, hide-off, and cold scans for 108 animals numbered 21 through 128. However, the usable data were available only for 98 animals numbered 27 through 124. The program used for data acquisition is called the "vertical scan"(See Appendix E). The "vertical scan" program acquires a set of RF echo data along the spine.

The animal data were collected in acoustic lines (RF echo data) of 3000 bytes representing 10 centimeters in depth, at each transducer location. Each complete scan includes RF data from 71 locations spaced 1 mm apart for total scanning range of 7 cm along the spine. Six RF data sets were collected at each location, with receiver gain values of 12, 18, 24, 30, 36 and 42 dB. The spine scan files are denoted in position 2 of the file

name with a "V" where the transducer scans over the spine. Typical spinal file names for data collected on a particular animal are:

Hide-on	nvaXXm05	(hide-on series 05)
Hide-off	fvaXXm07	(hide-off series 07)
Cold	cvaXXm07	(cold series 07)

Where, XX denotes the gain setting, n is for hide-on, f is for hide-off and c is for cold scans.

Two files are created: the binary file with the extension "bin", which contains the unscaled integer signal points (3000 for each scan), and an ASCII file with the extension "dat", which contains waveform and scan information. There are 3000 data points for each RF pulse. Furthermore, there are 71 RF signals with vertical increment of 1-mm step size that correspond to a scanning length of 7 cm.

Data Analysis

Our first objective was to decide which set of data would be most relevant to current beef grading procedures performed by USDA graders. Comparison of hide-on and hide-off RF signals for the same animal revealed that hide-off data were far simpler to interpret. Figures 15.a. and 15.b. show the RF signal along one scan line for animal #111 with hide-off and hide-on respectively. Both plots are from the same location, with the same gain setting (18 dB).

The first centimeter on both plots registers signals from within the transducer standoff, a boot-like protective cover for the transducer that couples the ultrasound energy to the carcass. The first spike following the standoff occurs at about 1.7 cm on the hide-on plot. The average thickness of cattle hide is about 0.7-1.0 cm (Charles Stites, University of Illinois Meat Science Laboratory, personal communication). Thus, it is not surprising that we see a spike at about 1.7 cm in the hide-on plot. The first spike on the hide off plot occurs at 1.7 cm however, this does not correspond to the first spike on the hide on plot which, also occurs at 1.7 cm. The first spike from the hide-on plot at 1.7 cm is missing on the hide-off plot due to the removal of hide. The distance between the

transducer standoff spike and the first spike on the hide off plot is 0.7 cm. Subcutaneous fat thickness of a cattle carcass is also estimated to be about 0.7-1.0 cm. The first spike following the transducer standoff on the hide-off plot occurs at 1.7 cm. This is in agreement with the thickness of 0.7-1.0 cm of fat. The location of the second spike at 2.4 cm on the hide-on plot is in agreement with the hide thickness corresponding to the hide/fat boundary. The second spike on the hide-on plot corresponds to the first spike on the hide-off plot. The third spike at 3.0 cm on the hide-on plot corresponds to the fat/cartilage boundary. The third spike on the hide-on plot corresponds to the second spike on the hide-off plot. The difference between the second spike and the third spike is 0.6 cm on the hide-on plot. This is in agreement with the difference of about 0.6 cm between the first and second spike on the hide-off plot. The highly attenuative characteristic of the hide is apparent by comparing Figure 15.a. with Figure 15.b. Since hide is very attenuating and distorts the reflected echo from the spine, it was decided to analyze only hide-off data for this research study. Moreover, signals coming back from the standoff material are ignored in the signal processing.

On the hide-off plot the second spike occurs at about 1 cm from the transducer standoff position which again is in agreement with the fat thickness for this animal. (This second spike is interpreted to reflect the location of the fat/spine boundary.) The analysis is performed on data from between 1 and 4 cm to ensure that the fat/spine boundary is always included in the analysis regardless of variation of tissue thickness from animal to animal.

Data analysis was done in MATLAB. The program "rf-to-ml" (See Appendix E) loads the acquired binary and ASCII files into MATLAB. The program "dnmab.m" (See Appendix E) squares the reflected amplitude and finds the maximum reflection for each RF signal and the location at which the maximum reflection has occurred. This program also integrates the area under the power signal. The program "ascan.m" (See Appendix E) takes the data from the dnmab.m program as input and generates five graphs. These are shown in Figure 16 as follows:

a) All 71 RF signals versus the distance from the transducer to the spine

b) One typical RF signal versus the distance from the transducer to the spine

c) Maximum power for each of 71 RF signals

d) The location of maximum power for all RF signals

e) The integral of the area under the power signal (energy signal)

Figure 16.a. is a plot of a superimposition of 71 RF signals. Each RF signal is a plot of received voltage as a function of time. The plot was acquired by taking the voltage data from the transducer as a function of time. The time axis was transformed into distance using the range equation. Transducer standoff data occupy the first centimeter in the graph as in Figure 15.a. and 15.b. (These standoff data are shown on Figures 16.a. and 16.b. but have been excluded from subsequent Figures). The first spike on Figure 16.a. corresponds to the fat/cartilage boundary. This first spike occupies about 5 mm on the graph, due to variation of fat thickness on the back of the beef as the scan proceeds from bottom to top. Before the second spike, which is the cartilage/bone boundary, there is observed an amplitude variation in the reflected signal, which is due to inhomogeneity within the cartilaginous part of the spinous processes. In this plot the relative values of amplitudes are important because the voltage data were taken directly from the transducer which means that they are proportional to pressure variation of the sound wave. The significance of this figure is that major echoes are relatively coincident as a function of distance. Figure 16.b. shows a single typical RF signal that is one of the signals that were plotted in 16.a. The amplitudes of RF echo signals differ according to distance from the transducer.

Figure 16.c. is a plot of maximum power of each RF signal. The plot is obtained as follows: First, all 71 RF signals were squared to obtain a plot of the relative power versus time. For each of these power plots the maximum value was found, and was plotted versus the index of the corresponding RF signal. A large value for maximum power means that at some depth there was a large impedance mismatch at a boundary. A small value for maximum power indicates that there was no boundary with a large impedance mismatch. Depending on what type of tissue the ultrasound is incident at (soft tissue versus hard tissue such as bone) the maximum power will be larger or smaller. For the first 20 RF signals the maximum power varies between 0 to 2000. This means that for

the first 2 cm of the scan there is inhomogeneity within the tissue being scanned. However, the reflected signals are not as large as at the 27^{th} scan line, where the maximum power occurs at approximately 6700. This plot indicates the profile of the tissue under investigation.

Each maximum power point in Figure 16.c. is associated with a depth at which the maximum reflected power occurs at some boundary location. This distance is plotted in Figure 16.d. versus RF signal index. Thus Figure 16.d. is interpreted to indicate the location of boundaries among different tissues. Figure 16.d. shows that the depth at which the maximum power has occurred for the 27^{th} scan line is about 3.3 cm. [Due to the large variation in the anatomy of the animals it was not feasible to compare the animals on a scan line to scan line basis].

Figure 16.e. is a plot of relative reflected energy as a function of transducer position. Taking the integral of the area of each RF signal after it had been squared created this plot. While 16.c. shows only the maximum reflected power, figure 16.e. shows the total reflected power for each RF signal. Figure 16.e. demonstrates the general profile of the spine of each animal. The larger the area under the maximum power signal, the harder the surface from which the ultrasound is reflected.

Because in larger and more mature animals there exists more ossification at the tip of the spinous processes, the larger area under the energy signal can be assumed to be from the old and mature category, which is a low quality grade. For example, the skeletal maturity for animals number 27 and 30 is A40 and A50 respectively. The skeletal maturity for animal number 28 is A30. The former two animals are in a lower skeletal maturity category than animal number 28. Figure 17 compares the area under the maximum power signal for animals 27, 28 and 30. A comparison of area under the maximum power for these three animals shows a smaller area for animal 28 and larger areas for the other two. This fact would have been even more apparent if the animals scanned had had a wider range of grade differences. It is worth exploring whether the area under energy signal is related to skeletal maturity.

CHAPTER 5
STATISTICAL ANALYSIS

Chapter 5 contains two sections. First, the animal data is explained and then the procedure for four statistical analysis is described.

Animal Data

Ninety-eight cattle were evaluated and slaughtered over an 18 months period. The cattle were selected from the University of Illinois beef-cow herds and various commercial feedlots. The chosen breeds and crosses represent genetically typical industry cattle type, which also provide variability of cattle necessary to supply cattle of different yield and quality grade. Live weight of the cattle ranged from 700 to 1500 pounds. Out of ninety-eight carcasses four were of "B", six were of "C", one was of "D", one was of "E" and the rest were of "A" skeletal maturity (with subscripts 0-100). Numerical quality grade values estimated by the USDA graders ranged from 0, for "C" and "E" skeletal maturity, to 303, for skeletal maturity of A60 and slight abundance of marbling. Figure 18 shows the distribution of numerical quality grading for all ninety-eight carcasses. The result of sensory judging showed that tenderness varies from 5 to 13 where, 15 is extremely tender and 0 is no tender. Flavor ranged from 7 to 11 where, 15 is the most flavorful and 0 is the least flavorful. Figures 19 and 20 show the distribution of Tenderness and Flavor for all the beef carcasses respectively. Figures 21, 22 and 23 present histograms of Ngrade, Tenderness and Flavor respectively.

Upon collection of data, research was performed to select the most appropriate variables for analysis purposes. Our data provided RF echo wave-forms from the region of the 13^{th} thoracic vertebrae. Skeletal maturity is determined from 10^{th} to 13^{th} thoracic vertebrae by the USDA graders, which is one of the attributes toward final determination of quality grade. It was deduced from the literature search that maturity increases as beef carcasses get older and heavier [Hamlin et al., 1995; Fitzhugh et al., 1971; Shackelford et

al., 1995]. Increase in maturity results in an increase in ossification in all bones as well as the spinous processes located in the spine [Mello et al., 1978]. In fact, the numerical grade assigned by USDA graders is calculated from the observation of ossification on the spinous processes at the thoracic vertebrae (called skeletal maturity) and marbling data. Gathered from all above-mentioned facts numerical grade (Ngrade) was chosen as one of our independent variables which best relates to skeletal maturity. Tenderness and Flavor are two of the sensory evaluation attributes. They are indirectly related to quality grading. The higher the quality grade the more tender and flavorful the meat must be. These two variables were chosen just to test the indirect relationship between the sensory attributes and quality grade attribute. It is expected that tenderness and flavor highly correlate with quality grade.

The increase in ossification as carcasses mature compared to unossified cartilaginous spinous processes creates an acoustic impedance difference for the ultrasound signal. The change of medium as an ultrasound wave travels in that medium represents a change in the acoustic impedance. Acoustic impedance is a function of density and the speed of sound in the medium (discussed in chapter 2, theoretical development). Due to the change in acoustic impedance the amplitude of the reflected ultrasound signal is also hypothesized to change. It was shown in the validation study of this thesis (chapter 3) that as ultrasound waves traveled from a medium containing plastic relative to a medium containing water the amplitude of reflected ultrasound wave decreased. Based on the information deduced from the validation study we could make the assumption that the larger amplitude of the reflected ultrasound signal is from the more ossified regions of the spinous processes compared to smaller amplitude of the reflected ultrasound signal from less ossified regions of the spinous processes. However, many other variables such as feed consumed by the beef cattle and genetics can change the amount of ossification in the spinous processes. Since these factors were not controlled in animal selection and there was no literature supporting a constant (same) type of ossification for all beef carcasses in the spinous processes, we had to look at a more general variable from our ultrasound data. The area under the energy signal (called Intave) provides us with a numerical value that is being investigated on how it might be related to carcass skeletal maturity. "Intave", thus serves

as our dependent variable. It is evident from previous studies that the ultrasonic energy signal with respect to skeletal maturity has not been investigated by ultrasound techniques.

In the original data, animals numbered 81(E80), 97(C30), 99(C0), 104(C50), 105(C20) and 120(C80) were assigned a value of zero for Ngrade. These animals were all C-maturity with the exception of animal number 81 that was E-maturity.

Statistical Analysis Procedure

Pearson correlation analysis was performed to determine whether the Ngrade and Intave values are correlated, That is, whether large values of one set are associated with large values of the other (positive correlation), small values of one set are associated with large values of the other (negative correlation), or values in both sets are unrelated (correlation near zero). A correlation coefficient is calculated for the two variables. The correlation coefficient varies from +1 (strong positive correlation) to –1 (strong negative correlation).

Pearson correlation coefficient, r, is a dimensionless index that ranges from -1.0 to 1.0 and reflects the extent of a linear relationship between two data sets. Following equation is used to compute r:

$$r = \frac{n(\Sigma xy) - (\Sigma x)(\Sigma y)}{\sqrt{[n\Sigma x^2 - (\Sigma x)^2][n\Sigma y^2 - (\Sigma y)^2]}} \qquad (20)$$

The dependent variable (Intave) is defined as a numerical value associated with the area under the ultrasonic energy signal. For a complete discussion of this variable refer to the previous chapter on ultrasonic data collection. The independent variables are:

1. Tenderness (Numerical values and distribution graph provided in chapter 4, animal selection) - - a component of sensory evaluation. In general the younger the animal the more tender the meat

2. Flavor (Numerical values and distribution graph provided in chapter 4, animal selection) - - another sensory component. Flavor varies directly with Tenderness.
3. Ngrade (Numerical values and distribution graph provided in chapter 4, animal selection) - - refers to numerical grading which is the numerical value assigned to skeletal maturity of the beef

For the list of numerical values of the dependent and independent variables refer to Appendix C.

In addition to the correlation matrix, multiple regression analyses were performed to determine effects of selected independent variable on "Intave". The independent variables include Tenderness, Flavor, and Ngrade. In the following section four sets of analyses will be conducted to examine the relationships among these variables.

Analysis 1:

This analysis was done using the original data (N=98). Table 4 presents correlation matrix among selected variables. Among the selected independent variables, Ngrade is correlated with "Intave" (r = -0.14), but not very strongly. This indicates the higher the value of Ngrade, the lower the value of "Intave". This was expected since higher Ngrade represents less mature (younger and smaller) beef cattle and, less mature carcasses do have less ossified spinous processes. A similar correlation between Ngrade and Flavor was observed(r = 0.17). Correlation between Tenderness and Ngrade is weaker than the correlation between Flavor and Ngrade (r = 0.11). A weak correlation is also observed between Tenderness and Flavor (r = 0.12). Next a scattered diagram was drawn between Ngrade and "Intave" to note any trend between the two variables. As shown in Figure 24 data points are spread on a wide range in the graph and depicting a specific trend is not obvious though neglecting the points to the right of point 6EE4 on the x-axis, a line with a negative slope is noticed. Figure 25 and 26 are scattered diagram between Intave and Flavor and Intave and Tenderness respectively.

For the multiple regression analysis, a linear model was adapted since no particular trend was noticed from the scattered diagram. The equations for the mathematical models are:

$$\text{Intave} = a + b\,(\text{Ngrade}) \tag{21}$$

$$\text{Intave} = a + b\,(\text{Ngrade}) + c\,(\text{Flavor}) \tag{22}$$

$$\text{Intave} = a + b\,(\text{Ngrade}) + c\,(\text{Tenderness}) + d\,(\text{Flavor}) \tag{23}$$

Table 5 shows regression coefficients, t-ratios, and level of significance for these models. The results of Table 4 and 5 support each other. Table 4 showed that Ngrade and Intave are correlated. Table 5 (column 3) showed the regression line for these two variables. Table 4 showed that Intave and Flavor are slightly correlated. This is also supported in Table 5 (column 2) where there was a slight increase in the significance level when Flavor was added to Ngrade. Similarly, Table 4 showed that Tenderness was not correlated to Intave. This was also shown from Table 5 where adding tenderness to Ngrade and Flavor did not increase the confidence level on the model. In summary, Ngrade is the most important variable in describing Intave.

Analysis 2:

Since "Intave" is widely distributed across 98 cases, a "Lintave" (natural log of Intave (shown in equation 24) was used to reduce the range of variation .

$$\text{Lintave} = \ln(1+\text{Intave}) \tag{24}$$

A second set of statistical analysis was performed using the same procedures with the same data set as before (N=98). However, this time "Lintave" is used in place of "intave".

Table 6 presents correlation matrix among selected variables. Among the selected independent variables, Ngrade is correlated with "Lintave" ($r = -0.197$). This indicates the

higher the value of Ngrade, the lower the value of "Intave". It appears that using "Lintave" has resulted in a slightly higher correlation coefficient than before when, "Intave" was used. Looking at scattered diagram (Figure 24) between "Lintave" and Ngrade show the trend of a line with a negative slope as it was before. The correlation values among other independent variables are not strong, except the relationship between Flavor and Ngrade (correlation coefficient, r = 0.17). Figures 25, 26, and 27 are the corresponding scattered diagrams.

The followings are the models used for the regression analysis:

$$\text{Lintave} = a + b\,(\text{Ngrade}) \tag{25}$$

$$\text{Lintave} = a + b\,(\text{Ngrade}) + c\,(\text{Flavor}) \tag{26}$$

$$\text{Lintave} = a + b\,(\text{Ngrade}) + c\,(\text{Tenderness}) + d\,(\text{Flavor}) \tag{27}$$

Table 7 shows regression coefficients, t-ratios, and level of significance. In this Table, three sets of regressions were performed. The results of Table 6 and 7 support each other. Table 6 showed that Ngrade and Intave are correlated. Table 7 (column 3) showed the regression line for these two variables. The confidence level explaining the relationship between Ngrade and Lintave has increased from 82 percent in analysis 1 (where, Intave was used) to 95 percent in analysis 2 (where, Lintave is used). Table 6 showed that Lintave and Flavor are correlated. This is also supported in Table 7 (column 2) where there was a slight increase in the significance level when Flavor was added to Ngrade. Similarly, Table 6 showed that Tenderness was very weakly correlated to Lintave. This was also shown from Table 7 where adding tenderness to Ngrade and Flavor did not increase the confidence level on the model. In summary, Ngrade is the most important variable in describing Lintave. It is clearly demonstrated from the two performed analysis that though replacing Intave with Lintave has resulted in stronger correlation and higher cofidence level between Ngrade and the ultrasonic derived parameter Lintave however, the trend of relationship between the two variables stayed the same. Namely, Ngrade is the most important variable in describing Lintave.

This indicates that the higher the value of Ngrade, the lower the value of "Lintave", verifying further our assumption mentioned earlier which is: higher value for Ngrade represents less mature beef carcasses, which means less ossification on the spinous processes. Based on our assumptions it is expected that the higher Ngrade values would be representing the smaller area under the energy signal. As shown in the third column of Table 7, eliminating insignificant variables does not change the significant effect of Ngrade on "Lintave". Among the three independent variables, Ngrade is the only variable that found to have significant impact on "Intave". This indicates that Flavor and Tenderness can be eliminated from equation 26 which, will become the same as equation 21.

Analysis 3:

For this analysis the animals with Ngrade of zero value were eliminated from the data set (N = 91). The same exact analysis as the one performed in Analysis 2 was conducted for Analysis 3. Tables 8 and 9 show the result of the correlation and regression analysis. Again, a significant correlation was observed between Ngrade and Lintave (r = -0.21). The correlation between Flavor and Ngrade is again significant (r = 0.25). Tables 8 and 9 support each other in the same manner as before. Namely, Ngrade is the best variable explaining Lintave. Figure 30 is the scattered diagram between Lintave and Ngrade.

Analysis 4:

The original data was modified for all the animals, recalculating the Ngrade value. This was done so that the animals with the numerical value of zero for Ngrade in the original data would contain a non-zero numerical value. The recalculated values are given in the Appendix D. The same statistical procedure as before was performed on this new data set (N = 98). Tables 10 and 11 show the result of correlation and regression analysis. As it can be observed from both tables the same relationship and trend exist among the same selected dependent and independent variables as it did with the last three analyses. It is

also evident from tables 10 and 11 that the magnitude of correlation coefficient and the significance of relationship between Ngrade and Lintave did not improve. Figure 31 is the scattered diagram between Lintave and Ngrade.

CHAPTER 6
DISCUSSION OF RESULTS

The main goal was to identify common features of the ultrasound data collected from ninety-eight beef carcasses that would facilitate evaluation of the skeletal maturity factor in the determination of quality grade. The first step was to identify the fat/spine boundary. Figure 16.a. gave us a general idea of where this boundary is located. Ultrasound data for this boundary in all the other beef carcasses were consistent with known hide thicknesses of 0.7-1.0 cm and fat thicknesses of 0.7-1.0 cm. Once the consistency of ultrasound data with direct measurement had been established (validation study), the question was what ultrasonic parameter would best represent the skeletal maturity. In answering this question our first approach was to determine where is the bone-cartilage boundary at the spinous processes and whether the ultrasound-determined boundary occurs at the same distance for animals that have similar maturity characteristics and have been categorized under the same quality grade by the USDA graders. However, due to tissue variation among the animals, uncertainty in the precise positioning of the transducer at exactly the same location for all the beef carcasses, as well as uncertainty in the process of ossification it was not possible to select an appropriate ultrasonic parameter representative of skeletal maturity from our data set. A more detailed and specific plan prior to conducting the experiment might have resulted in greater precision data collection and thus greater discrimination in data analysis.

Since skeletal maturity is evaluated by observing the spinous processes and the amount of ossification of the cartilaginous section at the tip of the processes, another question raised was whether we could estimate this thickness through ultrasound measurements. However the nature of ossification is a complex phenomenon that can be influenced by other factors than chronological age such as, sex, genetics and weight of the animals. Furthermore, there is some uncertainty in exactly how the process of ossification occurs. Whether this is a random process or starts at the tip of the spinous processes and progresses until it ossifies all the cartilagenous tip of the spinous processes is not well

understood. It was then decided to start from a general point and establish a general trend and subsequently work on details. Generally it is assumed that the more mature animals have larger bones, more ossified cartilage, and tougher muscles. Therefore the more mature animals fall under lower USDA grading once evaluated by the USDA graders. Because the characteristics of the tissue (bone and muscle) differs from a less mature to a more beef carcasses, the characteristics of the ultrasound reflected signal also differs for those two groups of beef carcasses. Examining and comparing total area under the energy signal among the beef carcasses provided us with enough evidence that we could assume the carcasses categorized at higher grades had smaller areas under their energy signals. This trend would have been more distinct if the pool of animals came from a wider range of skeletal maturity.

Correlation analyses did not show any noticeable correlation between Tenderness and Intave and Lintave. The same was true about Flavor and Intave and Lintave. However, there was significant correlation between Ngrade and Intave as well as Lintave. The trend was that the higher the value of Ngrade the lower the Intave and Lintave values. This supports that as the skeletal maturity (as reflected by Intave and Lintave values) decreases the numerical value of quality grade increases.

Regression analyses indicated that Ngrade was the most important variable in describing Intave and Lintave. Adding Flavor to the regression model very slightly improved the relationship between Lintave (and Intave) and numerical value of quality grade. However, adding Tenderness did not. Although a relationship was established between Intave (Lintave) and Ngrade, this relationship was not very strong.

For future studies in determining an ultrasonic parameter to represent the skeletal maturity, following recommendations are suggested:

1) Data should be collected from a wider variety of animals. For example, the database used for this research study contained all the animals from "A" skeletal maturity. This does not provide a wide range for comparison of skeletal maturity among the beef carcasses. Inclusion of more "C", "D", and "E" skeletal maturity would provide enough variation in the amount of ossification which in turn effects the numerical grade value (Ngrade). It is

indeed with "C", "D", and "E" skeletal maturity beef carcasses that the most of ossification of spinous processes occur.

2) Animal selection should be done controlling the sex, age, weight and genetics of the beef cattle.
3) Physical dimensions of the cross section of 13^{th} thoracic vertebrae should be measured to improve the match of ultrasound RF reflected signals with the tissue composition.

REFERENCES

Agemura, D.H., Ultrasonic Propagation Properties of Canine Myocardium and Bovine Articular Cartilage at 100 MHz. M.S. Thesis, University of Illinois, 1986.

Agemura, D.H., O'Brien, W.D., "Ultrasonic Propagation Properties of Articular Cartilage at 100 MHz," J. Acoust. Soc. Am., vol. 87, no. 4. pp. 1786-1791, 1991.

Amin, V.R., Doerr, V.J., Arul, P.R., and Carlson, D.L., "Application of Neural Network in Ultrasound Tissue Characterization Using Backscattered Signal Parameters," IEEE Proceedings, pp. 1357-1359, 1993.

Anderson, B.B., Busk, H., Chadwick, J.P., Cuthbertson, A., Fursey, G.A.J., Jones, D.W., Lewin, P., Miles, C.A. and Owen, M.G. "Comparison of Ultrasonic Equipment for Describing Beef Carcass Characteristics in Live Cattle," Livest. Prod. Sci., vol. 10, p. 133, 1983.

Bamber, J.C., Fry, M.J., Hill, C.R., Dunn, F. "Ultrasonic Attenuation and Backscattering by Mammalian Organs as a Function of Time After Excision," Ultrasound Med. Biol. vol. 3, pp. 15-20, 1977.

Brethour, J.R., "Relationship of ultrasound speckle to marbling score in cattle," J. Anim. Sci., vol. 68, pp. 2603, 1990.

Brethour, J.R."Estimating Marbling Score in Live Cattle from Ultrasound Images Using Pattern Recognition and Neural Network Procedures," J. Anim. Sci., vol. 72, pp. 1425-1432, June 1994.

Chang, Y.K., Carlson, D.L. "Utility of the Backscattered Ultrasonic A-Mode Signal for the Quantitative Grading of Beef," ISA, pp. 49-55, 1991.

Cross, H.R. and Belk, K.E. "Objective Measurements of Carcass and Meat Quality," Meat Science, vol. 36, pp. 191-202, 1994.

Dunn, F., Goss, S., Johnston, R., "Comprehensive compilation of empirical ultrasonic properties of mammalian tissues," J. Acoust. Soc. Am., vol. 64, pp. 423-457, Aug 1978.

Dyce, K.M., Sack, W.O., & Wensing, C.J.G., Textbook of Veterinary Anatomy, Saunders Company, Philadelphia, PA, 1987.

Faulkner, D.B., Parret, D.F., McKeith, F.K. and Berger, L.L. "Prediction of Fat Cover and Carcass Composition from Live and Carcass Measurements," J. Anim. Sci., vol. 68, p. 604, 1990.

Ferguson, D.M. "Ultrasonic Evaluation: Ultrasonic Measurements and Their Relation to Composition," Proceedings of the Symposium Electronic Evaluation of Meat in Support of Value-Based Marketing. pp. 49-58, West Lafayette, Indiana, March 27-28, 1991.

Fields, S., Dunn, F. "Correlation of Echographic Visualizability of Tissue with Biological Compositions and Physiological State," J. Acoust. Soc. Am., vol. 54, pp. 809-812, 1973.

Fitzhugh, H.A., Jr., Talor, C.S., St. "Genetic Analysis of Degree of Maturity," J. Anim. Sci., vol. 33, no. 4, pp. 717-725, 1971.

Goss, S.A., O'Brien, Jr. W.D., "Direct Ultrasonic Velocity Measurements of Mammalian Collagen Threads," J. Acoust. Soc. Am., vol. 65, pp. 507-511, 1979.

Green, R.D., Perkins, T.L., Hamlin, K.E., Fish, E.B., "Quality grade classification of feedlot cattle by video image analysis of ultrasound ribeye measurements," J. Anim. Sci., vol. 69(Suppl. 1), pp. 480, 1991.

Greenleaf, J.F. Tissue Characterization with Ultrasound, vol. I, CRC Press, Boca Raton, FL., 1986.

Guittet, C., Ossant, F., Remenieras, J.P., Pourcelot, L., Berson, M. "Ultrasonic Tissue Characterization for the Backscattering Estimation of the Attenuation Coefficient at High Frequencies: 20-100 MHz," IEEE Ultrasonics Symposium, pp. 1081-1084, 1996.

Hamlin, K.E., Green, R.D., Perkins, T.L., Cundiff, L.V., Miller, M.F. "Real-Time Ultrasonic Measurement of Fat Thickness and Longissimus Muscle Area: I. Description of Age and Weight Effects," J. Anim. Sci., vol. 73, pp. 1713-1724, 1995.

Haney, M.J., O'Brien, W. D., Jr. "Temperature Dependency of Ultrasonic Propagation Properties in Biological Materials," In Tissue Characterization with Ultrasound, vol. I, pp. 15-55, 1986.

Hazel, L.N., Kline, E.A. "Ultrasonic Measurement of Fatness in Swine," J. Anim. Sci., vol. 18, p. 815-819, 1959.

Hein, I.A., Novokofski, J.A., and O'Brien, W.D., Jr. Ultrasound Data Acquisition System Design for Collecting High Quality RF Data from Beef Carcasses in the Slaughter House Environment. IEEE Ultrasonics Symposium Proceedings, Tuscon, AZ., pp. 1039-1045, 1992.

Kinsler, L.E., Frey, A.R., Coppens, A.B., and Sanders, J.V. Fundamentals of Acoustics, 3rd Edition, John Wiley & Sons, 1982.

Kitamura, K., Pan, H., Ueha, S., Kimura, S., and Ohtomo, N. "Characterization of Bone Tissue by Analysis of the Ultrasonic Waves Scattered Around Cancellous bone," IEEE Ultrasonics Symposium, pp. 1119-1122, 1996.

Linzer, M., Parks, S.I.., Norton, S.J., Higgins, F.P., Dietz, D.R., Shideler, R.W., Shawker, T.H., Doppman, J.L.. "Comprehensive Ultrasonic Tissue Analysis system," In M. Linzer: Ultrasonic Tissue Characterization II, National Bureau of Standards Special publication 525, Washington, DC, US Government Printing Office, pp. 255-260, 1979.

Mariweb, E.N. Human Anatomy and Physiology, The Benjamin/Cummings Publishing Company, Redwood City, CA., 1989.

McLaren, D.G., McKeith, F.K. and Novakofski, J. "Prediction of Carcass Characteristics at Market Weight from Serial Real-Time Ultrasound Measures of Backfat and Loin Eye area in the Growing Pig," J. Anim. Sci., vol. 67, pp. 1657-1667, 1989.

McLaren, D.G., Novakofski, J., Parrett, D.F., Lo, L.L., Singh, S.D., Neumann, K.R. and McKeith, F.K. "A Study of Operator Effects on Ultrasonic Measures of Fat Depth and Longissimus Muscle Area in Cattle, Sheep and Pigs," J. Anim. Sci., vol. 69(1), pp. 54-66, 1990.

Meat Evaluation Handbook, National Live Stock and Meat Board, Chicago, IL, 1988.

Mello, F.C., Jr., Field, R.A., Riley, M.L. "Effect of Age and Anatomical Location on Composition of Bovine Bone," J. Food Sci., vol. 43, pp. 677-679, 1978.

Miles, C.A., Fisher, A.V., Fursey, G.A.J. and Page, S.J. "Estimating Beef Carcass Composition Using the Speed of Ultrasound," Meat Sci., vol. 21, p. 175-188, 1987.

Miles, C.A., Fursey, G.A.J., Page, S.J. and Fisher, A.V. "Progress Towards Using the Speed of Ultrasound for Beef Leanness Classification," Meat Sci., vol. 28, pp.19-130, 1990.

O'Brien, Jr., W.D., Erdman, Jr., J.W., Hebner, Tammy B. "Ultrasonic Propagation Properties (@ 100 MHz) in Excessively Fatty Rat Liver," J. Acoust. Soc. Am., vol. 83, no. 3, pp. 1159-1166, March 1988.

Official United States Standards for Grades of Carcass Beef, (Title 7,ch.1, pt.54, sections 54.102-54.107 of the CFR), 1997.

Parrish, Jr., F.C., Animal Science, Introductory Meats, Laboratory Manual. Paladin House, Lake Geneva, WI, 1994.

Patel, A., Amin R., Wilson D., Rouse B. "Beef quality grading using ultrasound signal processing," Proceedings of the 5th International Conference on Signal Processing Applications and Technology, vol. 2, 7 refs, pp. 1529-34, 1994.

Perry T C., Ainslie S.J., Traxler M.J., Fox D.J., and Stouffer J.R. "Uses of real-time and attenuation ultrasonic measurements to determine backfat thickness, rib eye area, carcass marbling and yield grade in live cattle," J. Anim. Sci., vol. 68, pp. 337, 1990.

Roberjot, V., Laugier, P., Droin, P., Giat, P., Berger G. "Measurement of Integrated Backscatter Coefficient of Trabecular Bone," IEEE Ultrasonics Symposium, pp. 1123-1126, 1996.

Robinson, D.E., Chen, F. and Wilson, L.S. "Measurement of Velocity of Propagation from Ultrasonic Pulse-Echo Data," Ultrasound in Med & Biol, vol. 4, pp. 413-420, 1982.

Scheer, R.L. "Computation of Acoustic Backscatter and Attenuation Coefficients in Muscle Tissue Utilizing a Reference Phantom," M.S. Thesis, University of Illinois, 1989.

Shackelford, S.D., Koohmaraie, M., Wheeler, T.L. "Effects of Slaughter Age on Meat Tenderness and USDA Carcass Maturity Scores of Beef Females," J. Anim. Sci., vol 73, pp. 3304-3309, 1995.

Shung, K.K., Smith, M.B., Tsu, B. Principals of Medical Imaging, Academic Press, 1992.

Sigelmann, R.A. and Reid, J.M. "Analysis and Measurement of Ultrasound Backscattering form an Ensemble of Scatterers Excited by Sine-Wave Bursts," J. Acoust. Soc. Am., vol. 53, pp. 1351-1355, 1973.

Smith, M.T., Oltjen, J.W., Dolezal, H.G., Gill, D.R., and Behrens, B.D. J. Anim. Sci., vol. 70, p. 29, 1992.

Stouffer, J.R., Vallentine, M.V. and Wellington, G.H. "Ultrasonic Measurements of Fat Thickness and Loin Eye Area on Live Cattle and Hogs," J. Anim. Sci, vol. 18, p. 1483, 1959.

Whittaker, A.D., Park, B., Thane, B.R., Miller, R.K., Savell, J.W., "Principles of ultrasound and measurement of intramuscular fat," J. Anim. Sci., vol. 70, pp. 942, 1992.

APPENDIX A

Table 1

Guidelines for Determining the Skeletal Maturity (Adapted from Burson)

Maturity	Age	Ossification measures	
		Lumbar vertebrae	Thoracic vertebrae
A	9-30 months	Cartilage nearly completely ossified	No to slight ossification
B	30-42 months	Nearly to completely ossified	Partial to moderate Ossification (10-25% ossified)
C	42-72 months	Complete ossification	Moderate to considerable Ossification (30-70%)
D	72-96 months	Complete ossification	Considerable ossification (70-100%)
E	Over 96 months	Complete ossification	Complete ossification

Table 2. Example of final quality grading (From Burson, University of Nebraska Extension Meat Specialist, Publication #357)

Example	Maturity	Marbling	Grade	Minimum Marbling For Grade	Excess Marbling	Marbling Level Adjustment	Quality Grade
1	A 70	Abund 40	Prime	Slightly Abundant 0	240	240/3	Prime 80
2	B 50	Modest 70	Choice	Slightly Modest 50	120	120/3	Choice 40
3	C 50	Slight 60	Utility	Partially Devoid 50	210	210/3	Utility 70
4	D 20	Traces 20	Utility	Traces 20	0	0/3	Utility 0
5	E 50	Moderate 50	Commercial	Moderate 50	0	0/3	Comercial 0

Table 3

Attenuation Coefficient and Velocity for Different Tissue Types (Adapted from Comprehensive Compilation of Empirical Ultrasonic Properties of Mammalian Tissues, Dunn et., 1978)

Tissue	Attentuation (dB/cm) (at ~ 1 MHz)	Speed of sound (m/sec)
Blood	0.019	1566
Fat	0.07	1467
Testis	0.07	—
Brain	0.09	1551
Liver	0.099	1578
Muscle	0.15	1566
Skin	0.24	1720
Tendon	0.45	1750
Cartilage	0.58	1665
Bone	1.61	3445

Table 4. Correlation among selected variables (Analysis 1)
(N = 98)

	T	F	N	I
Tenderness(T)	1[1]			
Flavor(F)	0.12[1]	1		
Ngrade(N)	0.11[1]	0.17[1]	1	
Intave(I)	-0.02[1]	0.09[1]	-0.14[1]	1

1- Correlation Coefficient (r-value)

Table 5. Regression analysis of Intave by selected independent variables (Analysis 1)

(N = 98)

	Equation 21 Coefficient (t-Ratio)	Equation 22 Coefficient (t-Ratio)	Equation 23 Coefficient (t-Ratio)
Tenderness	-378.3 (-0.16)		
Flavor	5534.6 (1.24)	5462.9 (1.24)	
Ngrade	-79.9 (-1.52)*	-80.66 (-1.54)*	-69.38 (-1.35)*

*Significant at the level of < 0.2

Table 6. Correlation among selected variables (Analysis 2)
(N = 98)

	F	T	N	L
Tenderness(T)	1[1]			
Flavor(F)	0.12[1]	1		
Ngrade(N)	0.17[1]	0.11[1]	1	
Lntave(L)	-0.01[1]	0.03[1]	-0.197[1]	1

1- Correlation Coefficient (r-value)

Table 7. Regression analysis of Lintave by selected independent variables (Analysis 2) (N = 98)

	Equation 25 Coefficient (t-Ratio)	Equation 26 Coefficient (t-Ratio)	Equation 27 Coefficient (t-Ratio)
Tenderness	-0.009 (-0.16)		
Flavor	0.05 (0.49)	0.05 (0.48)	
Ngrade	-0.003 (-1.98)*	-0.003 (-2.02)*	-0.002 (-1.97)*

*Significant at the level of < 0.05

Table 9. Regression analysis of Lintave by selected independent variables (Analysis 3) (N = 91)

	Equation 25 Coefficient (t-Ratio)	Equation 26 Coefficient (t-Ratio)	Equation 27 Coefficient (t-Ratio)
Tenderness	-0.014 (-0.23)		
Flavor	0.08 (0.7)	0.085 (0.73)	
Ngrade	-0.004 (-2.13)*	-0.004 (-2.13)*	-0.003 (-2.02)*

*Significant at the level of < 0.05

Table 10. Correlation among selected variables (Analysis 4)
(N = 98)

	F	T	N	L
Flavor(F)	1[1]			
Tenderness(T)	0.12[1]	1		
Ngrade(N)	0.18[1]	0.10[1]	1	
Lntave(L)	-0.11[1]	0.06[1]	-0.16[1]	1

1- Correlation Coefficient (r-value)

Table 11. Regression analysis of Lintave by selected independent variables (Analysis 4) (N = 98)

	Equation 25 Coefficient (t-Ratio)	Equation 26 Coefficient (t-Ratio)	Equation 27 Coefficient (t-Ratio)
Tenderness	-0.012 (-0.22)		
Flavor	0.044 (0.40)	0.04 (0.39)	
Ngrade	-0.001 (-1.39)	-0.001 (-1.4)*	-0.001 (-1.38)*

*Significant at the level of < 0.2

APPENDIX B

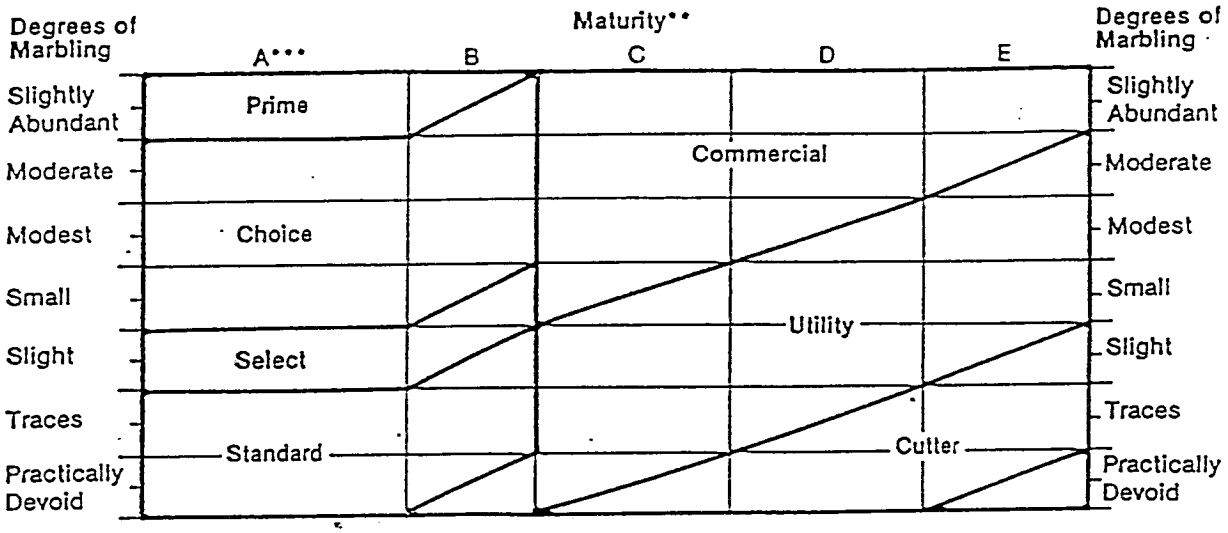

**Maturity increases from left to right (A through E).
***The A maturity portion of the Figure is the only portion applicable to bullock carcasses.

Figure 1. Relationship between marbling, maturity, and carcass quality grade (From Official United States Standards for Grades of Carcass Beef, 1997)

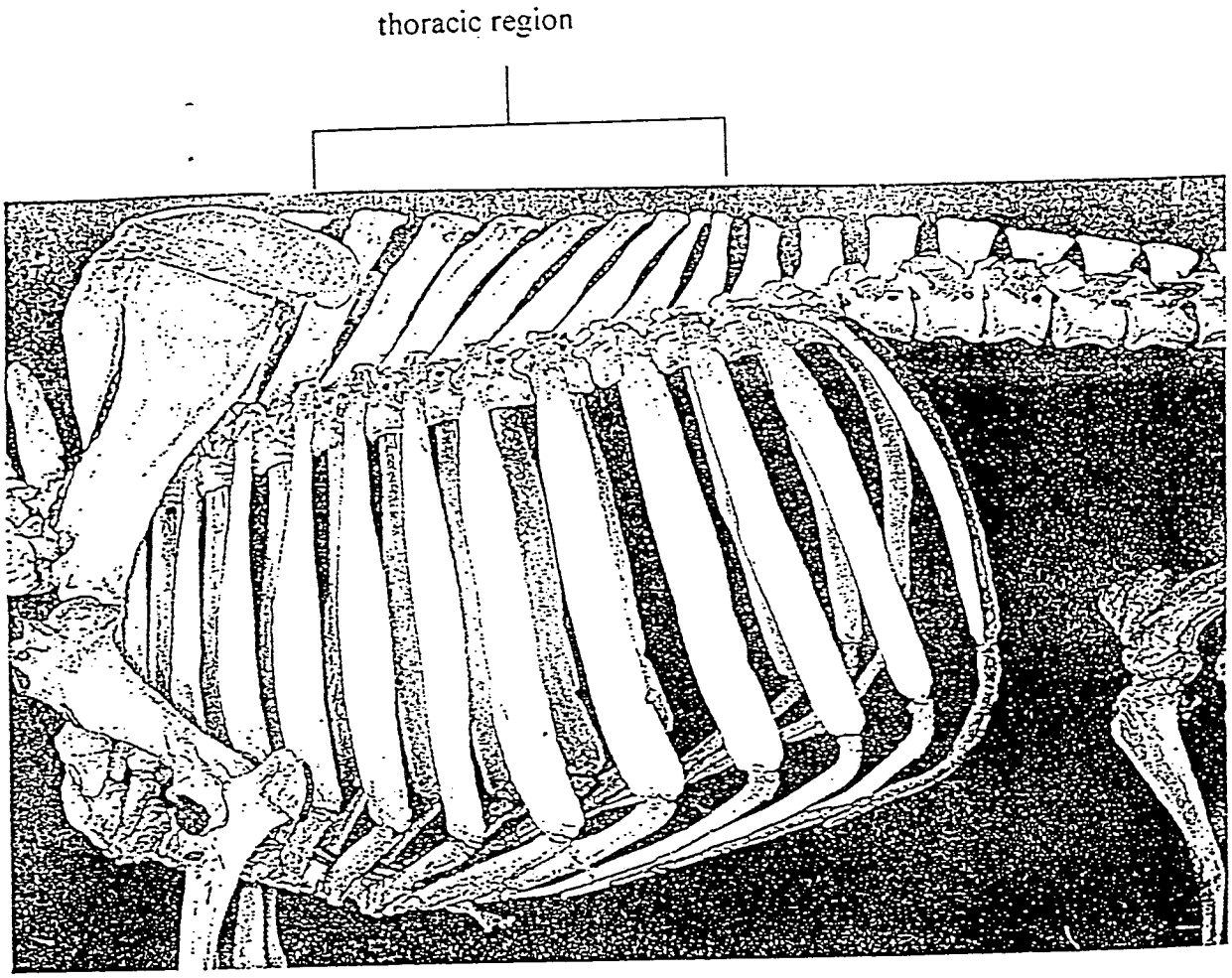

Figure 2.a. Textbook drawing of thoracic and lumbar region (From Textbook of Veterinary Anatomy, Dyce et al., 1987)

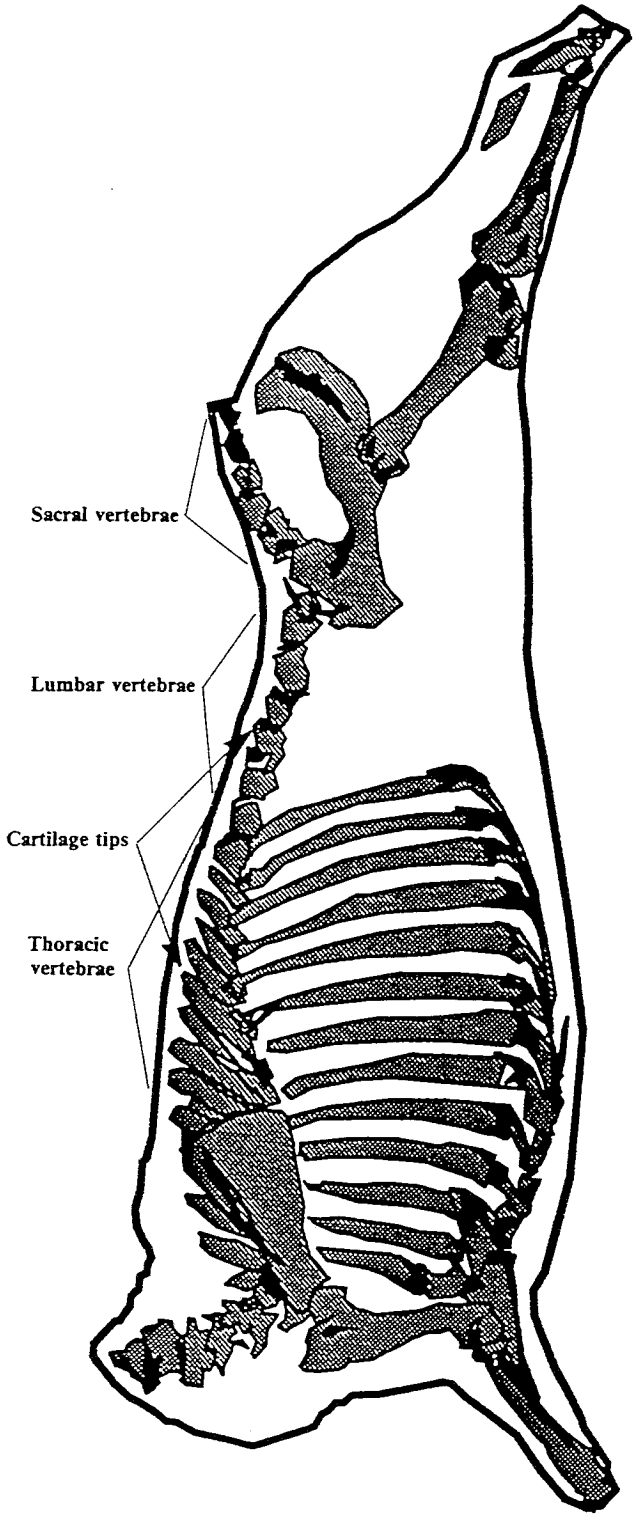

Figure 2.b. Location of cartilage and vertebrae for determination of maturity (From Cooperative Extension Services of Illinois)

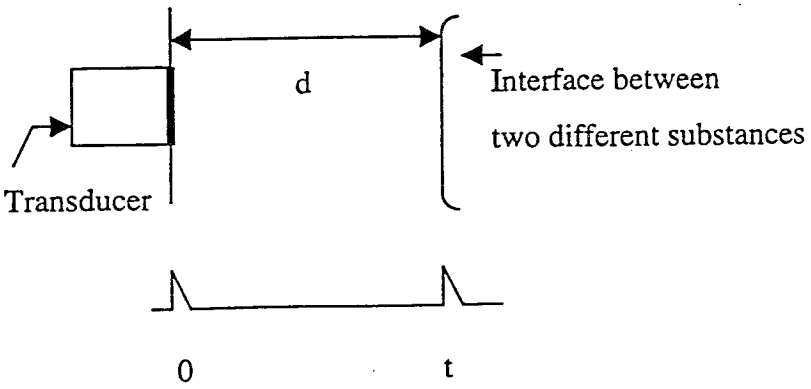

Figure 3. Illustration of "range equation"

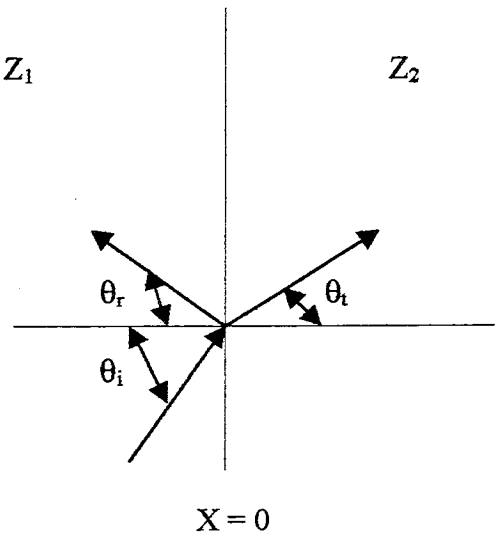

Figure 4. Oblique incidence of a plane wave.

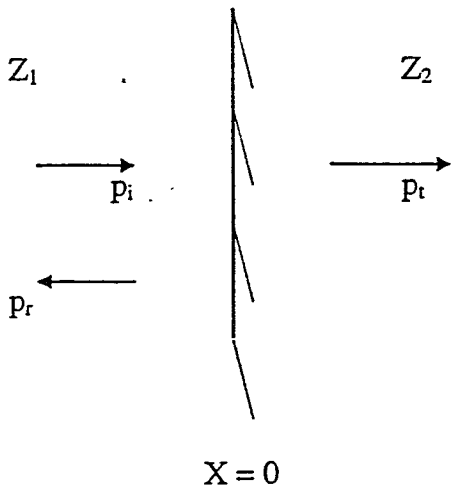

Figure 5. Reflection & transmission of plane wave normally incident

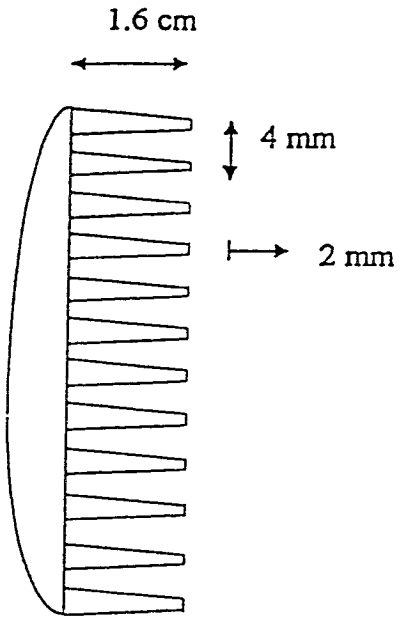

Figure 6. Diagram of the plastic comb

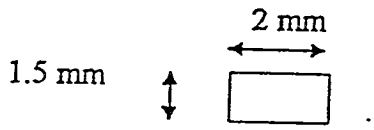

Figure 7.a. Cross section of the comb tooth

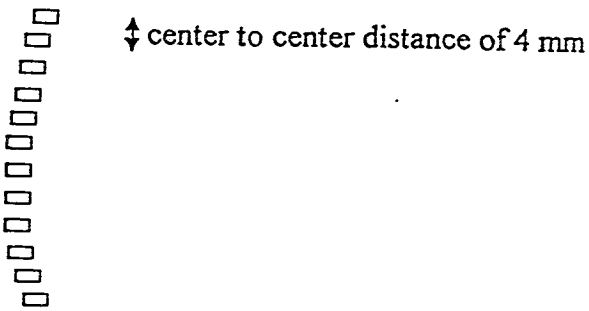

Figure 7.b. Schematic of tip of comb teeth

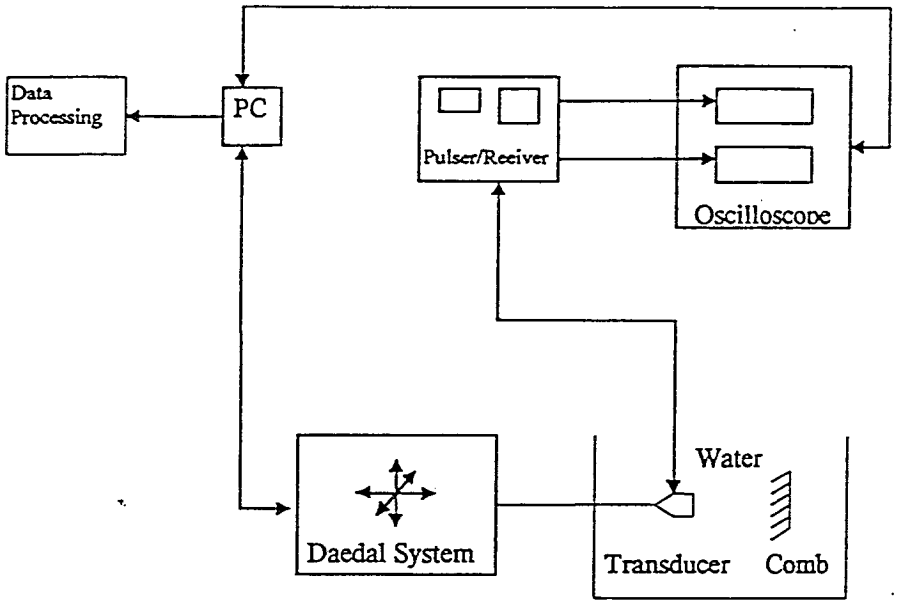

Figure 8.a. Block diagram of the main system component

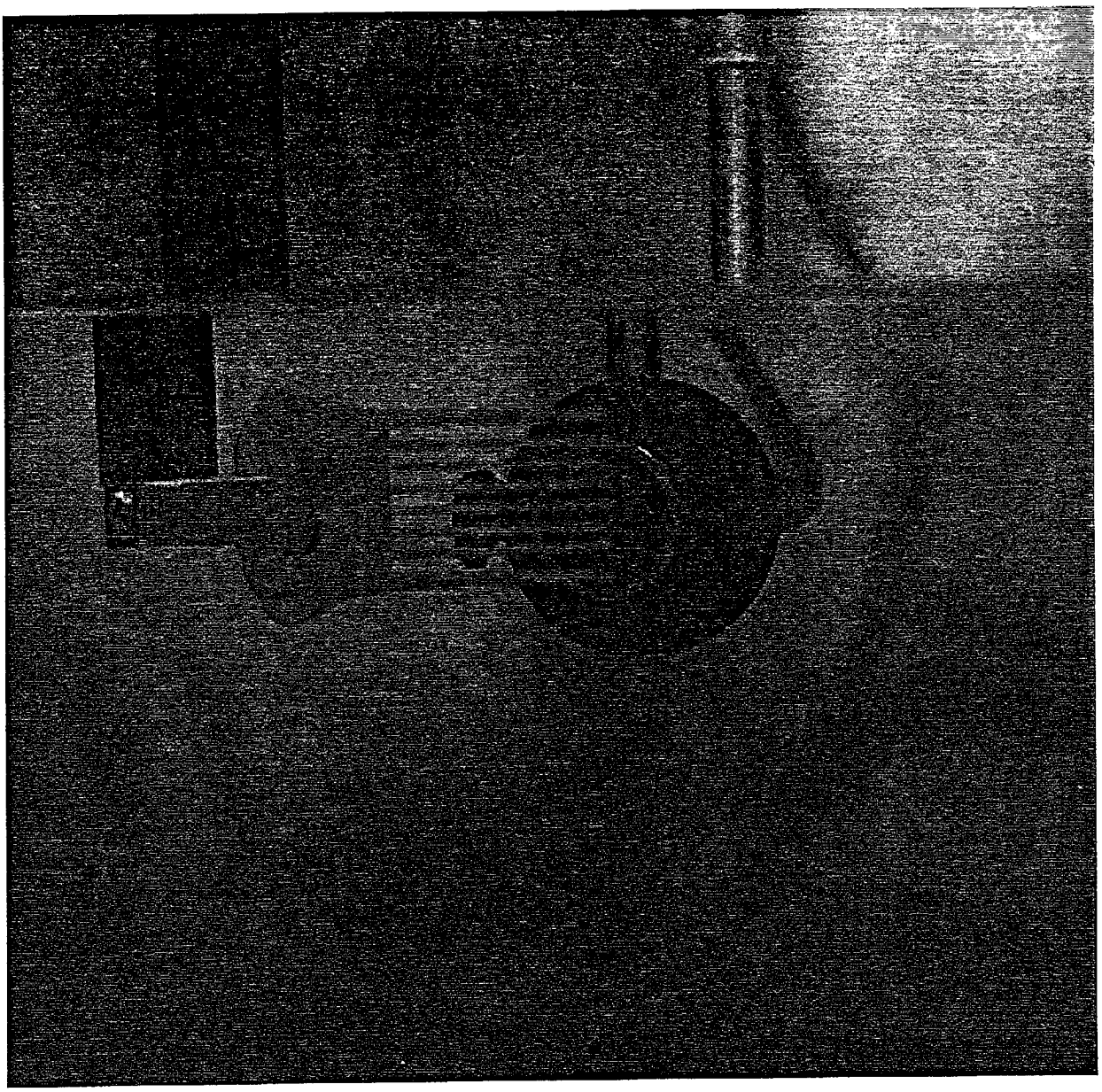

Figure 8.b. Photograph of comb position with respect to the transducer

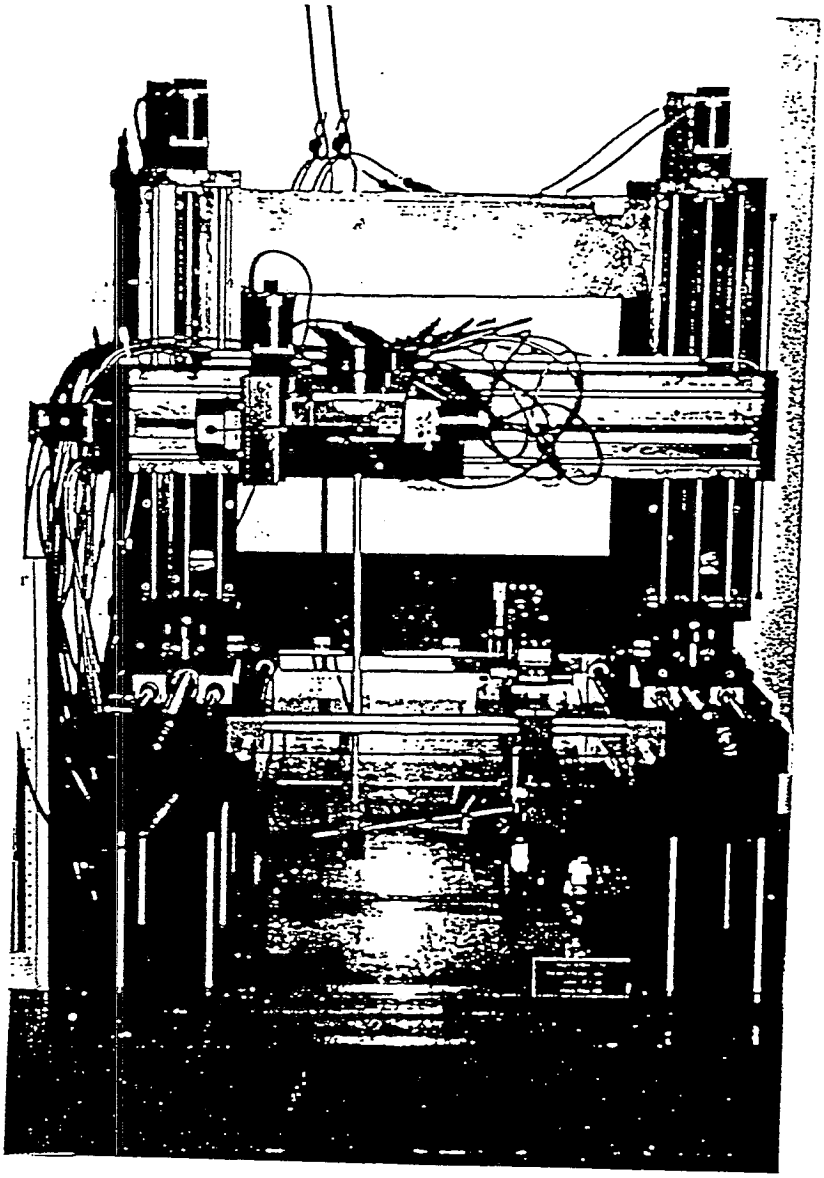

Figure 9. Photograph of the Daedal MC2000 Controller and MD23/ MD34 Motor / drive system

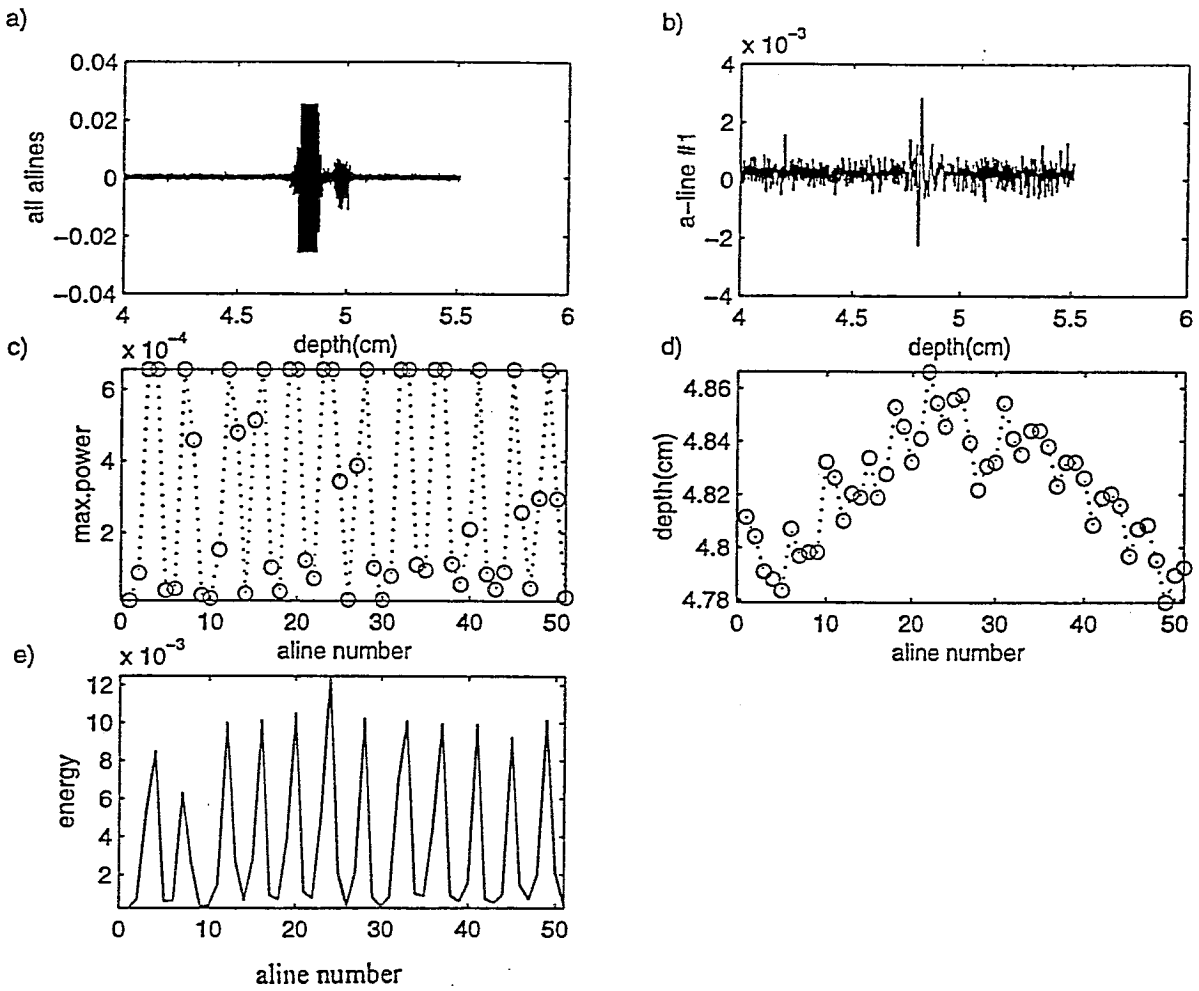

Figure 10. Five graphs generated by program "puscan" for the experimental object, a comb., (a) All 51 RF signals versus the distance from the transducer to the comb (b) One typical RF signal versus the difference from the transducer to the comb (c) Maximum power for 51 RF signals. (d) The location of maximum power for all RF signals. (e) The integral of area under the power signal (called energy)

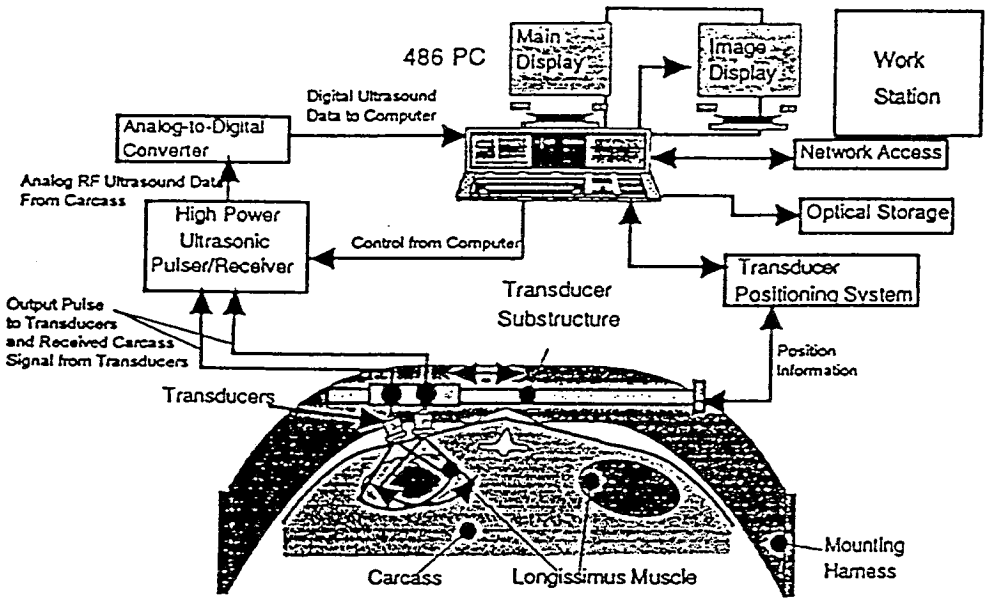

Figure 11: Overall design of BUGS system (From Hein et al., 1992)

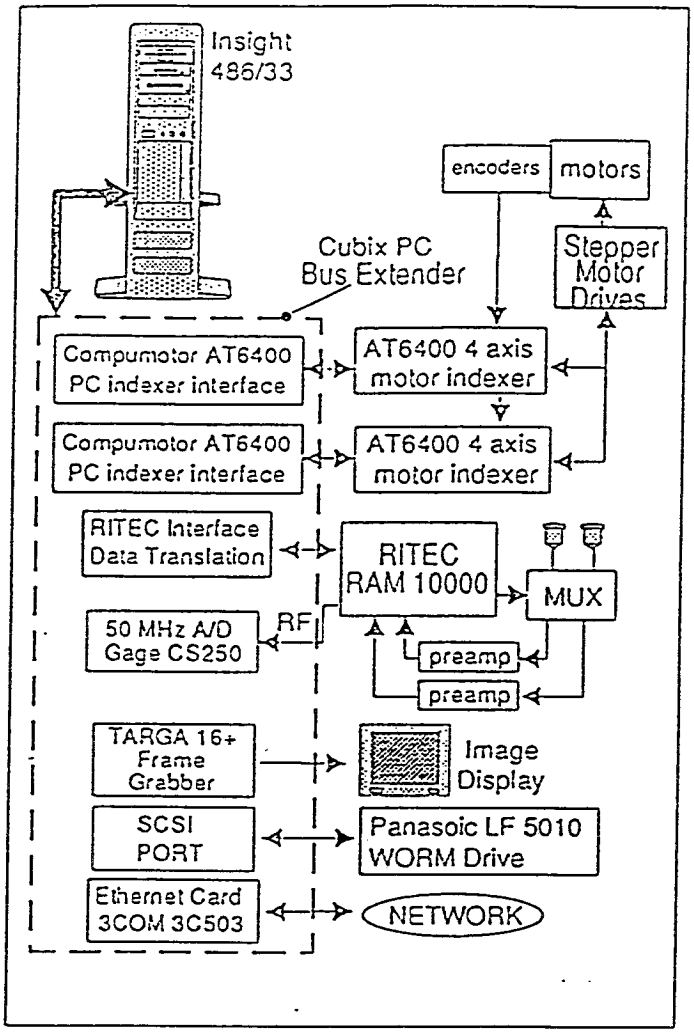

Figure 12: BUGS electronic system (From Hein et al., 1992)

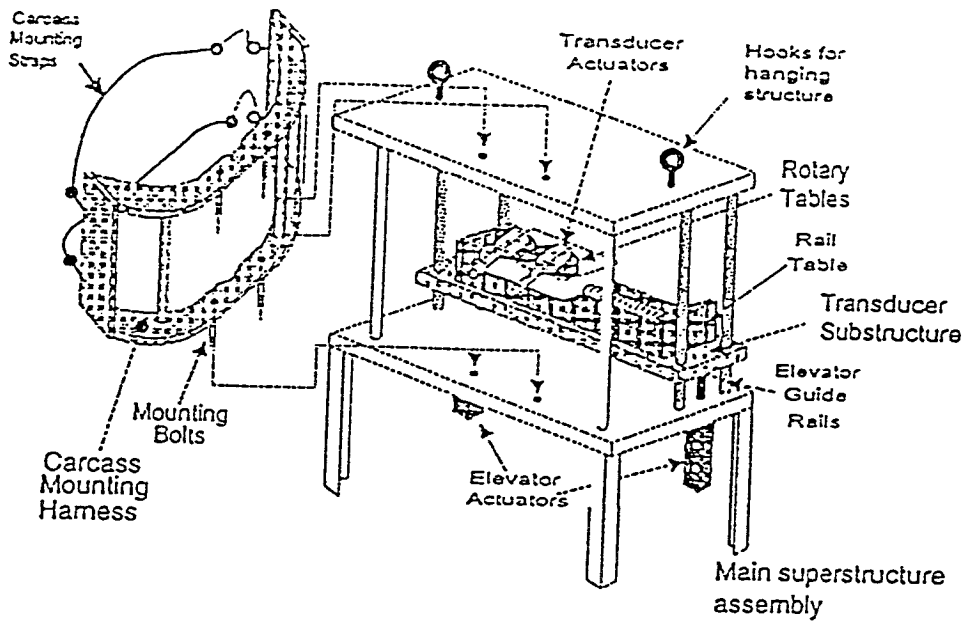

Figure 13: BUGS scanning table superstructure (From Hein et al., 1992)

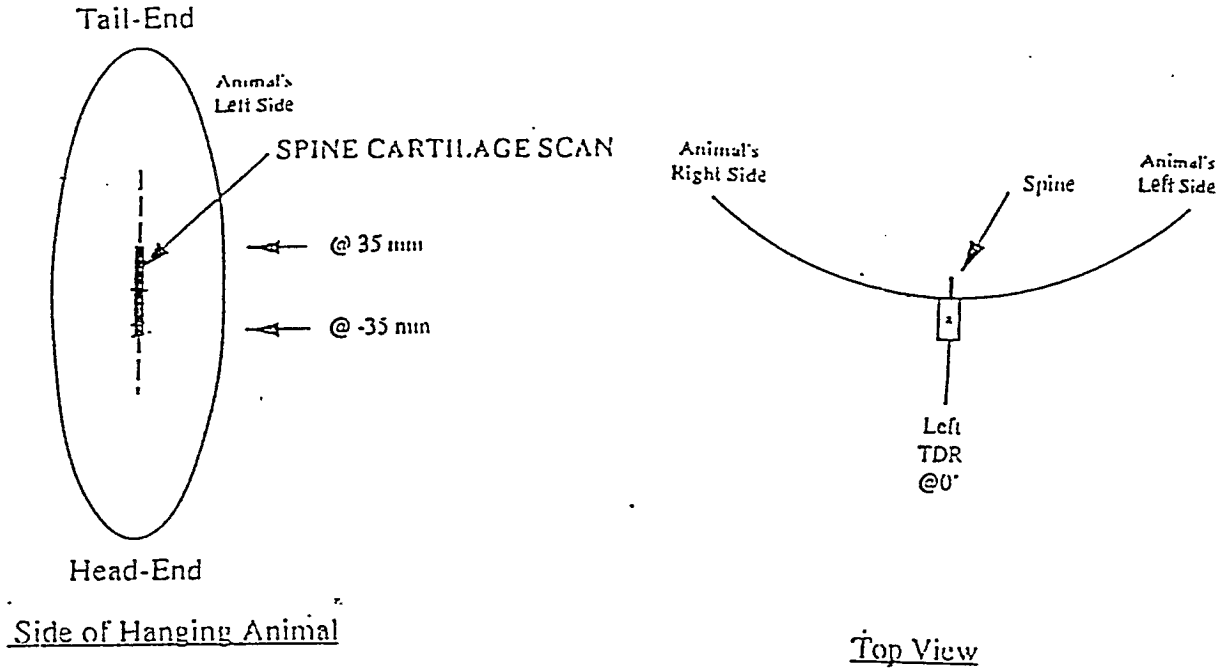

Figure 14: Spine cartilage scan

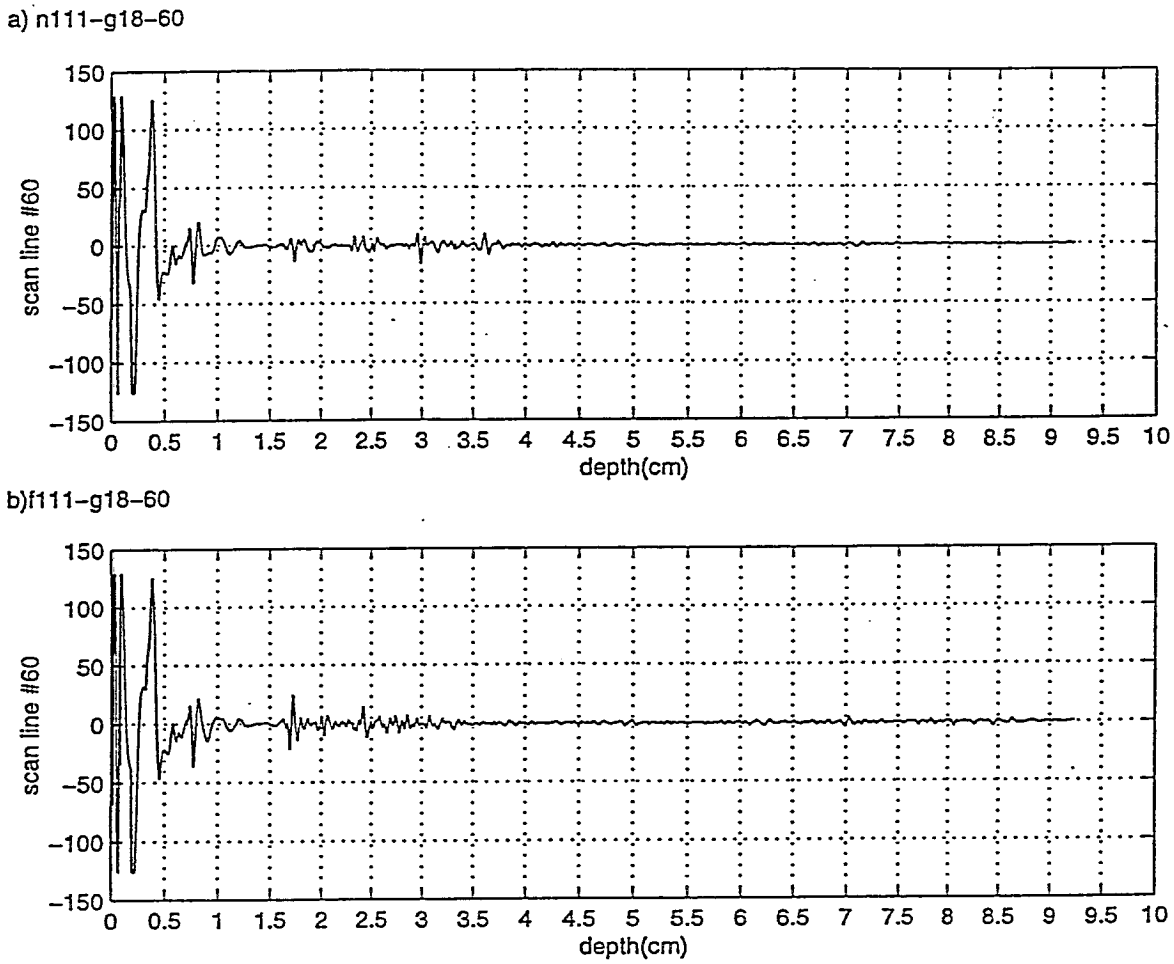

Figure 15. Comparison of hide-on and hide-off scan lines (a) Animal #111, hide-on, gain setting of 18, scan line 60 (b) Animal #111, hide-off, gain setting of 18, scan line 60. The first centimeter on both (a) and (b) registers signals from within the transducer standoff. The analysis is performed on data from 1 and 4 cm to ensure that the fat/spine boundary is always included.

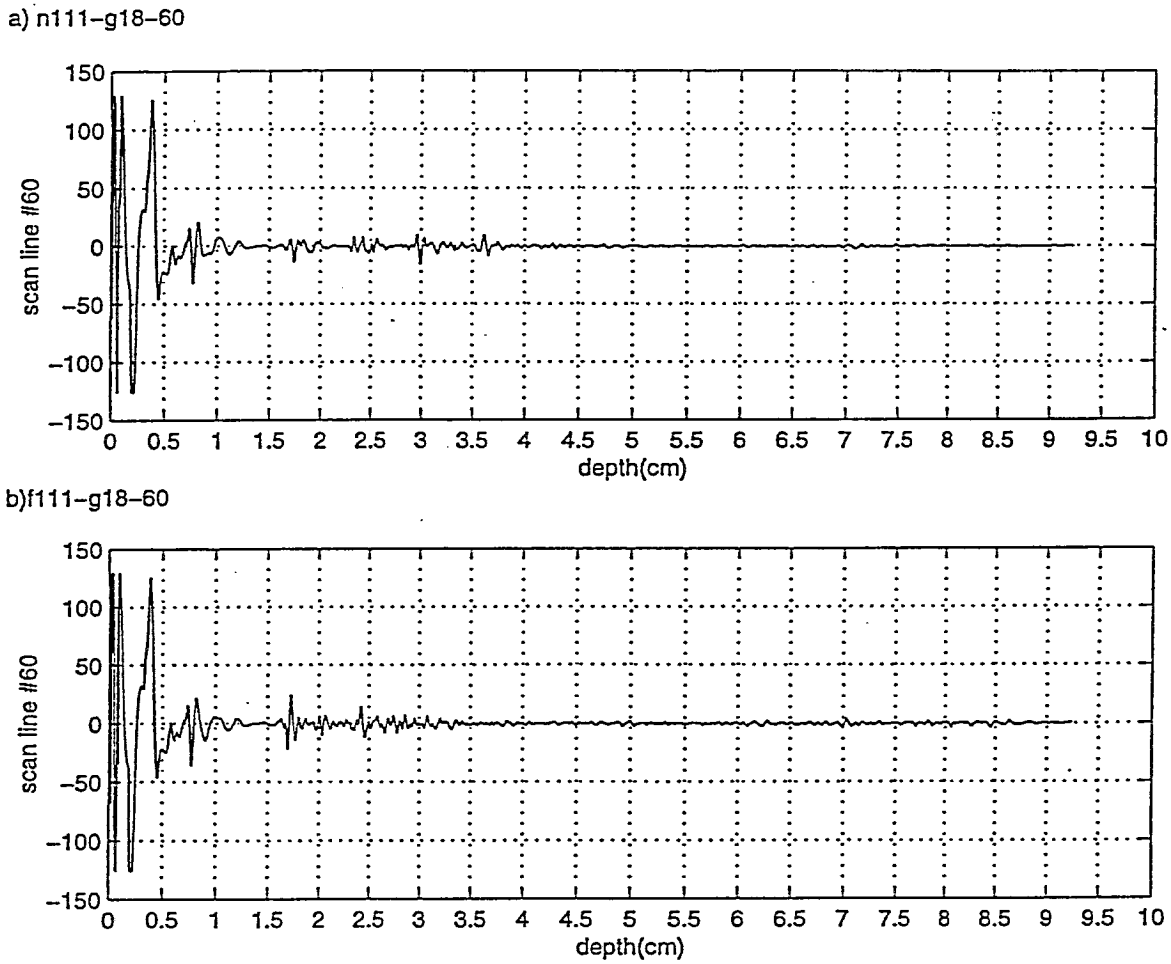

Figure 15. Comparison of hide-on and hide-off scan lines (a) Animal #111, hide-on, gain setting of 18, scan line 60 (b) Animal #111, hide-off, gain setting of 18, scan line 60. The first centimeter on both (a) and (b) registers signals from within the transducer standoff. The analysis is performed on data from 1 and 4 cm to ensure that the fat/spine boundary is always included.

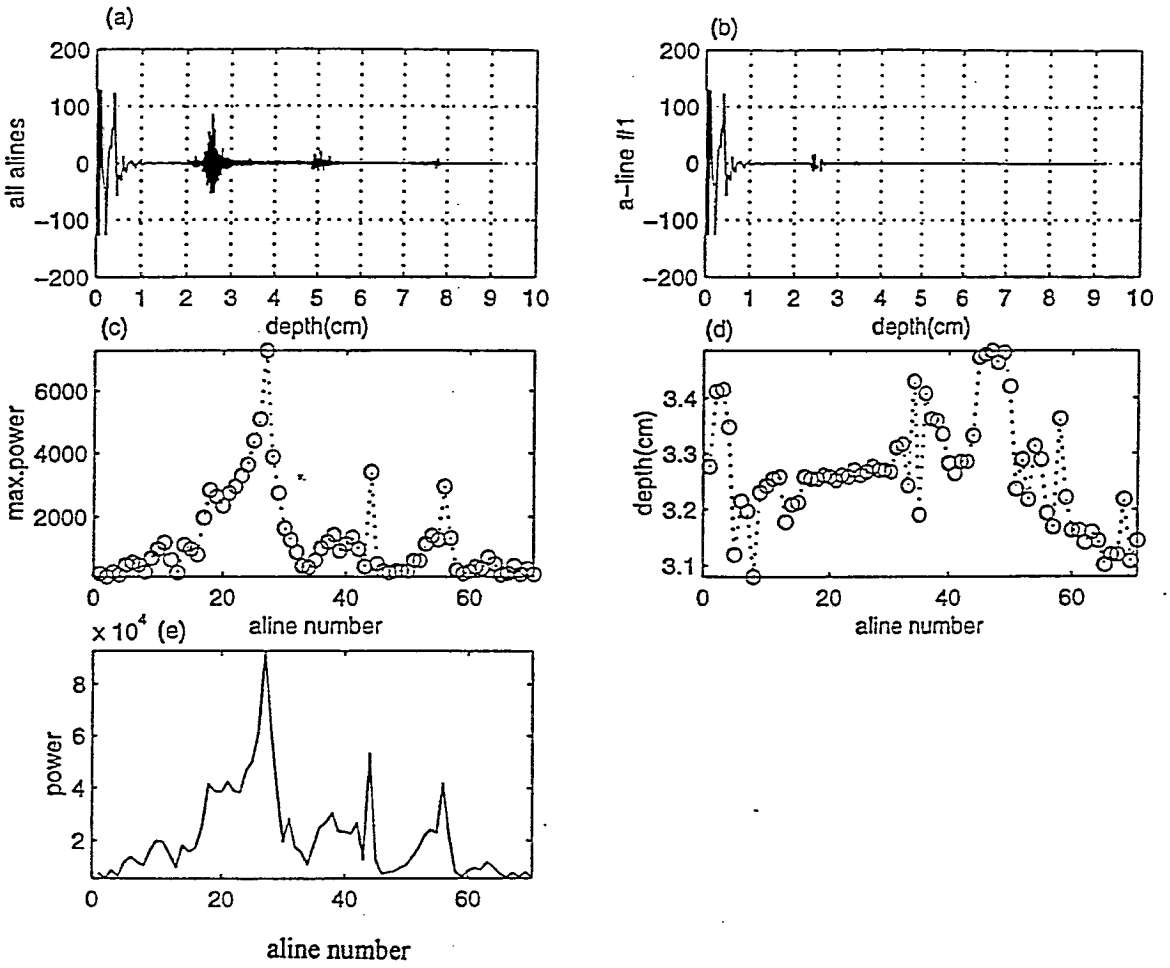

Figure 16. Five graphs generated by program "ascan" for animal #28, hide-off. (a) All 71 RF signals versus the distance from the transducer to the spine. (b) One typical RF signal versus the difference from the transducer to the spine. (c) Maximum power for 71 RF signals. (d) The location of maximum power for all RF signals. (e) The integral of area under the power signal (called energy)

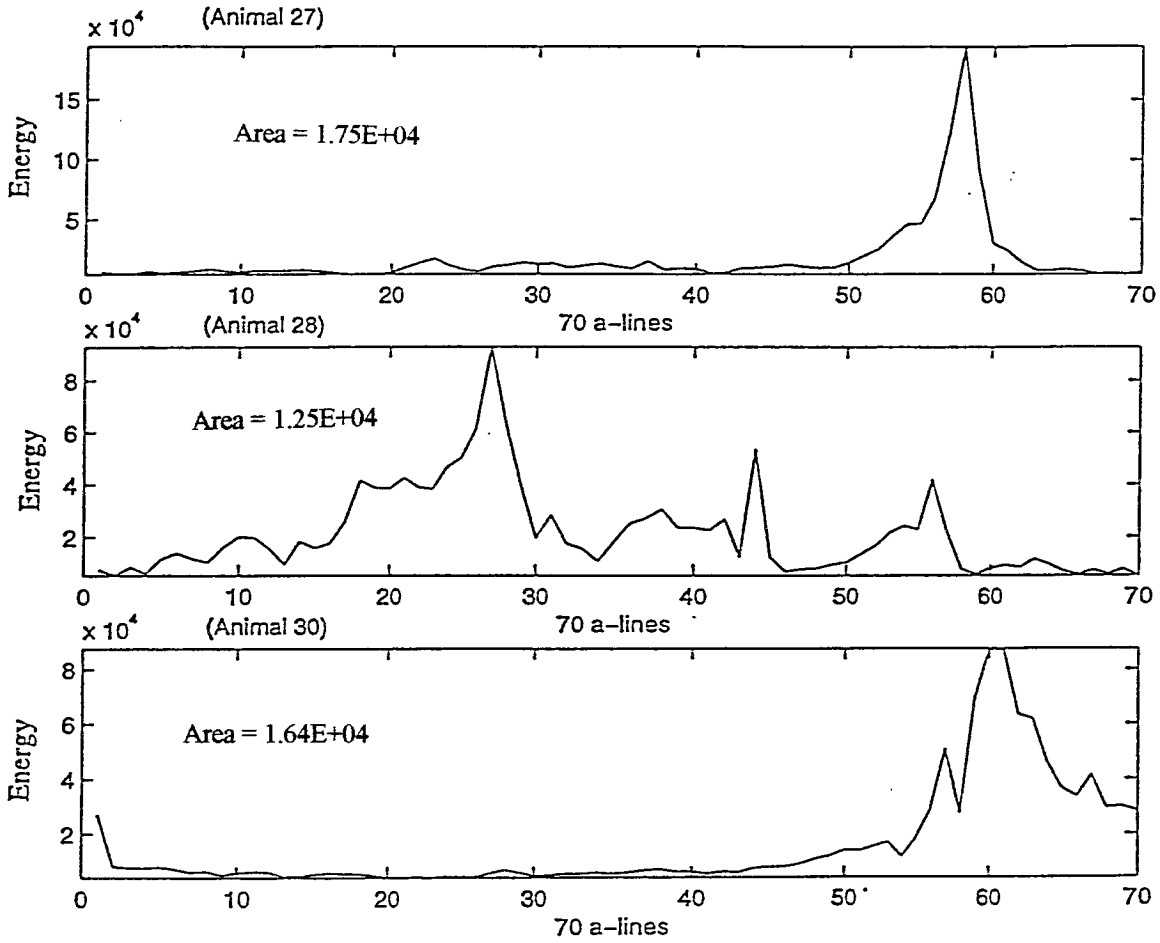

Figure 17. Comparison of area under the power signal (called energy) for animals 27, 28 and 30.

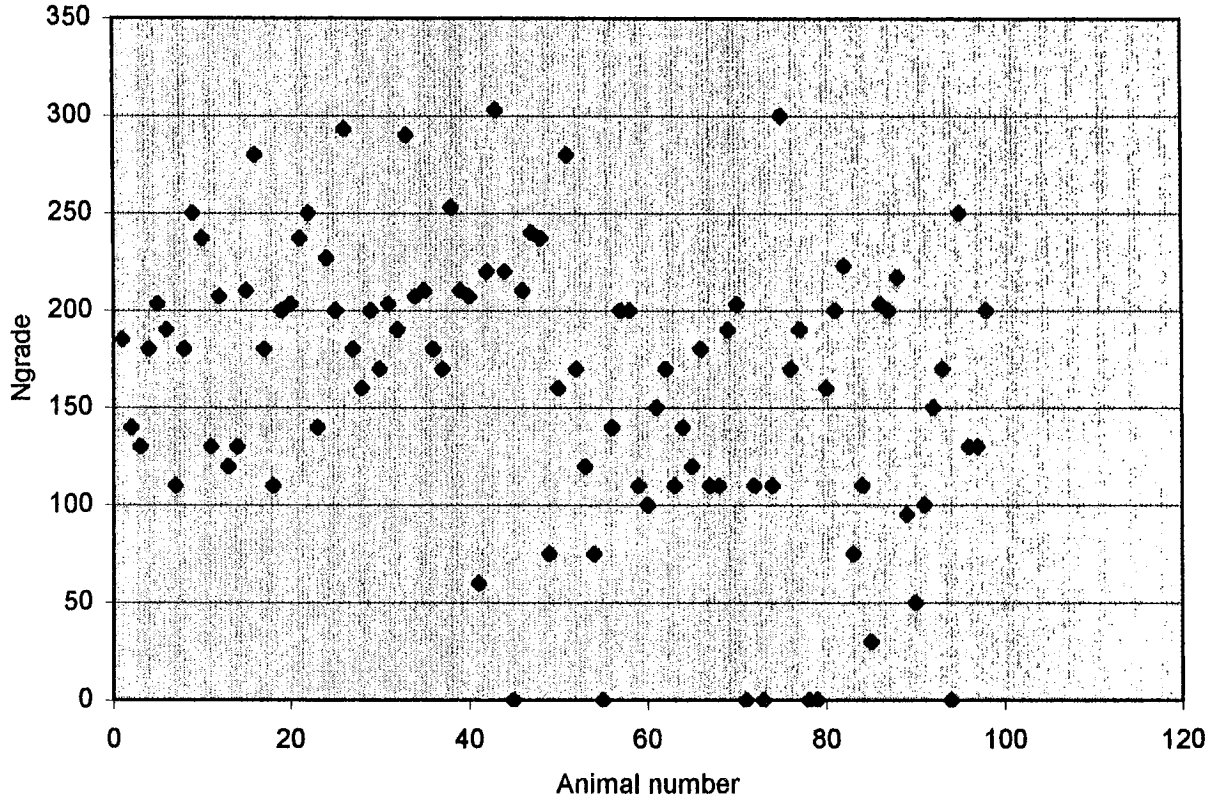

Figure 18. Distribution of Ngrade

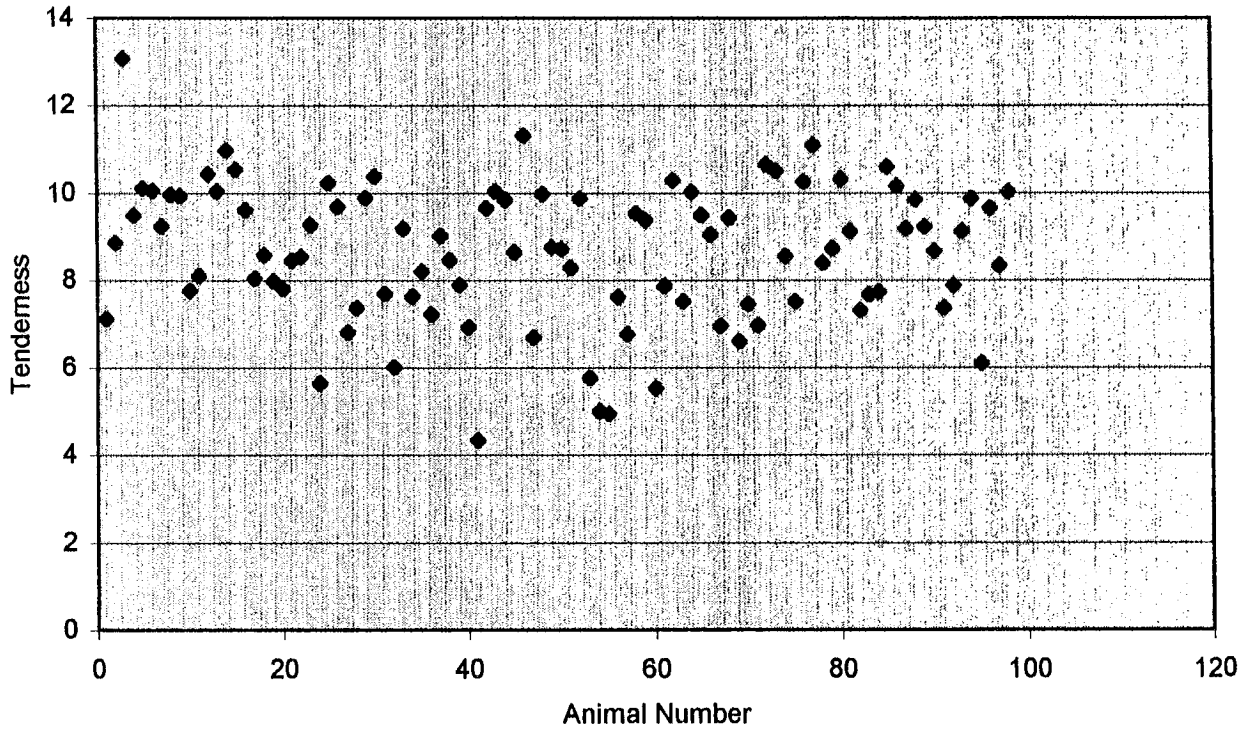

Figure 19. Distribution of Tenderness

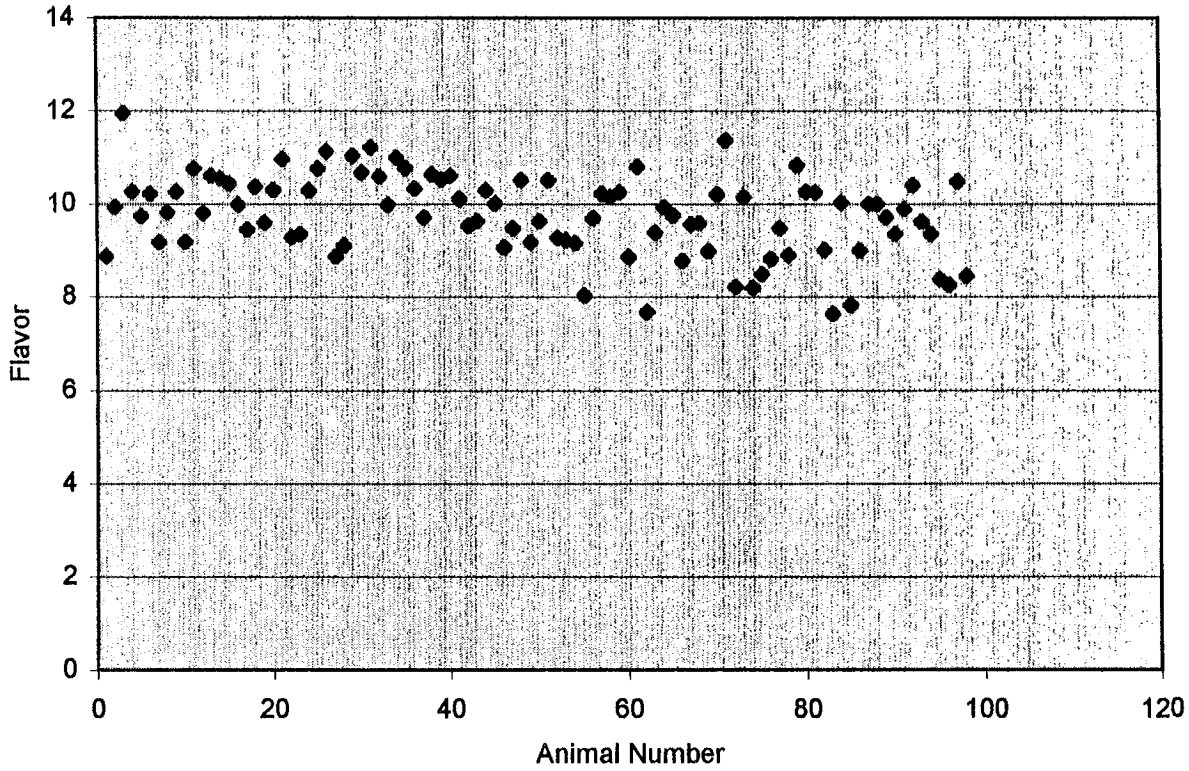

Figure 20. Distribution of Flavor

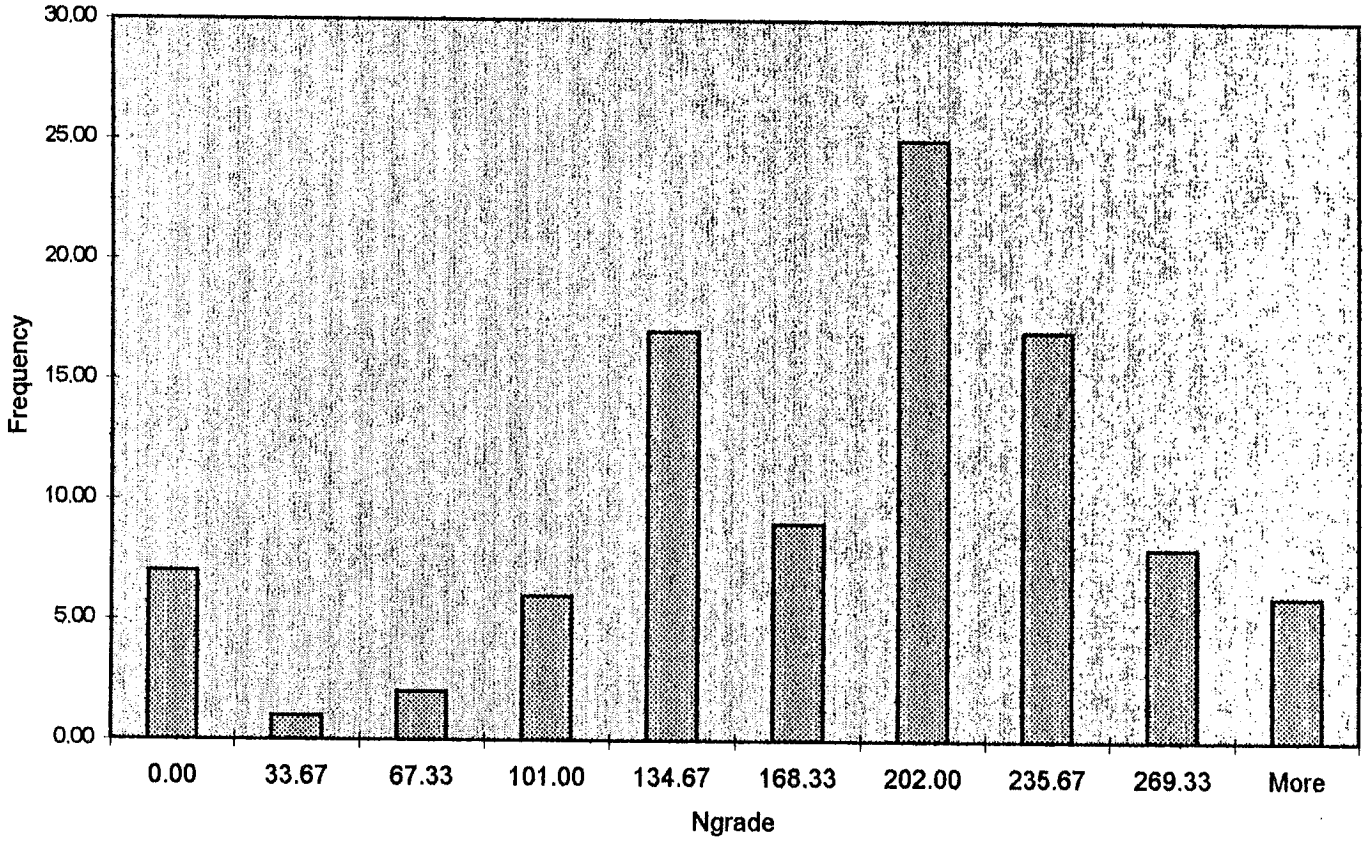

Figure 21. Ngrade Histogram

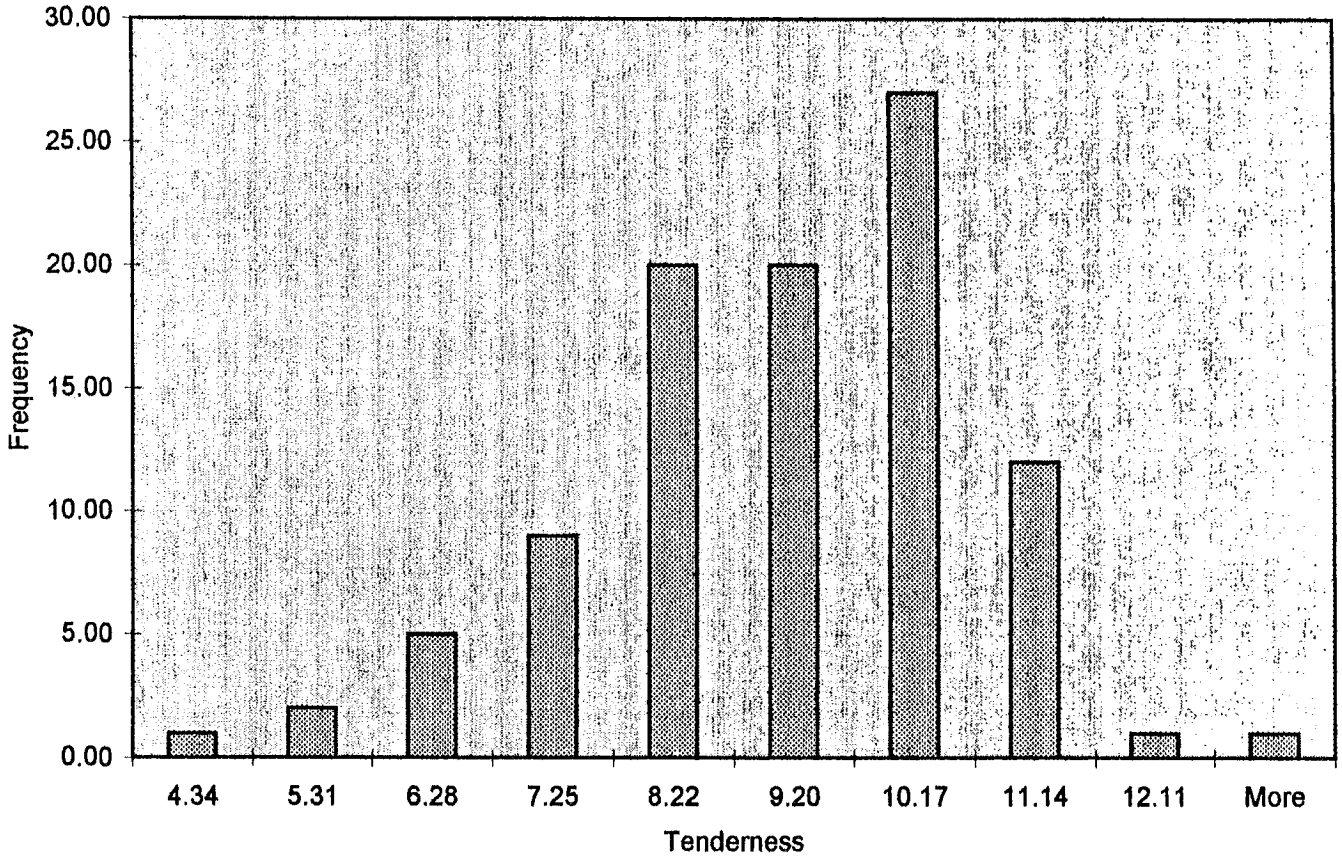

Figure 22. Tenderness Histogram

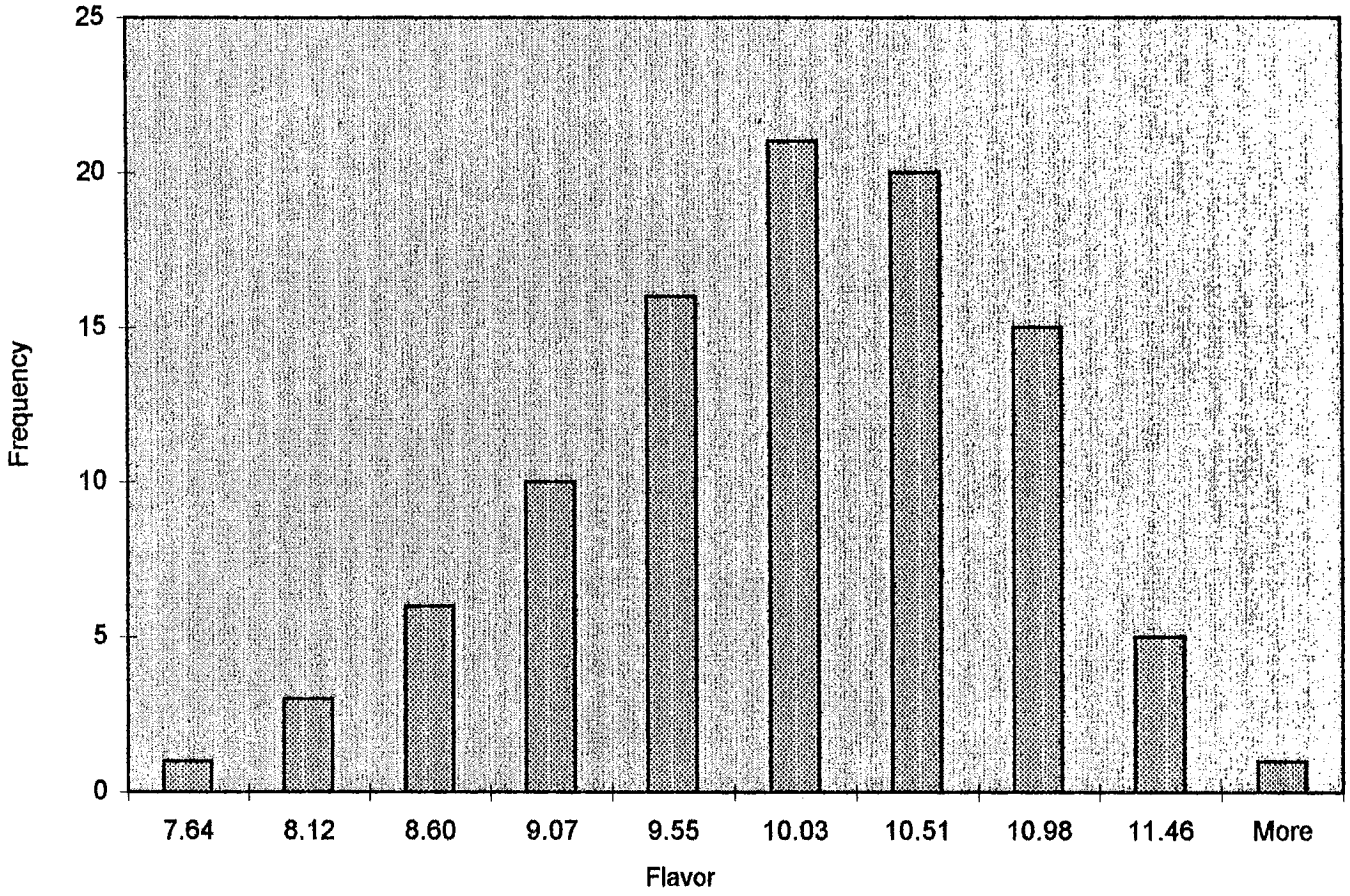

Figure 23. Flavor Histogram

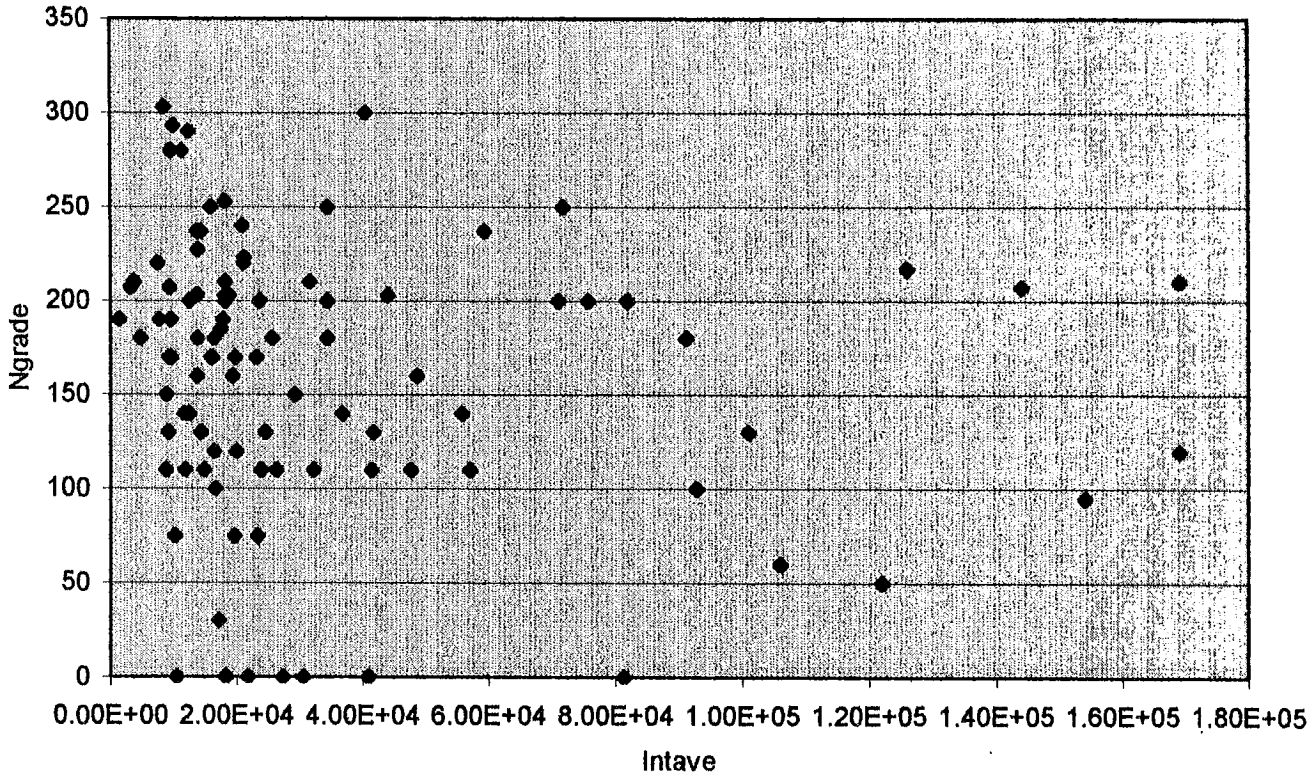

Figure 24: Intave vs. Ngrade

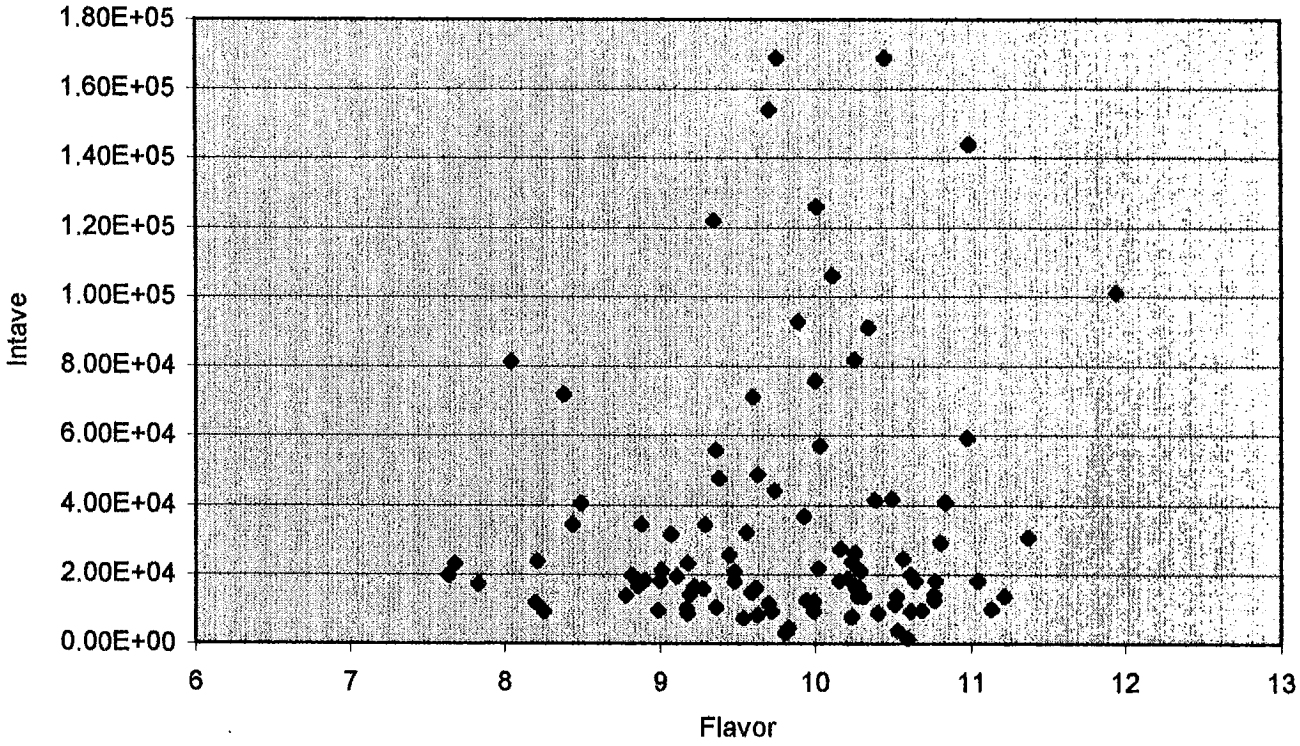

Figure 25. Intave vs. Flavor

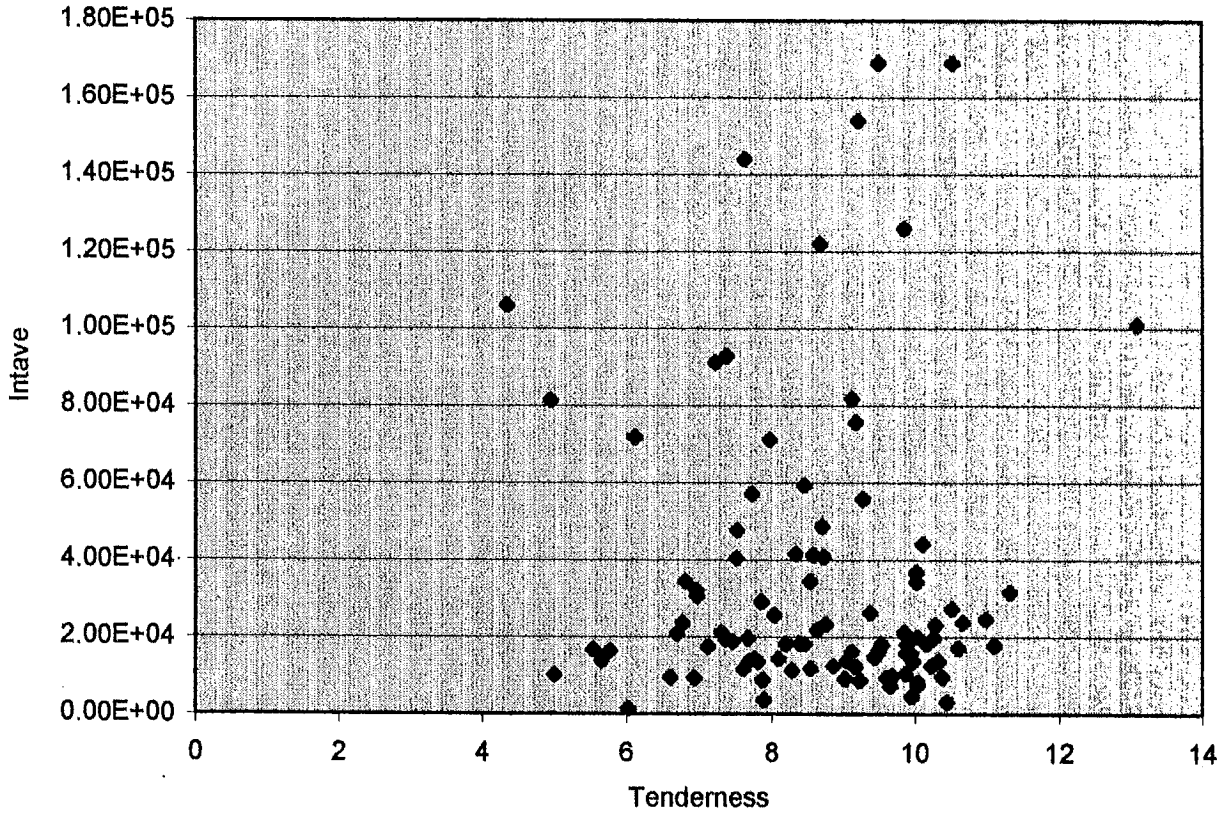

Figure 26. Intave vs. Tenderness

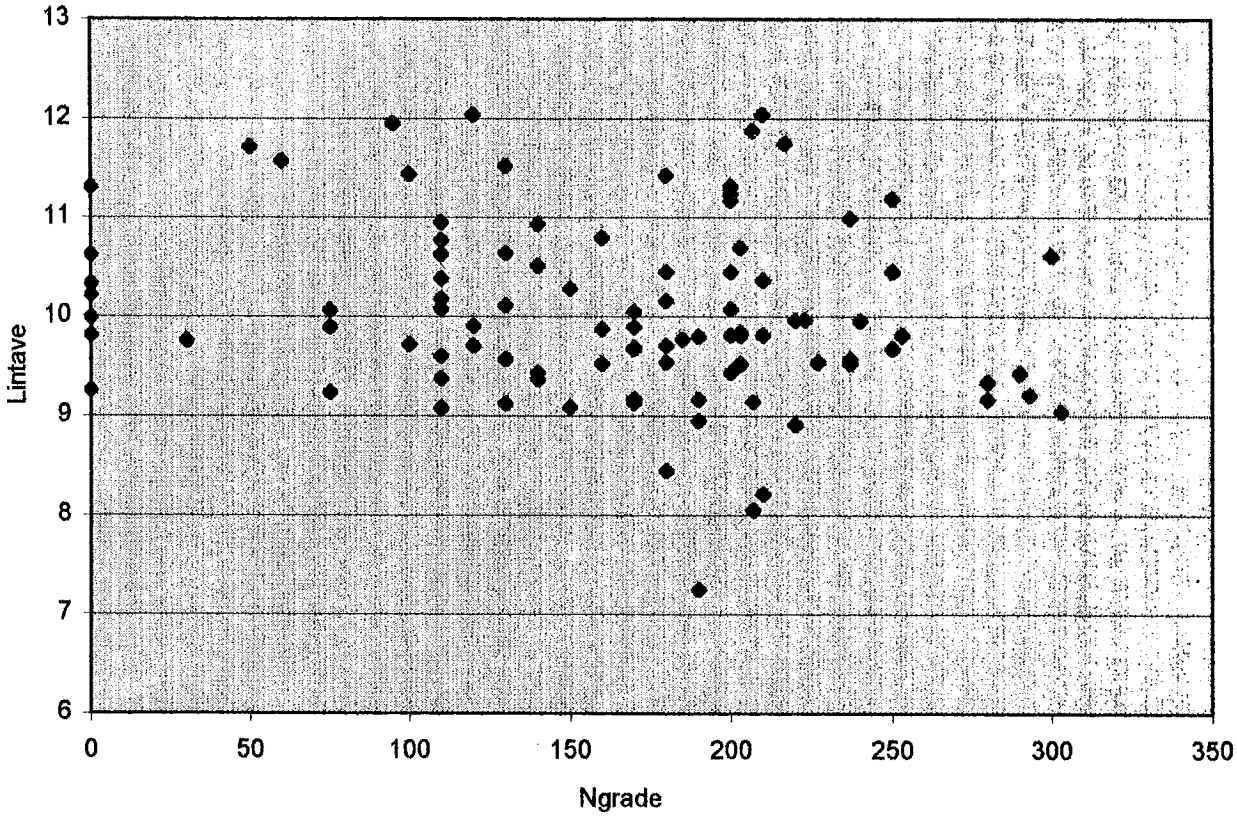

Figure 27. Lintave vs. Ngrade

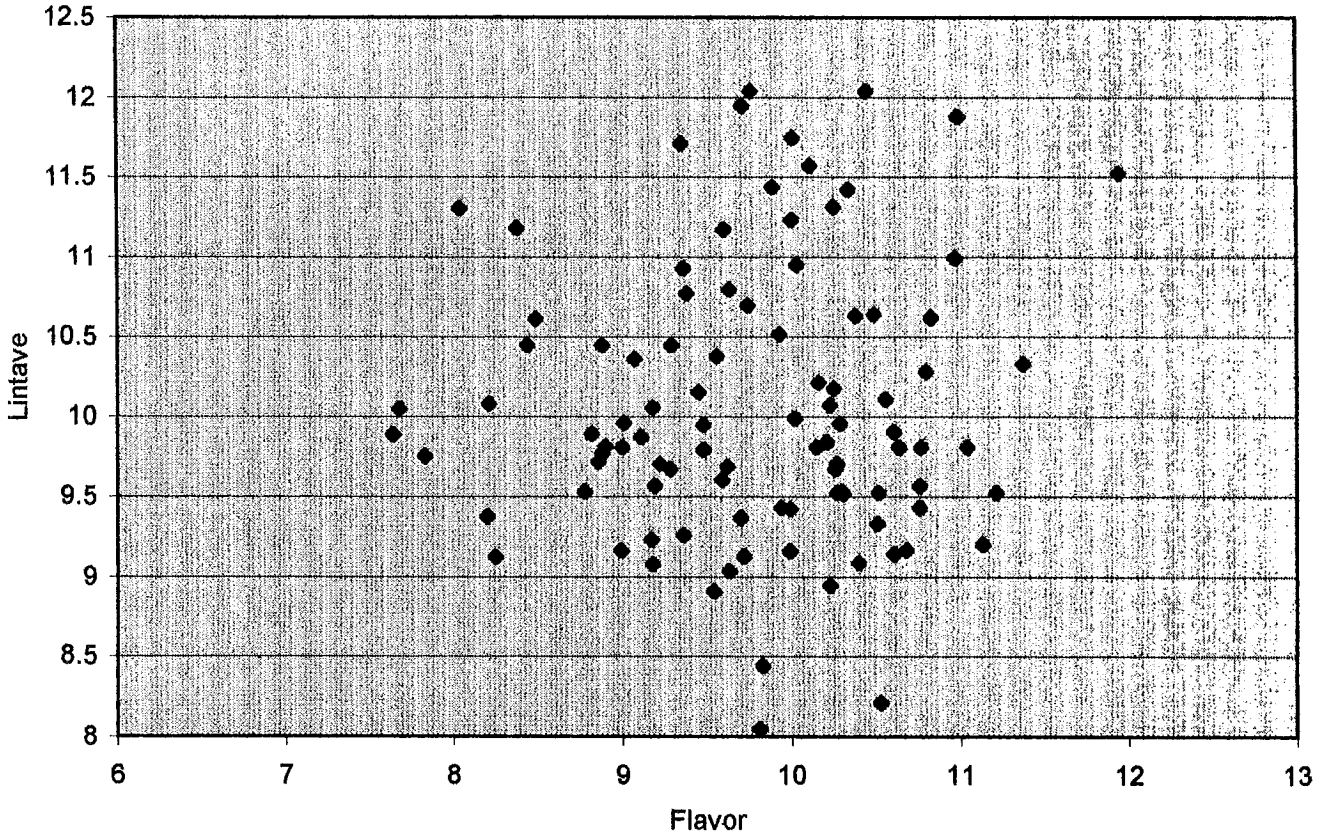

Figure 28. Lintave vs. Flavor

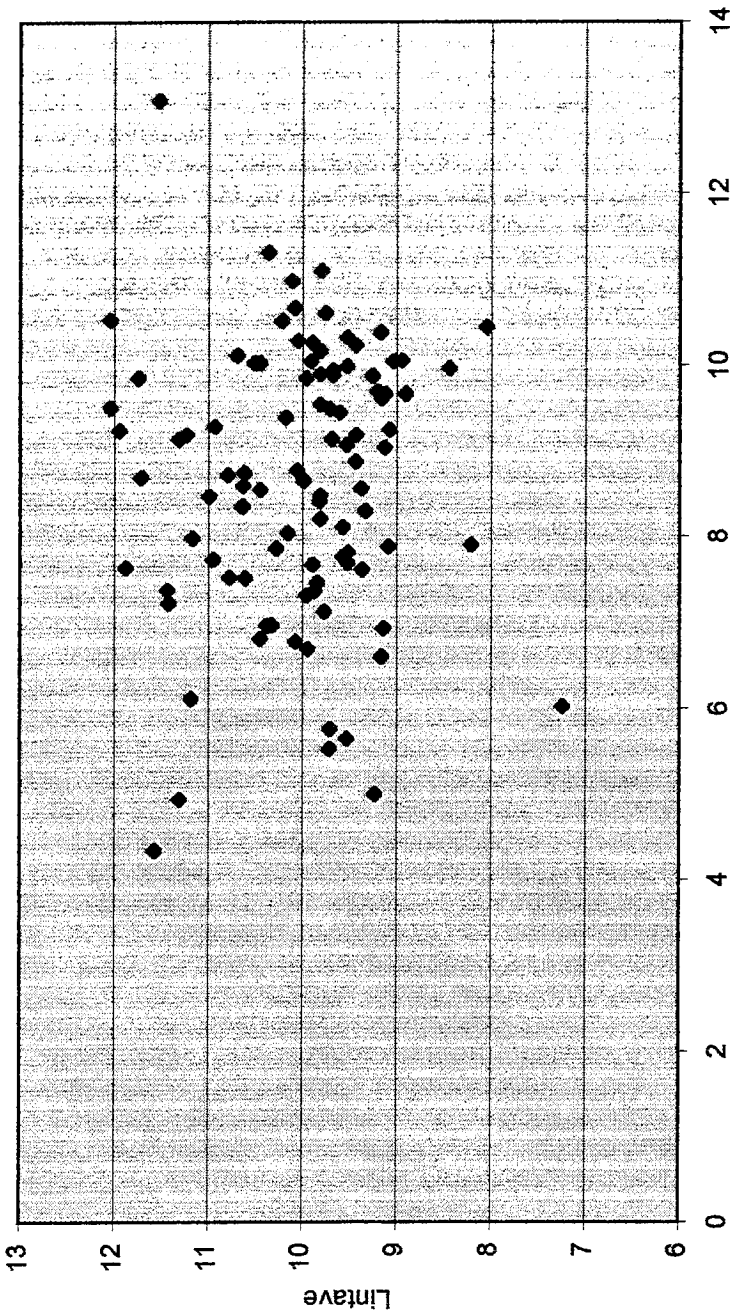

Figure 29. Lintave vs. Tenderness

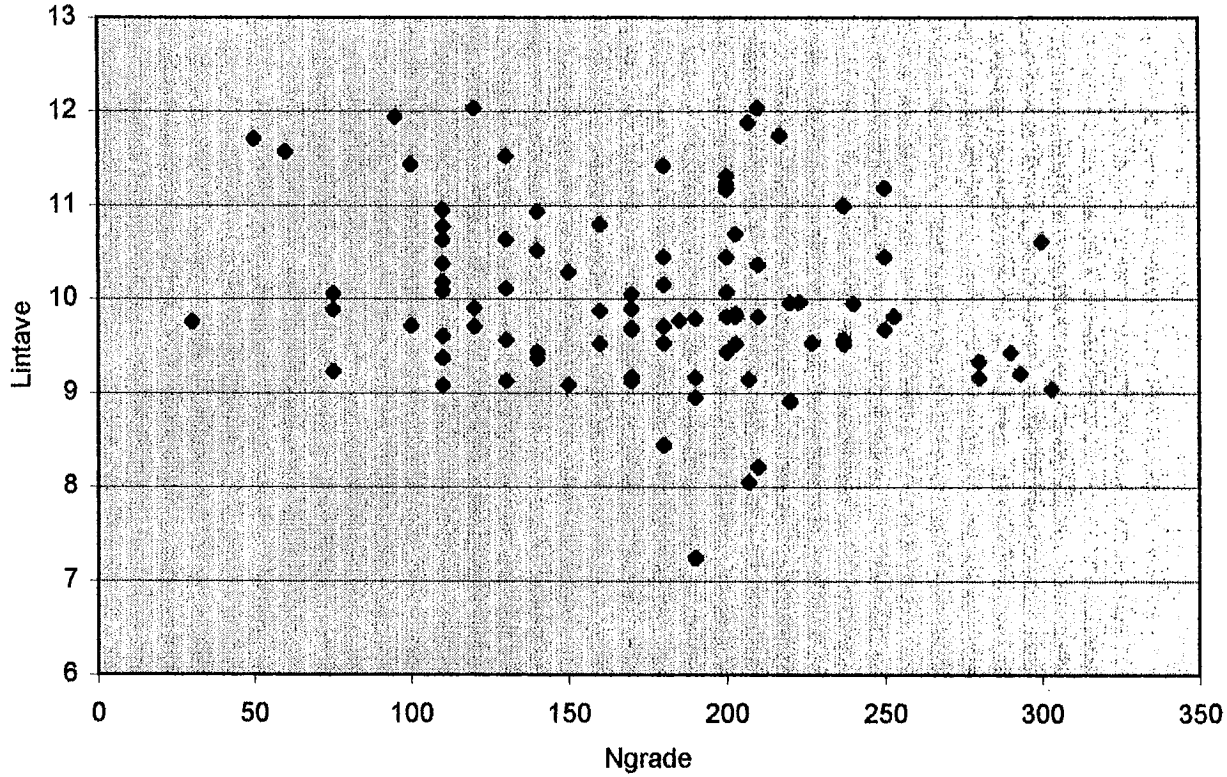

Figure 30. Lintave vs. Ngrade (Analysis 3)

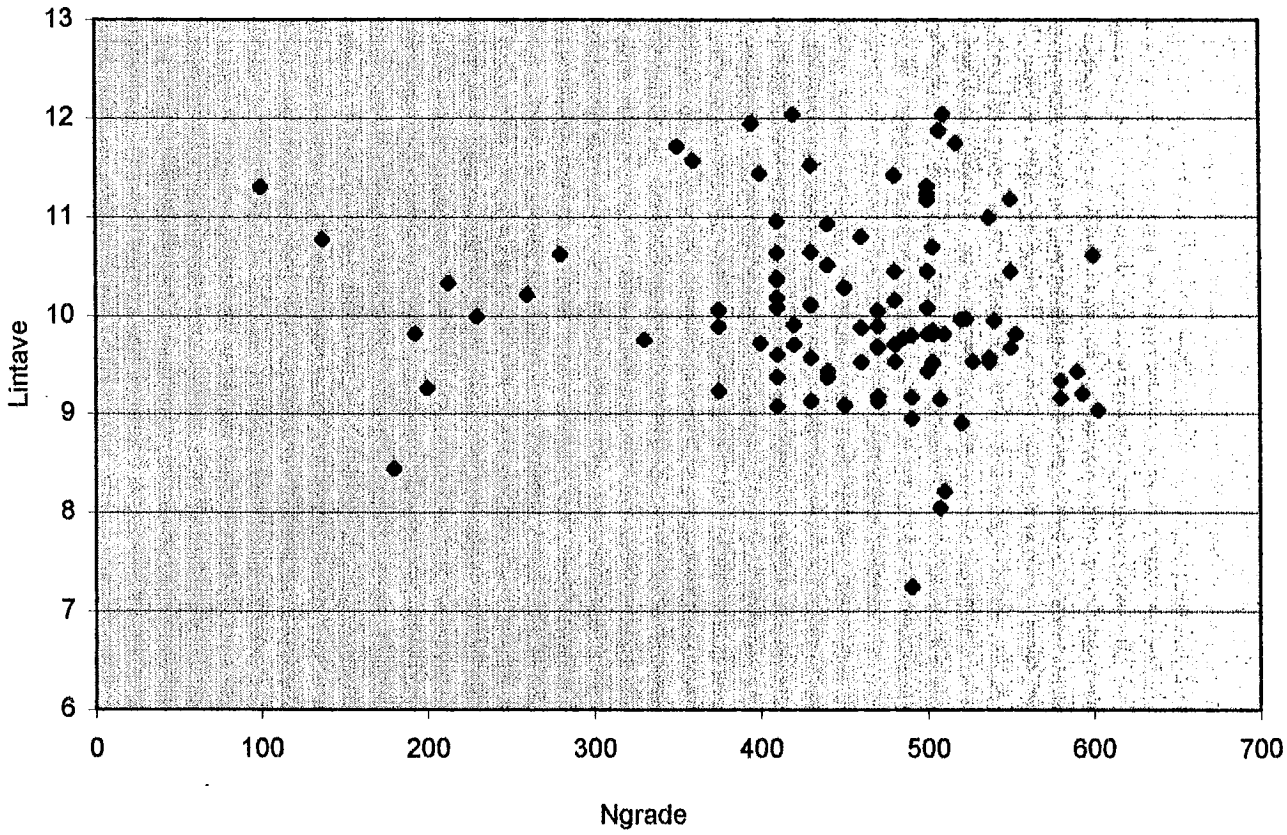

Figure 31. Lintave vs. Ngrade (Analysis 4)

APPENDIX C

Anml-#	Tenderness	Flavor	Ngrading	ln(1+intave)	IntAve(*10,000)
27	7.12	8.88	185	9.7700133	1.75E+04
28	8.87	9.94	140	9.4335639	1.25E+04
29	13.08	11.94	130	11.522886	1.01E+05
30	9.49	10.27	180	9.7050976	1.64E+04
31	10.11	9.74	203	10.694238	4.41E+04
32	10.05	10.23	190	8.9478061	7.69E+03
33	9.24	9.18	110	9.0769233	8.75E+03
34	9.96	9.83	180	8.4426851	4.64E+03
35	9.94	10.26	250	9.6741373	1.59E+04
36	7.76	9.19	237	9.5680847	1.43E+04
37	8.1	10.76	130	9.5680847	1.43E+04
38	10.44	9.81	207	8.0491077	3.13E+03
39	10.04	10.61	120	9.9035376	2.00E+04
40	10.98	10.56	130	10.110542	2.46E+04
41	10.53	10.45	210	12.03766	1.69E+05
42	9.61	9.99	280	9.1602043	9.51E+03
43	8.04	9.45	180	10.154285	2.57E+04
44	8.58	10.38	110	10.63106	4.14E+04
45	7.98	9.6	200	11.171857	7.11E+04
46	7.81	10.31	203	9.5178986	1.36E+04
47	8.46	10.97	237	10.992066	5.94E+04
48	8.54	9.29	250	10.44738	3.45E+04
49	9.28	9.36	140	10.929547	5.58E+04
50	5.65	10.3	227	9.5324963	1.38E+04
51	10.23	10.76	200	9.4335639	1.25E+04
52	9.69	11.13	293	9.2044229	9.94E+03
53	6.81	8.88	180	10.44738	3.45E+04
54	7.36	9.11	160	9.8730799	1.94E+04
55	9.89	11.04	200	9.8092318	1.82E+04
56	10.38	10.68	170	9.1685804	9.59E+03
57	7.69	11.21	203	9.5252241	1.37E+04
58	6.02	10.59	190	7.2449415	1.40E+03
59	9.18	9.99	290	9.4255324	1.24E+04
60	7.63	10.99	207	11.877576	1.44E+05
61	8.2	10.77	210	9.8092318	1.82E+04
62	7.22	10.34	180	11.420821	9.12E+04
63	9.03	9.72	170	9.1270675	9.20E+03
64	8.47	10.64	253	9.8092318	1.82E+04
65	7.9	10.53	210	8.2136527	3.69E+03
66	6.93	10.61	207	9.1432386	9.35E+03
67	4.34	10.11	60	11.571204	1.06E+05
68	9.66	9.54	220	8.9080183	7.39E+03
69	10.04	9.63	303	9.036106	8.40E+03
70	9.85	10.29	220	9.9570757	2.11E+04
71	8.64	10.02	0	9.9897111	2.18E+04
72	11.31	9.07	210	10.360944	3.16E+04
73	6.69	9.48	240	9.9475523	2.09E+04
74	9.98	10.52	237	9.5252241	1.37E+04
75	8.76	9.18	75	10.056252	2.33E+04
76	8.71	9.63	160	10.793455	4.87E+04

77	8.29	10.51	280	9.3326465	1.13E+04
78	9.88	9.28	170	9.6741373	1.59E+04
79	5.76	9.22	120	9.7050976	1.64E+04
80	5	9.17	75	9.230241	1.02E+04
81	4.94	8.04	0	11.305914	8.13E+04
82	7.61	9.7	140	9.3674296	1.17E+04
83	6.77	10.23	200	10.073273	2.37E+04
84	9.54	10.15	200	9.8092318	1.82E+04
85	9.38	10.25	110	10.177362	2.63E+04
86	5.53	8.86	100	9.7172182	1.66E+04
87	7.86	10.8	150	10.281958	2.92E+04
88	10.28	7.68	170	10.047631	2.31E+04
89	7.52	9.38	110	10.772708	4.77E+04
90	10.02	9.93	140	10.51328	3.68E+04
91	9.5	9.76	120	12.03766	1.69E+05
92	9.06	8.78	180	9.5324963	1.38E+04
93	6.96	9.56	110	10.379753	3.22E+04
94	9.44	9.59	110	9.60245	1.48E+04
95	6.6	8.99	190	9.1623049	9.53E+03
96	7.46	10.21	203	9.8416653	1.88E+04
97	6.97	11.37	0	10.328788	3.06E+04
98	10.66	8.21	110	10.081676	2.39E+04
99	10.51	10.16	0	10.214679	2.73E+04
100	8.55	8.2	110	9.3759396	1.18E+04
101	7.51	8.49	300	10.609082	4.05E+04
102	10.26	8.82	170	9.8934877	1.98E+04
103	11.1	9.48	190	9.7926119	1.79E+04
104	8.4	8.9	0	9.814711	1.83E+04
105	8.73	10.83	0	10.61891	4.09E+04
106	10.32	10.27	160	9.5252241	1.37E+04
107	9.13	10.25	200	11.313266	8.19E+04
108	7.31	9.01	223	9.9618036	2.12E+04
109	7.67	7.64	75	9.8884247	1.97E+04
110	7.73	10.03	110	10.952577	5.71E+04
111	10.6	7.83	30	9.7527228	1.72E+04
112	10.16	9	203	9.8092318	1.82E+04
113	9.18	10	200	11.234547	7.57E+04
114	9.85	10.01	217	11.744045	1.26E+05
115	9.23	9.71	95	11.944714	1.54E+05
116	8.68	9.35	50	11.711785	1.22E+05
117	7.37	9.89	100	11.438213	9.28E+04
118	7.88	10.4	150	9.0860235	8.83E+03
119	9.13	9.62	170	9.6866367	1.61E+04
120	9.87	9.36	0	9.2592258	1.05E+04
121	6.11	8.38	250	11.181654	7.18E+04
122	9.66	8.25	130	9.1248914	9.18E+03
123	8.34	10.49	130	10.63828	4.17E+04
124	10.02	8.44	200	10.445841	3.44E+04

APPENDIX D

Anml-#	Flavor	Tenderness	Ngrading	ln(intave)	IntAve(*10,000)
27	8.88	7.12	485	9.770013	17500.00
28	9.94	8.87	440	9.433564	12500.00
29	11.94	13.08	430	11.52289	101000.00
30	10.27	9.49	480	9.705098	16400.00
31	9.74	10.11	503	10.69424	44100.00
32	10.23	10.05	490	8.947806	7690.00
33	9.18	9.24	410	9.076923	8750.00
34	9.83	9.96	180	8.442685	4640.00
35	10.26	9.94	550	9.674137	15900.00
36	9.19	7.76	537	9.568085	14300.00
37	10.76	8.10	430	9.568085	14300.00
38	9.81	10.44	507	8.049108	3130.00
39	10.61	10.04	420	9.903538	20000.00
40	10.56	10.98	430	10.11054	24600.00
41	10.45	10.53	510	12.03766	169000.00
42	9.99	9.61	580	9.160204	9510.00
43	9.45	8.04	480	10.15429	25700.00
44	10.38	8.58	410	10.63106	41400.00
45	9.60	7.98	500	11.17186	71100.00
46	10.31	7.81	503	9.517899	13600.00
47	10.97	8.46	537	10.99207	59400.00
48	9.29	8.54	550	10.44738	34453.00
49	9.36	9.28	440	10.92955	55800.00
50	10.30	5.65	527	9.532496	13800.00
51	10.76	10.23	500	9.433564	12500.00
52	11.13	9.69	593	9.204423	9940.00
53	8.88	6.81	480	10.44738	34453.00
54	9.11	7.36	460	9.87308	19400.00
55	11.04	9.89	500	9.809232	18200.00
56	10.68	10.38	470	9.16858	9590.00
57	11.21	7.69	503	9.525224	13700.00
58	10.59	6.02	490	7.244942	1400.00
59	9.99	9.18	590	9.425532	12400.00
60	10.99	7.63	507	11.87758	144000.00
61	10.77	8.20	510	9.809232	18200.00
62	10.34	7.22	480	11.42082	91200.00
63	9.72	9.03	470	9.127067	9200.00
64	10.64	8.47	553	9.809232	18200.00
65	10.53	7.90	510	8.213653	3690.00
66	10.61	6.93	507	9.143239	9350.00
67	10.11	4.34	360	11.5712	106000.00
68	9.54	9.66	520	8.908018	7390.00
69	9.63	10.04	603	9.036106	8400.00
70	10.29	9.85	520	9.957076	21100.00
71	10.02	8.64	230	9.989711	21800.00
72	9.07	11.31	410	10.36094	31600.00
73	9.48	6.69	540	9.947552	20900.00
74	10.52	9.98	537	9.525224	13700.00
75	9.18	8.76	375	10.05625	23300.00
76	9.63	8.71	460	10.79345	48700.00

77	10.51	8.29	580	9.332646	11300.00
78	9.28	9.88	470	9.674137	15900.00
79	9.22	5.76	420	9.705098	16400.00
80	9.17	5.00	375	9.230241	10200.00
81	8.04	4.94	100	11.30591	81300.00
82	9.70	7.61	440	9.36743	11700.00
83	10.23	6.77	500	10.07327	23700.00
84	10.15	9.54	500	9.809232	18200.00
85	10.25	9.38	410	10.17736	26300.00
86	8.86	5.53	400	9.717218	16600.00
87	10.80	7.86	450	10.28196	29200.00
88	7.68	10.28	470	10.04763	23100.00
89	9.38	7.52	137	10.77271	47700.00
90	9.93	10.02	440	10.51328	36800.00
91	9.76	9.50	420	12.03766	169000.00
92	8.78	9.06	480	9.532496	13800.00
93	9.56	6.96	410	10.37975	32200.00
94	9.59	9.44	410	9.60245	14800.00
95	8.99	6.60	490	9.162305	9530.00
96	10.21	7.46	503	9.841665	18800.00
97	11.37	6.97	213	10.32879	30600.00
98	8.21	10.66	410	10.08168	23900.00
99	10.16	10.51	260	10.21468	27300.00
100	8.20	8.55	410	9.37594	11800.00
101	8.49	7.51	600	10.60908	40500.00
102	8.82	10.26	470	9.893488	19800.00
103	9.48	11.10	490	9.792612	17900.00
104	8.90	8.40	193	9.814711	18300.00
105	10.83	8.73	280	10.61891	40900.00
106	10.27	10.32	460	9.525224	13700.00
107	10.25	9.13	500	11.31327	81900.00
108	9.01	7.31	523	9.961804	21200.00
109	7.64	7.67	375	9.888425	19700.00
110	10.03	7.73	410	10.95258	57100.00
111	7.83	10.60	330	9.752723	17200.00
112	9.00	10.16	503	9.809232	18200.00
113	10.00	9.18	500	11.23455	75700.00
114	10.01	9.85	517	11.74405	126000.00
115	9.71	9.23	395	11.94471	154000.00
116	9.35	8.68	350	11.71178	122000.00
117	9.89	7.37	400	11.43821	92800.00
118	10.40	7.88	450	9.086024	8830.00
119	9.62	9.13	470	9.686637	16100.00
120	9.36	9.87	200	9.259226	10500.00
121	8.38	6.11	550	11.18165	71800.00
122	8.25	9.66	430	9.124891	9180.00
123	10.49	8.34	430	10.63828	41700.00
124	8.44	10.02	500	10.44584	34400.00

APPENDIX E

rowscan.c

```
/*
   |          This program is written by Kay Raum                          |
   | I used some good ideas from Nadine B. Smith and Kate Hillsley.        |
   |                                                                       |
   | It is written to create a set of A-scan lines along one axis.         |
   | The distance between two A-scan lines (stepsize) and the total        |
   | length of a scan row is selectable as well as the axis of the         |
   | daedal system, wich is used. The direction of the scan                |
   | is always in the positive axis direction. You have to select the      |
   | trace of the signal, wich you want to grab from the tektronix         |
   | scope, too.                                                           |
   | You should take care, that the scope is running in enhanced mode,     |
   | otherwise scan information will not stored correctly.                 |
   | Two files will be created. A binary file with extension .bin          |
   | contains the unscaled integer signal points (1024 for each scan).     |
   | Th second file is an ASCII file, wich contains waveform and scan      |
   | information. You have to transfer the files separatly in binary       |
   | or ascii mode, respectively. To read the files in matlab, you         |
   | should use my function file.m                                         |
   |                                                                       |
   | For questions and suggestions, send an e-mail to                      |
   |  raum@uibrl.brl.uiuc.edu                                              |
   |                                                                       |
   ^^^^^^^^^^^^^^^^^^^^^^^^^^^^^^^^^^^^^^^^^^^^^^^^^^^^^^^^^^^^^^^^^^^^^^^ */
#include <conio.h>
#include <stdio.h>
#include <string.h>
#include <stdlib.h>
#include "c:\qc2\include\msgraph.h"
#include <time.h>
#include "c:\at-gpib\c\decl.h"

#define ERR     (1<<15)      /* Error detected           */
#define TIMO    (1<<14)      /* Timeout                  */
#define RQS     (1<<11)      /* Device needs service     */

void introduction(void);
void init_parameter(void);
void init_files(void);
void init_device(void);
void measure(void);
void disable_device(void);

FILE
        *fopen(),
        *ptr_dat,
        *ptr_bin;

char filebin[25],
         filedat[25],
         command[30],
         wait[20],
         wfm[250],
         op,
         asr[4];

char ax_number;

unsigned long int inter;

int     gpib0,
        dev0,
        dev1,
        dev2,
        dev3;
```

rowscan.c

```
struct data
  {
  unsigned long int number_point,
                                        numscan;
  float                           xincr,xmult,xzero,ymult,yzero;
  };

struct data info;

main()
  {
  introduction();
  init_parameter();
  init_device();
  init_files();
  measure();
  disable_device();
  }

void introduction()
  {
  _clearscreen(_GCLEARSCREEN);
  printf("\n\n\n\n ROWSCAN.C");
  printf("\n Collects RF data on a row.");
  printf("\n You can select the distance between two scanpoints (stepsize)");
  printf("\n and the total length of the row.\n");
  printf("\n Scaninformation will be stored in c:\\kay\\wave\\file_nam.dat");
  printf("\n Unscaled Values will be stored in c:\\kay\\wave\\file_nam.bin");
  }

void init_parameter()
  {
  static char fileout[5],
                          filenam[50]="c:\\kay\\wave\\",
                          intervall[3],
                          distance[20];

  unsigned long int dist;

  printf("\n Enter a 6 char output filename            : ");
  scanf("%s",fileout);
  strcat(filenam,fileout);
  strcpy(filebin,filenam);
  strcat(filebin,".bin");
  strcpy(filedat,filenam);
  strcat(filedat,".dat");
  printf(" Enter the scanaxis (1, 2 or 3)            : ");
  ax_number=getche();
  op=getche();
  printf("\n Enter the distance between collected waves: ");
  scanf("%s",intervall);
  printf(" Enter the length of the row in mm         : ");
  scanf("%s",distance);
  inter=atoi(intervall);
  dist=atoi(distance);
  info.numscan=(1000*dist/inter+1);
  printf("\n %u Scans of a row will be created.",info.numscan);
  switch(ax_number)
          {
          case'1':
                dev1=ibfind("axis1");
                strcpy(command, "MN A10 1V.01 D");
                strcat(command, intervall);
                strcat(command, " G ");
```

rowscan.c

```
                strcpy(wait," 1R ");
                break;
          case'2':
                dev1=ibfind("axis2");
                strcpy(command, "MN A10 2V.01 D");
                strcat(command, interval1);
                strcat(command, " G ");
                strcpy(wait," 2R ");
                break;
          case '3':
                dev1=ibfind("axis3");
                strcpy(command, "MN A10 3V.01 D");
                strcat(command, interval1);
                strcat(command, " G ");
                strcpy(wait," 3R ");
                break;
          default:
                printf("\n unknown axis");
                op=getche();
                _clearscreen(_GCLEARSCREEN);
                exit(0);
          }
  }

void init_device(void)
  {
  static char trace[4],
                        output[12],
                        select[12];

  printf("\n\n Enter Trace (e.g. tra3)            : ");
  scanf("%s",trace);
  gpib0=ibfind("gpib0");
  dev0=ibfind("tekdev1");
  ibwrt(dev0,"DIG RUN ",8);
  strcpy(output,"OUTPUT ");
  strcpy(select,"SELECT ");
  strcat(output,trace);
  strcat(select,trace);
  printf("\n--%s--",output);
  printf("\n--%s--",select);

  ibwrt(dev0,output,strlen(output));

  ibwrt(dev0,select,strlen(select));
  ibwrt(dev0,"ENC WAV:bin ",12);
  ibwrt(dev0,"BYT LSB ",8);
  ibwrt(dev0,"ABB ON ",7);
  ibwrt(dev0,"WFM YMU:1 ",10);
  ibwrt(dev0,"WFM NR.pt:1024 ",14);
  ibwrt(dev0,"wfm?",4);
  ibrd(dev0,wfm,250);
  sscanf(wfm,"WFMPRE ACSTATE:ENHANCED,NR.PT:%lu,PT.FMT:Y,XINCR:%g,XMULT:%g,XZERO:%g,YMULT:%g
,YZERO:%g",
  &info.number_point,&info.xincr,&info.xmult,&info.xzero,
  &info.ymult,&info.yzero);
  printf("\n\nPoints : %lu",info.number_point);
  printf("    Xincr : %g",info.xincr);
  printf("    Xmult : %g",info.xmult);
  printf("    Xzero : %g",info.xzero);
  printf("\nYmult  : %g",info.ymult);
  printf("    Yzero  : %g",info.yzero);
  printf("\n%s",wfm);
  ibwrt(dev1," F ",3);
  ibwrt(dev1," E ",3);
```

```
  }

void init_files()
  {

  if ((ptr_dat = fopen(filedat,"w")) == NULL)
        {
        printf(" error opening data file \n");
        exit(0);
        }
  if ((ptr_bin = fopen(filebin,"wb")) == NULL)
        {
        printf(" error opening binary file \n");
        exit(0);
        }
  fprintf(ptr_dat,"%g %g %g %lu %lu %g %g %lu",info.ymult,info.yzero,
  info.xincr,info.number_point,info.numscan,info.xmult,info.xzero,inter);
  fprintf(ptr_dat,"\nymult yzero xincr number_point numscan xmult xzero stepsize\n");
  fclose(ptr_bin);
  fclose(ptr_dat);
  }

void measure()
  {
  unsigned long int i,j,delay;
  static char curv[2060];

  if ((ptr_bin = fopen(filebin,"ab")) == NULL)
        {
        printf(" error appending to binary file \n");
        exit(0);
        }
  printf("\n\nPlease wait!!!  ");
  for(i=0;i<=(info.numscan-1);i++)
        {
        printf(".");
        ibwrt(dev0,"curve?",6);
        for(delay=0;delay<=900;delay++)
          {
          printf("\n Scheiss delay, sau Du, alberne....");
          }
        printf("\n->");

        ibrd(dev0,curv,2058);
        ibwrt(dev1, command, strlen(command));
        for (j=9;j<=2056;j++)
          {
          fputc(curv[j],ptr_bin);
          }
        while (asr[1] != 'R')
          {
          ibwrt(dev1,wait,strlen(wait));
          ibrd(dev1,asr,3);
          }
        asr[1] = 'B';

  }
  fclose(ptr_bin);
  }

void disable_device()
  {
  ibwrt(dev1, "F ",2);
  ibwrt(dev2, "F ",2);
  ibwrt(dev3, "F ",2);
```

rowscan.c

```
  /* ibsic(gpib0);       */
  /* ibonl(gpib0,0); */
  }
```

```
% file.m
% This function loads bin and dat file
% each A-Scanline is one column of matrix B


n=input('Enter a filename : ','s');


bin=[n '.bin'];
dat=[n '.dat'];

fid=fopen(dat,'r');
A=fscanf(fid,'%f',[8,1]);
ymult=A(1,1);
yzero=A(2,1);
xincr=A(3,1);
number_point=A(4,1);
numscan=A(5,1);
xmult=A(6,1);
xzero=A(7,1);
stepsize=A(8,1);
status=fclose(fid);

fid=fopen(bin,'rb','g');
B=zeros(number_point,numscan);
B=fread(fid,[number_point,numscan],'short');
status=fclose(fid);

B=B';

clear n;
clear bin;
clear dat;
clear fid;
clear status;
clear A;
```

```
%sanity.m
%this program is written to calculate the maximum reflected signal,
%the location of max.power and integral of the area under max. power signal
%this program is written for the comb experiment


for i= 1:numscan
    s=B(i,:);
    im=s;
    imn=s.^2;
    [a,b] = max(imn);
    power(i)=a;
    location(i)=((1480/2)*(xincr*b+xzero)*100);
    int(i)=sum(imn);
    time=(xzero+xincr:xincr:xzero+1024*xincr);
    distance=(1480/2)*time*100;
    end
intave=mean(int);
mavg = mean(power);
```

```
%puscan.m, written for the comb experiment
%this program makes a scaled plot of signals converted to distance
%there are six graphs generated


subplot(3,2,1);
plot(distance,B);
xlabel('depth(cm)')
ylabel('all alines')
%subplot(3,2,5);
%plot(location,power,'.');
%xlabel('depth(cm)');
%ylabel('max.power');
subplot(3,2,3);
aline=(1:1:51);
plot(aline,power,'o',aline,power,':');
axis([0 51 min(power) max(power)])
xlabel('aline number');
ylabel('max.power')
subplot(3,2,4);
plot(aline,location,'o',aline,location,':')
axis([0 51 min(location) max(location)]);
xlabel('aline number');
ylabel('depth(cm)')
subplot(3,2,2)
plot(distance,B(1,:))
xlabel('depth(cm)')
ylabel('a-line #1')
subplot(3,2,5)
plot(int)
xlabel('51 alines')
ylabel('energy')
axis([0 51 min(int) max(int)])
```

```
    /*-------------------------------------------------------------------*/
    /*    Procedure for performing a vertical scan of the spinal cord.   */
    /* The procedure assumes that the transducer is at the zero position,*/
    /* that is at the spinal cord midway between the upper and lower     */
    /* elevator position and that all counters has been set to zero.     */
    /* Further, the transducer must be fully retracted and parallel.     */
    /* One scan of the animal is performed at one vertical position      */
    /* using only the left transducer.                                   */
    /* The transducers are brought back to the original                  */
    /* position after the scan.                                          */
    /*-------------------------------------------------------------------*/

extern void cartilage_scan (capture_attrb_type *data_systems,
                            xducer *xducer_a,
                            motion_type *motion,
                            int gain_settings_max, int *gain_values,
                            header *hdr1)

{int a_line_counter;        /*  Counter for the number of a-lines          */
 int tgc_length;            /*  Segment of data for particular gain setting */
 int gain_setting;          /*  Current gain setting                       */
 char filename[50];         /*  File name                                  */
 int c;                     /*  Loop counter                               */
 float pos;                 /*  Position of motor                          */
 int err;                   /*  Error code returned from the MCL library   */
 int offset;                /*  Offset for picking out gain values         */
 float width;               /*  Width of the displayed A-lines             */
 int width1;                /*  Width of the displayed A-lines             */
 char side_char;            /*  Character indicating side of animal        */


  mcl_err_trace (0);

     /*  Make the directories for the scan  */

  make_directory (hdr1->animal.number,hdr1->animal.hide);

  tgc_length = data_systems->adc_samples/gain_settings_max;
  width = 480.00 / motion->num_a_lines;
  width1 = (int) (width + 0.5);
  if (width1 < 1)
    width1=2;

     /*   Move the transducer to their correct position    */
     /*   This also centers the rail table midway between  */
     /*   scanning start point.                            */

  CLS;
  printf ("Moving transducers and structure to initial position....");
  goto_position (0,
                 -motion->elevator*motion->num_a_lines/2.0,
                 motion->left_rotary_table,0);

  CLS;
  printf("Total of %d Gain Settings\n", gain_settings_max );

      /*        Find initial position and final position        */

  mcl_pos_rail_table(&pos);
```

```
hdr1->position.scan_xstart=pos;
hdr1->position.scan_xend=pos;
mcl_pos_elevator(&pos);
hdr1->position.scan_ystart=pos;
if (motion->scan_direction == UP)
   hdr1->position.scan_yend=pos + motion->elevator*motion->num_a_lines/2;
else
   hdr1->position.scan_yend=pos - motion->elevator*motion->num_a_lines/2;
mcl_pos_left_actuator (&pos);
hdr1->position.scan_zstart=pos;
hdr1->position.scan_zend=pos;

     /*   Generate the files for this scan    */
for( gain_setting=0; gain_setting<gain_settings_max; gain_setting++ )
  {xducer_a->angle=motion->left_rotary_table;

       /* Create filename for each gain setting    */
   make_filename (hdr1->animal.number,
                  hdr1->animal.hide,'v','a',
                  gain_values[gain_setting],
                  'm',
                  filename );
   printf("Creating file %s\n", filename );
   strcpy( gain_file[gain_setting], filename );
   if( ( access( filename, 00) ) == 0 )
     print_file_error (filename);
   else              /* If filename is OK, then set RITEC gain, generate the hea
                     /* file, and write the header to the file.
     {
      generate_header(data_systems, gain_values[gain_setting],
                      xducer_a,
                      motion, "Vertical scan", hdr1);
      write_header(filename, hdr1);
      }
  }
     /*  Move actuators fully into phantom      */
mcl_move_left_actuator (100);
while (mcl_move_left_actuator (100) == 0)
  ;

     /* get ready to start -- set up targa screen, */
CLS;
targa_clear_screen();
targa_draw_depth_scale(10.0);

    /* display current header info to VGA display */
show_header(hdr1,xducer_a,xducer_a);

printf("Gain settings: ",' ');
for(c=0; c<gain_settings_max; c++) printf("%d ",gain_values[c] );
printf (" dB, ");

printf(" Scan direction: %s (%6.2f mm)", motion->scan_dir_string, motion->elev

      /*   Main loop for data acquisition    */
 /* Set the mutipliexer to the correct transducer    */
rtc_set_trig (data_systems->ritec_trig_source,
              data_systems->ritec_rept_freq,
              0);
```

```
for (a_line_counter = 0; a_line_counter< motion->num_a_lines; a_line_counter++
  {
         /* Repeat data acquisition for all gain settings   */

   for( gain_setting=0; gain_setting<gain_settings_max; gain_setting++ )
     {          /* all desired gain settings   */
      STP (22, 1);
      printf("A-line: %d  gain: %d  ", a_line_counter, gain_values[gain_settin
      rtc_set_rcvr_and_gain (0,gain_values[gain_setting]);

            /* Capture data at current gain setting          */
      if (adc_get_data(data_systems->adc_samples,data_systems->buffer))
        {fatal_error_init();
         printf("      Error capturing data!\n");
         exit(0);
         }

          /* Append RF data to current gain setting file       */
      append_data(gain_file[gain_setting],
                  data_systems->buffer,data_systems->adc_samples);

          /*   Make data for display on Targa board   */
      offset=gain_setting * tgc_length/2;
      for(c=0; c<=tgc_length/2; c++ )
        tgc_rf_data[offset + c] = data_systems->buffer[offset + c];
      }
         /* Display tgc B-line constructed from all the gain settings */

   for (c=gain_settings_max*tgc_length/2; c<=data_systems->adc_samples; c++)
     tgc_rf_data[c] =data_systems->buffer[c];

   display_a_line (tgc_rf_data, data_systems->adc_samples,
                   (int) (width*a_line_counter), width1+1, 10.0);

          /*  Store the position of the transducers  */

   find_position (&xyz_pos[a_line_counter]);

      /*   Retract the transducers, move the rail table and compress  */

   retract_left_actuator (motion->left_xducer_actuator);

   if (motion->scan_direction == UP )
     err=mcl_move_elevator( motion->elevator );
   else
     err=mcl_move_elevator( -motion->elevator );
   if (err)
     {fatal_error_init();
      printf ("      Not possible to move elevator to correct position\n");
      motor_problem();
     }

   mcl_move_left_actuator (100);
   while (mcl_move_left_actuator (100) == 0)
     ;
   }

      /*  Store the position indication at the end of the files  */
      /*  and generate the information file for the scanning     */
```

```
    for( gain_setting=0; gain_setting<gain_settings_max; gain_setting++ )
      {
      append_position (gain_file[gain_setting],
                       xyz_pos,motion->num_a_lines,
                       gain_setting>=gain_settings_max);
      store_information (gain_file[gain_setting],
                         data_systems,
                         xducer_a,xducer_a,
                         motion,
                         gain_settings_max,gain_values);
      }


        /*  Update the file counter number   */

    update_file_counter (hdr1->animal.number,hdr1->animal.hide);

    /*   Move the transducers to the initial position   */
  motors_initial_position();
}

  /*-------------------------------------------------------*/
  /* Capture a single line of data and store it in a file */
  /*-------------------------------------------------------*/

void capture_data (capture_attrb_type *data_systems)
{
char file_name[80];
FILE *fptr;           /* File pointer for reading/writing the file */

  printf ("Currently not implemented\n");
/*  printf ("Input file name: ");
  scanf ("%s",file_name);
  if( (fptr = fopen(file_name, "w+b" ) ) == NULL )
    {fatal_error_init();
     printf("Cannot open the file %s for output\n",file_name);
     exit(0);
  }
  else
    if (adc_get_data(16384,data_systems->buffer))
      {fatal_error_init();
       printf("      Error capturing data!\n");
       exit(0);
       }
    else
      if (fwrite (data_systems->buffer,sizeof(unsigned char), 16384, fptr) != 16
        {fatal_error_init();
         printf("Cannot append binary data to %s!\n", file_name);
         exit(0);
        }
   fclose (fptr);
*/
}

  /*-------------------------------------------------------------*/
  /* Capture data from calibration phantom and store it in a file */
  /*-------------------------------------------------------------*/

void calibrate (capture_attrb_type *data_systems)
{
```

```
char file_name[80];
FILE *fptr;           /* File pointer for reading/writing the file */
int  animal_no;

  printf ("Input animal number: ");
  scanf ("%d",&animal_no);
  make_directory (animal_no, "phantom");

      /*         Move the transducers to the initial position   */
  motors_initial_position();

     /*  Do measurement for transducer a  */

  mcl_move_left_actuator (33.0);
  rtc_set_rcvr_and_gain (0,6);
        /* Set the mutipliexer to the correct transducer        */
  rtc_set_trig (data_systems->ritec_trig_source,
                data_systems->ritec_rept_freq,
                0);

  printf ("Hold phantom on left transducer and press RETURN when ready: ");
  get_key();
  printf ("\n");

  sprintf (file_name,"c:\\data\\anml_%03d\\phantom\\xduc_a.dat",animal_no);
  printf ("File name %s \n",file_name);
  if( (fptr = fopen(file_name, "w+b" ) ) == NULL )
    {fatal_error_init();
     printf("Cannot open the file %s for output\n",file_name);
     exit(0);
    }
  else
        /*     Capture data at current gain setting        */
    if (adc_get_data(8192,data_systems->buffer))
      {fatal_error_init();
       printf("      Error capturing data!\n");
       exit(0);
      }
    else
      if (fwrite (data_systems->buffer,sizeof(unsigned char), 8192, fptr) != 819
        {fatal_error_init();
         printf("Cannot append binary data to %s!\n", file_name);
         exit(0);
        }
   fclose (fptr);

     /*  Do measurement for transducer b  */

  mcl_move_right_actuator (33.0);
  rtc_set_rcvr_and_gain (1,6);
        /* Set the mutipliexer to the correct transducer        */
  rtc_set_trig (data_systems->ritec_trig_source,
                data_systems->ritec_rept_freq,
                1);

  printf ("Hold phantom on right transducer and press RETURN when ready: ");
  get_key();
  printf ("\n");

  sprintf (file_name,"c:\\data\\anml_%03d\\phantom\\xduc_b.dat",animal_no);
```

```
   printf ("File name %s \n",file_name);
   if( (fptr = fopen(file_name, "w+b" ) ) == NULL )
     {fatal_error_init();
      printf("Cannot open the file %s for output\n",file_name);
      exit(0);
     }
   else
         /*     Capture data at current gain setting        */
     if (adc_get_data(8192,data_systems->buffer))
       {fatal_error_init();
        printf("      Error capturing data!\n");
        exit(0);
        }
     else
       if (fwrite (data_systems->buffer,sizeof(unsigned char), 8192, fptr) != 819
         {fatal_error_init();
          printf("Cannot append binary data to %s!\n", file_name);
          exit(0);
         }
    fclose (fptr);

       /*         Move the transducers to the initial position   */
   motors_initial_position();

   printf ("Calibration data stored, press RETURN: ");
   get_key();
}

   /*-------------------------------------------------------------------*/
   /*    Get  the name of the configuration file fo the experiment   */
   /*-------------------------------------------------------------------*/

get_config_file_name (char config_file[80],int scan_type)

{int selection;

   switch (scan_type)
    {
     case F1: strcpy (config_file,"cf_files\\hor_");
              break;
     case F2: strcpy (config_file,"cf_files\\ski_");
              break;
     case F3: strcpy (config_file,"cf_files\\car_");
              break;
     case F4: strcpy (config_file,"cf_files\\lin_");
              break;
    }
   head_scan();
   printf ("Select name of configuration file: \n\n");
   printf ("            [F1] - Hide on experiment  \n");
   printf ("            [F2] - Hide off experiment \n");
   printf ("            [F3] - Cold experiment     \n");
   printf ("            [F4] - Phantom experiment  \n");
   printf ("            [F5] - User input of file name\n\n");
   printf ("Input selection: ");
   selection = get_key();
   switch (selection)
     {
     case F1: config_file = strcat (config_file,"hon.cf");
              break;
```

```
    case F2: config_file = strcat (config_file,"hoff.cf");
             break;
    case F3: config_file = strcat (config_file,"cold.cf");
             break;
    case F4: config_file = strcat (config_file,"phan.cf");
             break;
    default: printf ("Input file name: ");
             scanf ("%s",config_file);
             break;
    }
}

  /*-----------------------------------------*/
  /*      Show the options for doing a scan  */
  /*-----------------------------------------*/

void show_scan_menu (void)
{
     head_scan ();
     printf("                [F1]  Complete horizontal scan with new protocol\n");
     printf("                [F2]  Skin thickness scan\n");
     printf("                [F3]  Cartilage scan\n");
     printf("                [F4]  Capture of single line data (not implemented) \
     printf("                [F5]  Make phantom scan\n");
     printf("                [F6]  Make transducer calibration scan\n\n");
     printf("                [F7]  Complete scan of hide-on animal\n");
     printf("                [F8]  Complete scan of hide-off animal\n");
     printf("                [F9]  Complete scan of cold animal\n\n");

     printf("               [ESC] Go back to the main menu\n");
}

   /*-------------------------------------------------*/
   /*    Select between the different scan options    */
   /*-------------------------------------------------*/

extern void scan_options (capture_attrb_type *data_systems,
                          xducer *xducer_a, xducer *xducer_b,
                          motion_type *motion,
                          int *gain_settings_max, int *gain_values,
                          header *hdr1)

{int key;              /* Extended keyboard code                  */
 int number_of_scans; /* Number of horizontal scans to perform  */
 char config_file[80];/* Name of configuration file              */

  while (1)
   {
   show_scan_menu();
   key = get_key();
   if ((key == F1) | (key == F2) | (key == F3))
     {get_config_file_name (config_file,key);
      read_config_file (config_file,data_systems,
                    xducer_a,xducer_b,
                    motion,
                    gain_settings_max,gain_values);
     change_ritec_values (data_systems);
     move_motors ();
     edit_motion_values (motion);
     edit_gain_settings (gain_settings_max,gain_values);
```

```
  input_header_data (hdr1);
  }
switch( key )
    {
        /* -------  Go back to the main menu---------------------- */

        case ESC:
                  return ;
                  break;

        /* --------- Make a horizontal scan with new protocol  --- */
        case F1:
                  printf ("Number of horizontal scans: ");
                  number_of_scans=input_int(1,9);
                  generate_header(data_systems, 0, xducer_a,
                                  motion, "Horizontal scan", hdr1);
                  show_header (hdr1,xducer_a,xducer_b);
                  printf ("Press RETURN to make experiment and ESC to cancel
                  key = get_key();
                  if (key != ESC)
                    hor_scan2 (number_of_scans,
                               data_systems,
                               xducer_a,xducer_b,
                               motion,
                               *gain_settings_max,gain_values,
                               hdr1);
                  break;

        /* --------- Make a skin thickness scan with new protocol   --- */
        case F2:
                  printf ("Number of horizontal scans: ");
                  number_of_scans=input_int(1,9);
                  generate_header(data_systems, 0, xducer_a,
                                  motion, "Skin scan", hdr1);
                  show_header (hdr1,xducer_a,xducer_b);
                  printf ("Press RETURN to make experiment and ESC to cancel
                  key = get_key();
                  if (key != ESC)
                    skin_scan (number_of_scans,
                               data_systems,
                               xducer_a,xducer_b,
                               motion,
                               *gain_settings_max,gain_values,
                               hdr1);
                  break;

        /* --------- Make a cartilage scan with new protocol        --- */
        case F3:
                  generate_header(data_systems, 0, xducer_a,
                                  motion, "Cartilage scan", hdr1);
                  show_header (hdr1,xducer_a,xducer_a);
                  printf ("Press RETURN to make experiment and ESC to cancel
                  key = get_key();
                  if (key != ESC)
                    cartilage_scan (data_systems,
                                    xducer_a,
                                    motion,
                                    *gain_settings_max,gain_values,
                                    hdr1);
                  break;
```

```
/* --------- Capture a single line of data  - */
case F4:  capture_data(data_systems);
          break;

/* --------- Make a complete scan of the phantom    --- */
case F5:  read_config_file ("cf_files\\phantom.cf",
                            data_systems,
                            xducer_a,xducer_b,
                            motion,
                            gain_settings_max,gain_values);
          move_motors ();
          input_header_data (hdr1);
          number_of_scans=1;
          generate_header(data_systems, 0, xducer_a,
                          motion, "Phantom scan", hdr1);
          show_header (hdr1,xducer_a,xducer_b);
          printf ("Press RETURN to make experiment and ESC to cancel
          key = get_key();
          if (key != ESC)
            phantom (data_systems,
                     xducer_a,xducer_b,
                     motion,
                     *gain_settings_max,gain_values,
                     hdr1);
          break;

/* --------- Make transducer calibration scans ----- */
case F6:  calibrate (data_systems);
          break;

/* --------- Make a complete scan of a hide_on animal       --- */
case F7:  read_config_file ("cf_files\\hor_hon.cf",
                            data_systems,
                            xducer_a,xducer_b,
                            motion,
                            gain_settings_max,gain_values);
          move_motors ();
          input_header_data (hdr1);
          number_of_scans=1;
          generate_header(data_systems, 0, xducer_a,
                          motion, "Horizontal scan", hdr1);
          show_header (hdr1,xducer_a,xducer_b);
          printf ("Press RETURN to make experiment and ESC to cancel
          key = get_key();
          if (key != ESC)
           {
            hor_scan2 (number_of_scans,
                       data_systems,
                       xducer_a,xducer_b,
                       motion,
                       *gain_settings_max,gain_values,
                       hdr1);
            read_config_file ("cf_files\\ski_hon.cf",
                              data_systems,
                              xducer_a,xducer_b,
                              motion,
                              gain_settings_max,gain_values);
            number_of_scans=3;
            generate_header(data_systems, 0, xducer_a,
```

```
                                motion, "Skin scan", hdr1);
                skin_scan (number_of_scans,
                           data_systems,
                           xducer_a,xducer_b,
                           motion,
                           *gain_settings_max,gain_values,
                           hdr1);
                read_config_file ("cf_files\\car_hon.cf",
                                  data_systems,
                                  xducer_a,xducer_b,
                                  motion,
                                  gain_settings_max,gain_values);
                generate_header(data_systems, 0, xducer_a,
                                motion, "Cartilage scan", hdr1);
                cartilage_scan (data_systems,
                                xducer_a,
                                motion,
                                *gain_settings_max,gain_values,
                                hdr1);
                }
              break;

/* --------- Make a complete scan of a hide_off animal       --- */
case F8:  read_config_file ("cf_files\\hor_hoff.cf",
                            data_systems,
                            xducer_a,xducer_b,
                            motion,
                            gain_settings_max,gain_values);
          move_motors ();
          input_header_data (hdr1);
          number_of_scans=3;
          generate_header(data_systems, 0, xducer_a,
                          motion, "Horizontal scan", hdr1);
          show_header (hdr1,xducer_a,xducer_b);
          printf ("Press RETURN to make experiment and ESC to cancel
          key = get_key();
          if (key != ESC)
           {
            hor_scan2 (number_of_scans,
                       data_systems,
                       xducer_a,xducer_b,
                       motion,
                       *gain_settings_max,gain_values,
                       hdr1);
            read_config_file ("cf_files\\ski_hoff.cf",
                              data_systems,
                              xducer_a,xducer_b,
                              motion,
                              gain_settings_max,gain_values);
            number_of_scans=3;
            generate_header(data_systems, 0, xducer_a,
                            motion, "Skin scan", hdr1);
            skin_scan (number_of_scans,
                       data_systems,
                       xducer_a,xducer_b,
                       motion,
                       *gain_settings_max,gain_values,
                       hdr1);
            read_config_file ("cf_files\\car_hoff.cf",
                              data_systems,
```

```
/*  rf_to_ml.c                                                    */
/*  C program to convert the animal binary data files to Matlab format    */
/*  I.  C include files */

#include <math.h>
#include <stdio.h>

/* II.  Default Parameters */
#define LENGTH_HEADER           1024
#define MAX_NUMBER_A_LINE       150
#define MAX_LENGTH_A_LINE       5000

/* invoke by
rf_to_ml infile.dat output.mat
*/

extern void savemat();

main(argc, argv)
int argc;
char *argv[];
        {
        FILE            *infile, *outfile;
        unsigned char
        buff[LENGTH_HEADER+MAX_NUMBER_A_LINE*MAX_LENGTH_
A_LINE];
        double          dbuff[MAX_LENGTH_A_LINE],
rfsignal[MAX_NUMBER_A_LINE*MAX_LENGTH_A_LINE];
        int             header_len, length_a_line, number_a_line;
        int             n, m, x, y;

        infile = fopen(argv[1], "r");
        fread(buff, sizeof(char), LENGTH_HEADER, infile);
        fclose(infile);
        header_len = LENGTH_HEADER;
      length_a_line = buff[210]*256+buff[209];
      number_a_line = buff[212]*256+buff[211];

/* read in data */
        infile = fopen(argv[1], "r");
```

```
        fread(buff, sizeof(char),
LENGTH_HEADER+number_a_line*length_a_line, infile);
        fclose(infile);
        for (n = 0; n < number_a_line; n++)
                for (m = 0; m < length_a_line; m++)
                        rfsignal[m*number_a_line+n] =
(double)buff[header_len+n*5000+m];
        outfile = fopen(argv[2], "w");
        savemat(outfile, 1000, "im", number_a_line, length_a_line, 0, rfsignal,
(double *) 0);
        fclose(outfile);

        } /* End of main */
```

```
% fnmab.m
% This program squares the reflected signals and finds the maximum power
% for each signal and the location of where the maximum power has occured.
% It then takes the integral of the area under the squared of the reflected
% signal.  It also finds the average of the maximum power.

name = input('Enter the name of the data file without extension:' ,'s');
filename = [name '.mat'];
eval(['load ' filename]);
im=im-mean(mean(im));
   for i=1:70
    s=im(i,270:1400);
    imn=s.^2;
    [a,b] = max(imn);
    power(i)=a;
    location(i)=((b+270)*40/13000);
    int(i)=sum(imn);
    end
intave=mean(int);
mavg = mean(power);
result1 = [name 'res1'];
eval(['save ',result1,' power -ascii']);
result2 = [name 'res2'];
eval(['save ',result2,' intave -ascii']);
result4=[name 'res4'];
eval(['save ' ,result4,' location -ascii']);
%clear
```

```
% ascan.m
% graphs
% this program makes a scaled plot of signals converted to distance

distance=1:1:3000;
j=(40/13000)*distance;
subplot(3,2,1);
plot(j,im);
xlabel('depth(cm)')
ylabel('all alines')
set(gca,'XTickMode','manual')
set(gca,'XTick',[0:1:10])
grid
subplot(3,2,3);
aline=(1:1:70);
plot(aline,power,'o',aline,power,':');
axis([0 70 min(power) max(power)])
xlabel('aline number');
ylabel('max.power')
%set(gca,'XTickMode','manual')
%set(gca,'XTick',[0:5:70])
%grid
subplot(3,2,4);
plot(aline,location,'o',aline,location,':')
axis([0 70 min(location) max(location)]);
xlabel('aline number');
ylabel('depth(cm)')
subplot(3,2,2)
plot(j,im(60,:))
xlabel('depth(cm)')
ylabel('a-line #1')
set(gca,'XTickMode','manual')
set(gca,'XTick',[0:1:10])
grid
subplot(3,2,5)
plot(int)
xlabel('70 alines')
ylabel('power')
axis([0 70 min(int) max(int)])
```

```
/*  rf_to_ml.c                                                    */
/*  C program to convert the animal binary data files to Matlab format    */
/*  I.  C include files */

#include <math.h>
#include <stdio.h>

/* II.  Default Parameters */
#define LENGTH_HEADER           1024
#define MAX_NUMBER_A_LINE       150
#define MAX_LENGTH_A_LINE       5000

/* invoke by
rf_to_ml infile.dat output.mat
*/

extern void savemat();

main(argc, argv)
int argc;
char *argv[];
        {
        FILE            *infile, *outfile;
        unsigned char
        buff[LENGTH_HEADER+MAX_NUMBER_A_LINE*MAX_LENGTH_
A_LINE];
        double          dbuff[MAX_LENGTH_A_LINE],
rfsignal[MAX_NUMBER_A_LINE*MAX_LENGTH_A_LINE];
        int             header_len, length_a_line, number_a_line;
        int             n, m, x, y;

        infile = fopen(argv[1], "r");
        fread(buff, sizeof(char), LENGTH_HEADER, infile);
        fclose(infile);
        header_len = LENGTH_HEADER;
      length_a_line = buff[210]*256+buff[209];
      number_a_line = buff[212]*256+buff[211];

/* read in data */
        infile = fopen(argv[1], "r");
```

```
        fread(buff, sizeof(char),
LENGTH_HEADER+number_a_line*length_a_line, infile);
        fclose(infile);
        for (n = 0; n < number_a_line; n++)
                for (m = 0; m < length_a_line; m++)
                        rfsignal[m*number_a_line+n] =
(double)buff[header_len+n*5000+m];
        outfile = fopen(argv[2], "w");
        savemat(outfile, 1000, "im", number_a_line, length_a_line, 0, rfsignal,
(double *) 0);
        fclose(outfile);

        } /* End of main */
```

APPENDIX F

anl31g18

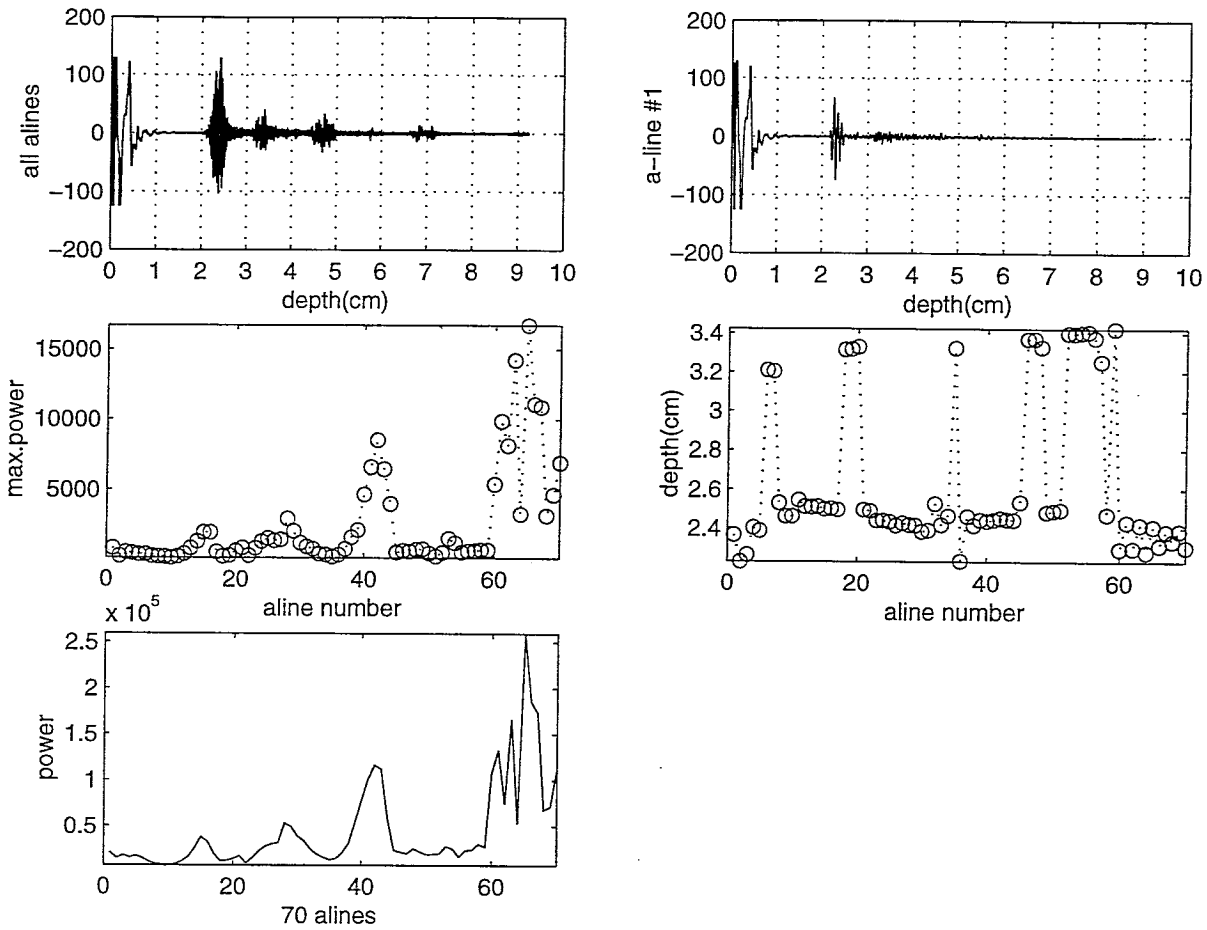
all alines
depth(cm)
a-line #1
depth(cm)
max.power
aline number
depth(cm)
aline number
x 10^5
power
70 alines

anl32g18

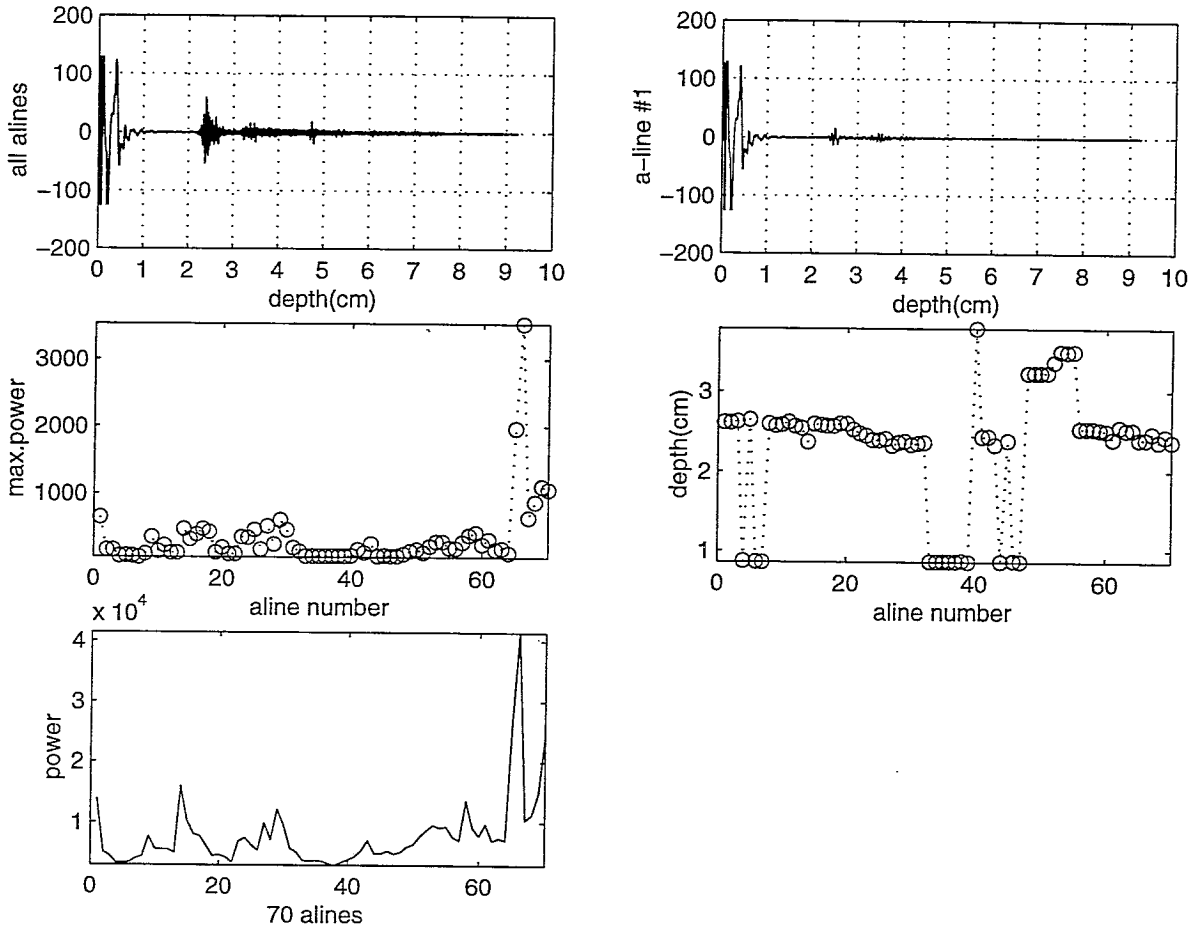
all alines
depth(cm)
a-line #1
depth(cm)
max.power
x 10^4
aline number
depth(cm)
aline number
power
70 alines

anl33g18

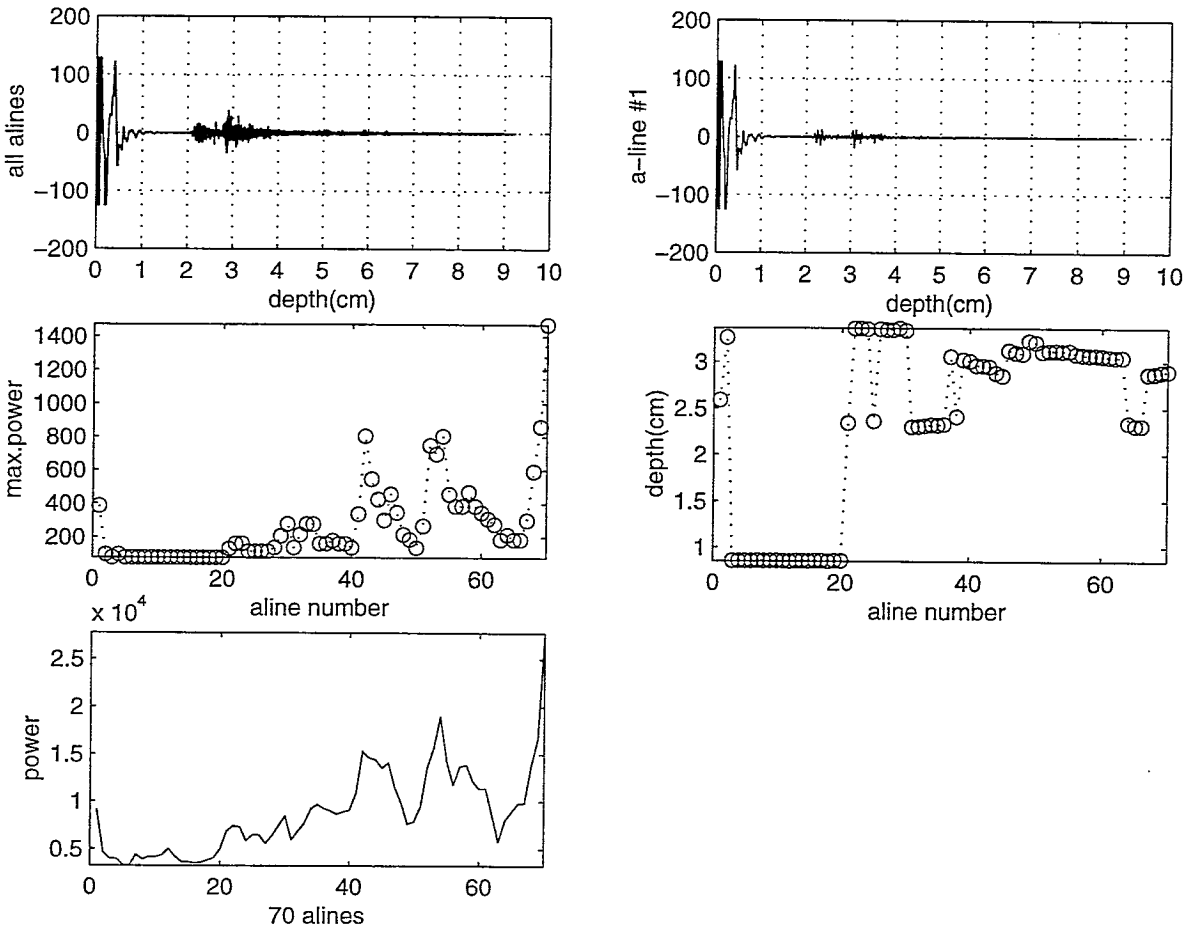
all alines
depth(cm)
a-line #1
depth(cm)
max.power
aline number
x 10^4
depth(cm)
aline number
power
70 alines

anl34g18

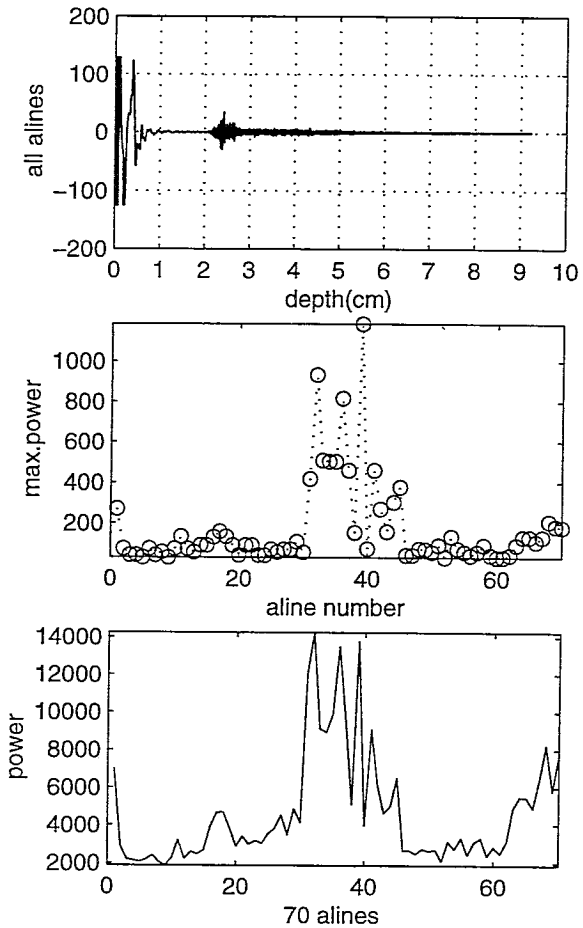
all alines
depth(cm)
max.power
aline number
power
70 alines

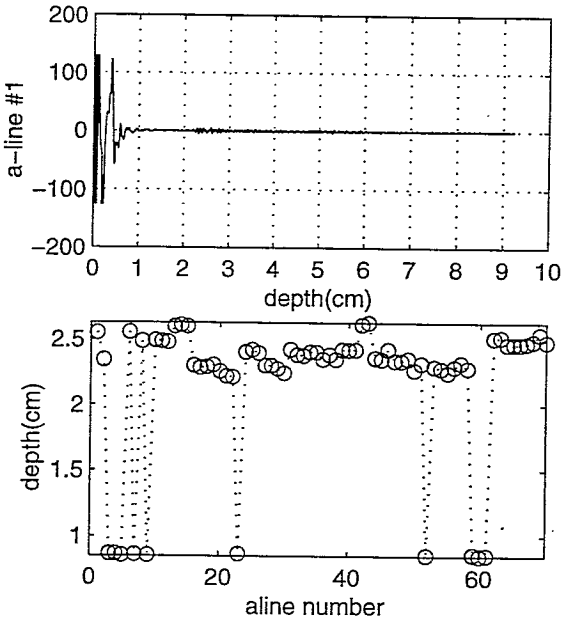
a-line #1
depth(cm)
depth(cm)
aline number

anl35g18

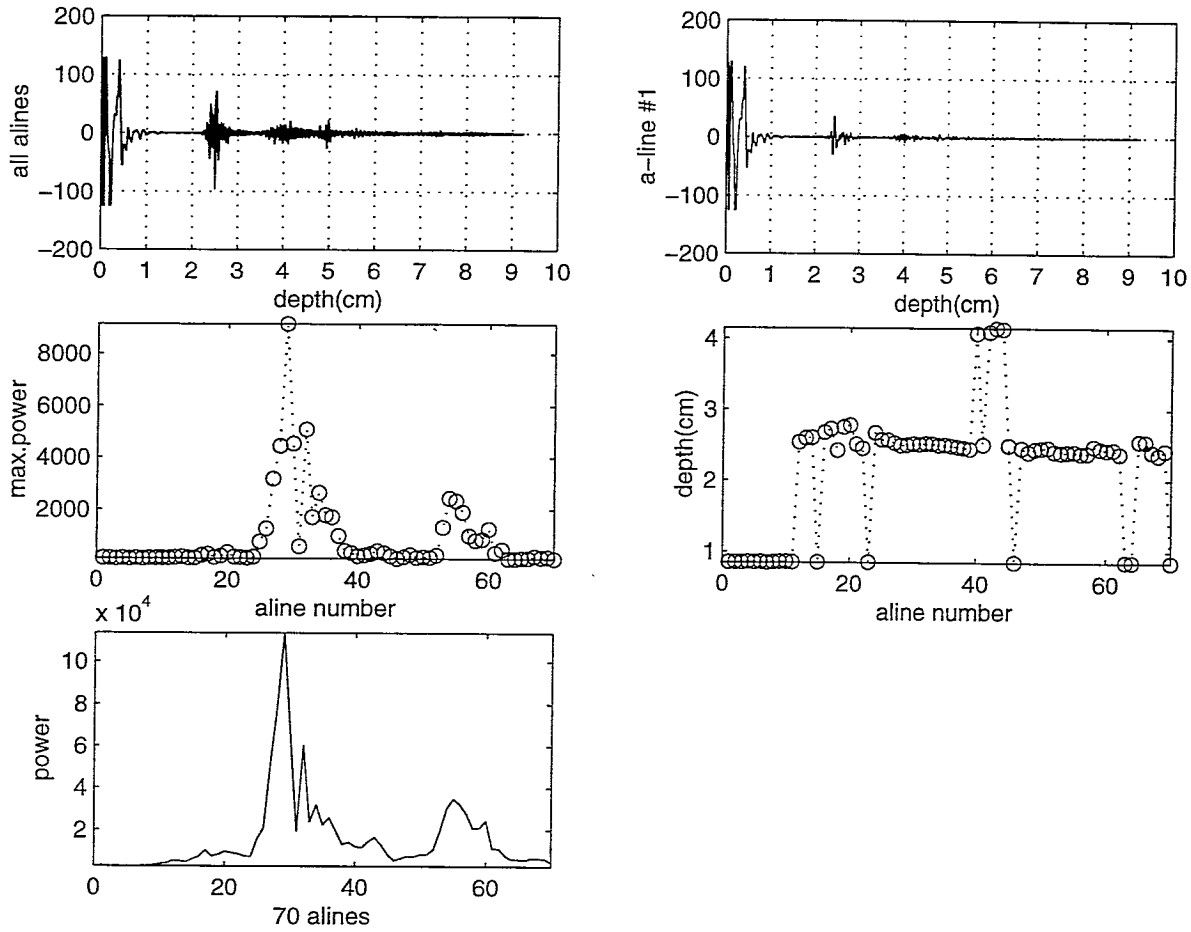
all alines
depth(cm)
a-line #1
depth(cm)
max.power
aline number
depth(cm)
aline number
x 10^4
power
70 alines

anl36g18

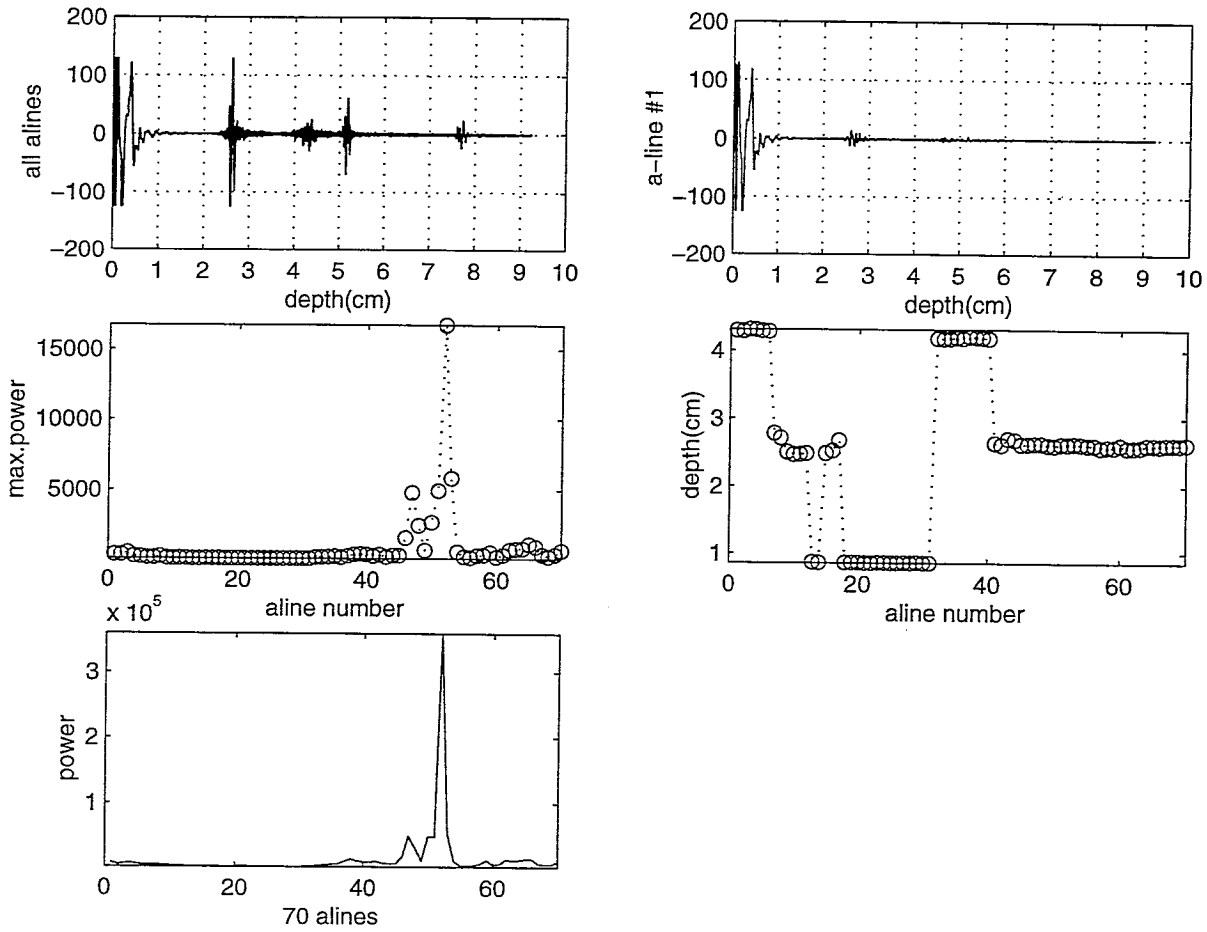
all alines
depth(cm)
a-line #1
depth(cm)
max.power
aline number
depth(cm)
aline number
x 10^5
power
70 alines

anl37g18

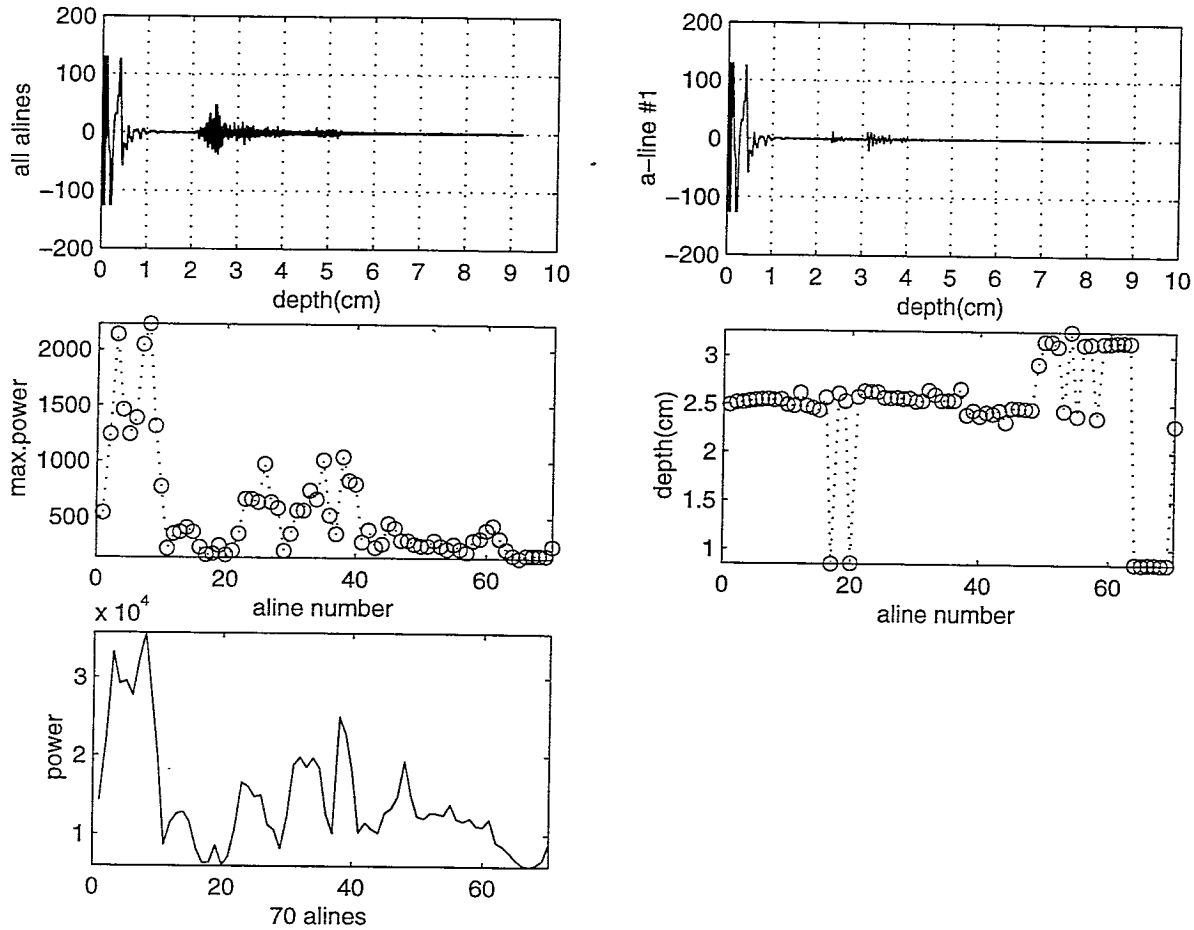
all alines
depth(cm)
a-line #1
depth(cm)
max.power
aline number
depth(cm)
aline number
x 10^4
power
70 alines

anl38g18

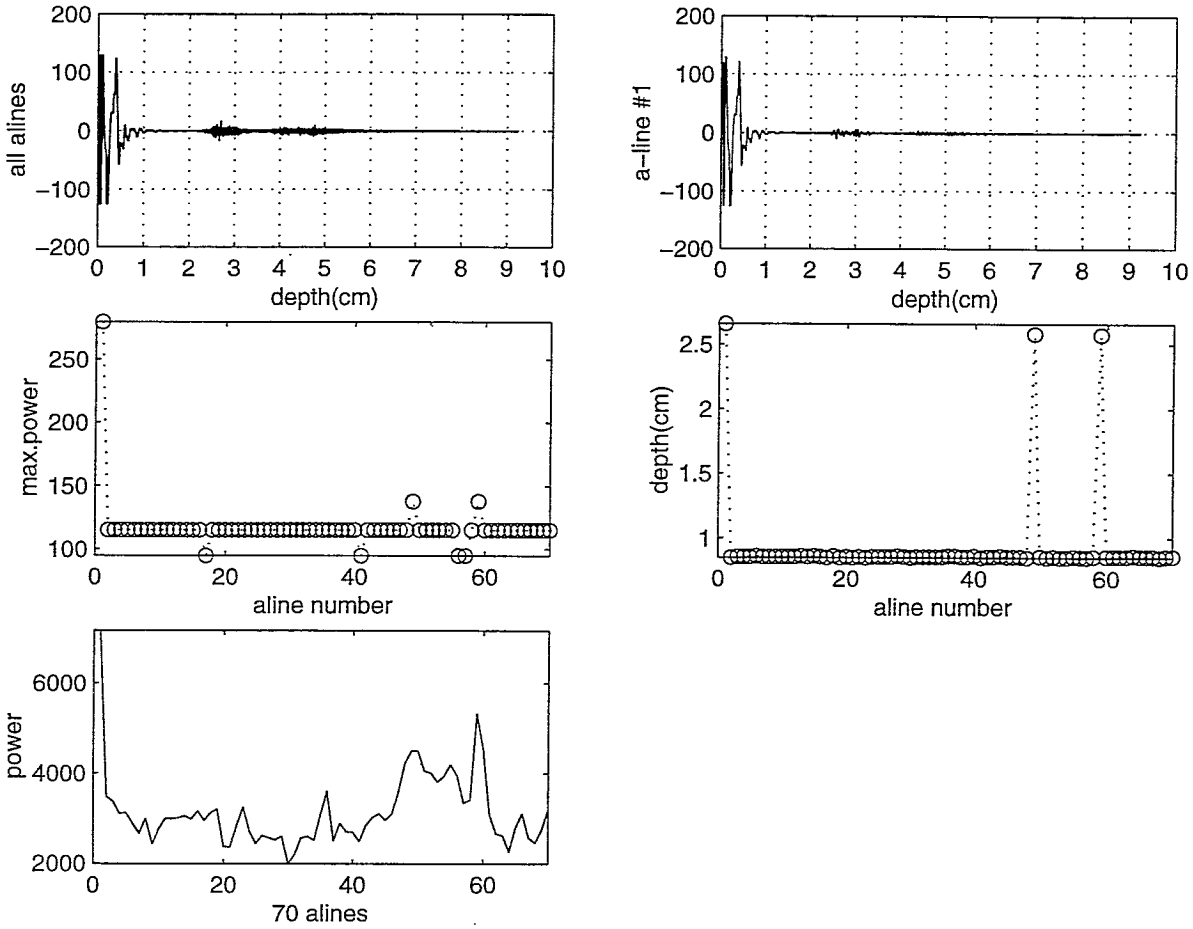
all alines
depth(cm)
a-line #1
depth(cm)
max.power
aline number
depth(cm)
aline number
power
70 alines

anl39g18

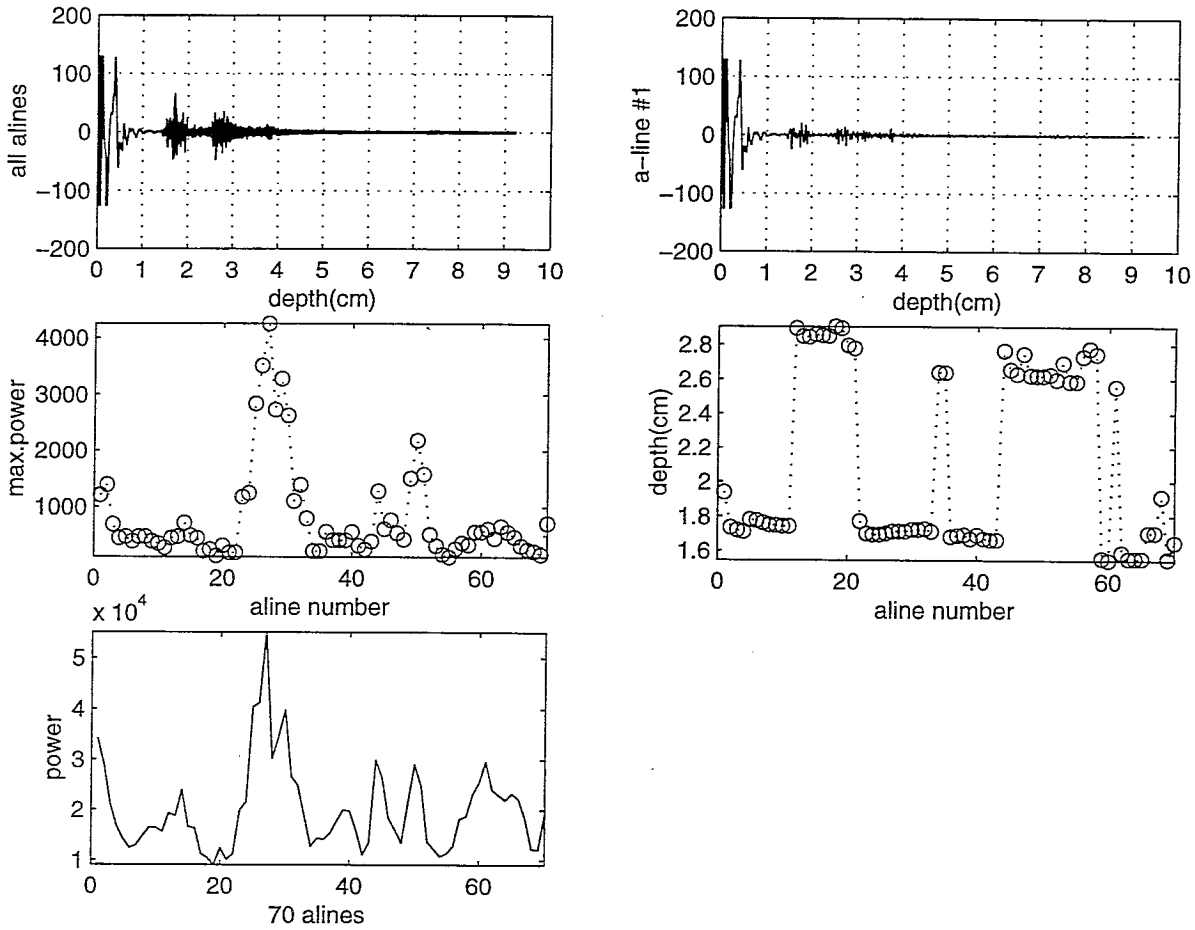
all alines
depth(cm)
a-line #1
depth(cm)
max.power
aline number
depth(cm)
aline number
x 10^4
power
70 alines

anl40g18

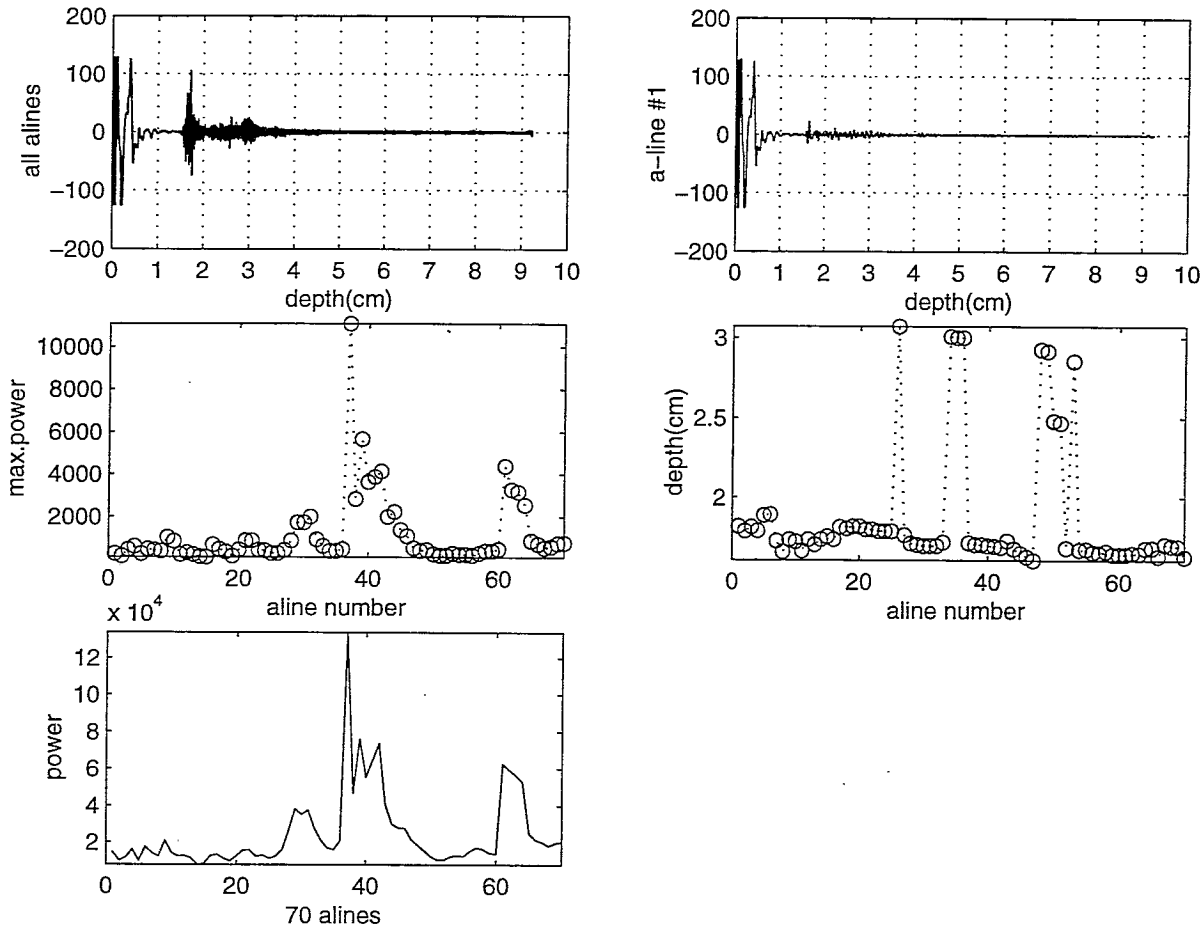
all alines
depth(cm)
a-line #1
depth(cm)
max.power
aline number
depth(cm)
aline number
x 10^4
power
70 alines

anl41g18

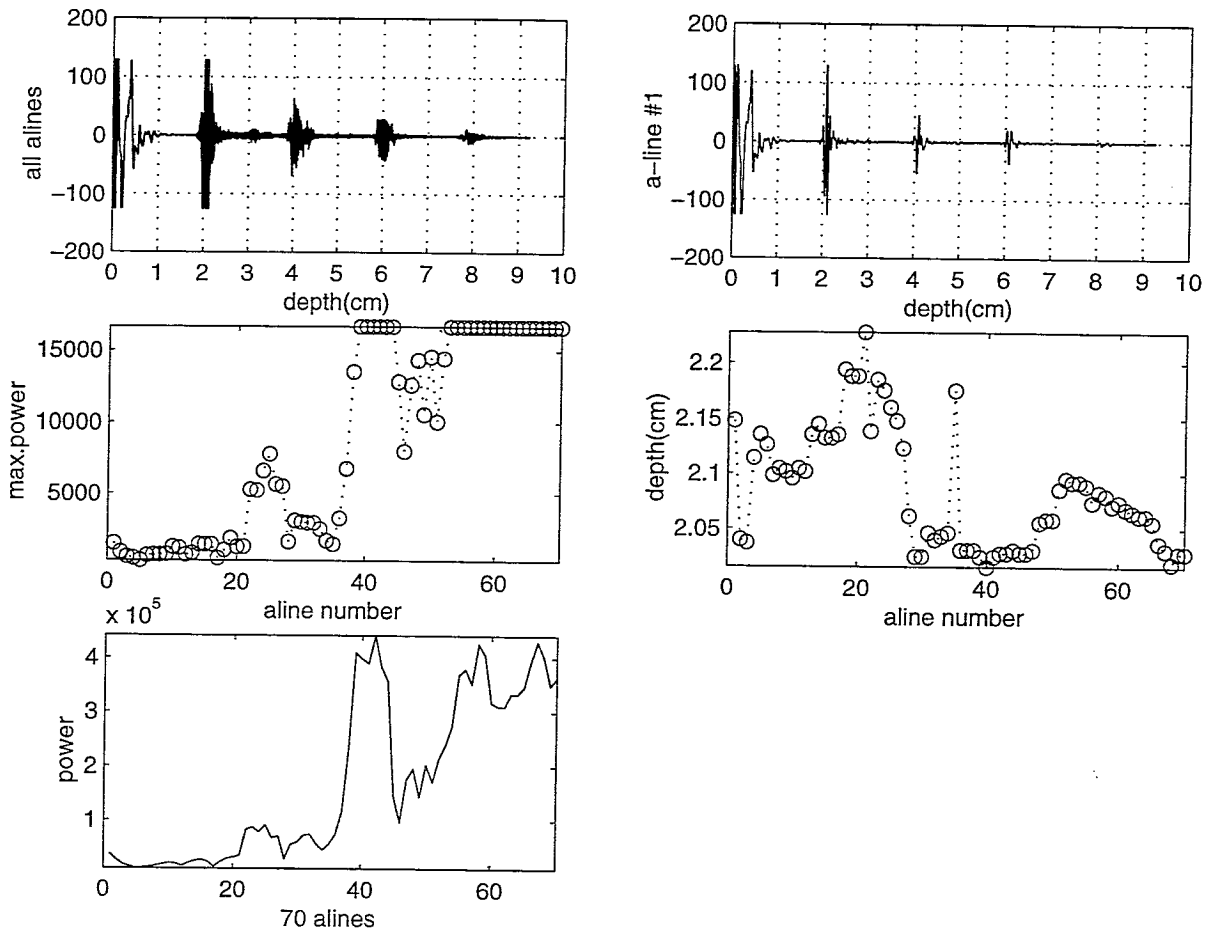
all alines
depth(cm)
a-line #1
depth(cm)
max.power
aline number
depth(cm)
aline number
x 10^5
power
70 alines

anl42g18

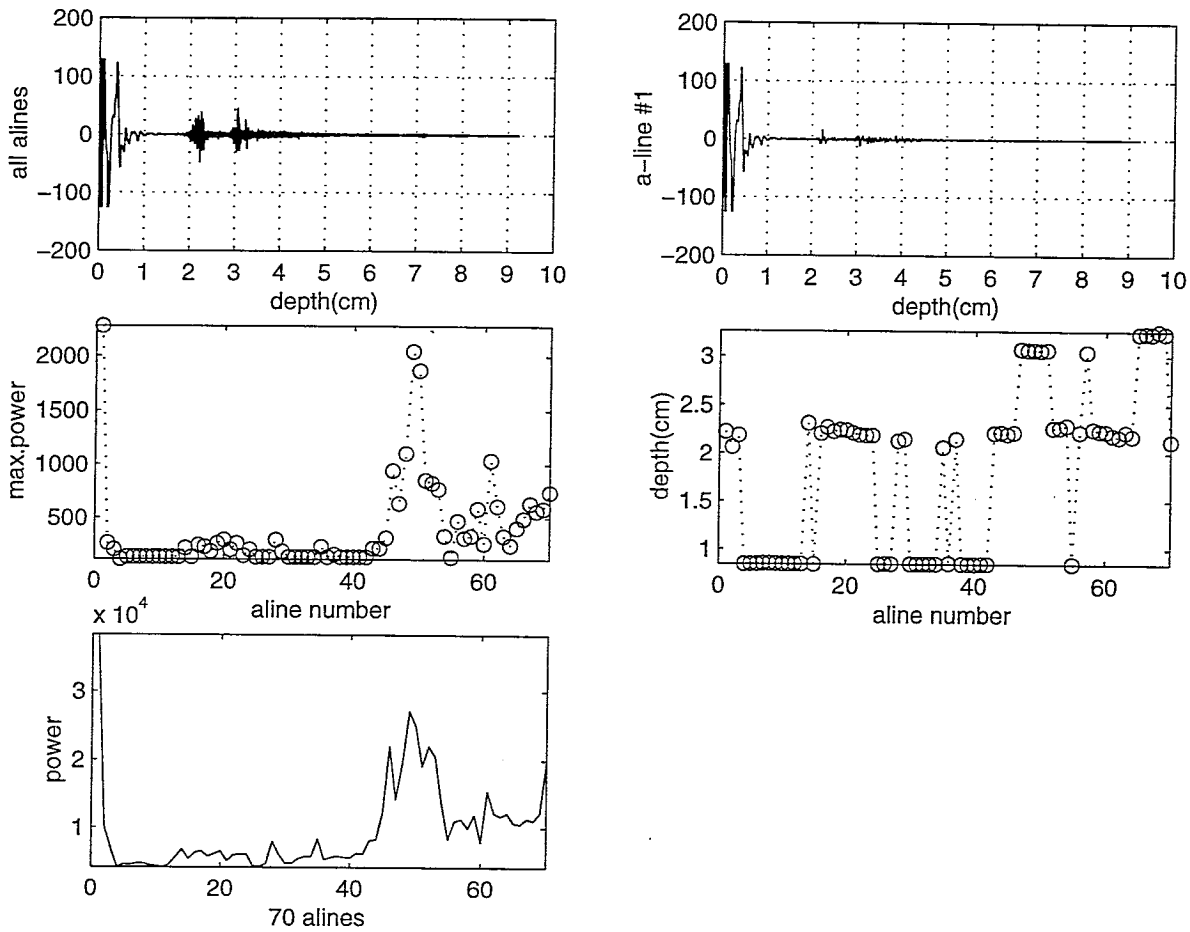
all alines
depth(cm)
a-line #1
depth(cm)
max.power
aline number
depth(cm)
aline number
x 10^4
power
70 alines

anl43g18

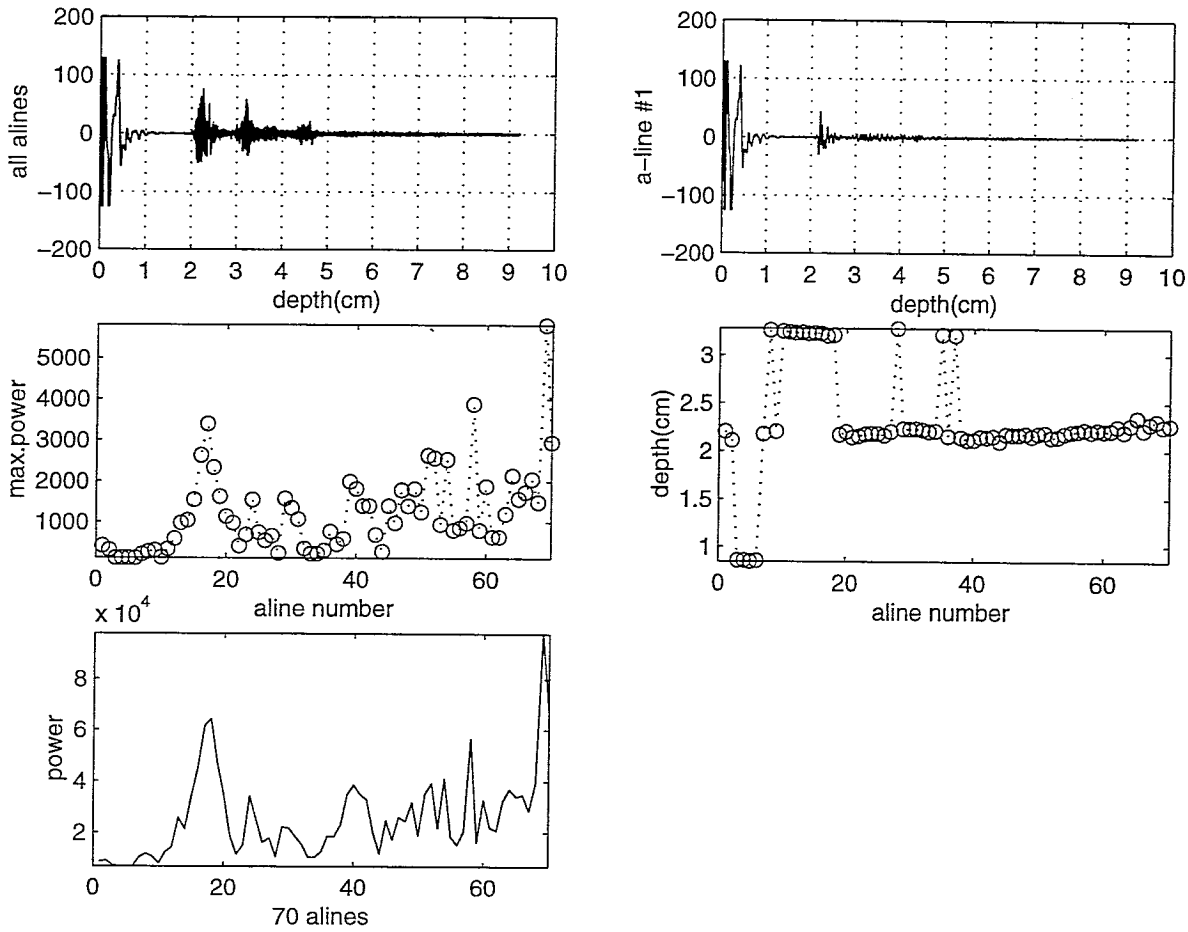
all alines
depth(cm)
a-line #1
depth(cm)
max.power
aline number
depth(cm)
aline number
x 10^4
power
70 alines

anl44g18

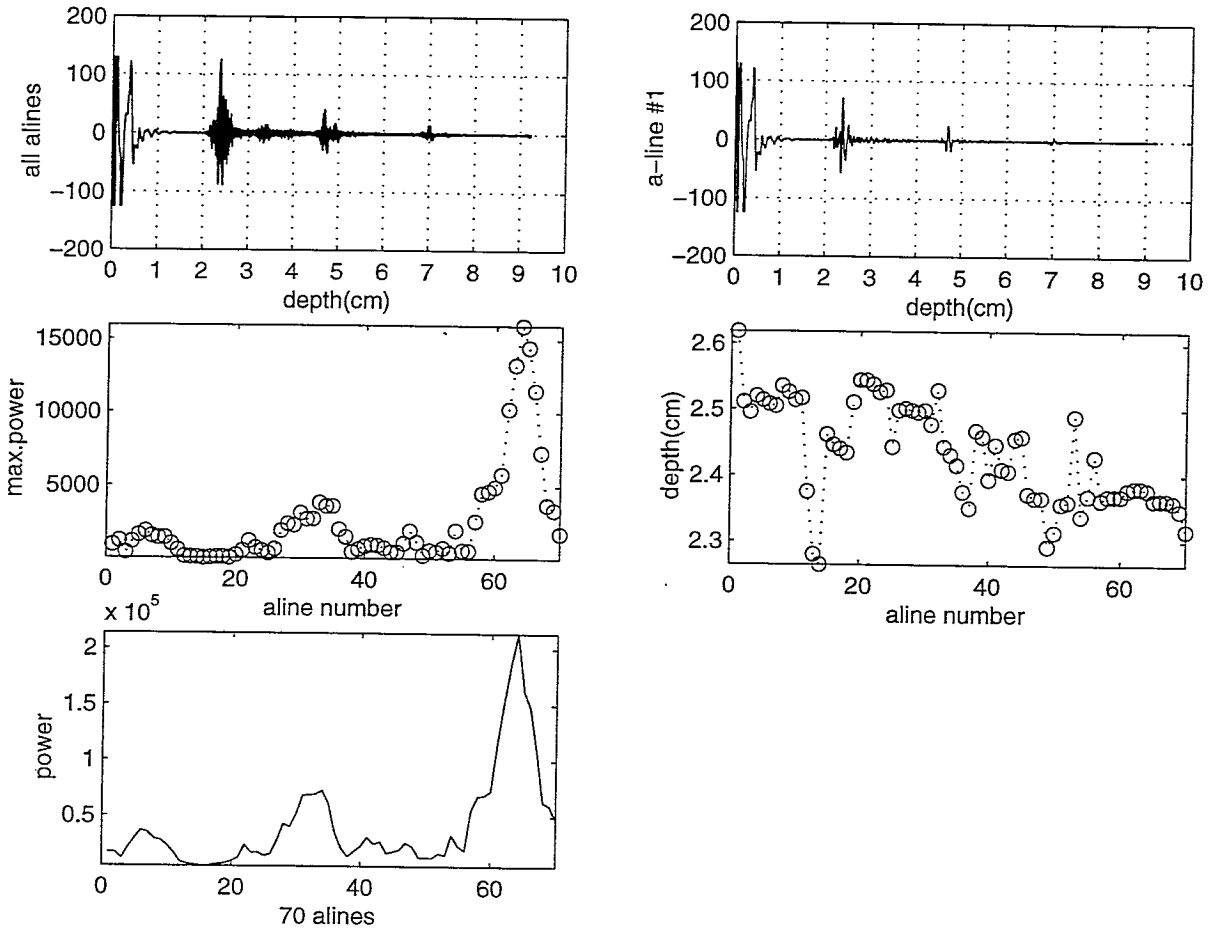
all alines
depth(cm)
a-line #1
depth(cm)
max.power
aline number
depth(cm)
aline number
x 10^5
power
70 alines

anl45g18

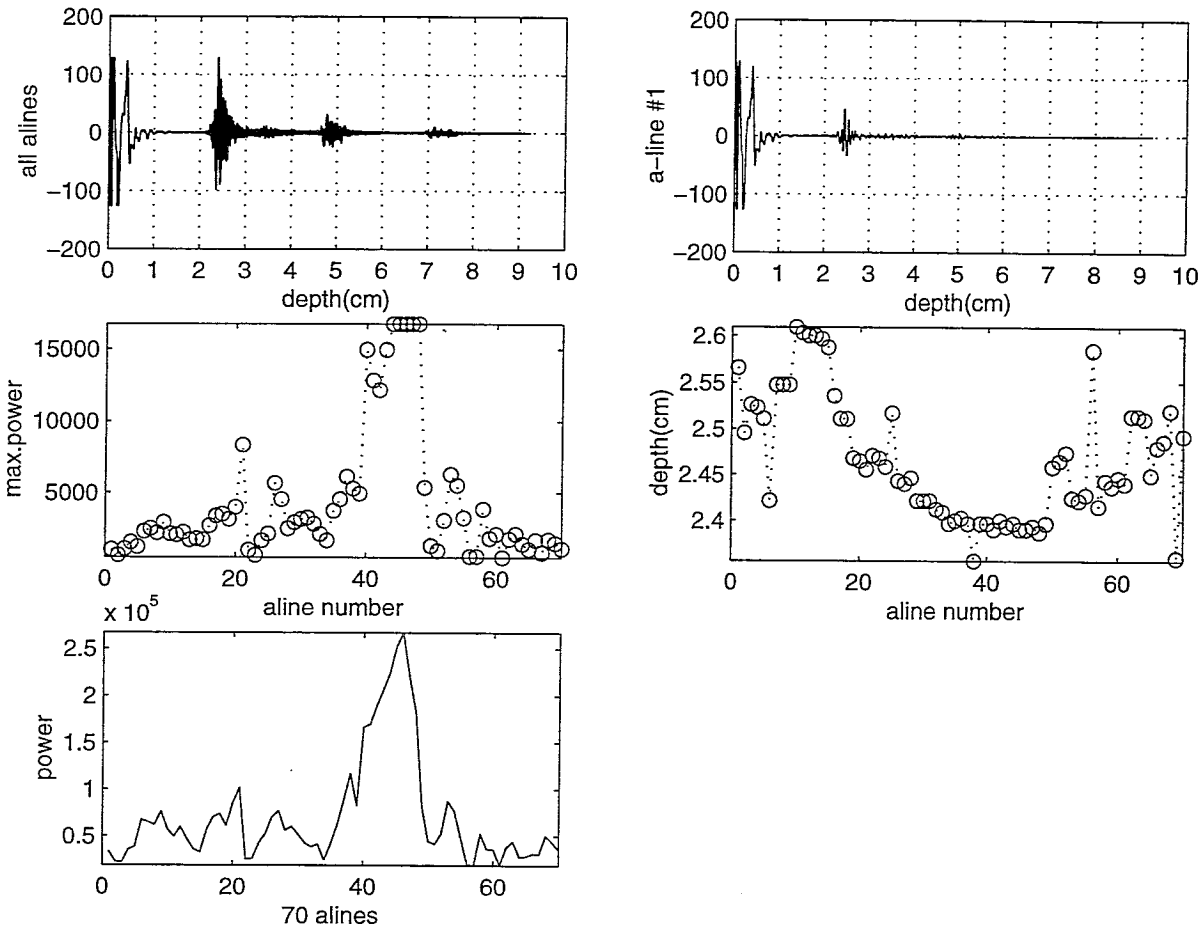
all alines
depth(cm)
a-line #1
depth(cm)
max.power
aline number
depth(cm)
aline number
x 10^5
power
70 alines

anl46g18

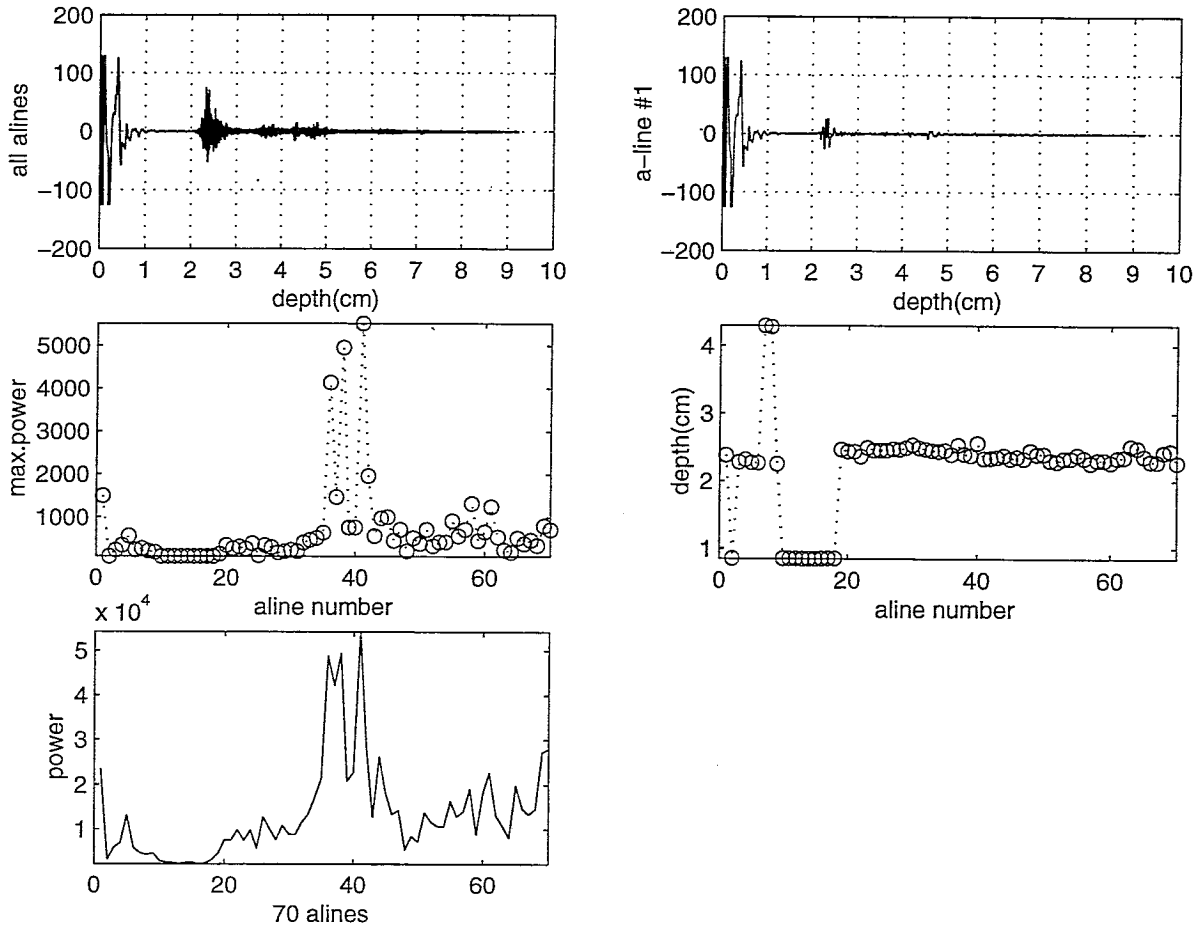
all alines
depth(cm)
a-line #1
depth(cm)
max.power
aline number
depth(cm)
aline number
x 10^4
power
70 alines

anl47g18

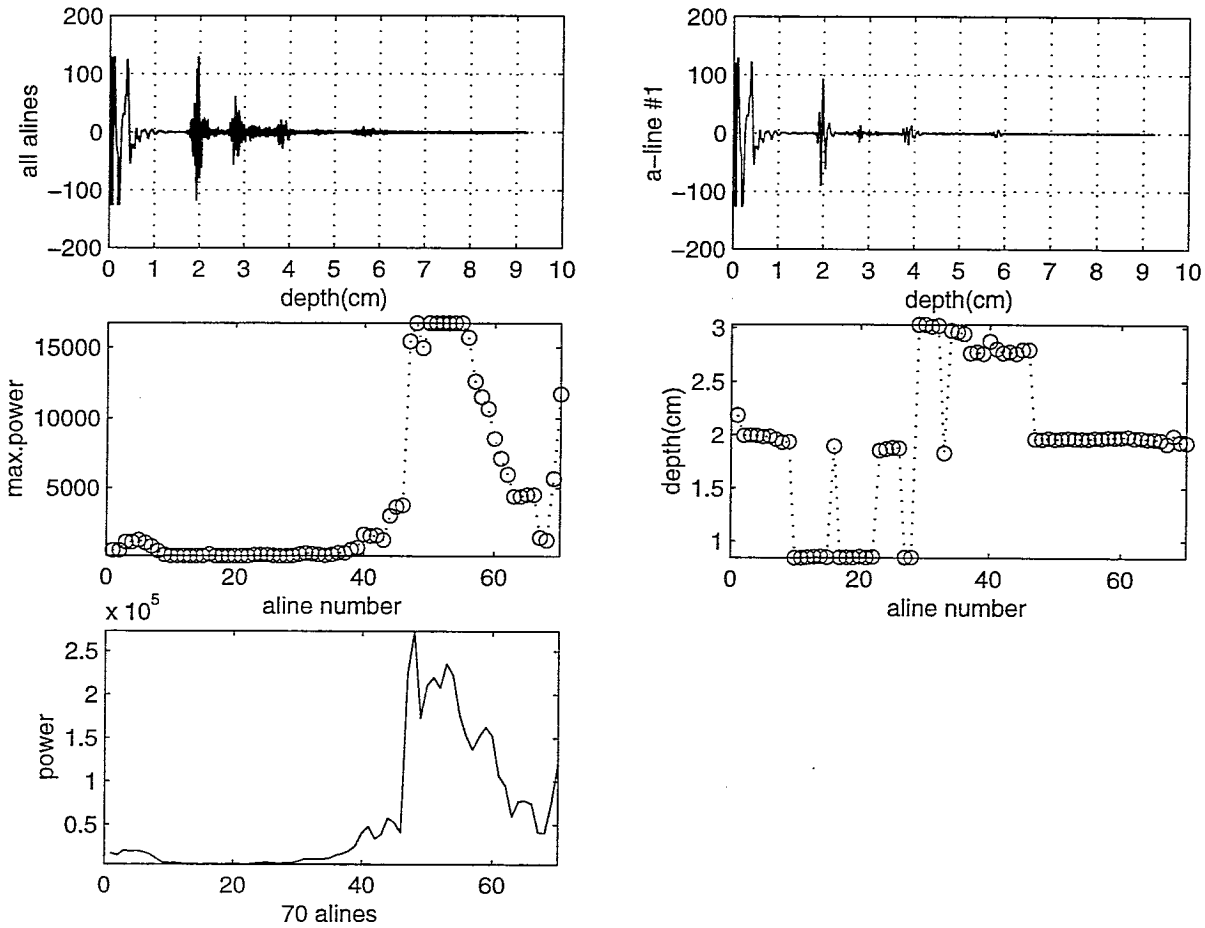
all alines
depth(cm)
a-line #1
depth(cm)
max.power
aline number
depth(cm)
aline number
x 10^5
power
70 alines

anl49g18

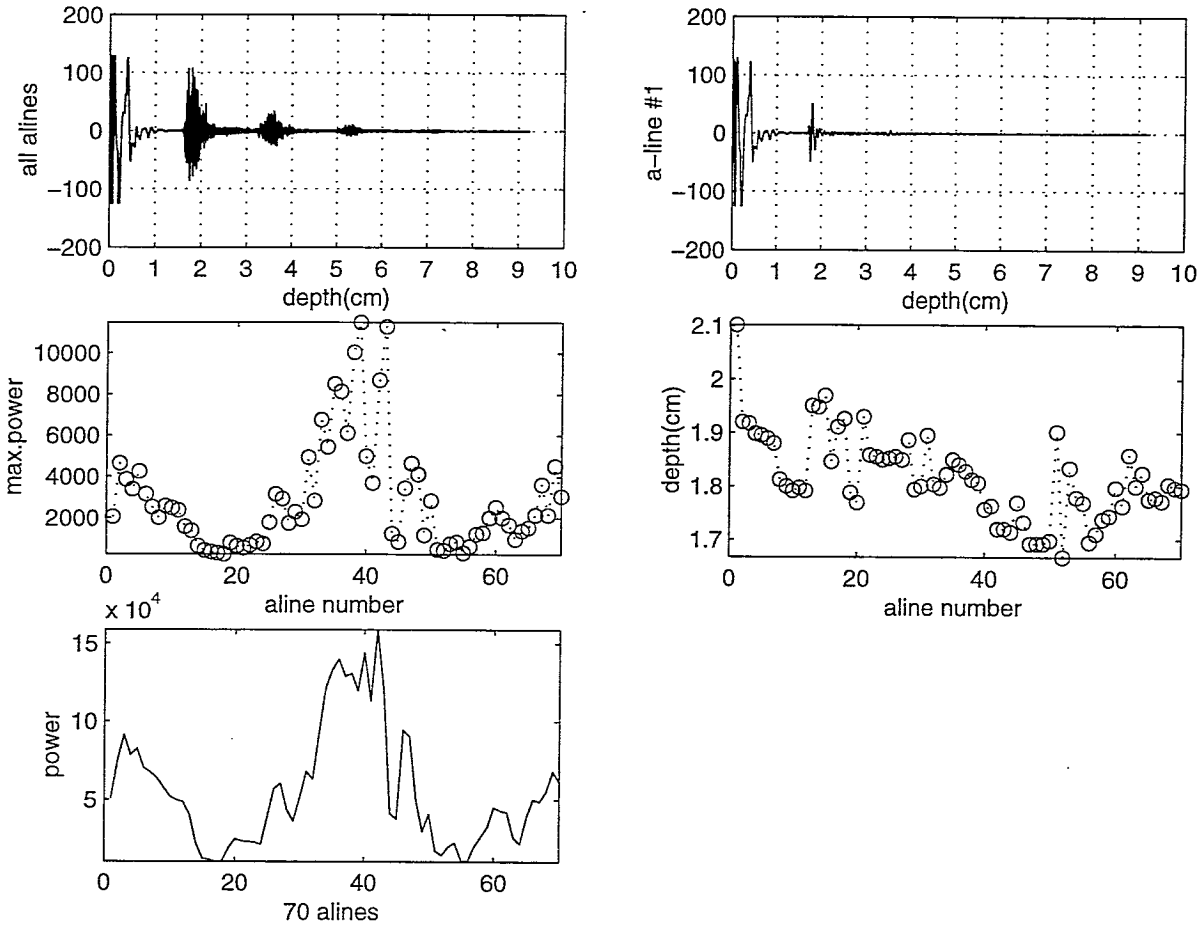
all alines
depth(cm)
a–line #1
depth(cm)
max.power
aline number
depth(cm)
aline number
x 10^4
power
70 alines

anl50g18

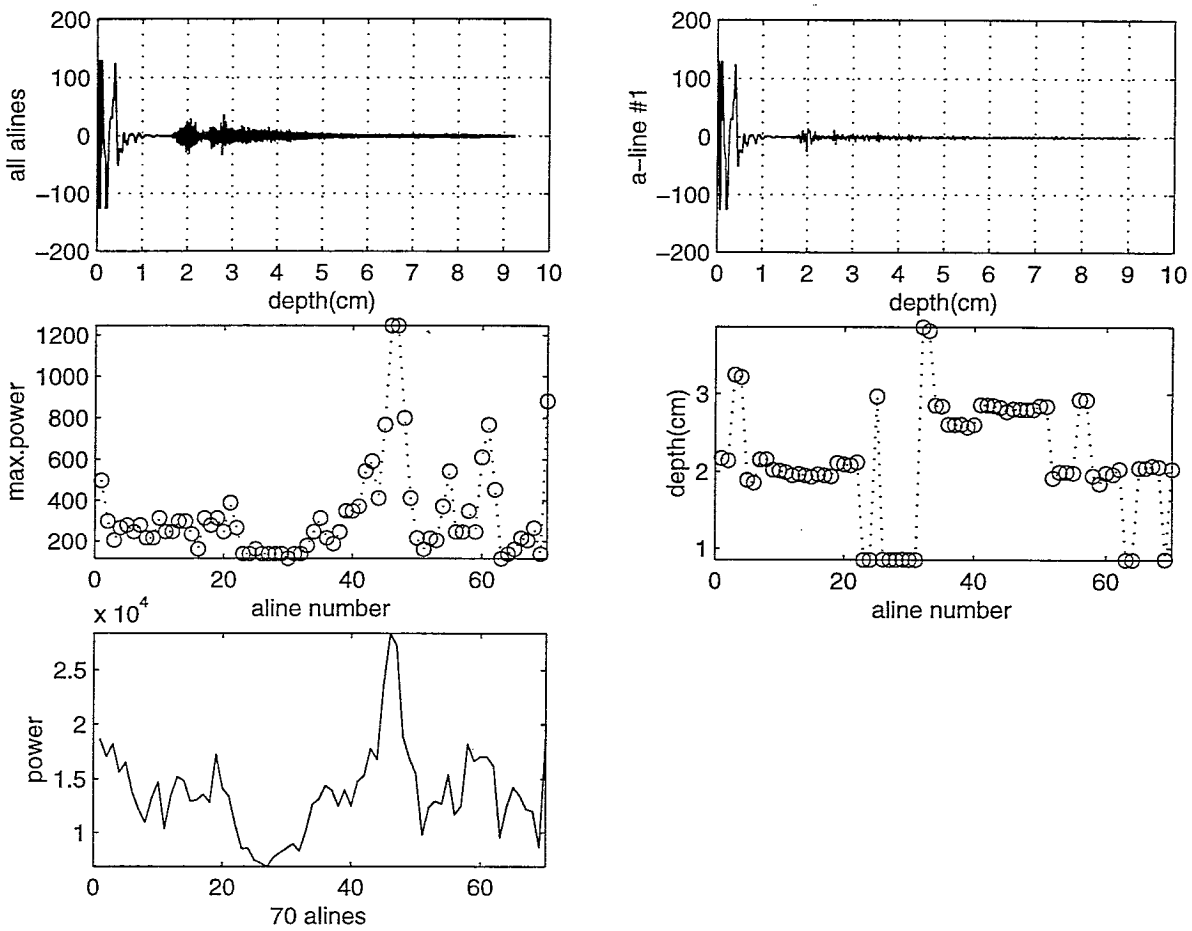
all alines
depth(cm)
a-line #1
depth(cm)
max.power
aline number
depth(cm)
aline number
x 10^4
power
70 alines

anl51g18

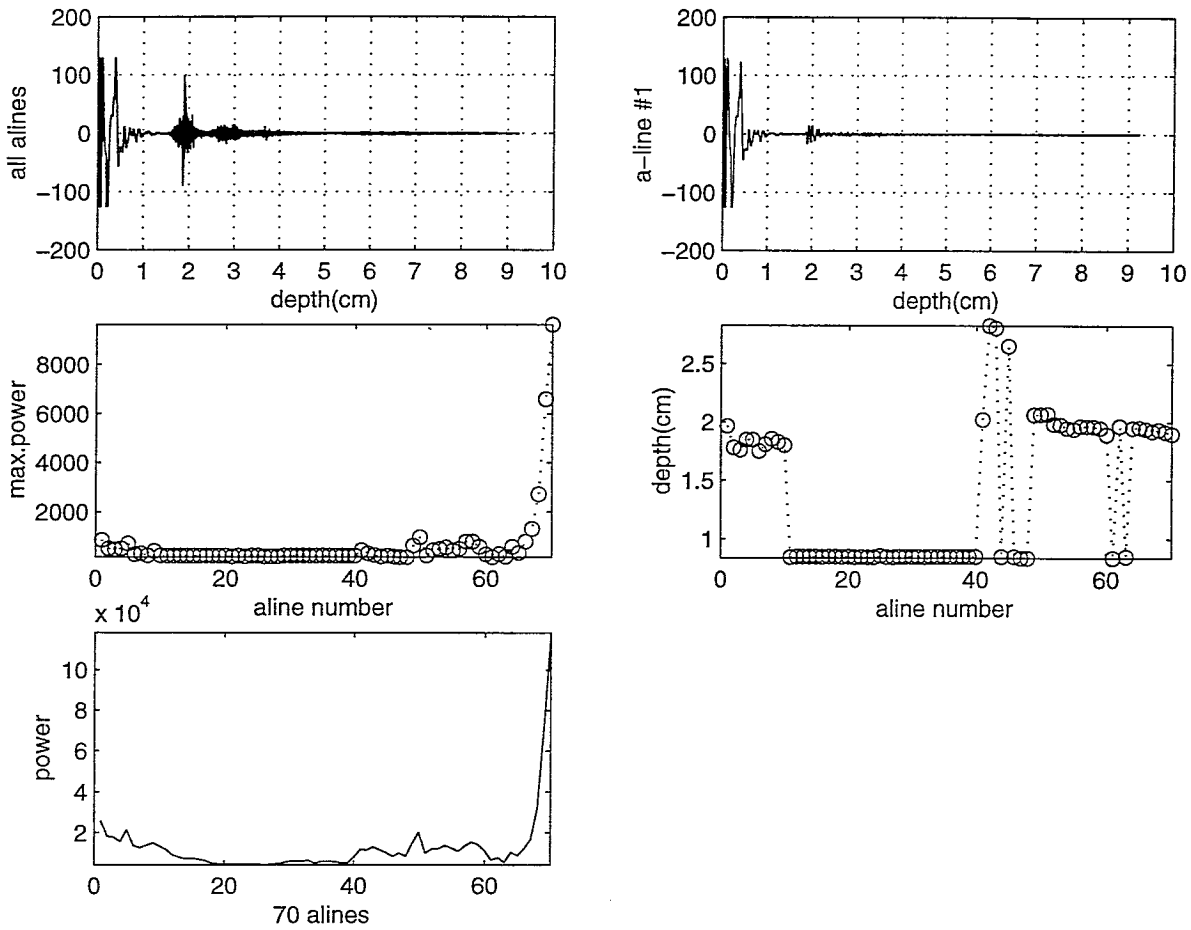
all alines
depth(cm)
a-line #1
depth(cm)
max.power
aline number
depth(cm)
aline number
x 10^4
power
70 alines

anl52g18

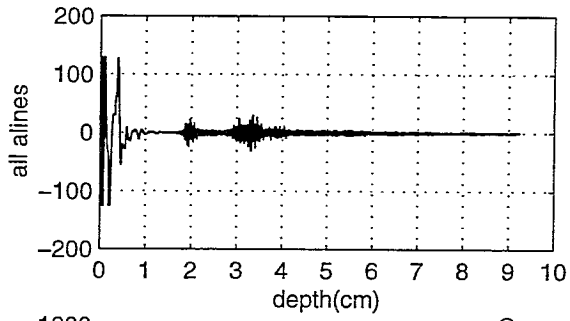
all alines
depth(cm)

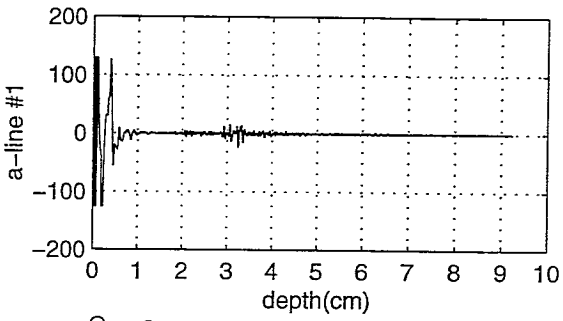
a-line #1
depth(cm)

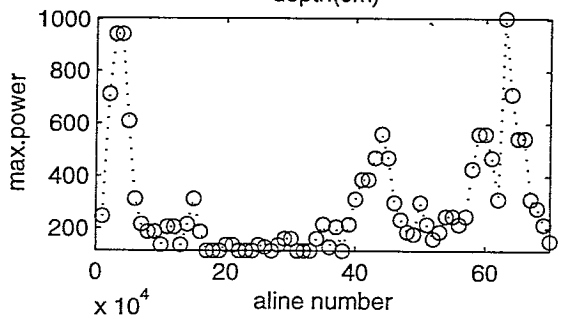
max.power
aline number

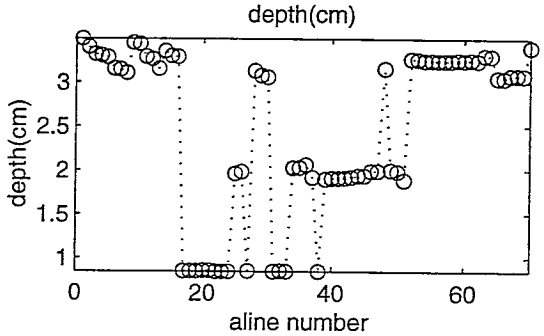
depth(cm)
aline number

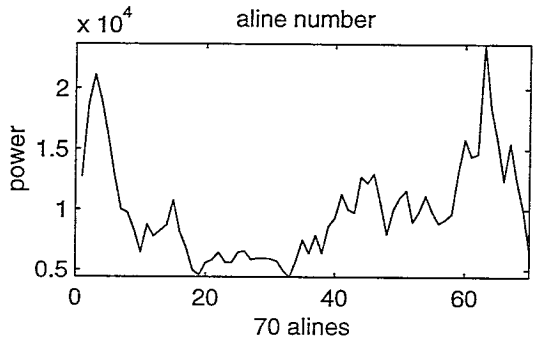
x 10^4
power
70 alines

anl53g18

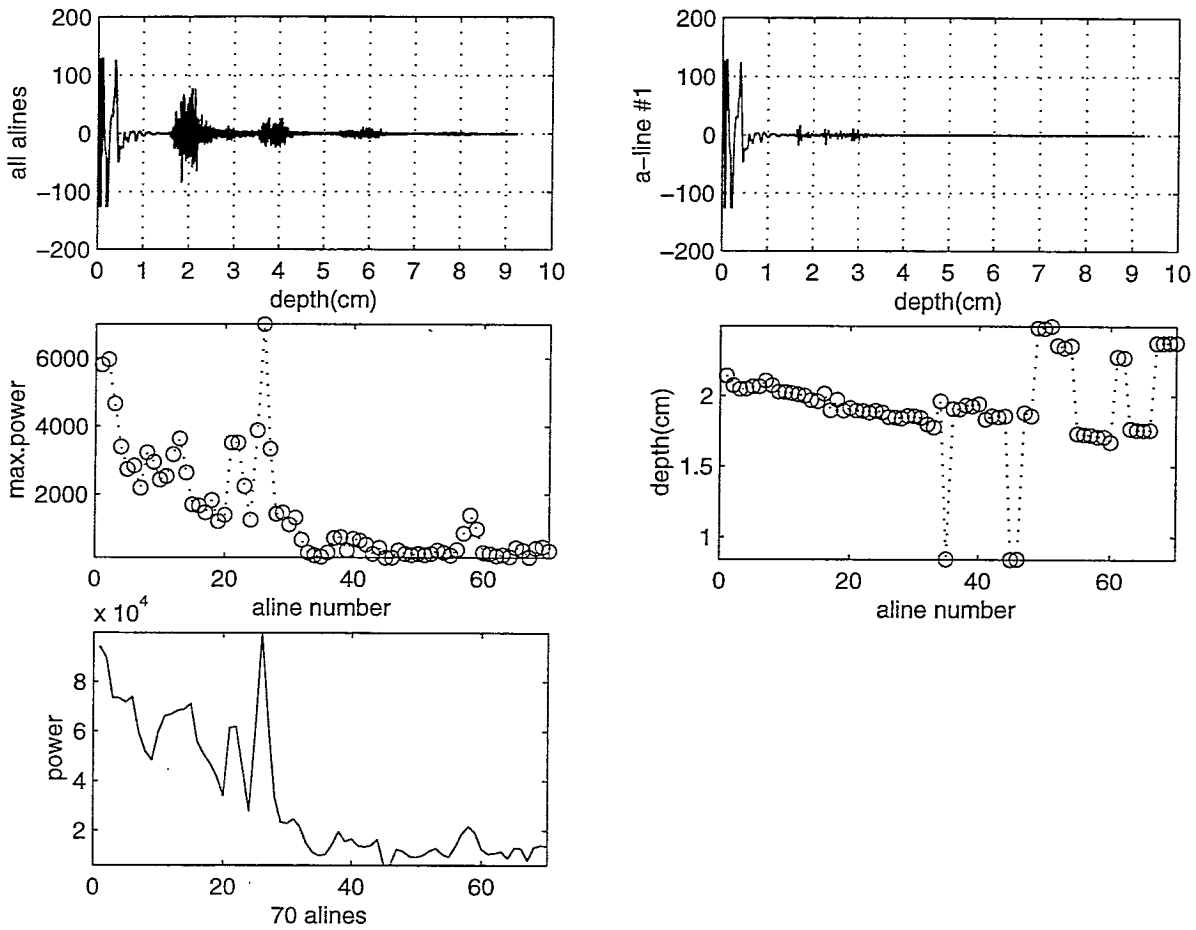
all alines
depth(cm)
a-line #1
depth(cm)
max.power
aline number
depth(cm)
aline number
x 10^4
power
70 alines

anl54g18

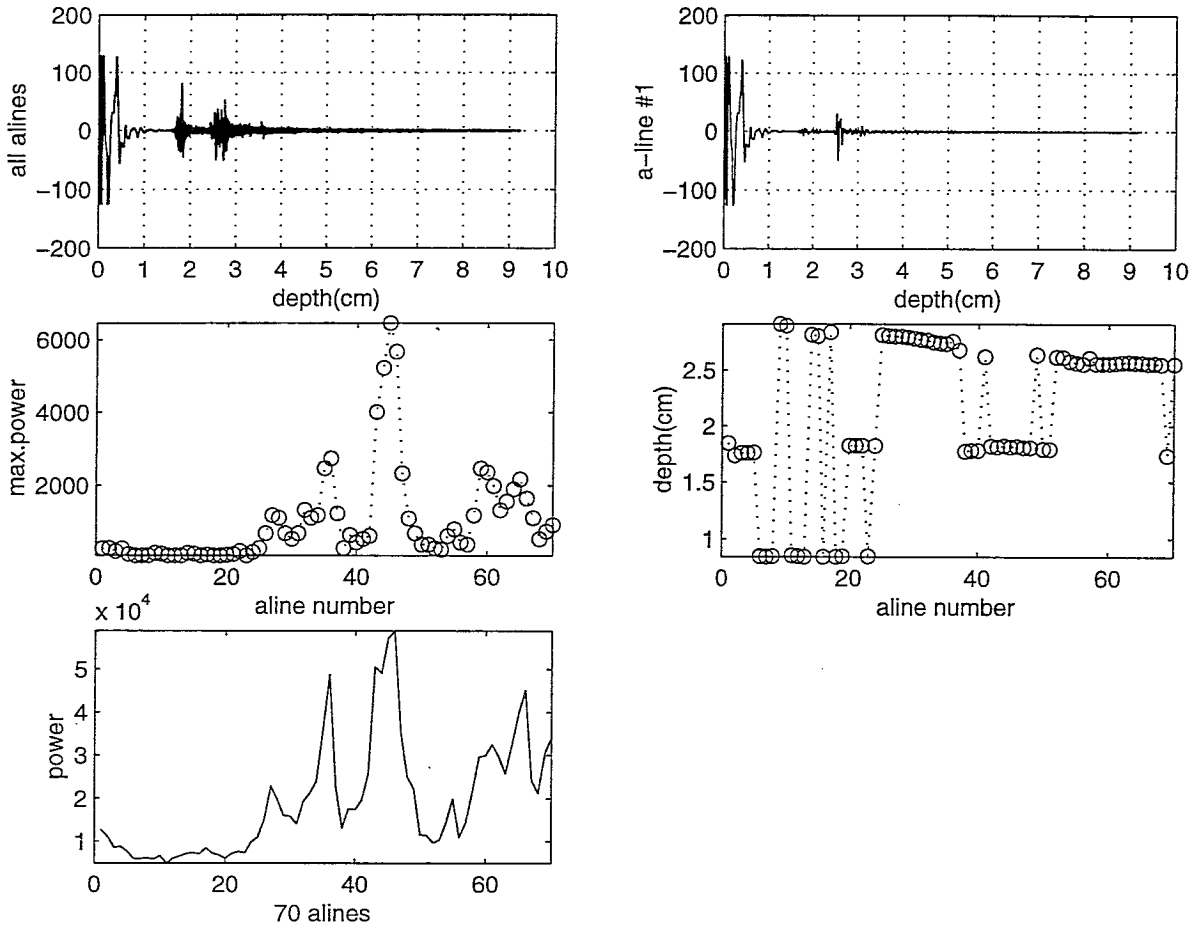
all alines
depth(cm)
a-line #1
depth(cm)
max.power
aline number
depth(cm)
aline number
x 10^4
power
70 alines

anl55g18

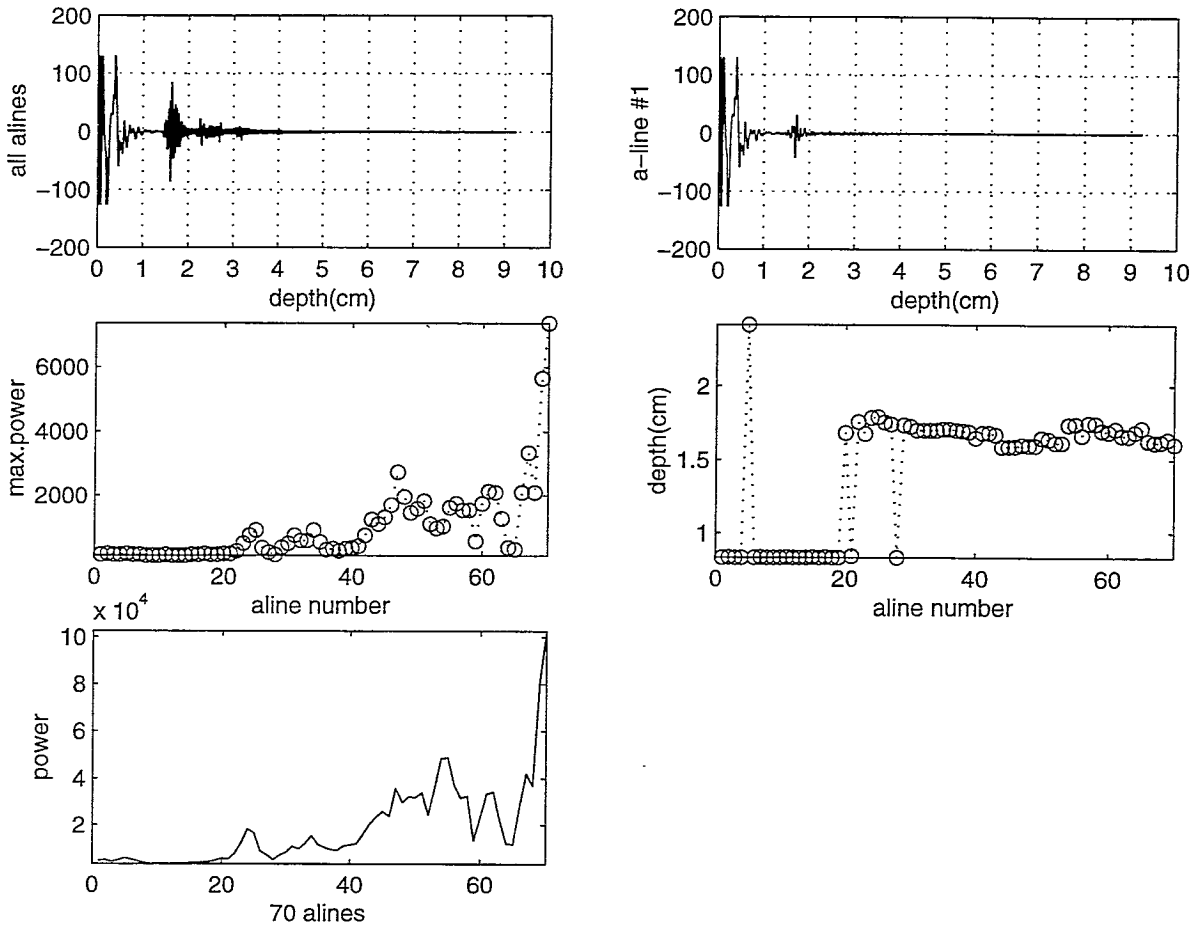
all alines
depth(cm)
a–line #1
depth(cm)
max.power
aline number
depth(cm)
aline number
x 10^4
power
70 alines

anl56g18

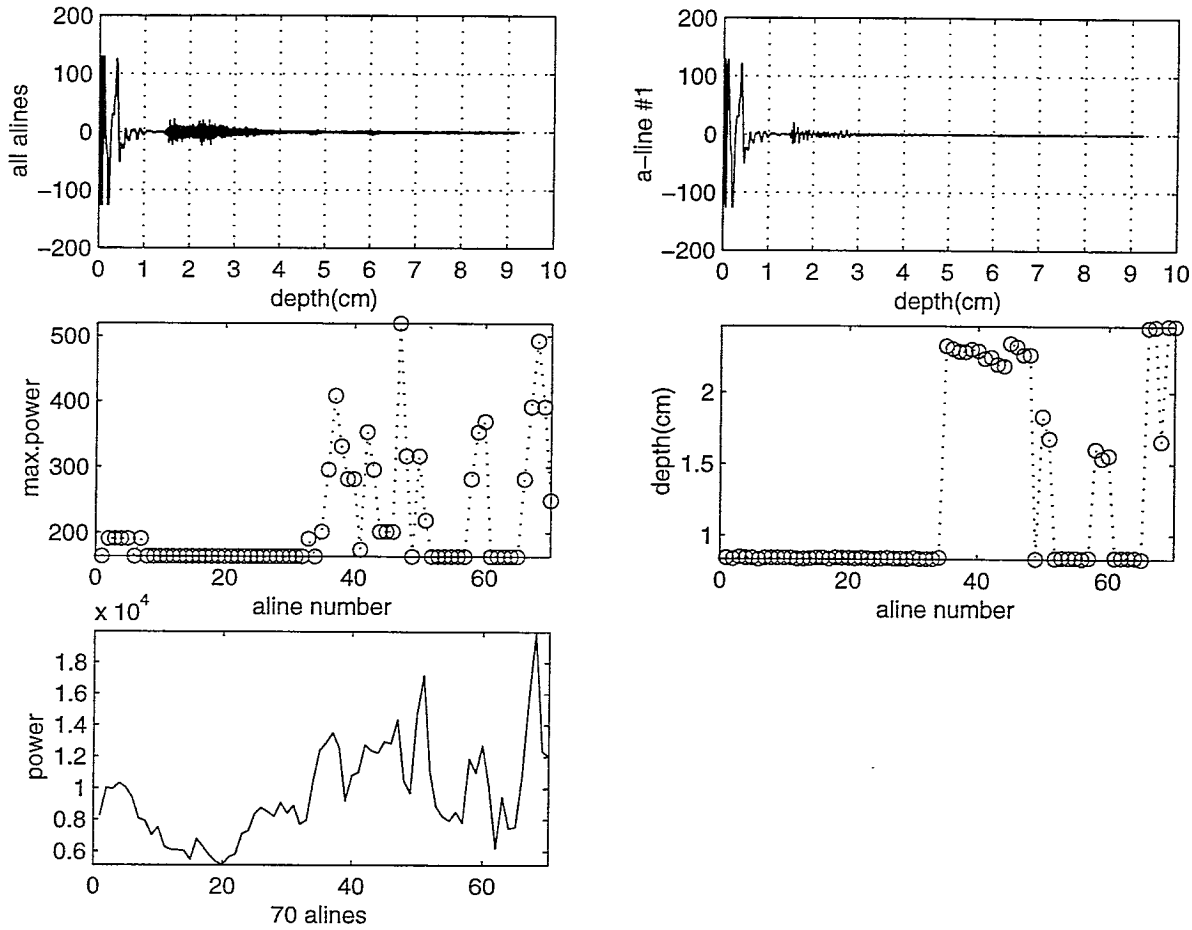
all alines
depth(cm)
a-line #1
depth(cm)
max.power
aline number
depth(cm)
aline number
x 10^4
power
70 alines

anl57g18

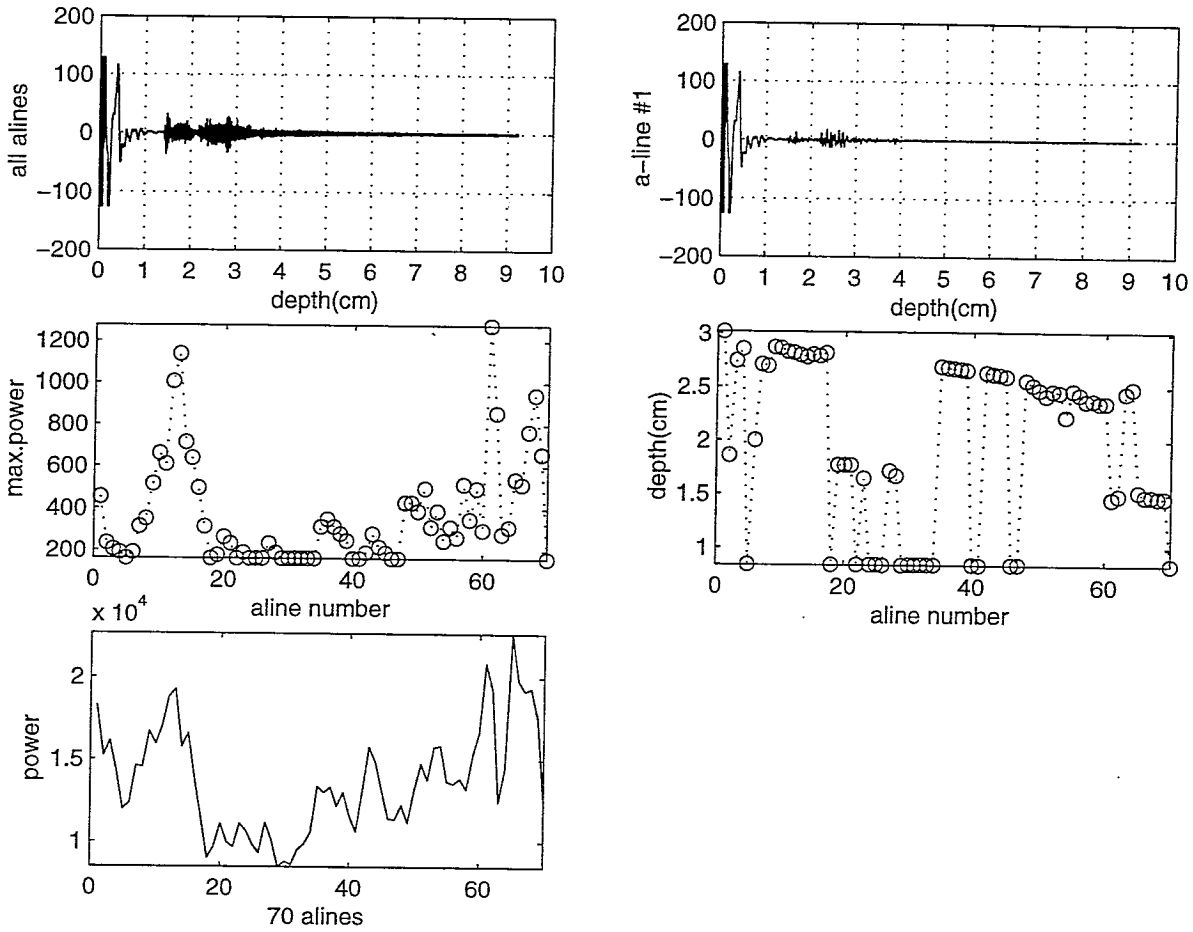
all alines
depth(cm)
a-line #1
depth(cm)
max.power
x 10^4
aline number
depth(cm)
aline number
power
70 alines

anl58g18

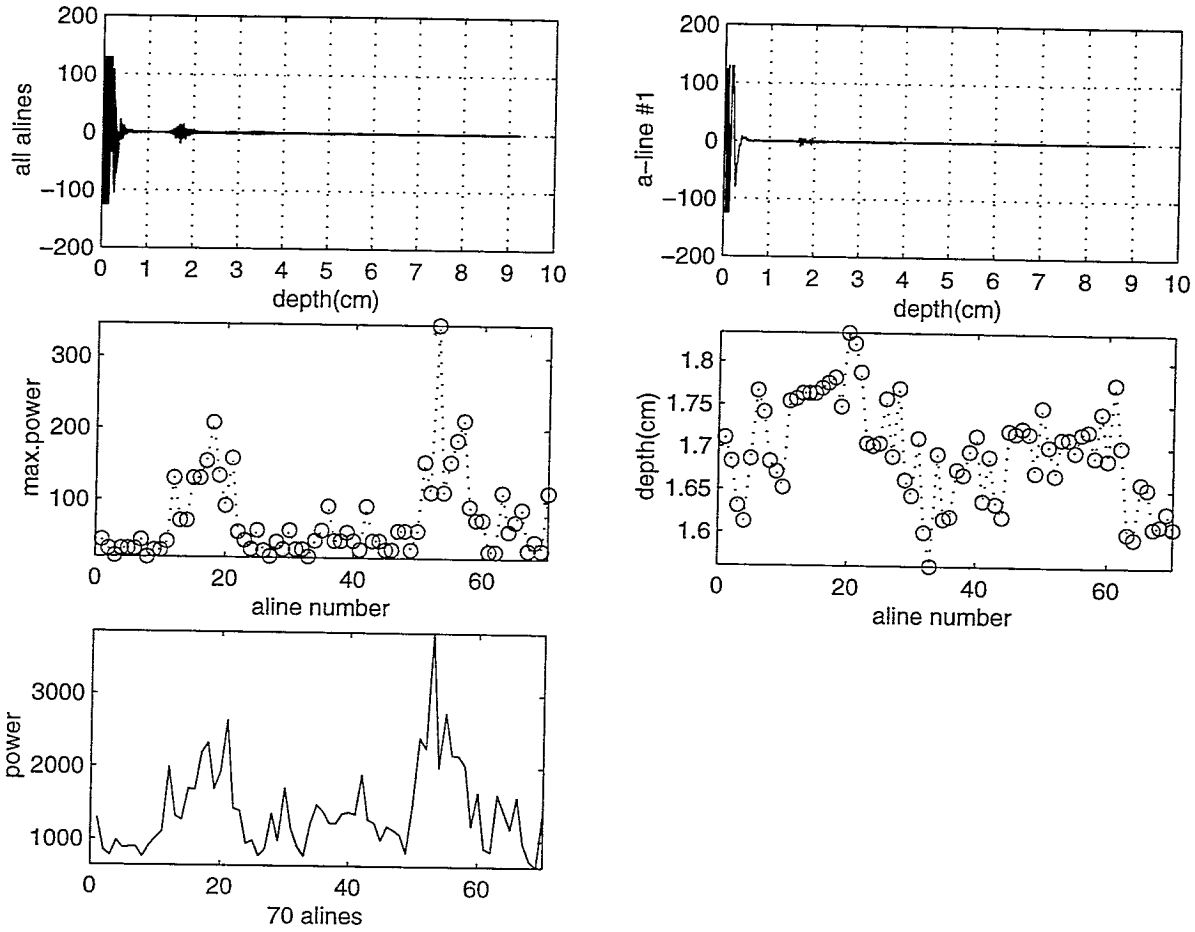
all alines
depth(cm)
a-line #1
depth(cm)
max.power
aline number
depth(cm)
aline number
power
70 alines

anl59g18

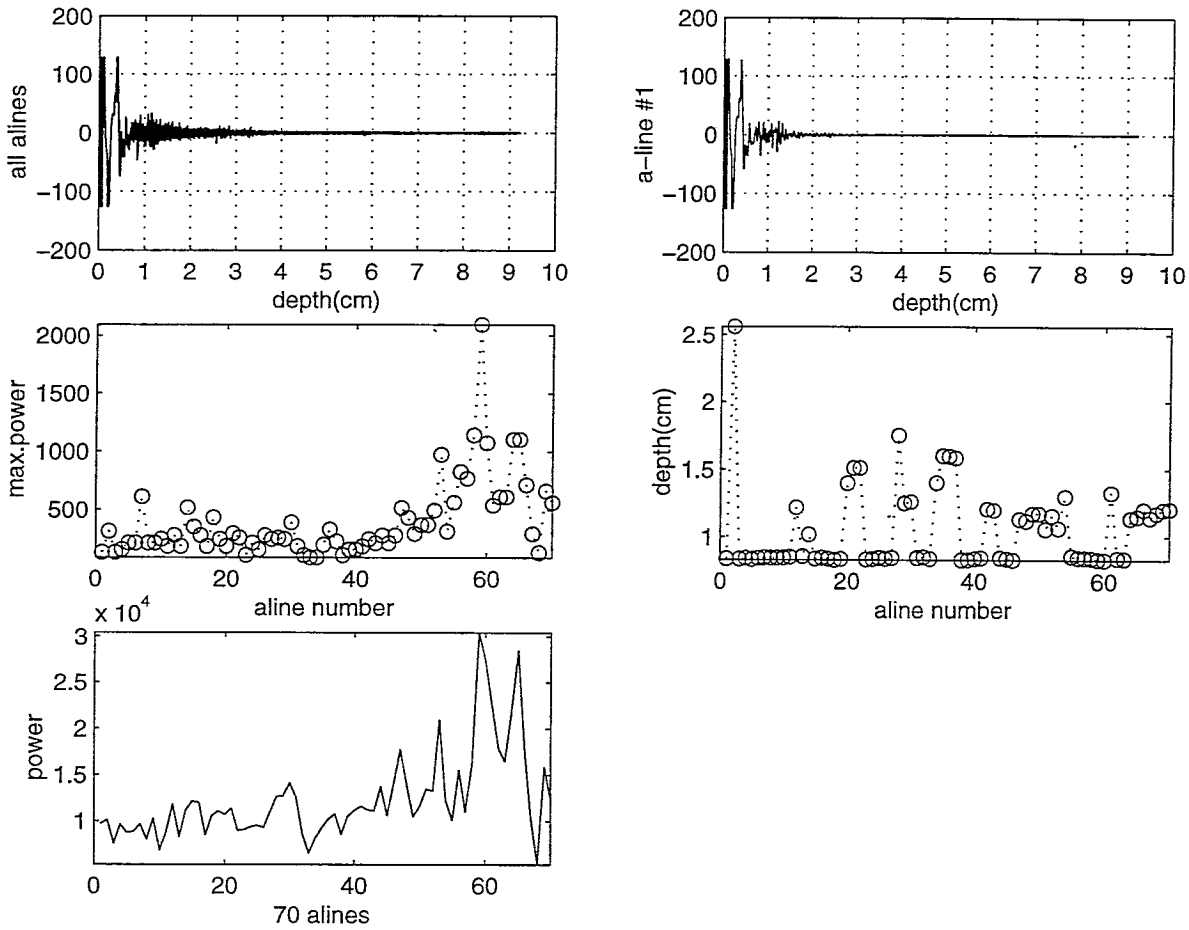
all alines
depth(cm)
a-line #1
depth(cm)
max.power
aline number
depth(cm)
aline number
x 10^4
power
70 alines

anl60g18

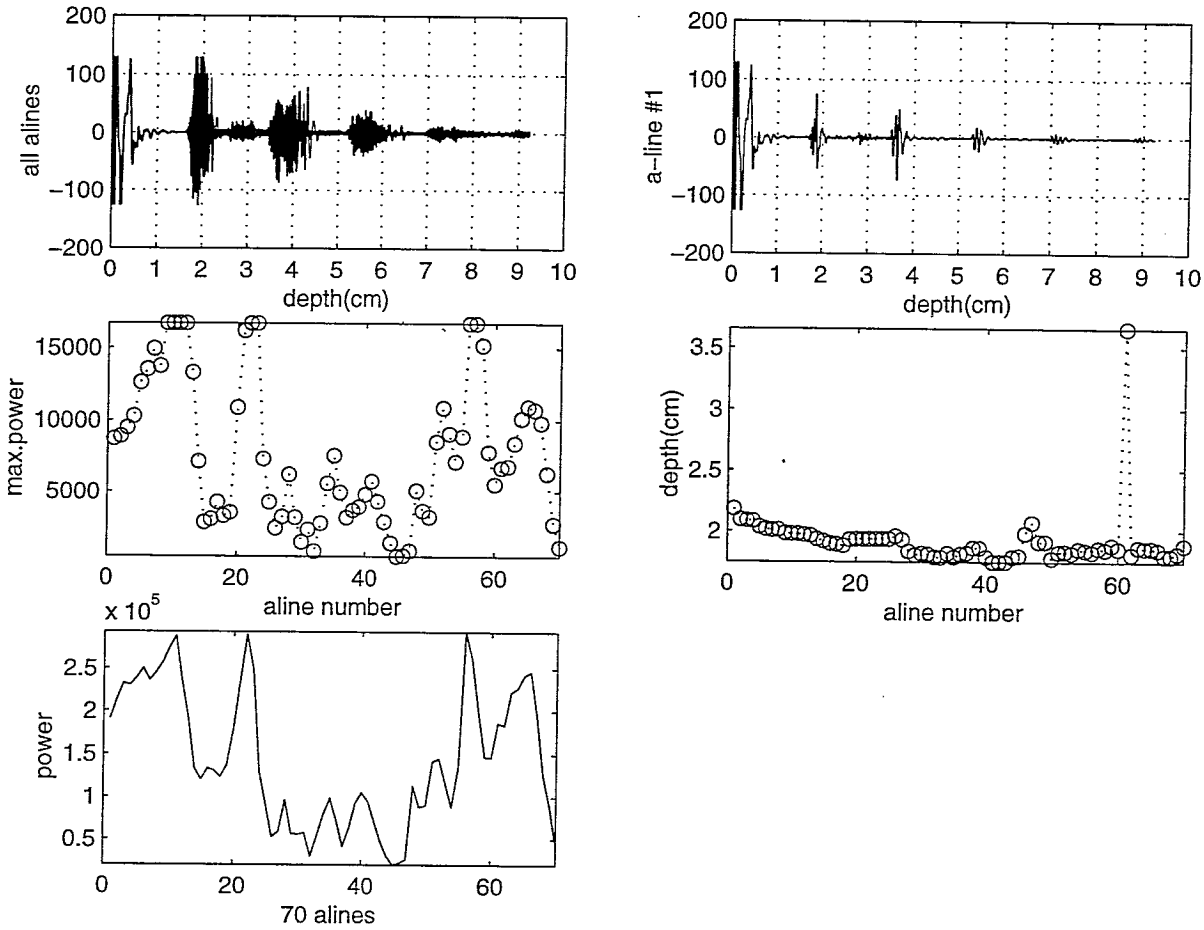
all alines
depth(cm)
a-line #1
depth(cm)
max.power
aline number
depth(cm)
aline number
x 10^5
power
70 alines

anl61g18

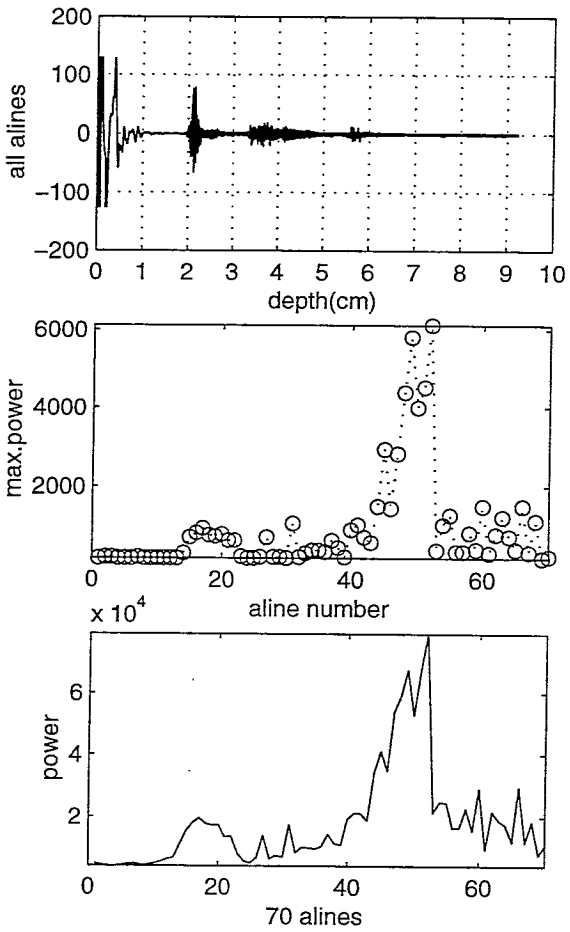
all alines
depth(cm)
max.power
aline number
x 10^4
power
70 alines

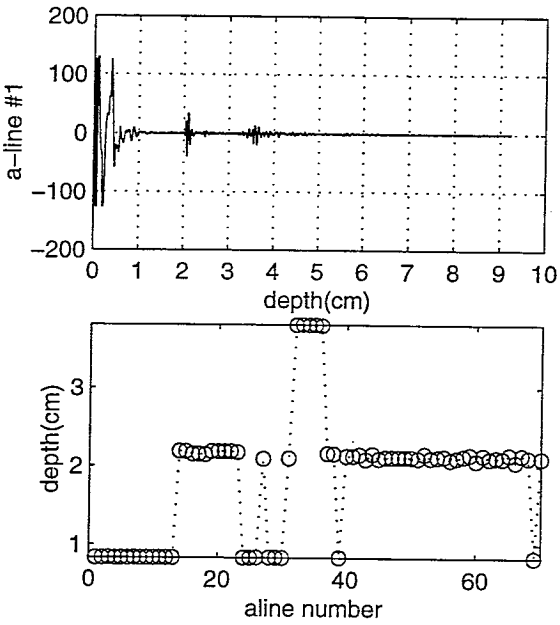
a-line #1
depth(cm)
depth(cm)
aline number

anl62g18

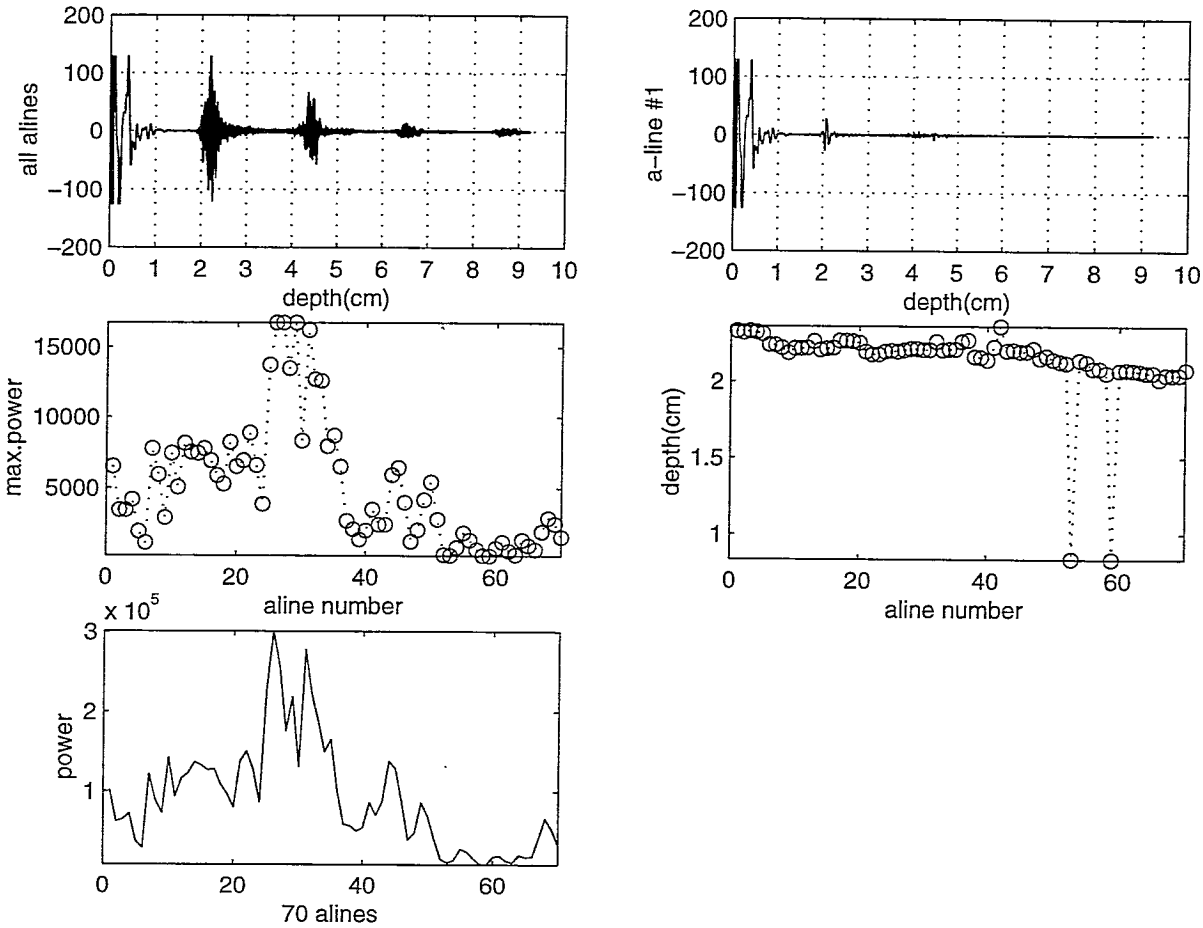
all alines
depth(cm)
a-line #1
depth(cm)
max.power
aline number
depth(cm)
aline number
x 10^5
power
70 alines

anl63g18

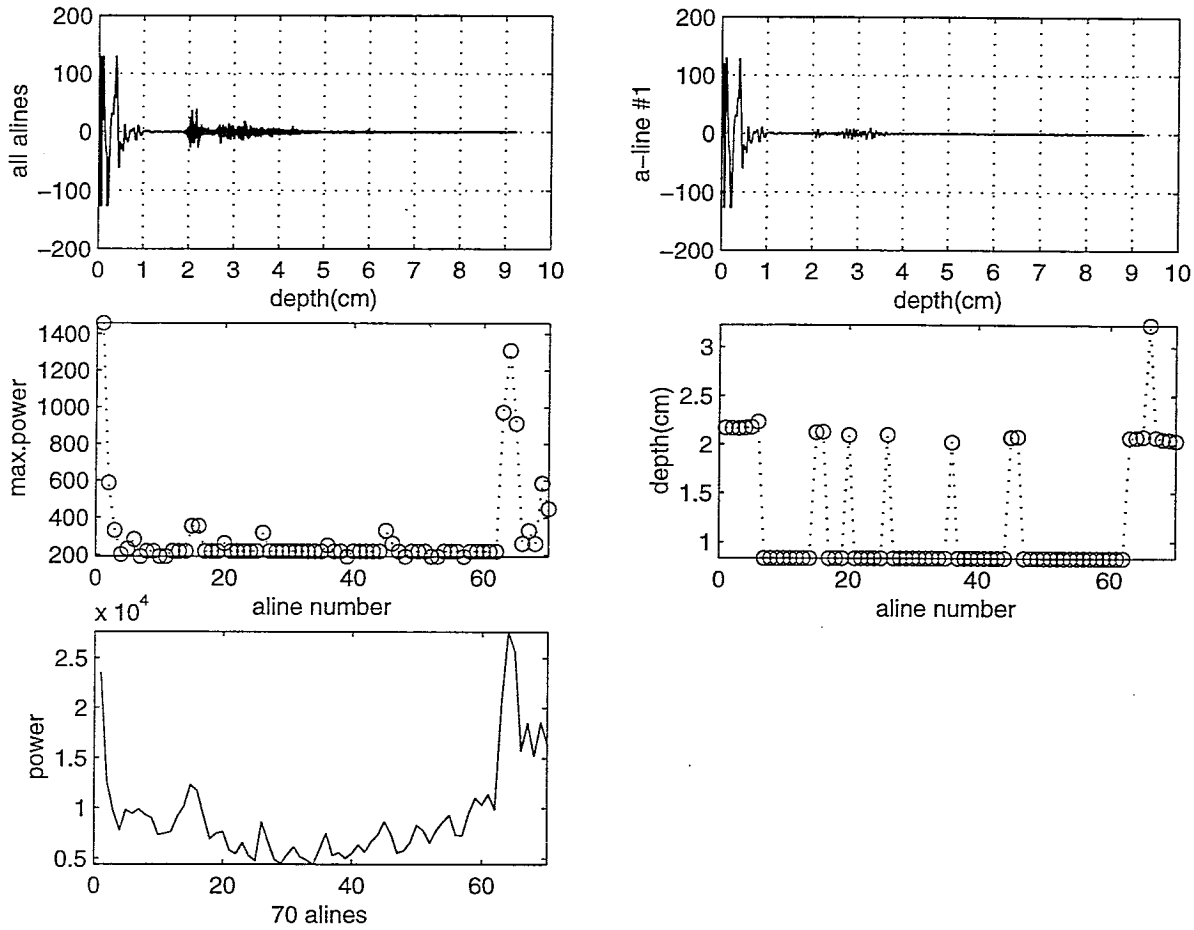
all alines
depth(cm)
a-line #1
depth(cm)
max.power
aline number
depth(cm)
aline number
x 10^4
power
70 alines

anl64g18

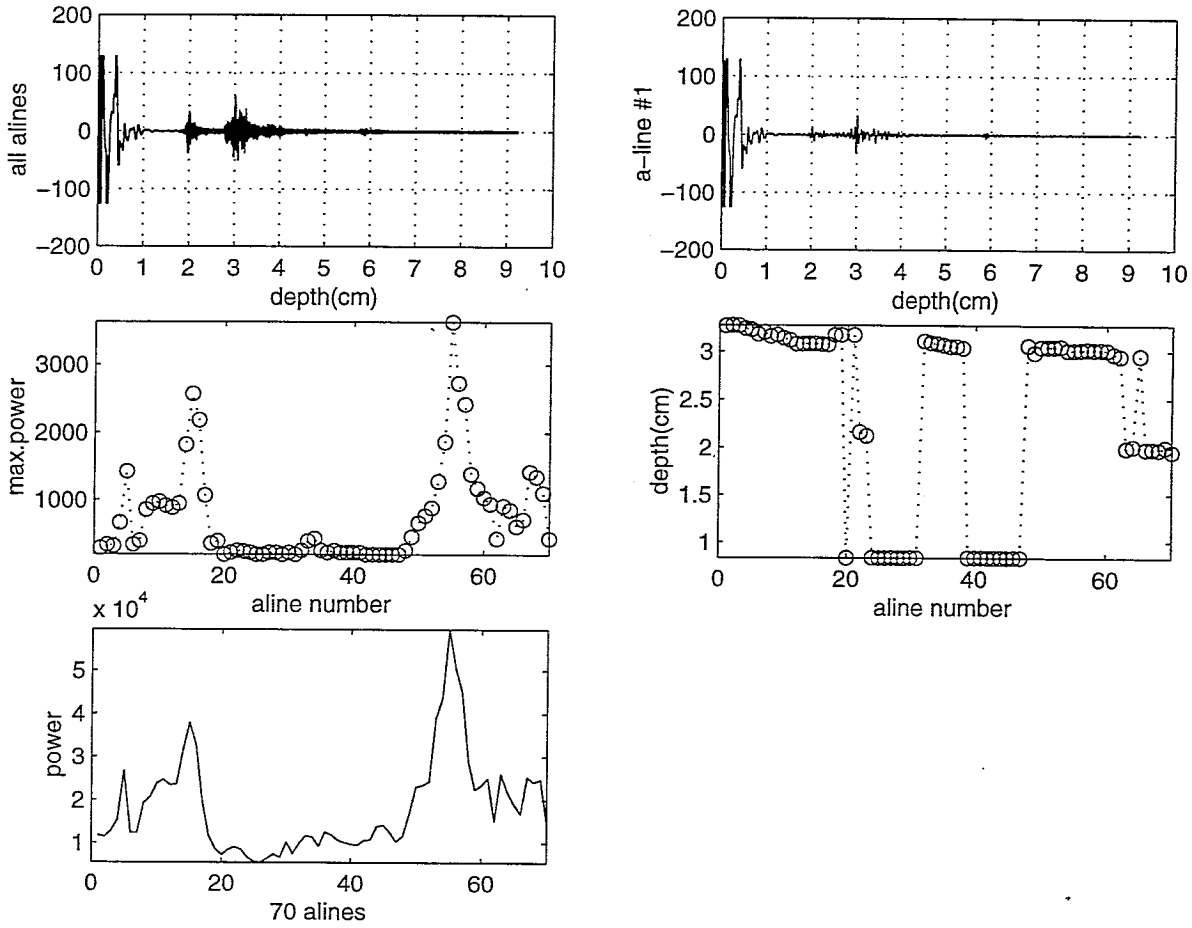
all alines
depth(cm)
a-line #1
depth(cm)
max.power
aline number
depth(cm)
aline number
x 10^4
power
70 alines

anl65g18

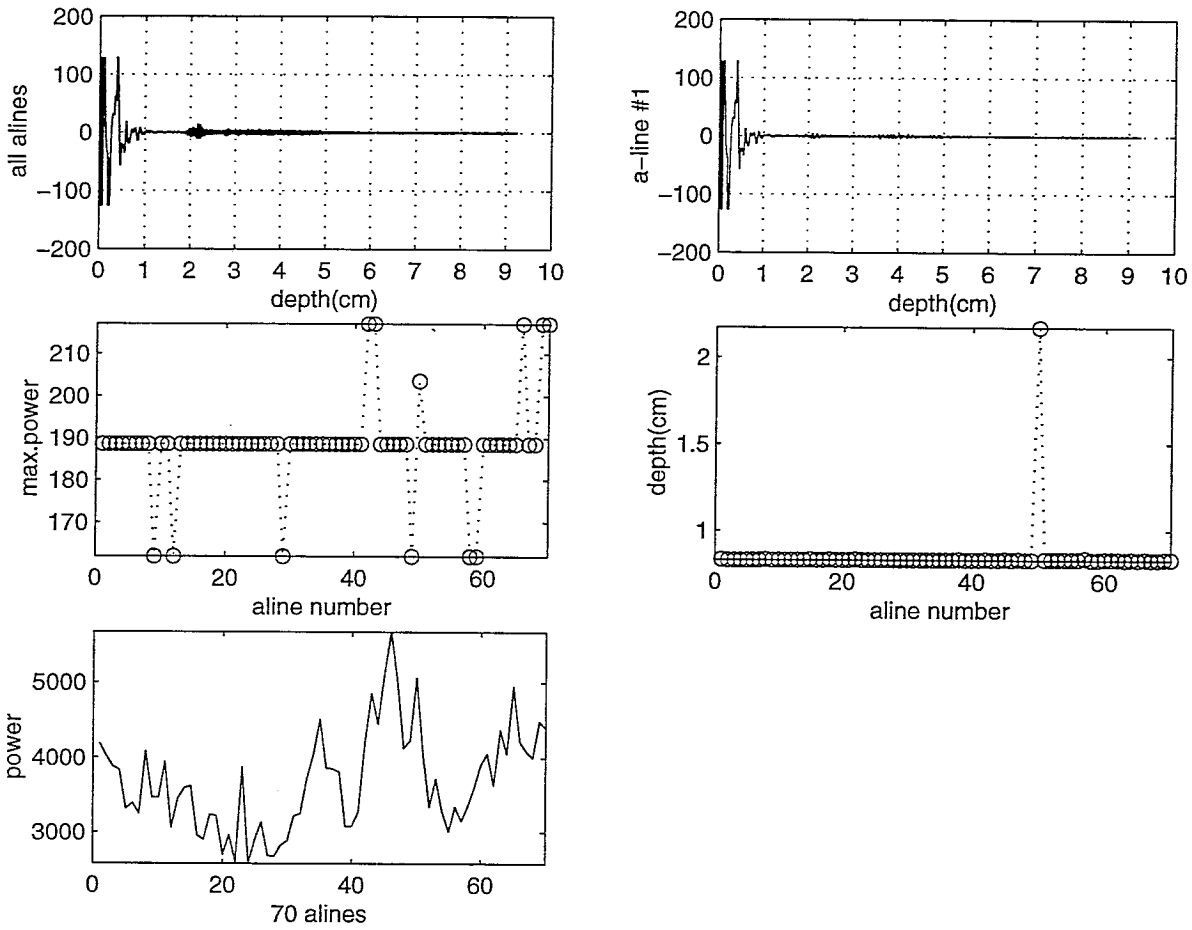
all alines
depth(cm)
a-line #1
depth(cm)
max.power
aline number
depth(cm)
aline number
power
70 alines

anl66g18

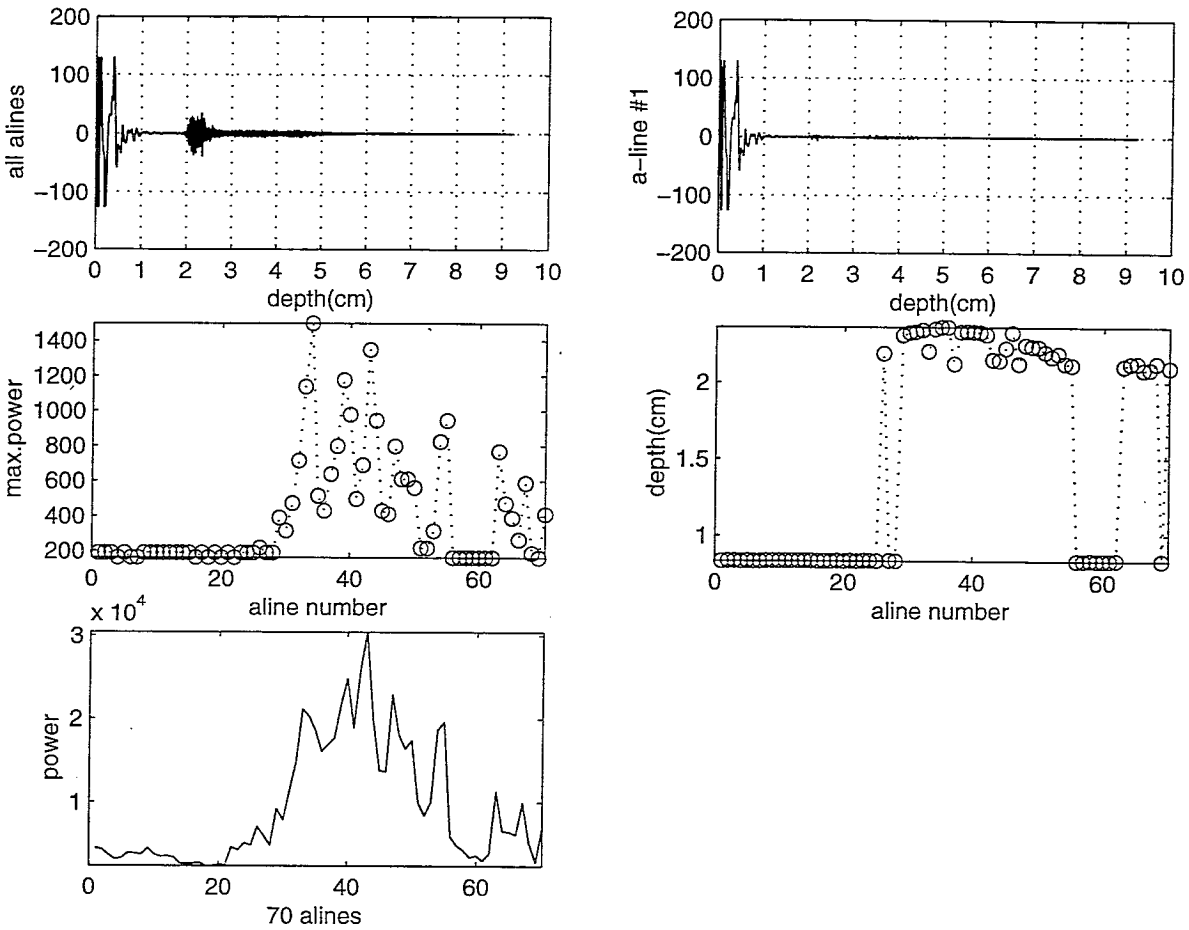
all alines
depth(cm)
a-line #1
depth(cm)
max.power
aline number
depth(cm)
aline number
x 10^4
power
70 alines

anl67g18

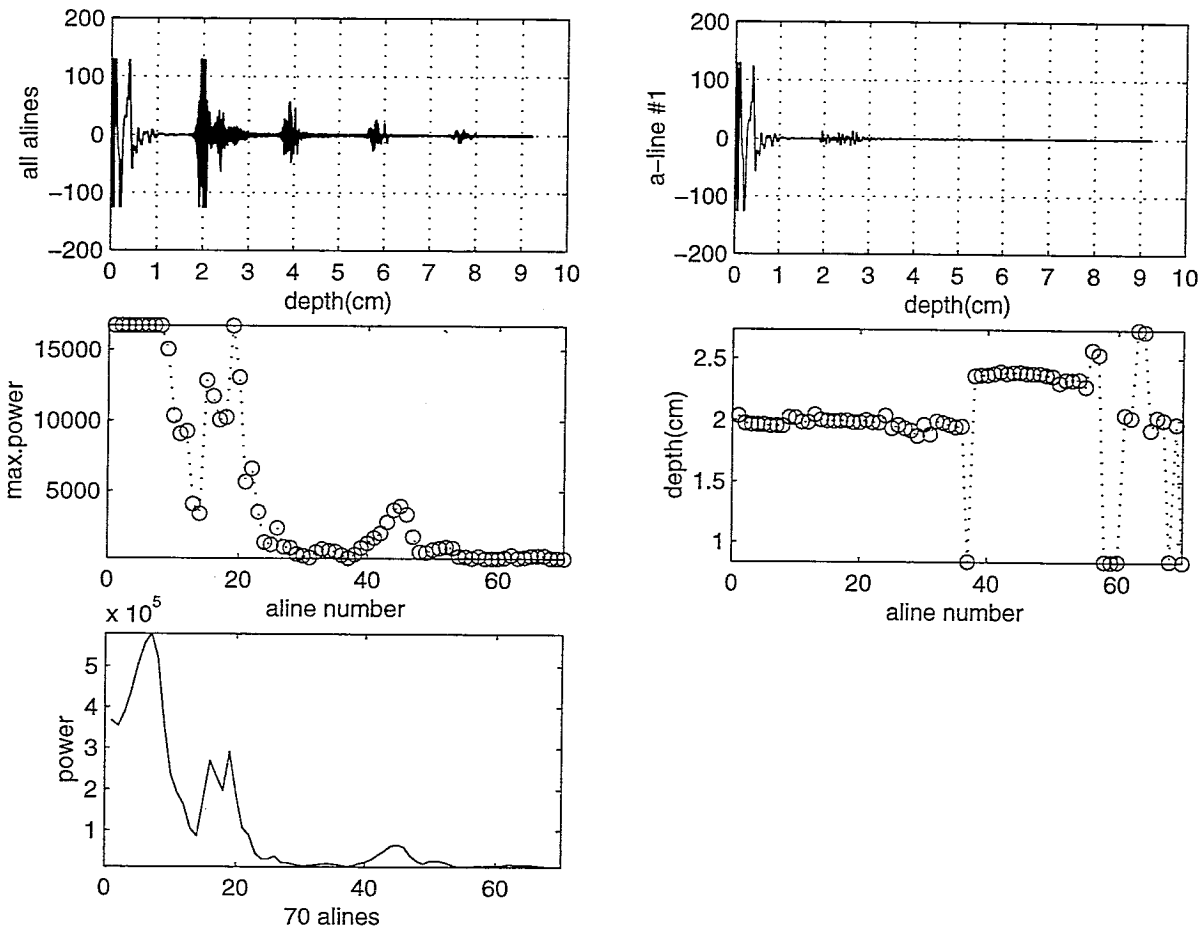
all alines
depth(cm)
a-line #1
depth(cm)
max.power
aline number
depth(cm)
aline number
x 10^5
power
70 alines

anl68g18

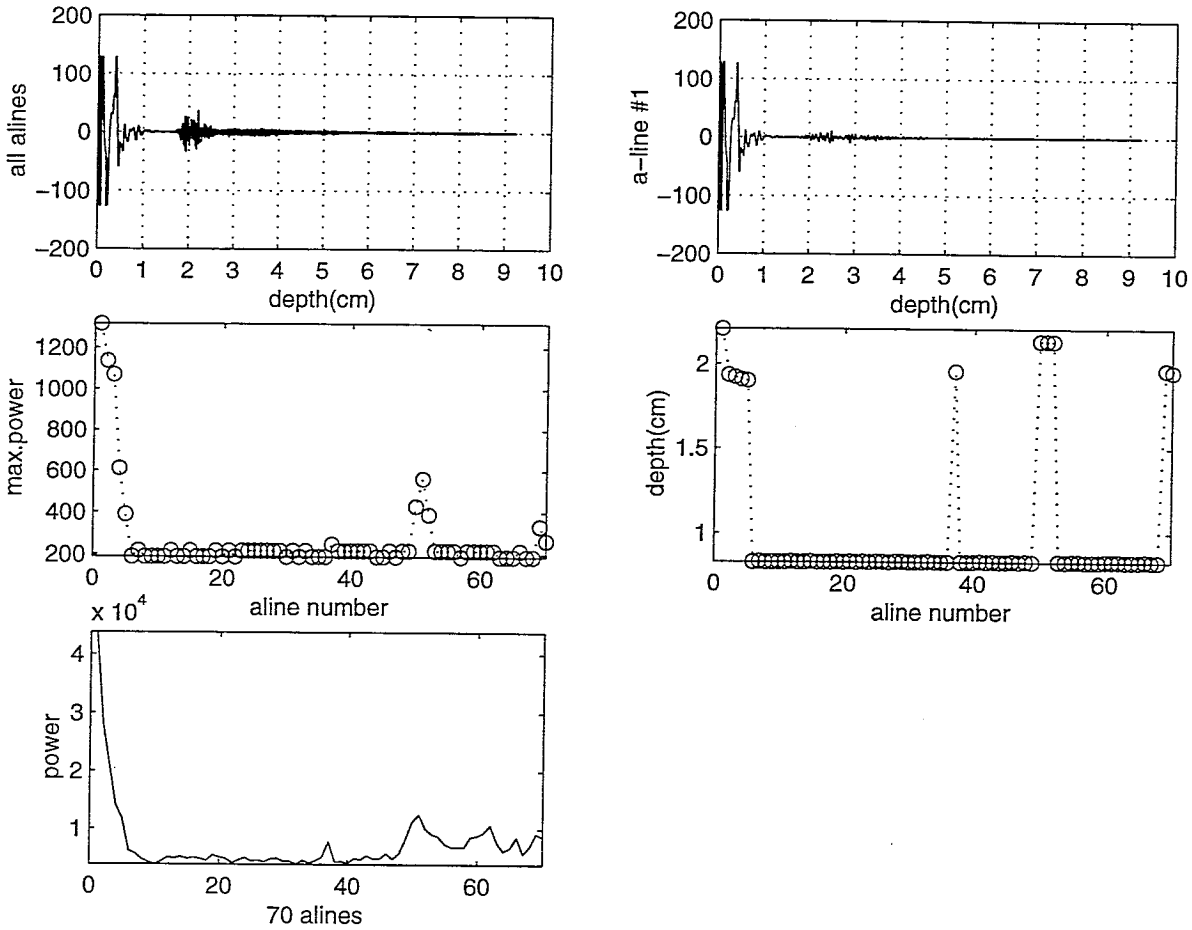
all alines
depth(cm)
a-line #1
depth(cm)
max.power
aline number
depth(cm)
aline number
x 10^4
power
70 alines

anl69g18

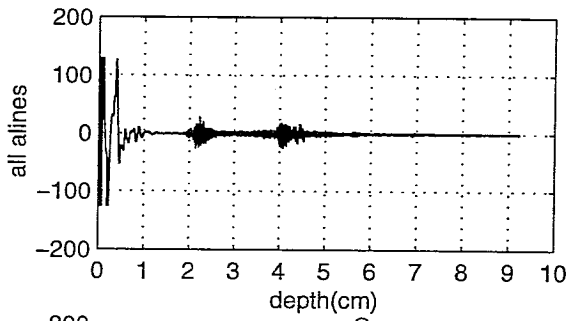
all alines
depth(cm)

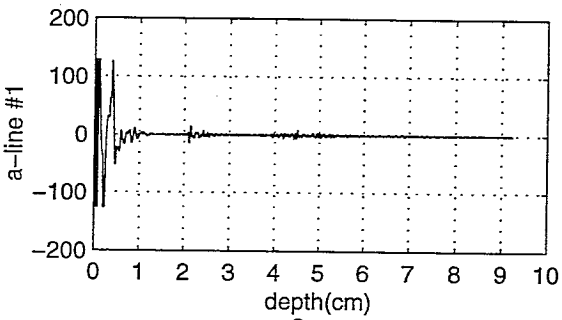
a–line #1
depth(cm)

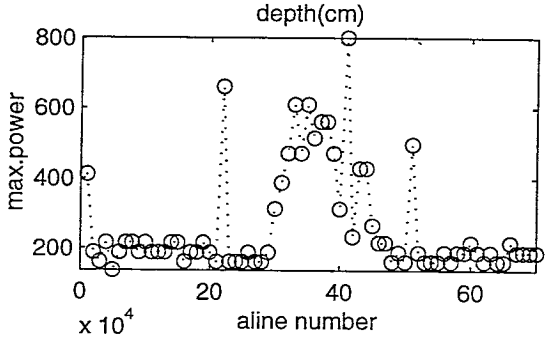
max.power
aline number

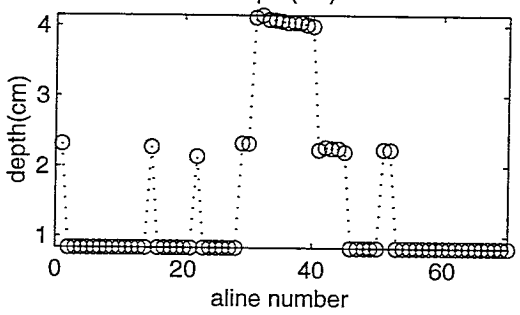
depth(cm)
aline number

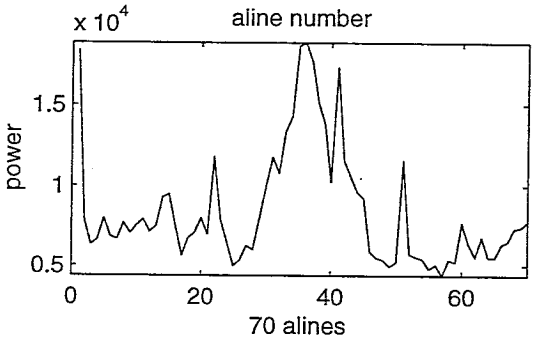
x 10^4
power
70 alines

anl70g18

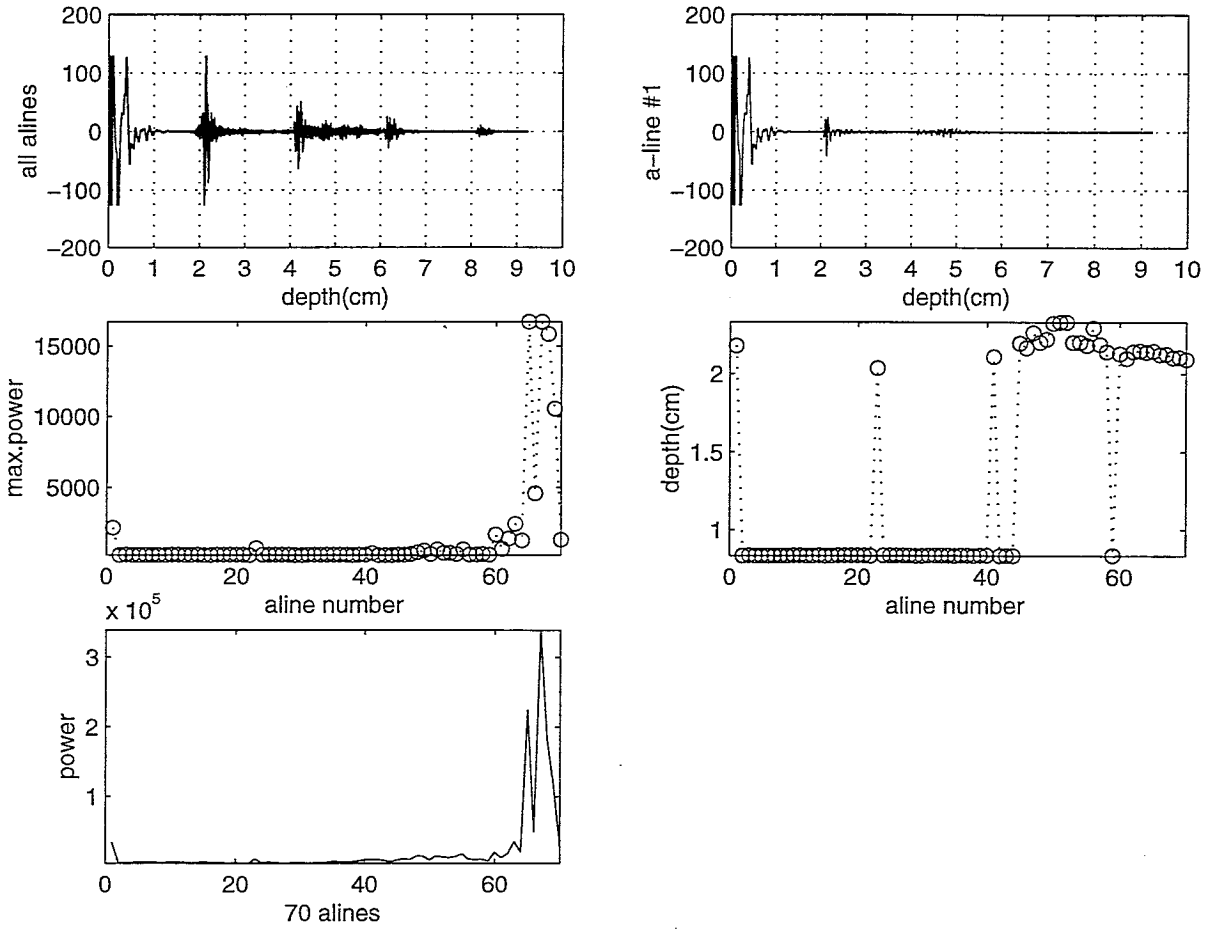
all alines
depth(cm)
a-line #1
depth(cm)
max.power
aline number
depth(cm)
aline number
x 10^5
power
70 alines

anl71g18

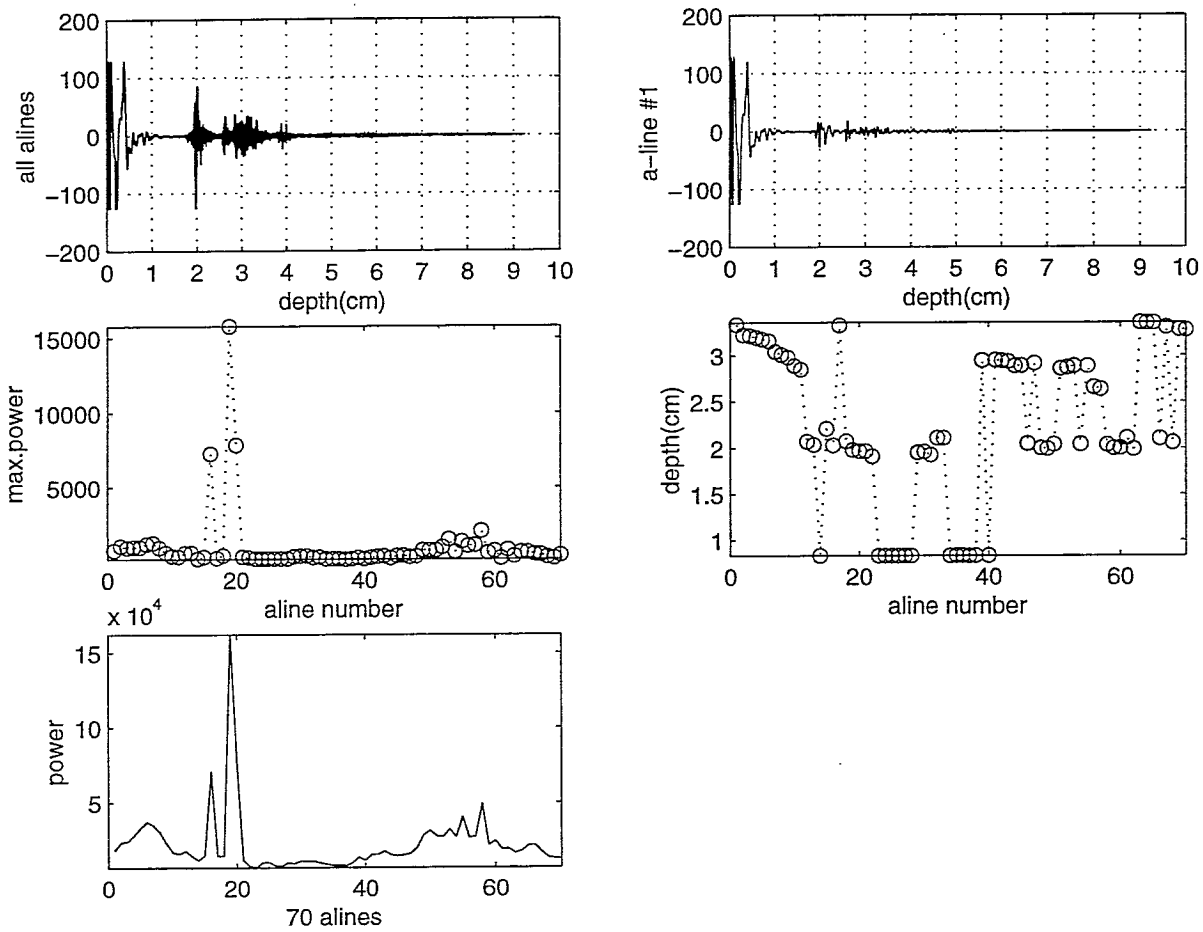
all alines
depth(cm)
a-line #1
depth(cm)
max.power
aline number
depth(cm)
aline number
x 10^4
power
70 alines

anl72g18

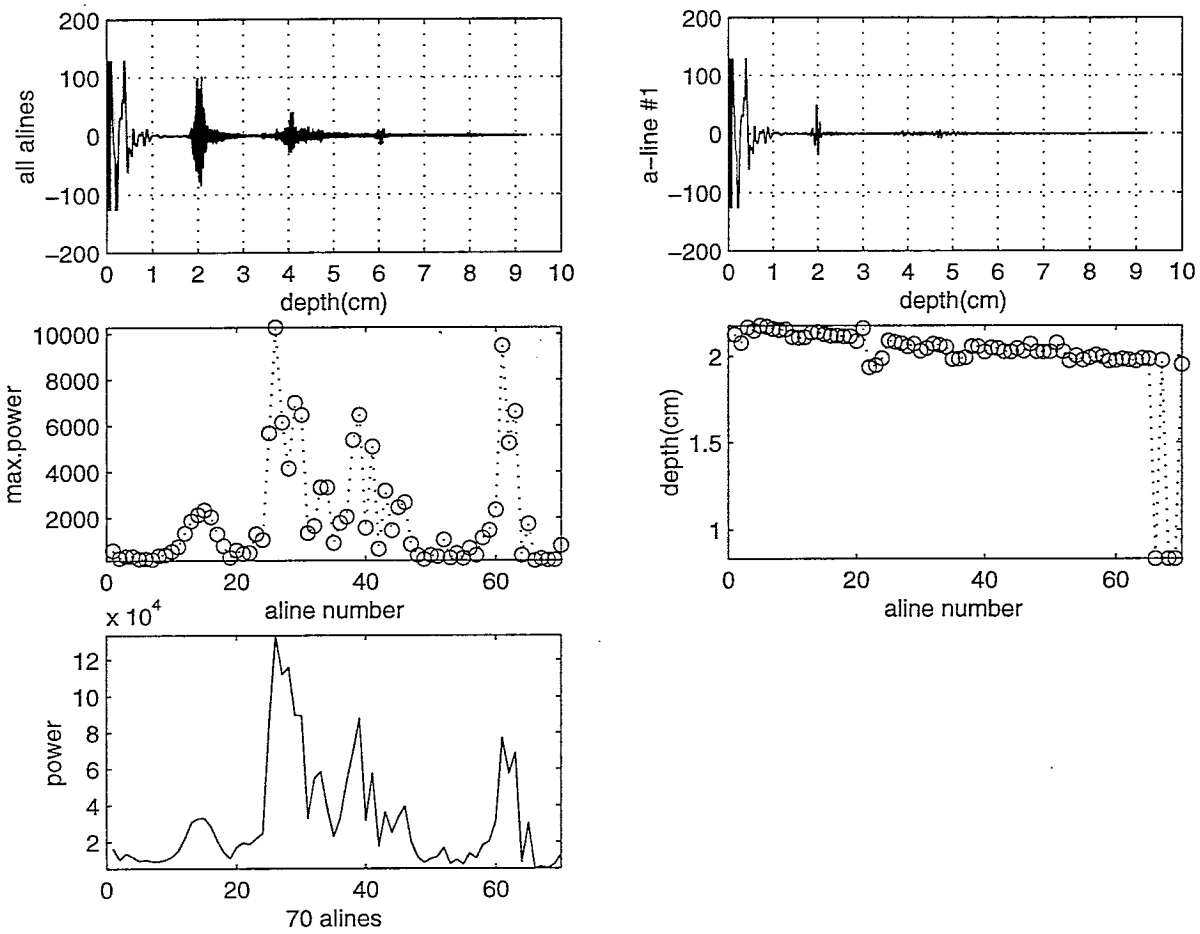
all alines
depth(cm)
a-line #1
depth(cm)
max.power
aline number
depth(cm)
aline number
x 10^4
power
70 alines

anl73g18

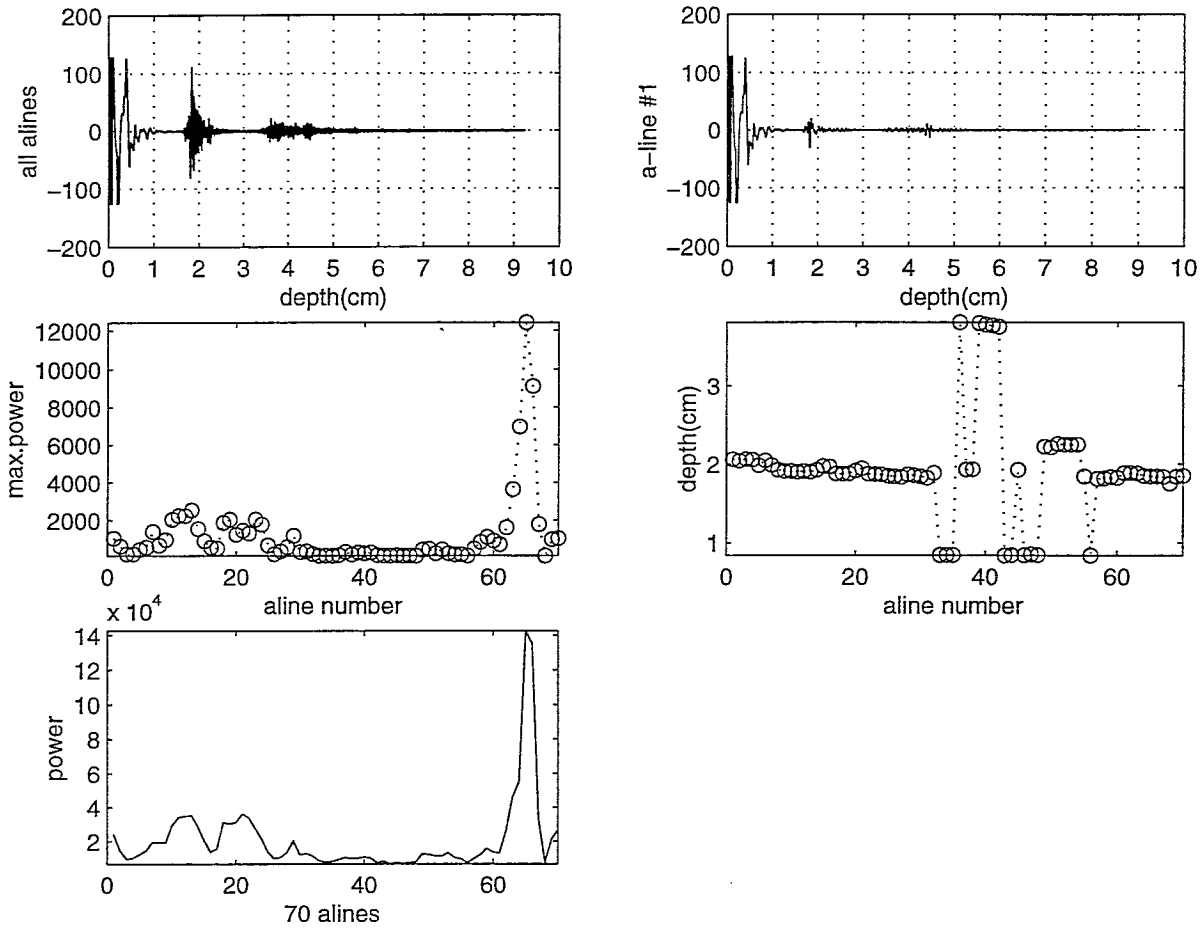
all alines
depth(cm)
a-line #1
depth(cm)
max.power
aline number
depth(cm)
aline number
x 10^4
power
70 alines

anl74g18

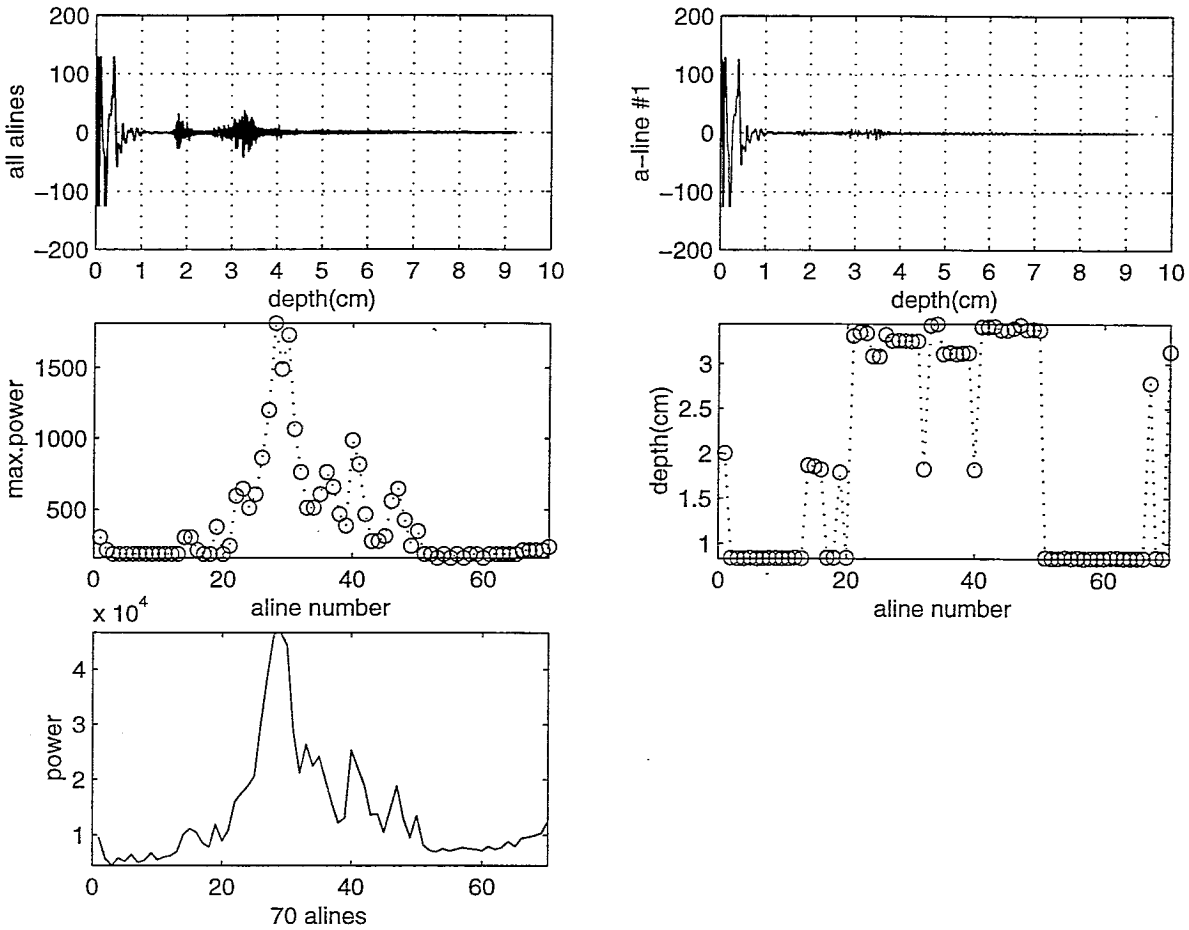
all alines
depth(cm)
a-line #1
depth(cm)
max.power
aline number
depth(cm)
aline number
x 10^4
power
70 alines

anl75g18

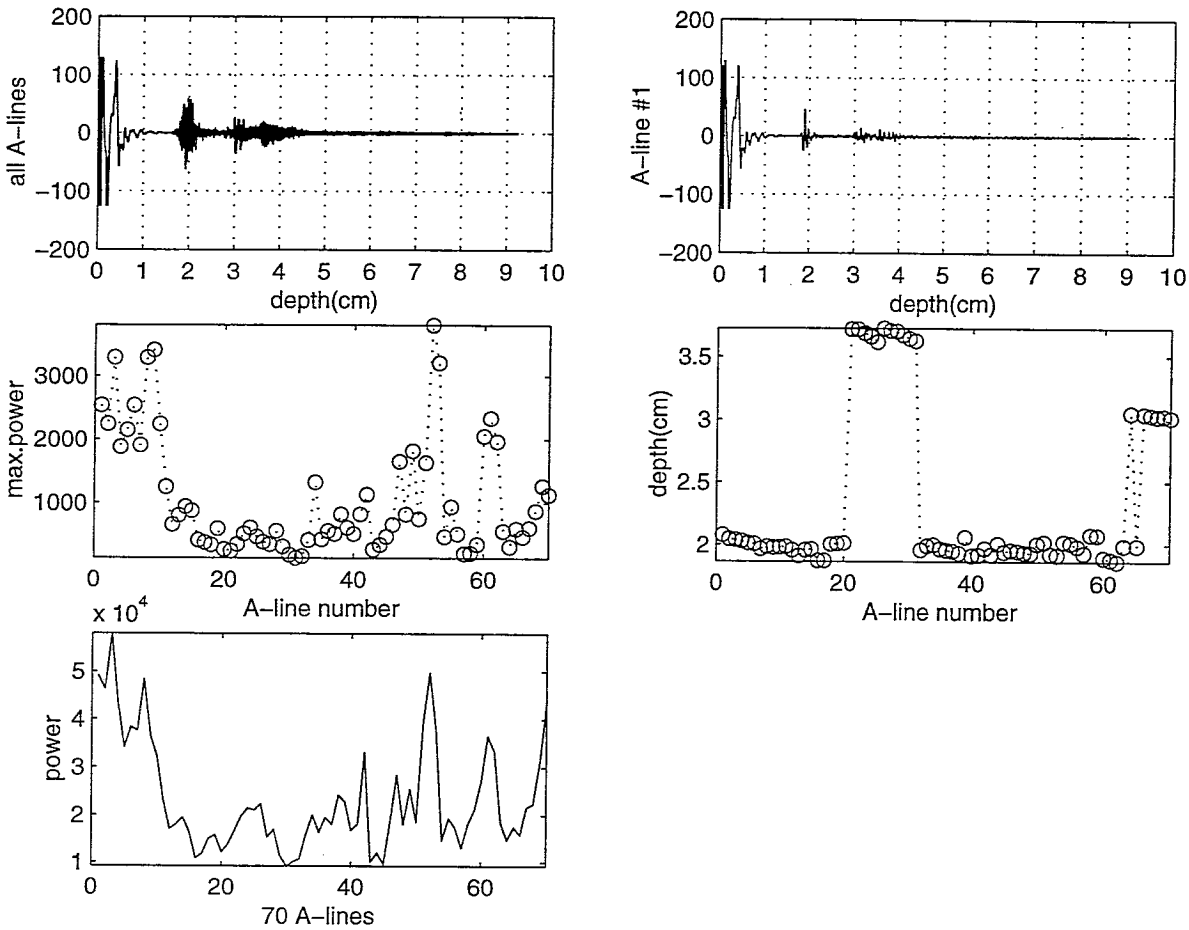
all A–lines
depth(cm)
A–line #1
depth(cm)
max.power
A–line number
depth(cm)
A–line number
x 10^4
power
70 A–lines

anl76g18

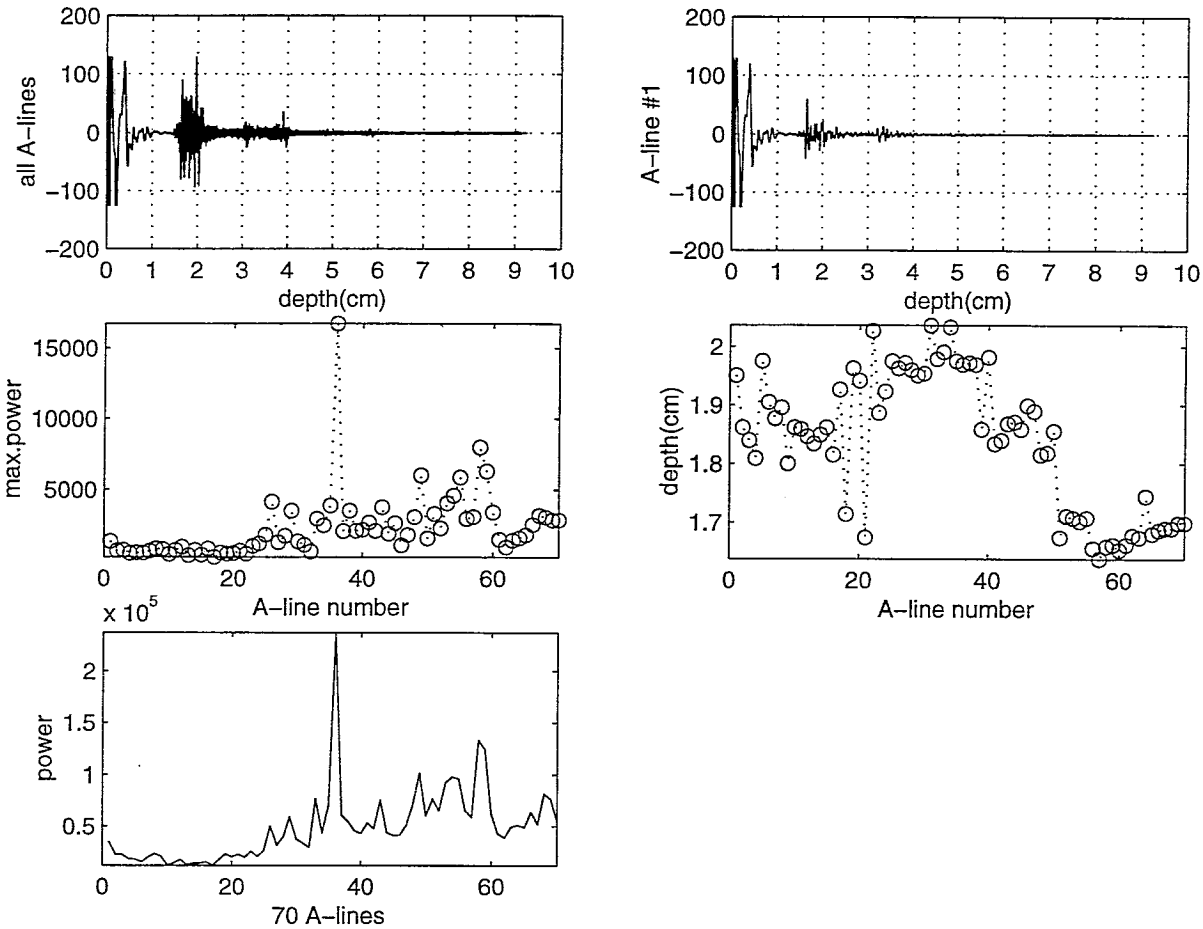
all A–lines
depth(cm)
A–line #1
depth(cm)
max.power
A–line number
depth(cm)
A–line number
x 10^5
power
70 A–lines

anl77g18

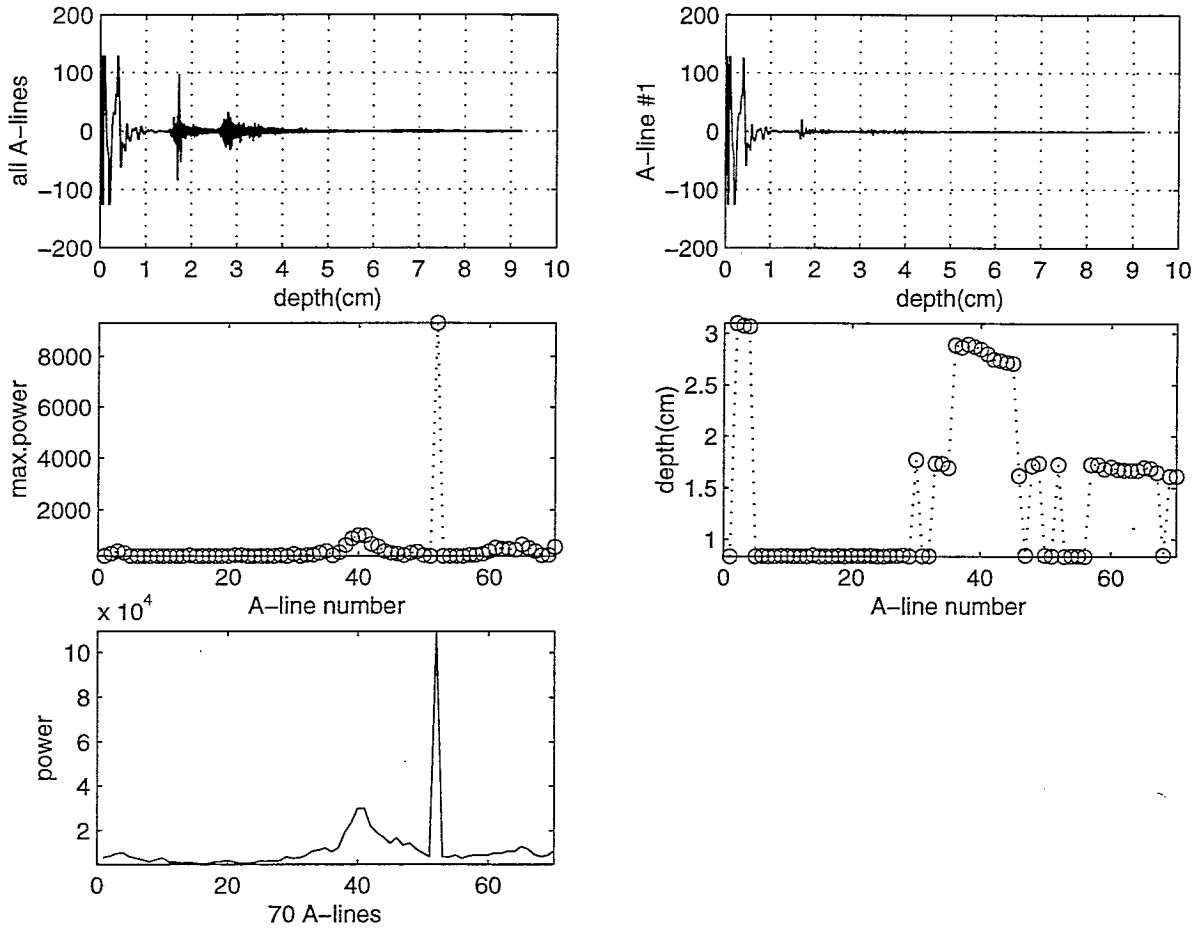
all A–lines
depth(cm)
A–line #1
depth(cm)
max.power
A–line number
depth(cm)
A–line number
x 10^4
power
70 A–lines

anl78g18

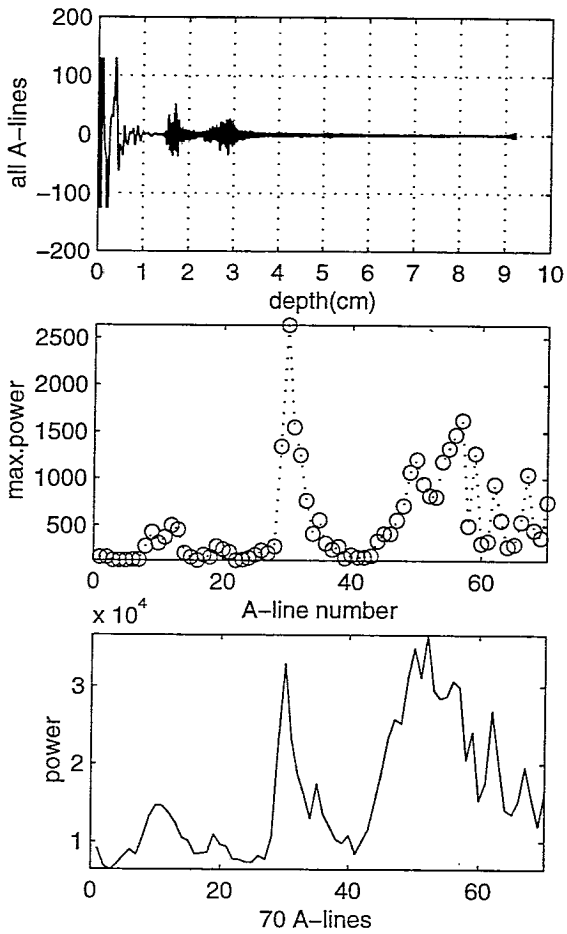
all A–lines
depth(cm)
max.power
A–line number
x 10^4
power
70 A–lines

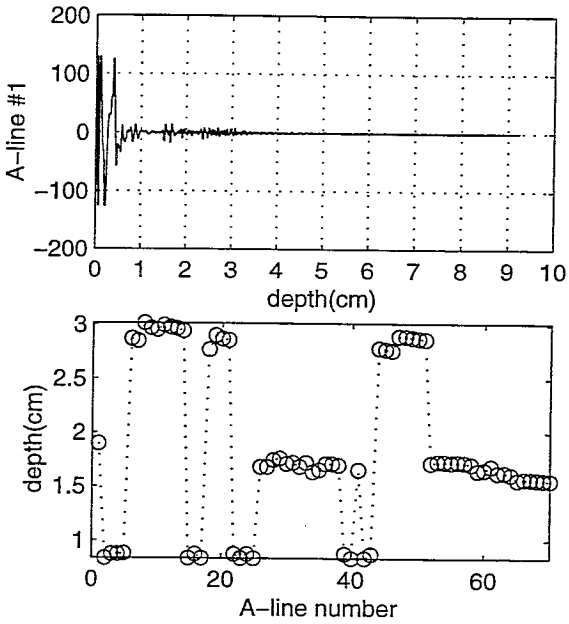
A–line #1
depth(cm)
depth(cm)
A–line number

anl79g18

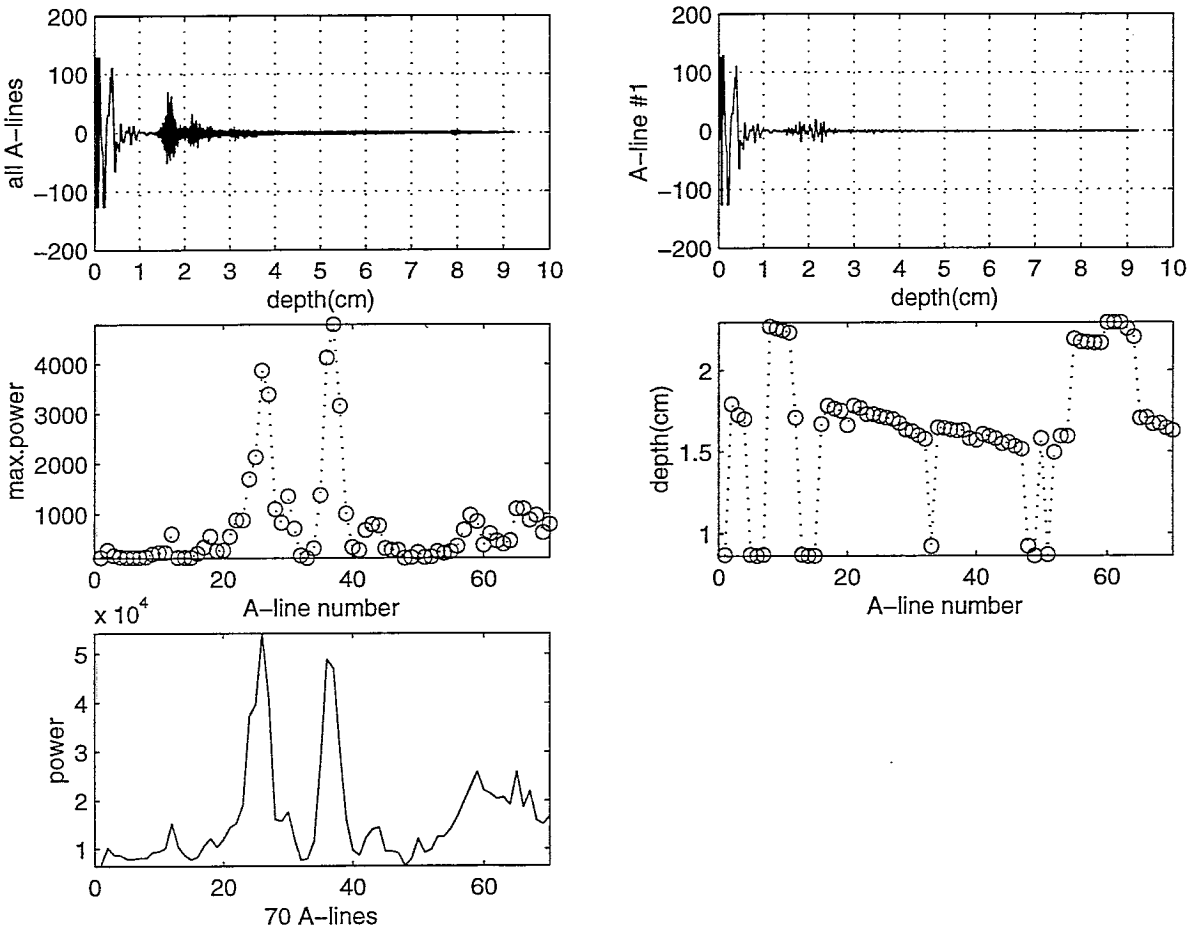
all A–lines
depth(cm)
A–line #1
depth(cm)
max.power
A–line number
depth(cm)
A–line number
x 10^4
power
70 A–lines

anl80g18

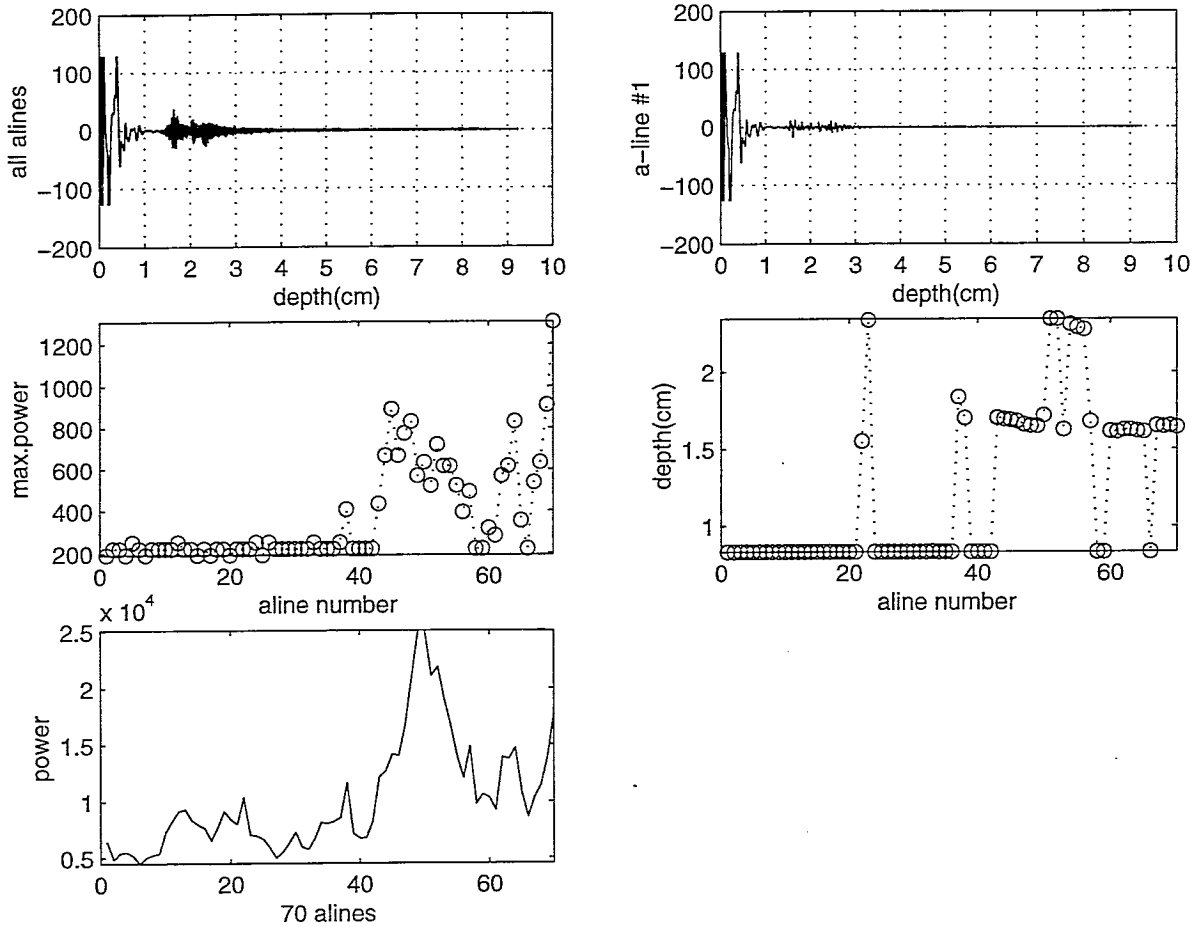
all alines
depth(cm)
a-line #1
depth(cm)
max.power
aline number
depth(cm)
aline number
x 10^4
power
70 alines

anl81g18

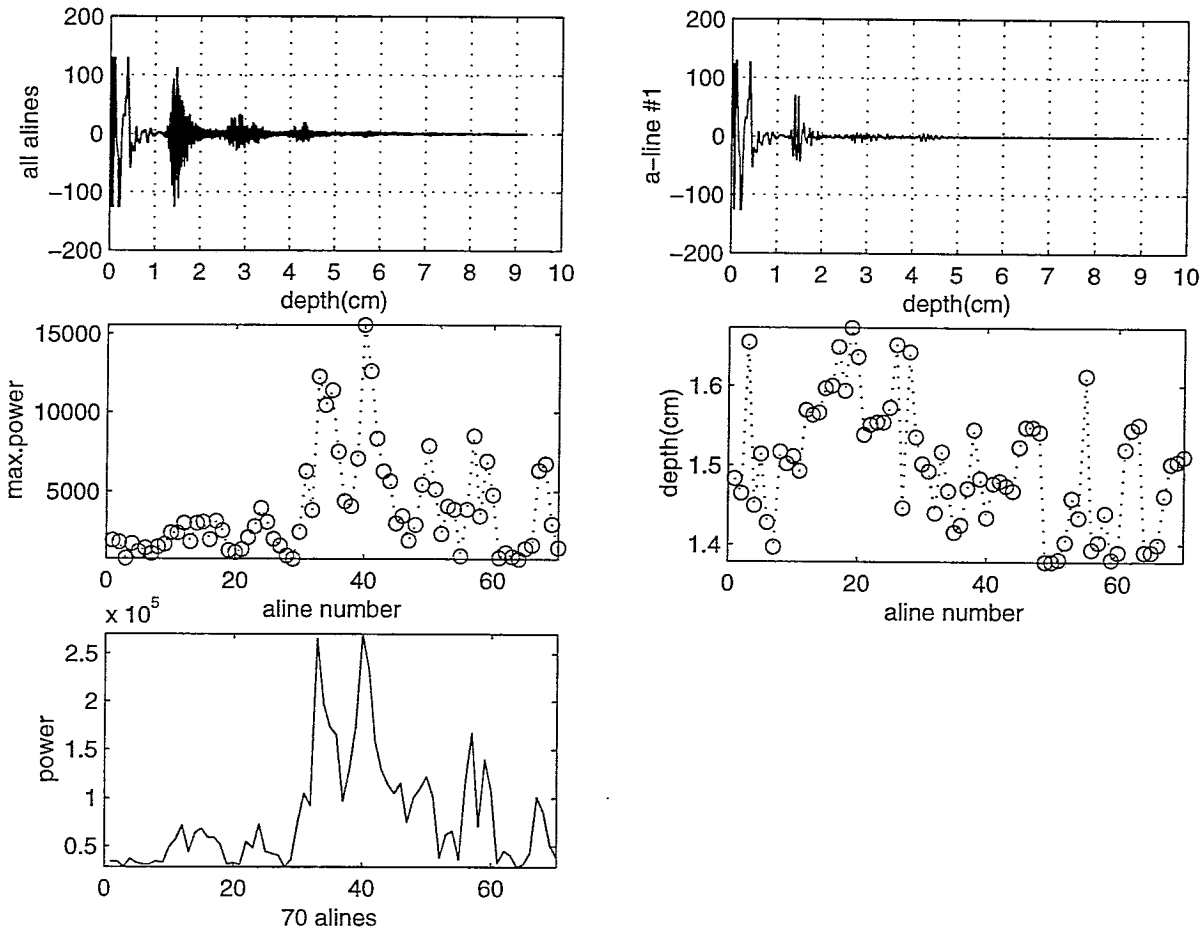
all alines
depth(cm)
a-line #1
depth(cm)
max.power
aline number
depth(cm)
aline number
x 10^5
power
70 alines

anl82g18

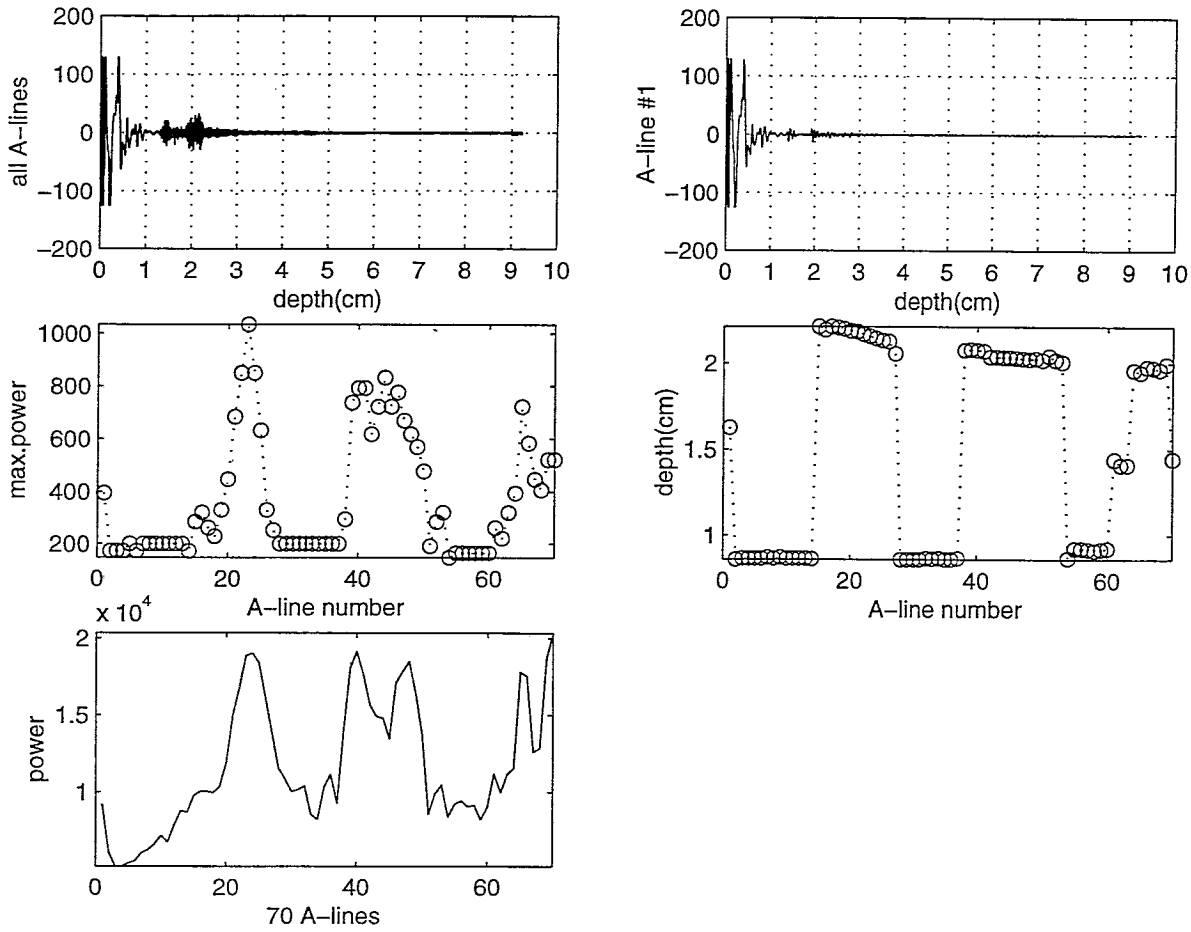
all A–lines
depth(cm)
A–line #1
depth(cm)
max.power
A–line number
depth(cm)
A–line number
x 10^4
power
70 A–lines

anl83g18

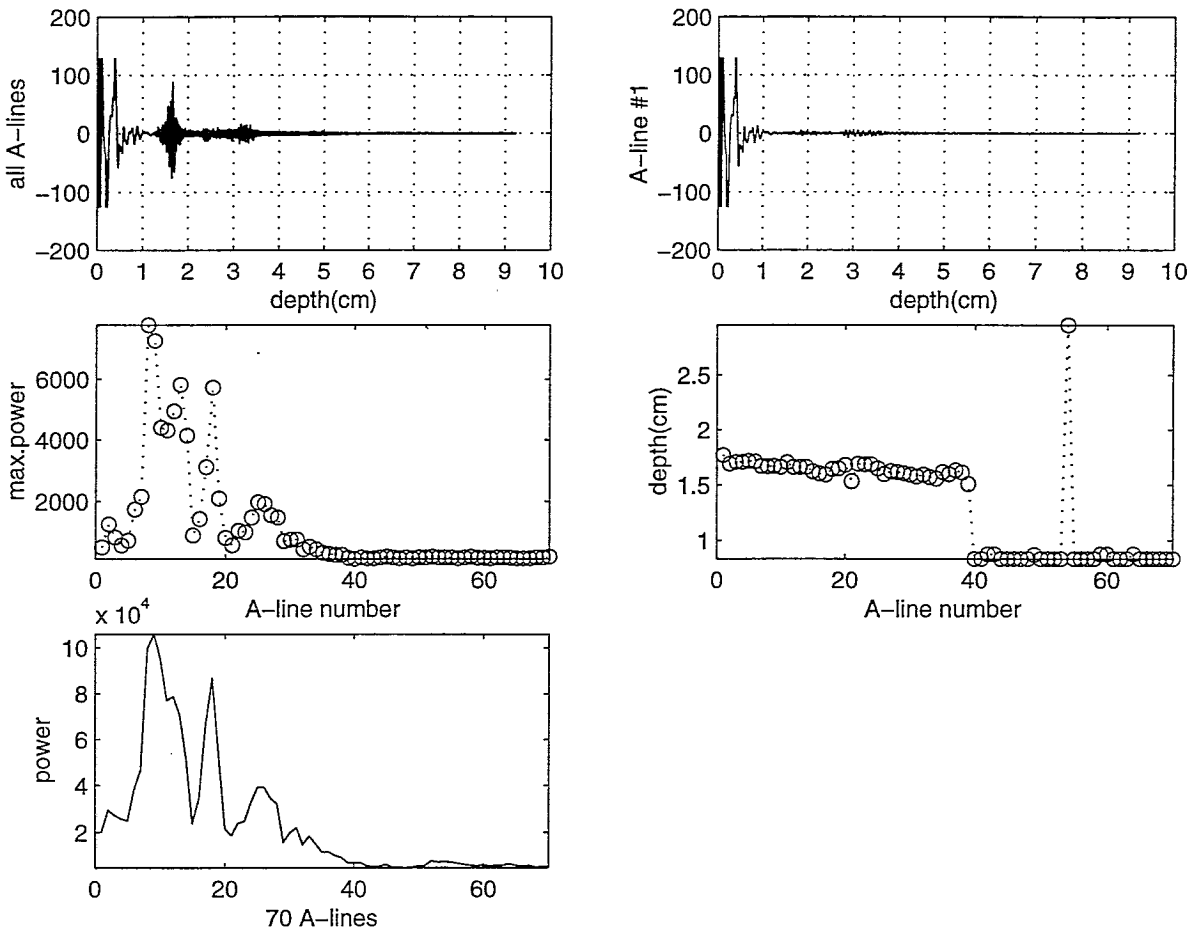
all A–lines
depth(cm)
A–line #1
depth(cm)
max.power
A–line number
depth(cm)
A–line number
x 10^4
power
70 A–lines

anl84g18

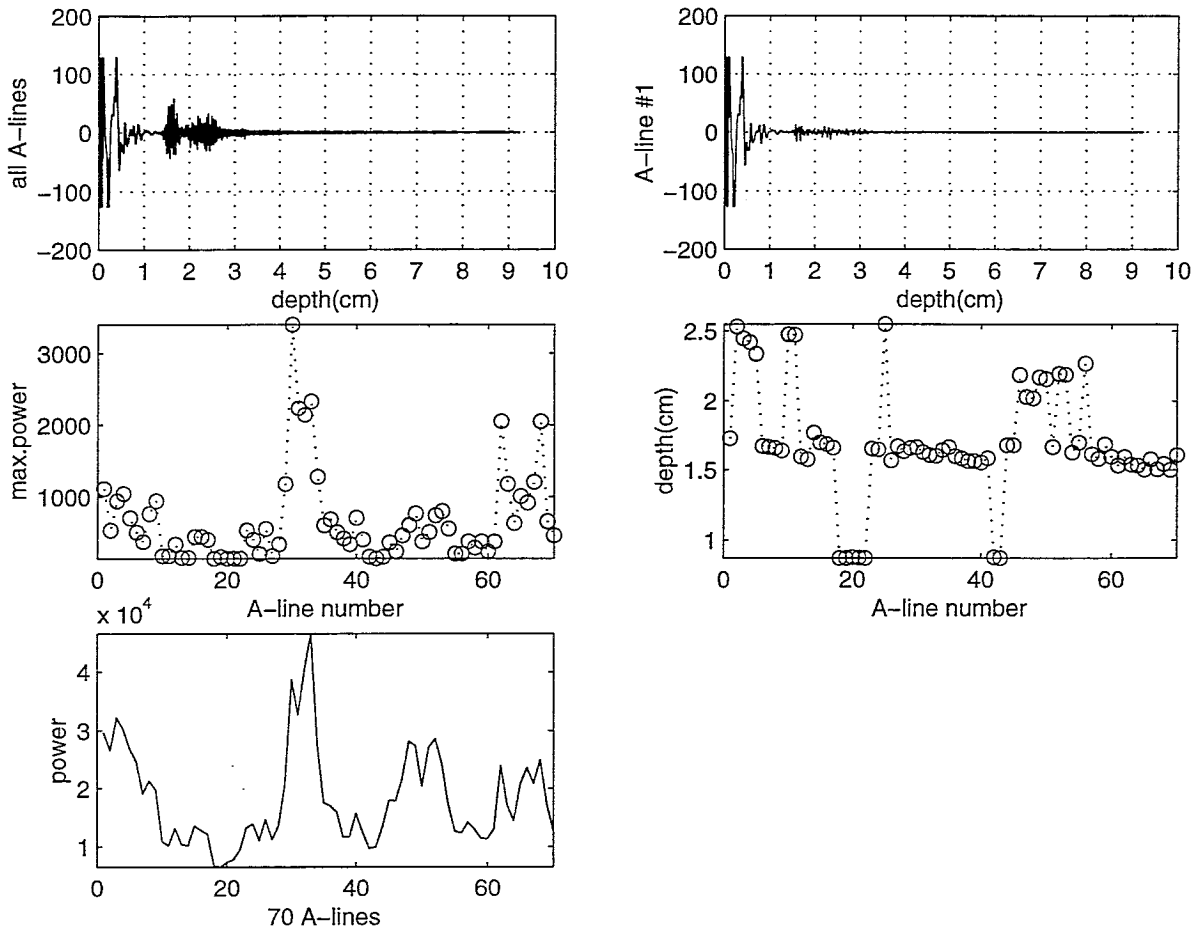
all A–lines
depth(cm)
A–line #1
depth(cm)
max.power
A–line number
depth(cm)
A–line number
x 10^4
power
70 A–lines

anl85g18

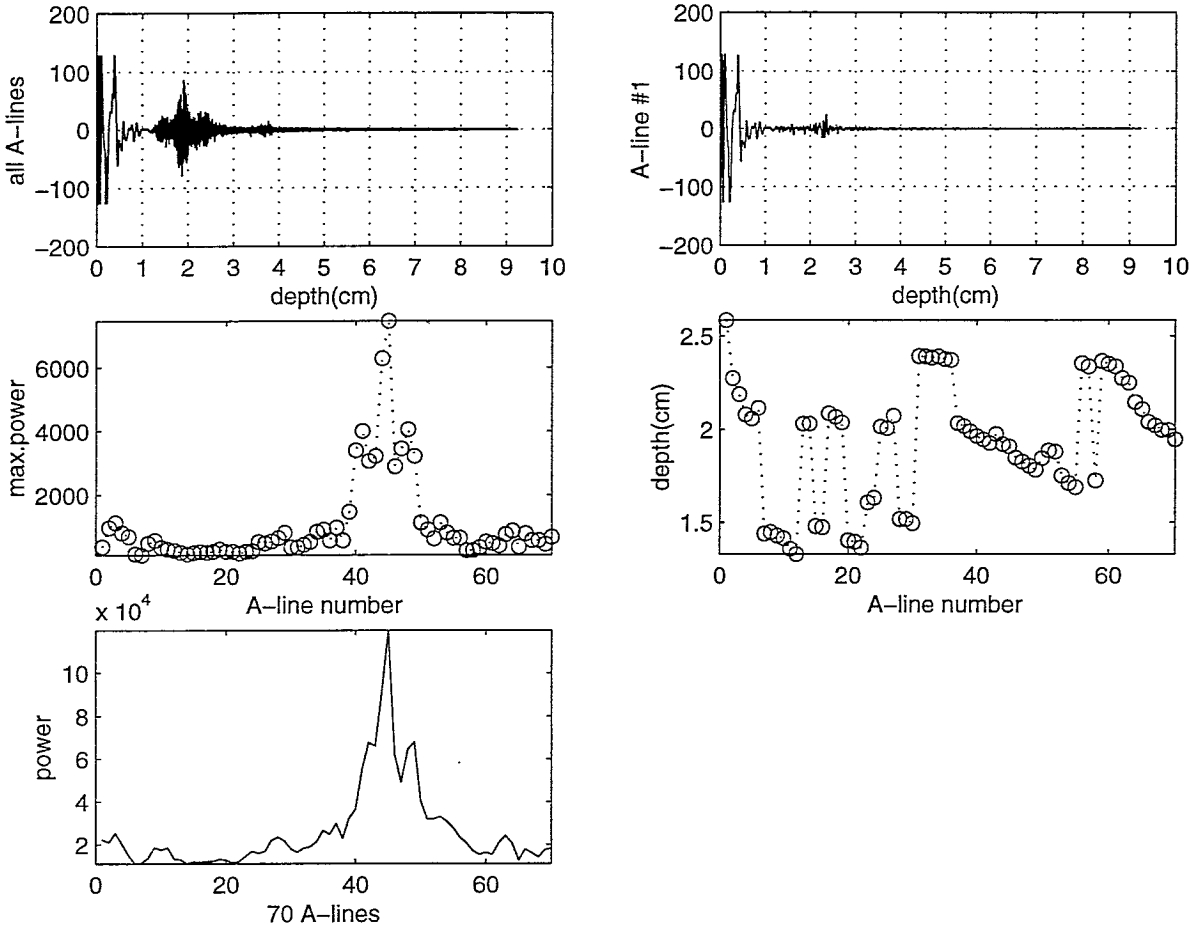
all A–lines
depth(cm)
A–line #1
depth(cm)
max.power
A–line number
depth(cm)
A–line number
x 10^4
power
70 A–lines

anl86g18

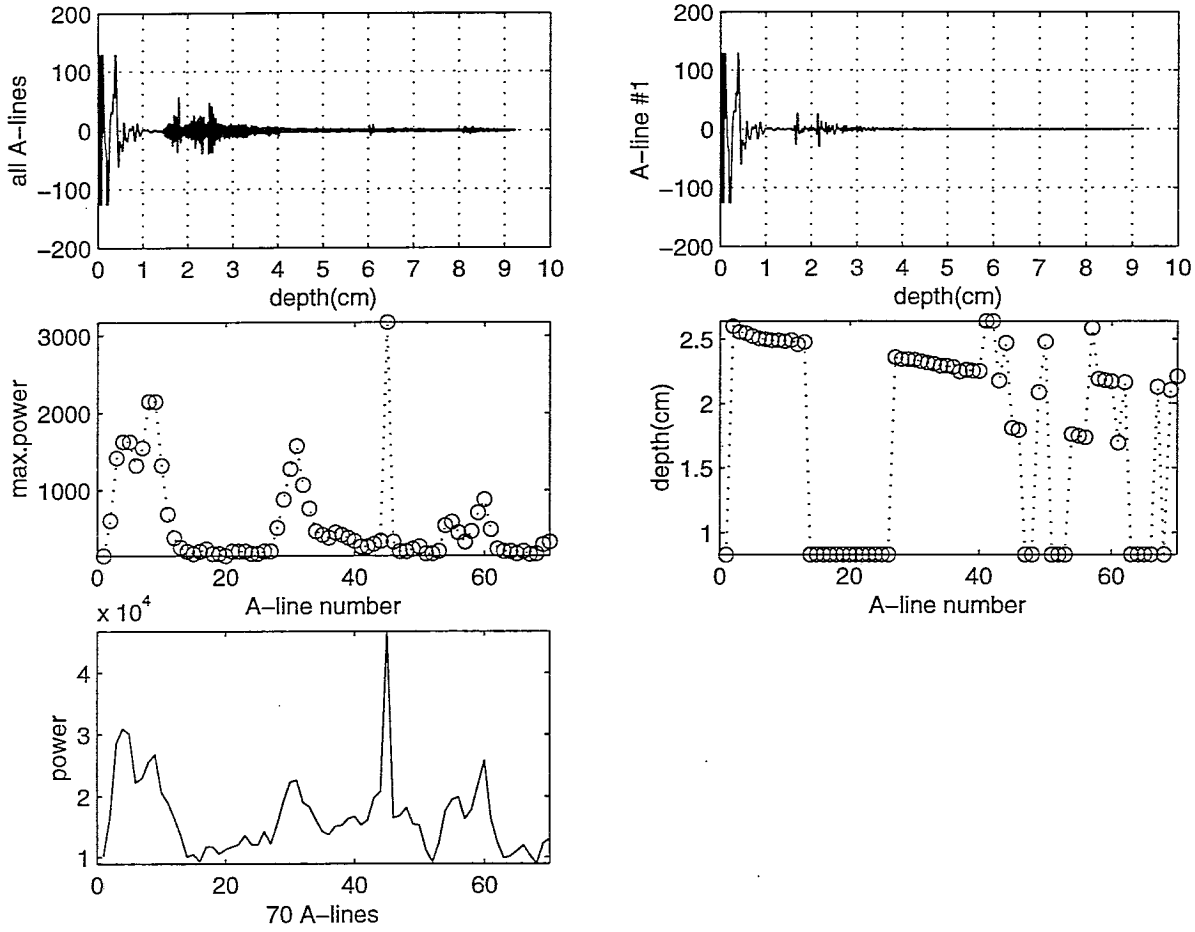
all A–lines
depth(cm)
A–line #1
depth(cm)
max.power
A–line number
depth(cm)
A–line number
x 10^4
power
70 A–lines

anl87g18

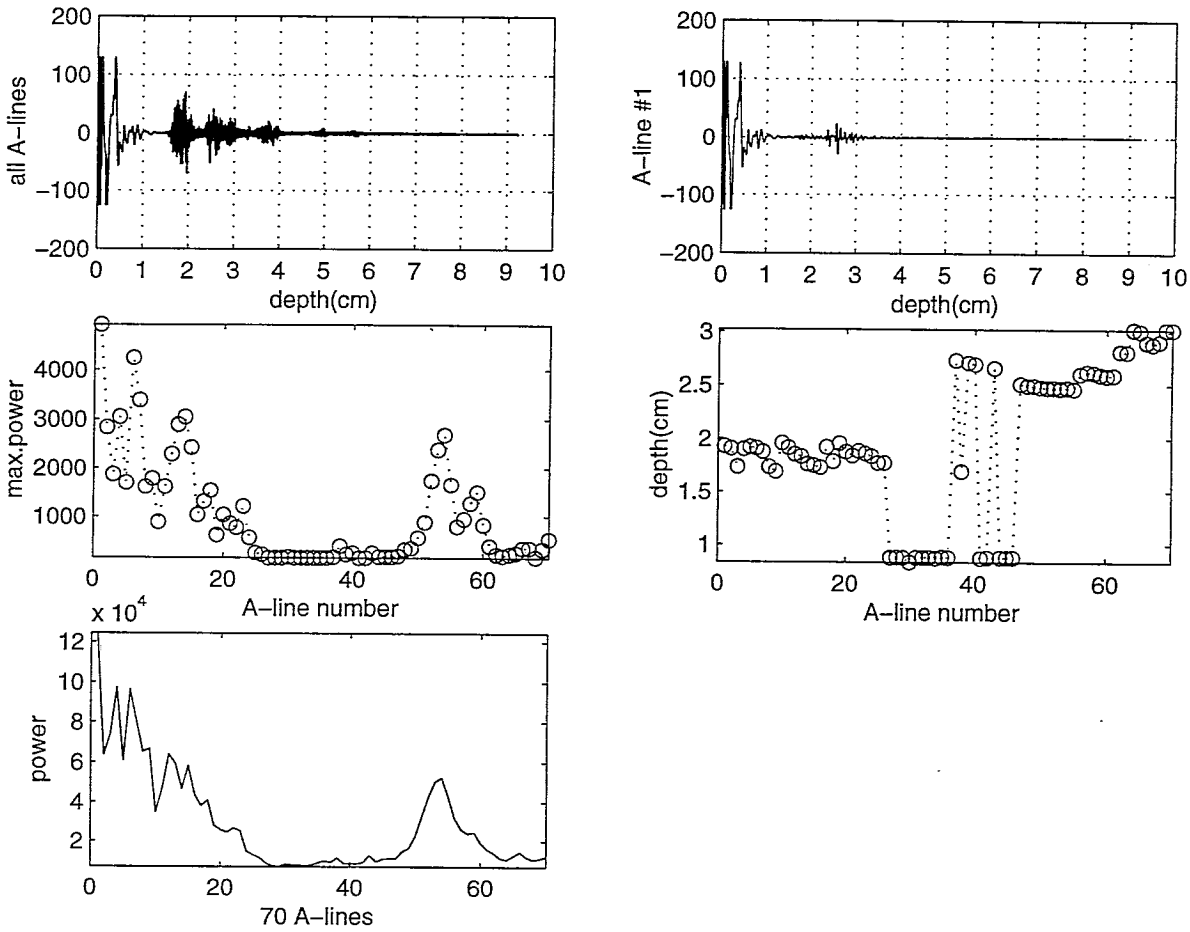
all A–lines
depth(cm)
A–line #1
depth(cm)
max.power
A–line number
depth(cm)
A–line number
x 10^4
power
70 A–lines

anl88g18

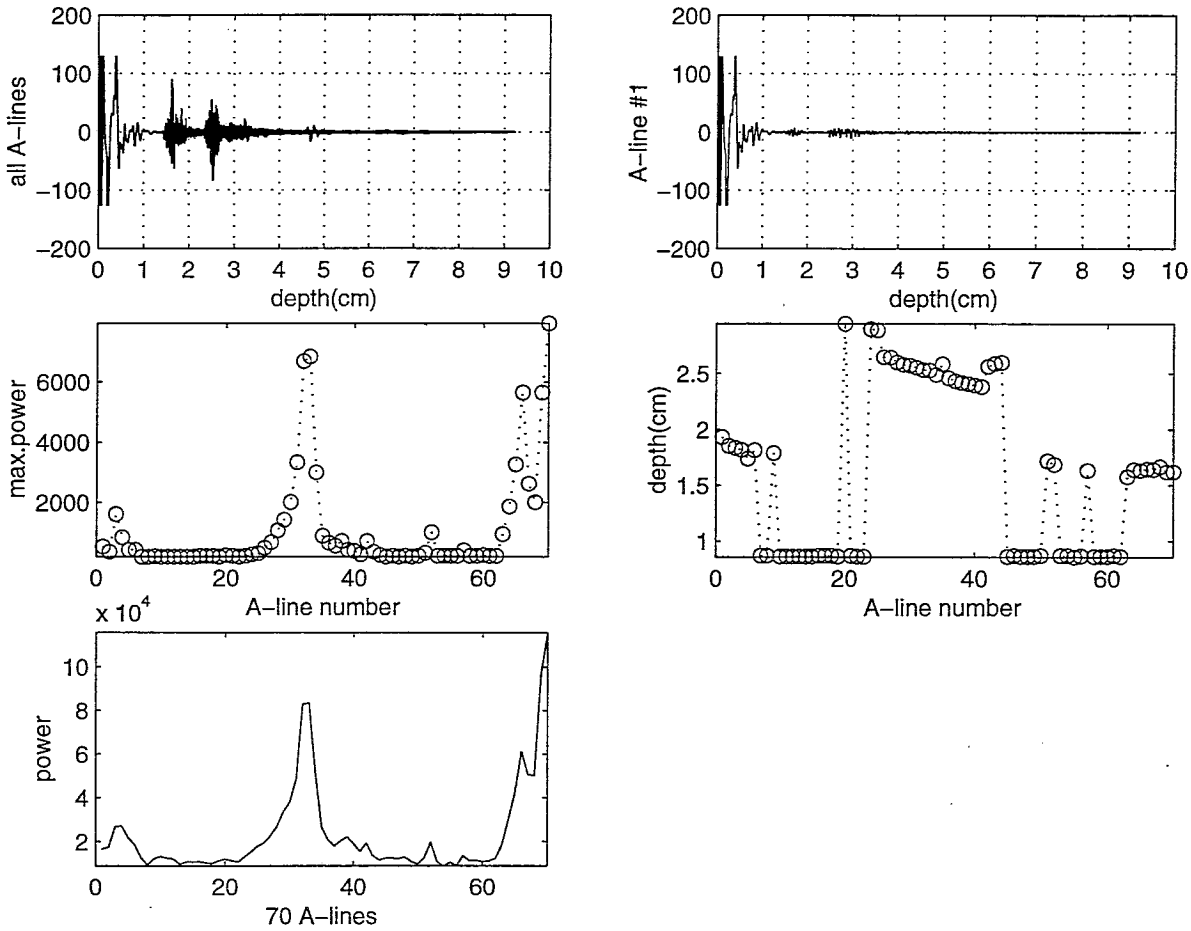
all A–lines
depth(cm)
A–line #1
depth(cm)
max.power
A–line number
depth(cm)
A–line number
x 10^4
power
70 A–lines

anl89g18

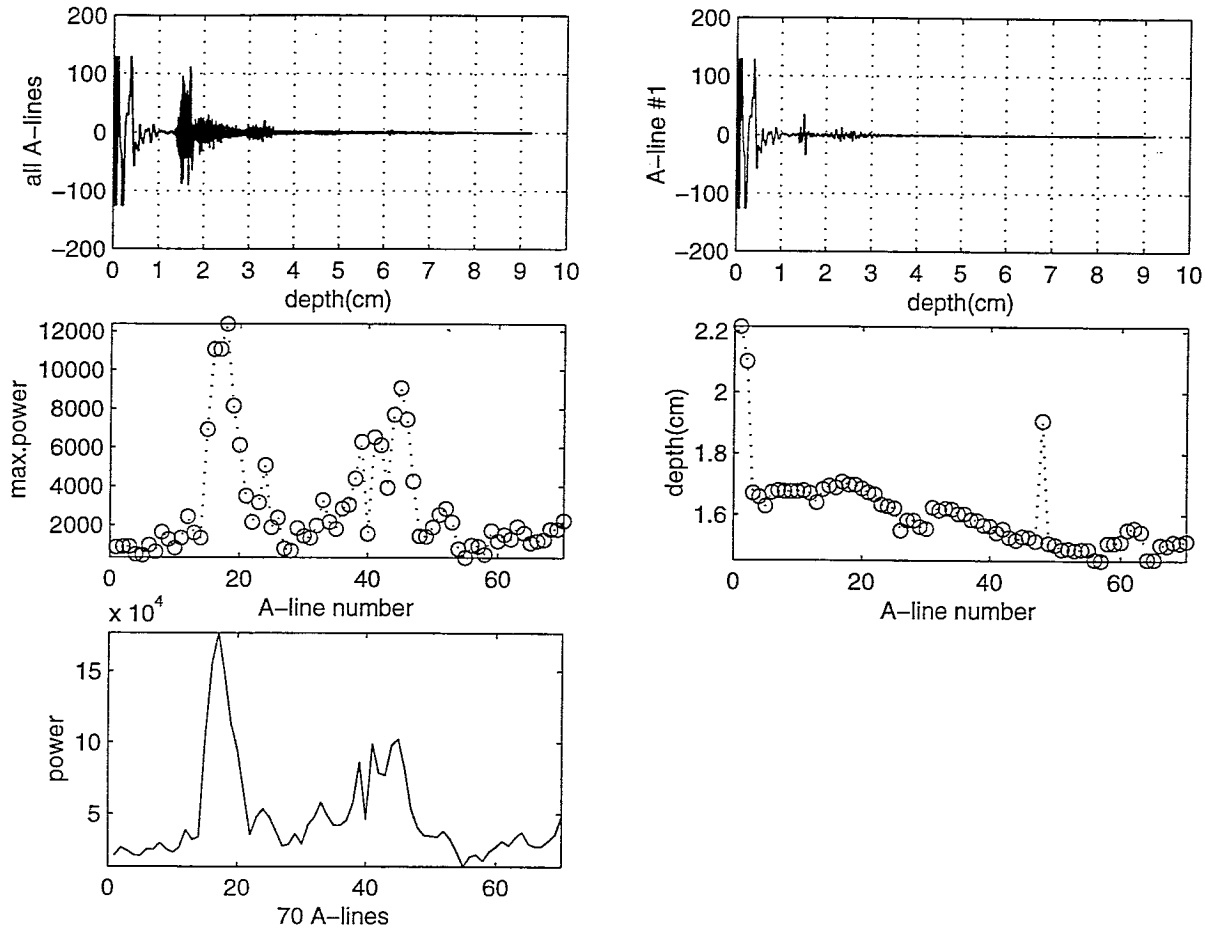
all A–lines
depth(cm)
A–line #1
depth(cm)
max.power
A–line number
depth(cm)
A–line number
x 10^4
power
70 A–lines

anl90g18

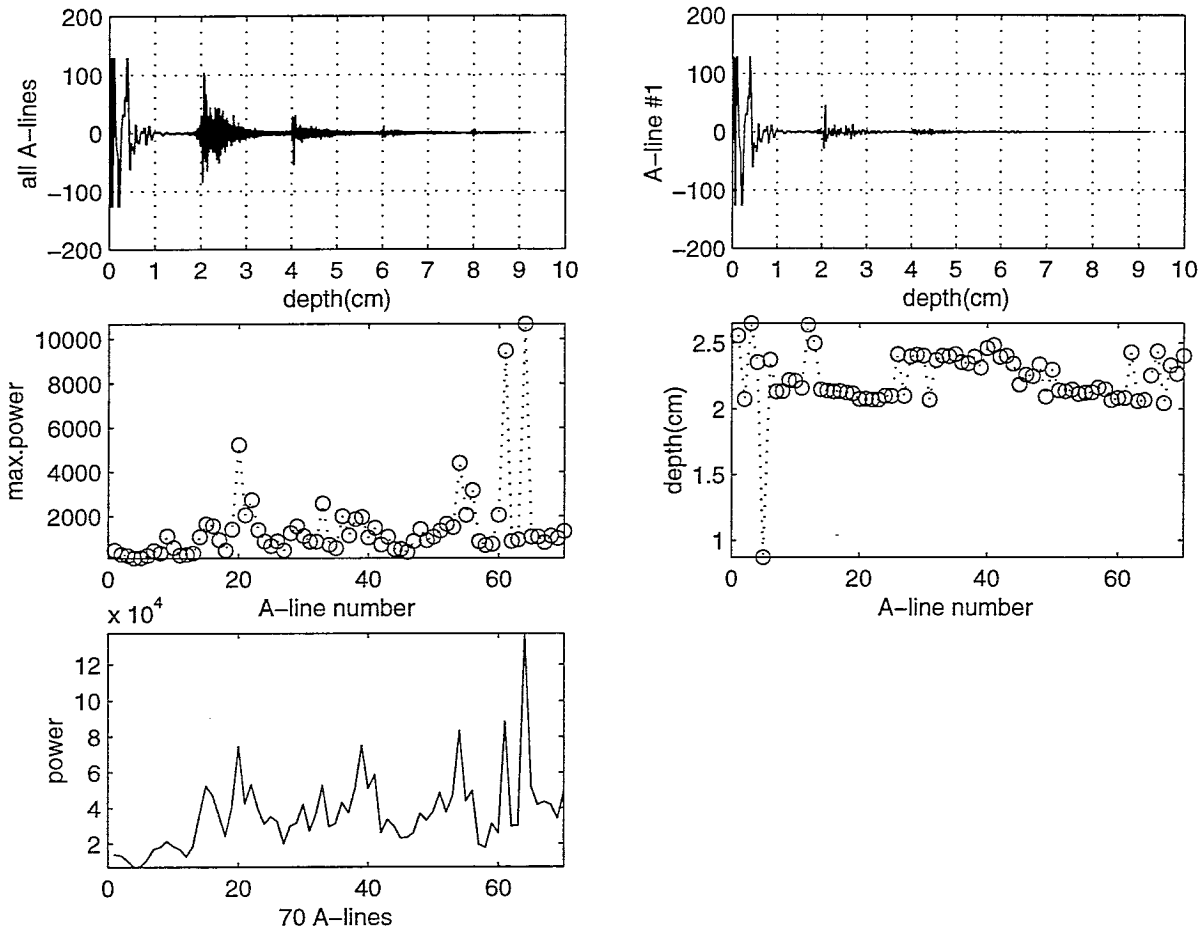
all A–lines
depth(cm)
A–line #1
depth(cm)
max.power
A–line number
depth(cm)
A–line number
x 10^4
power
70 A–lines

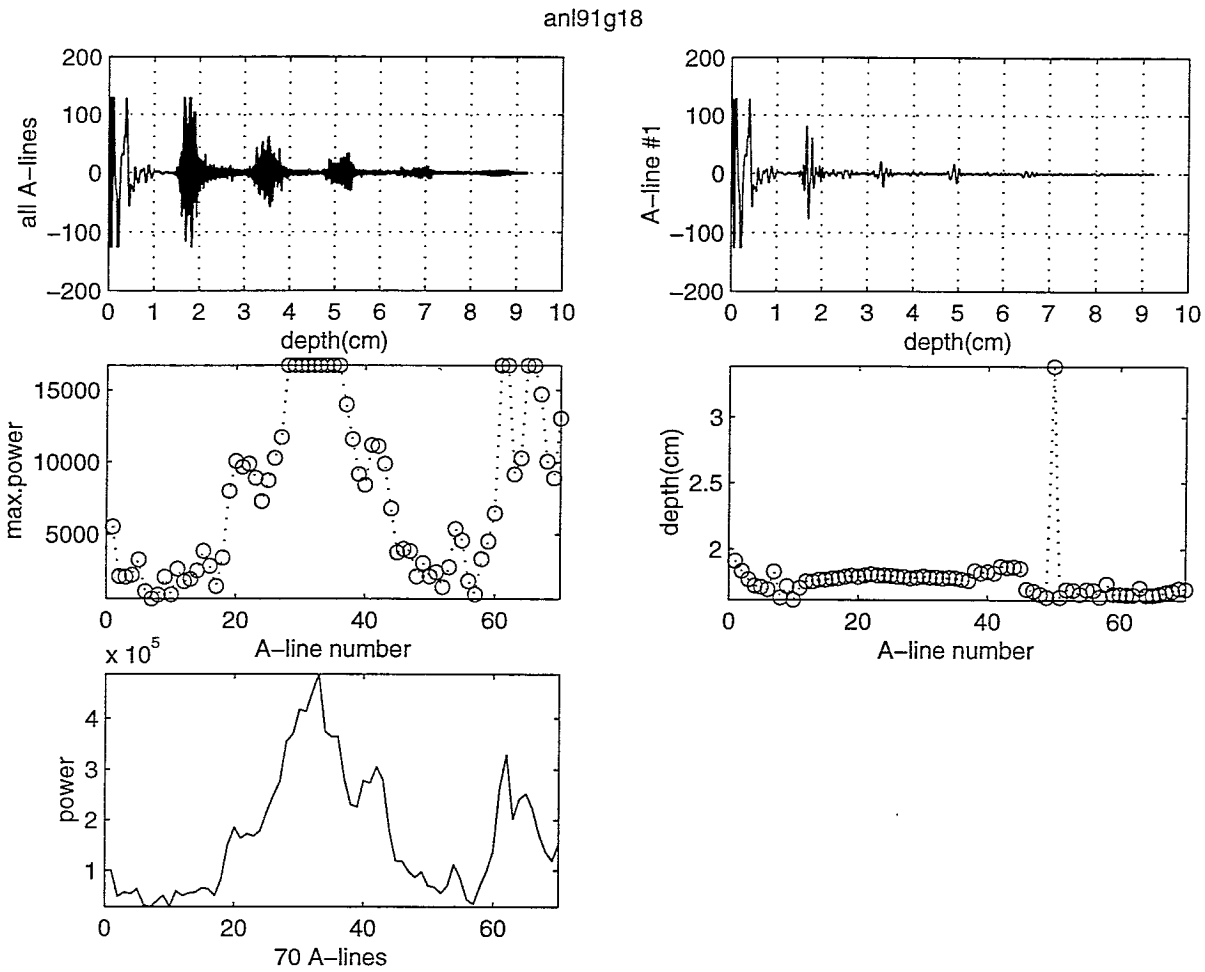
anl91g18
all A–lines
depth(cm)
A–line #1
depth(cm)
max.power
A–line number
depth(cm)
A–line number
x 10^5
power
70 A–lines

anl92g18

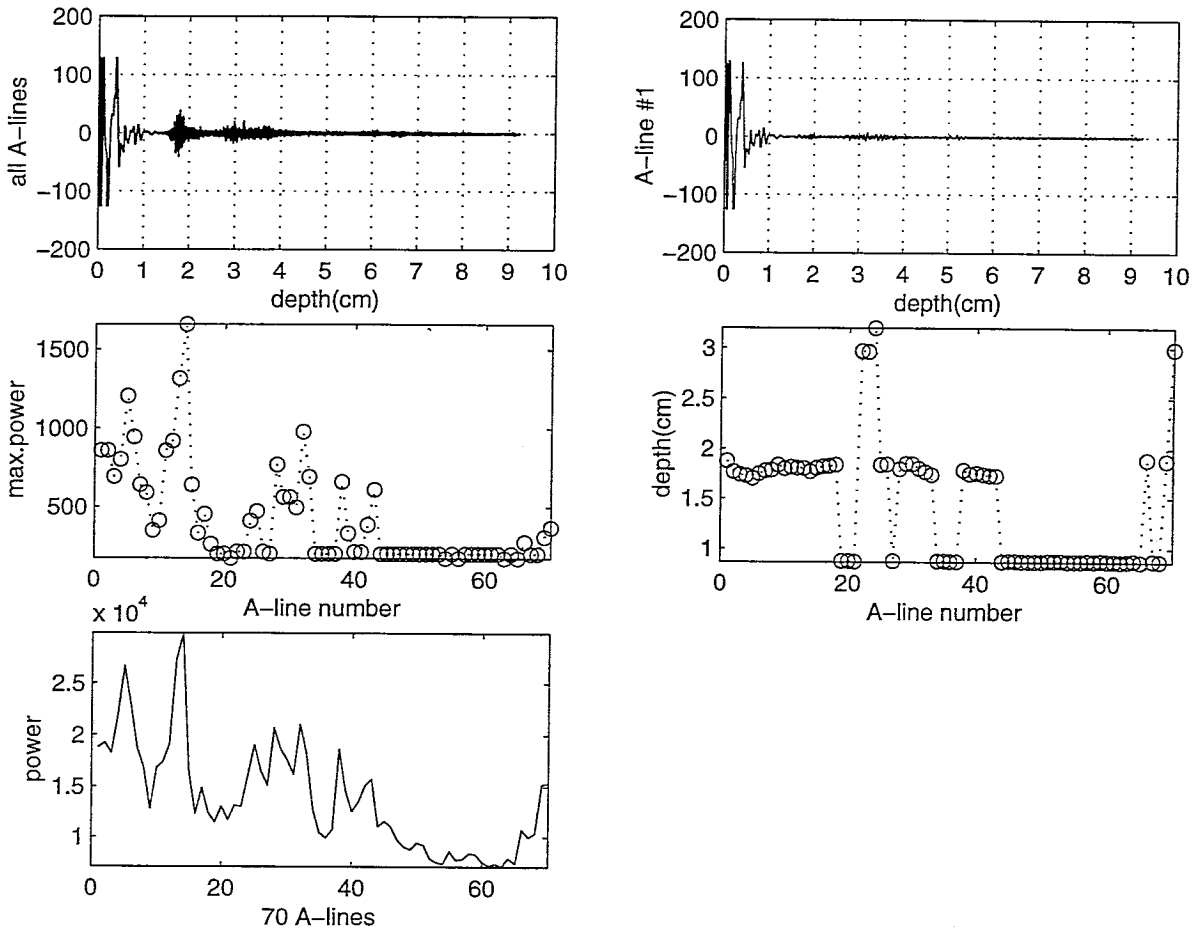
all A–lines
depth(cm)
A–line #1
depth(cm)
max.power
A–line number
depth(cm)
A–line number
x 10^4
power
70 A–lines

anl93g18

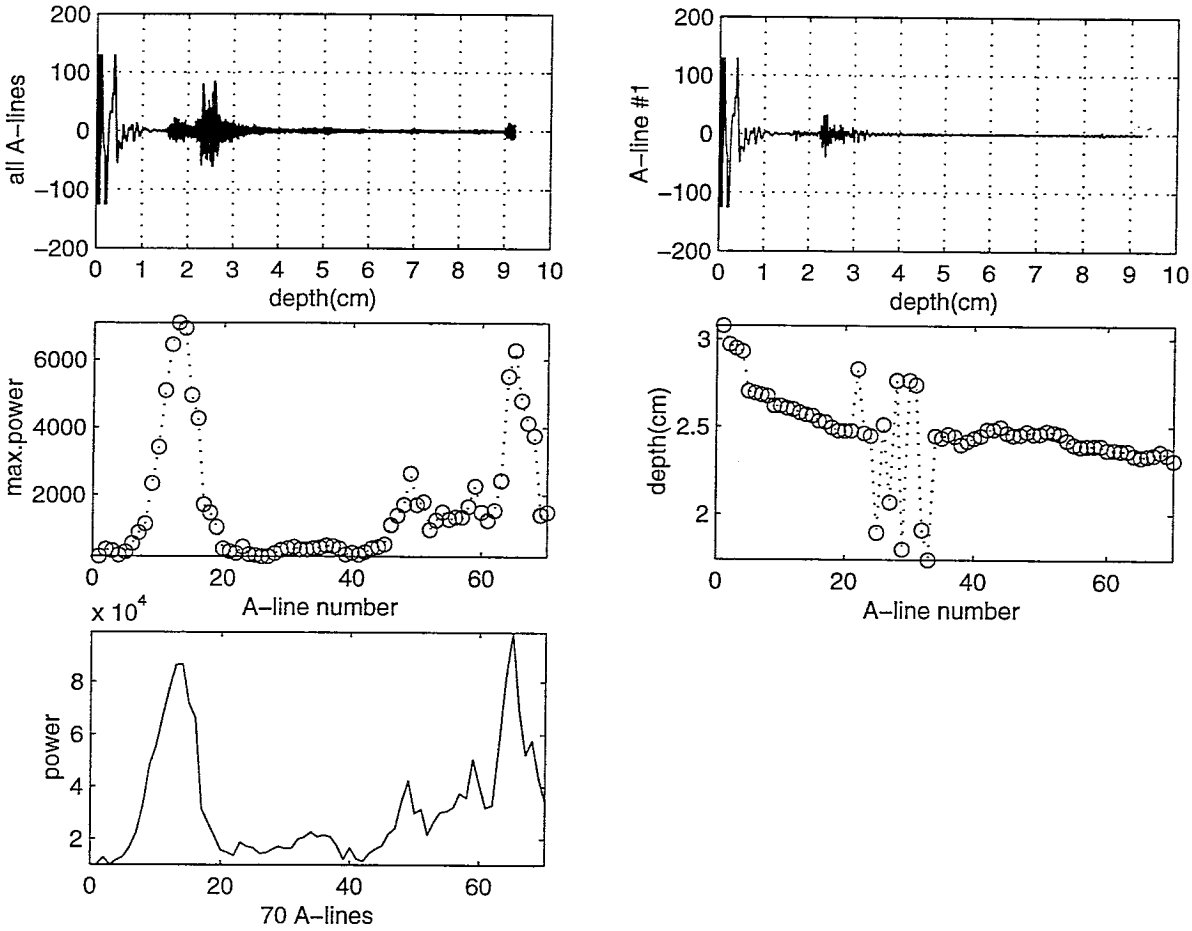
all A–lines
depth(cm)
A–line #1
depth(cm)
max.power
A–line number
depth(cm)
A–line number
x 10^4
power
70 A–lines

anl94g18

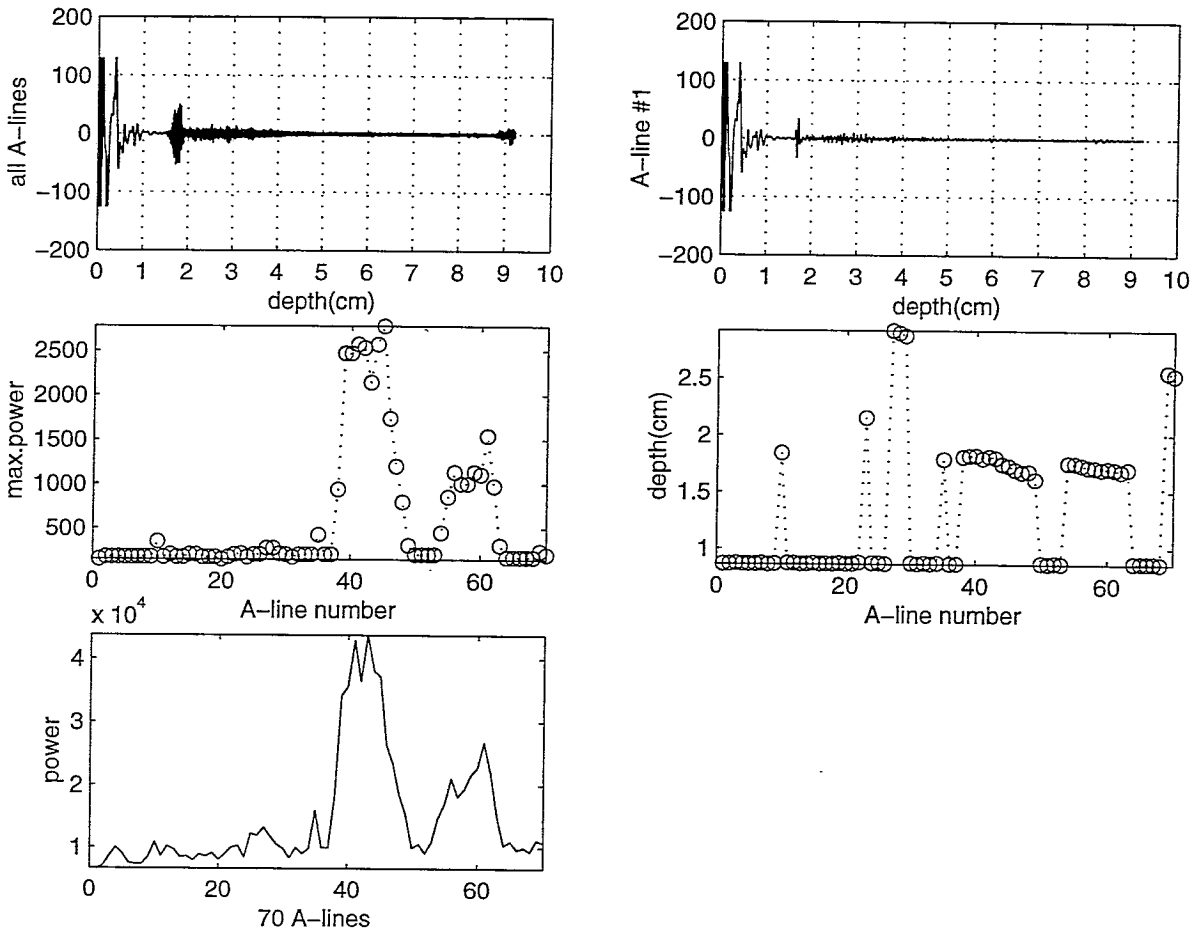
all A–lines
depth(cm)
A–line #1
depth(cm)
max.power
A–line number
depth(cm)
A–line number
x 10^4
power
70 A–lines

anl95g18

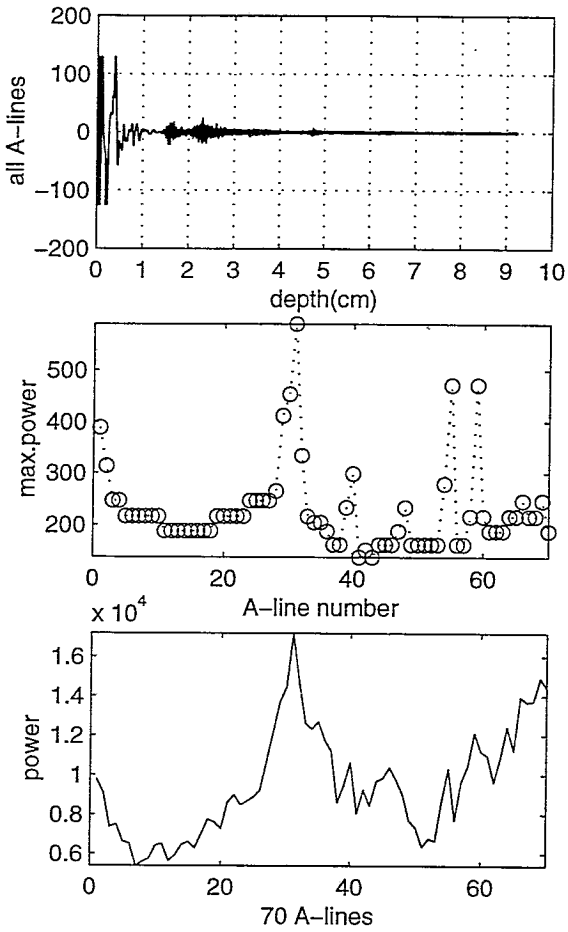
all A-lines
depth(cm)
max.power
A-line number
x 10^4
power
70 A-lines

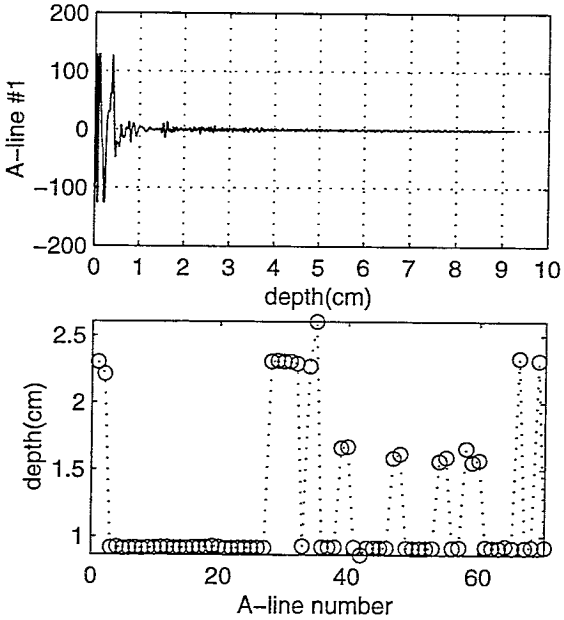
A-line #1
depth(cm)
depth(cm)
A-line number

anl96g18

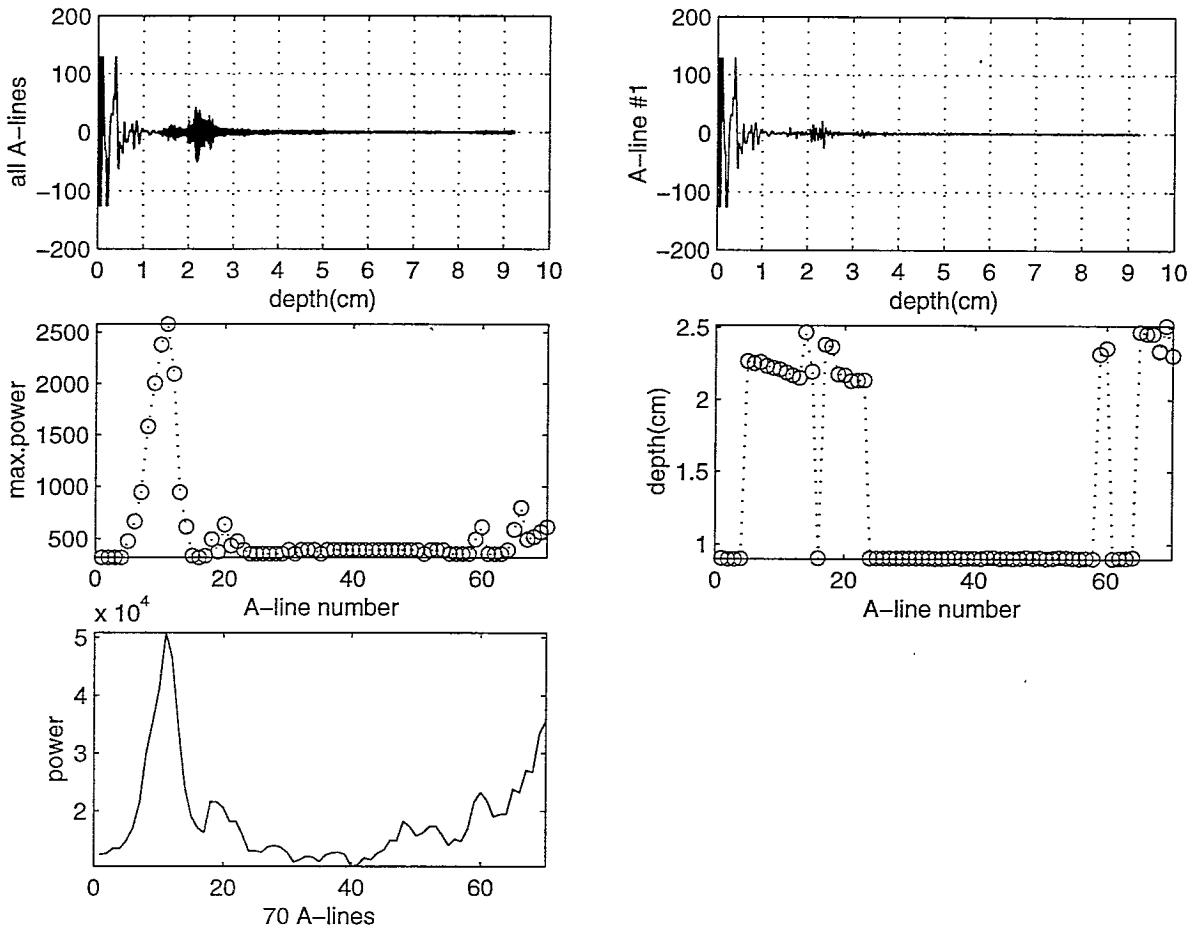
all A–lines
depth(cm)
A–line #1
depth(cm)
max.power
A–line number
depth(cm)
A–line number
x 10^4
power
70 A–lines

anl97g18

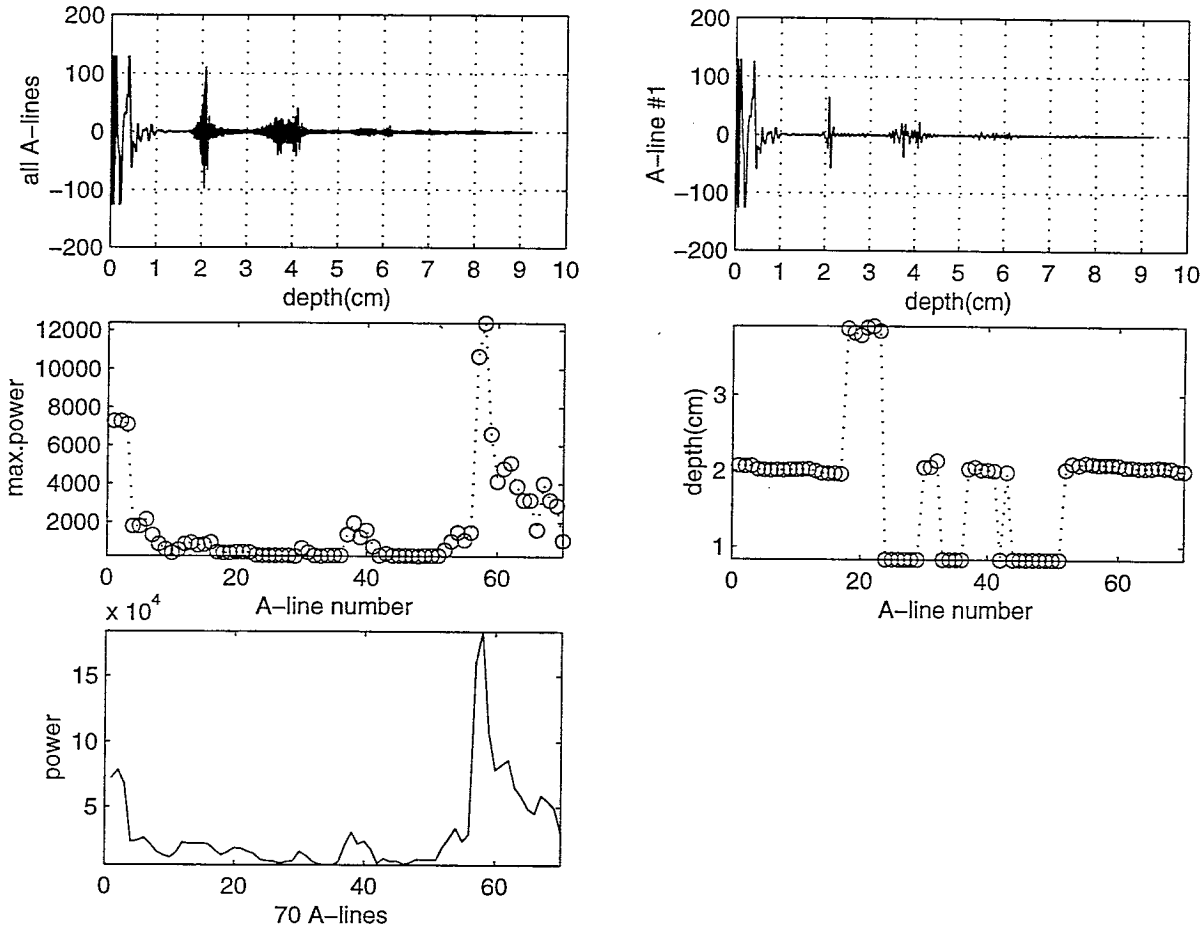
all A–lines
depth(cm)
A–line #1
depth(cm)
max.power
A–line number
depth(cm)
A–line number
x 10^4
power
70 A–lines

anl98g18

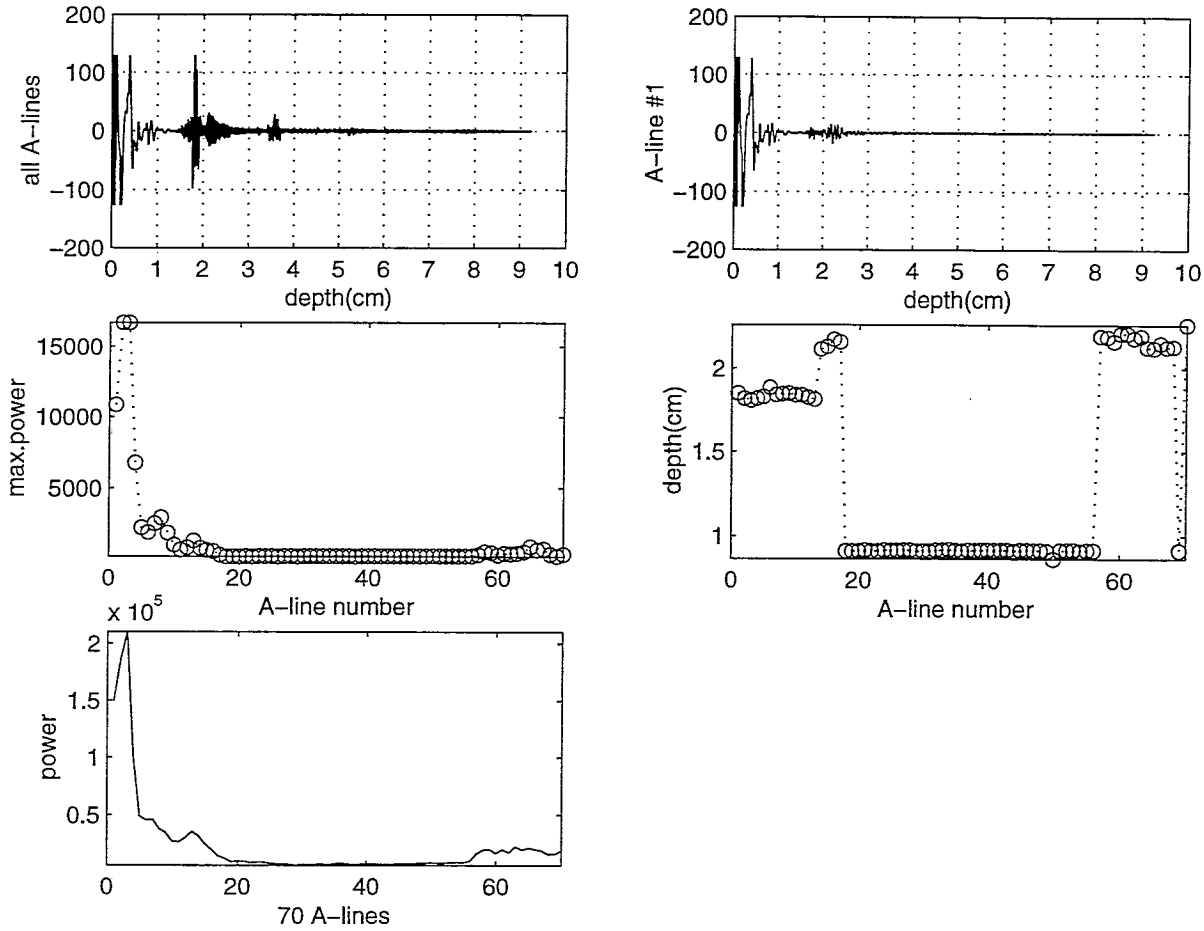
all A–lines
depth(cm)
A–line #1
depth(cm)
max.power
A–line number
depth(cm)
A–line number
x 10^5
power
70 A–lines

anl99g18

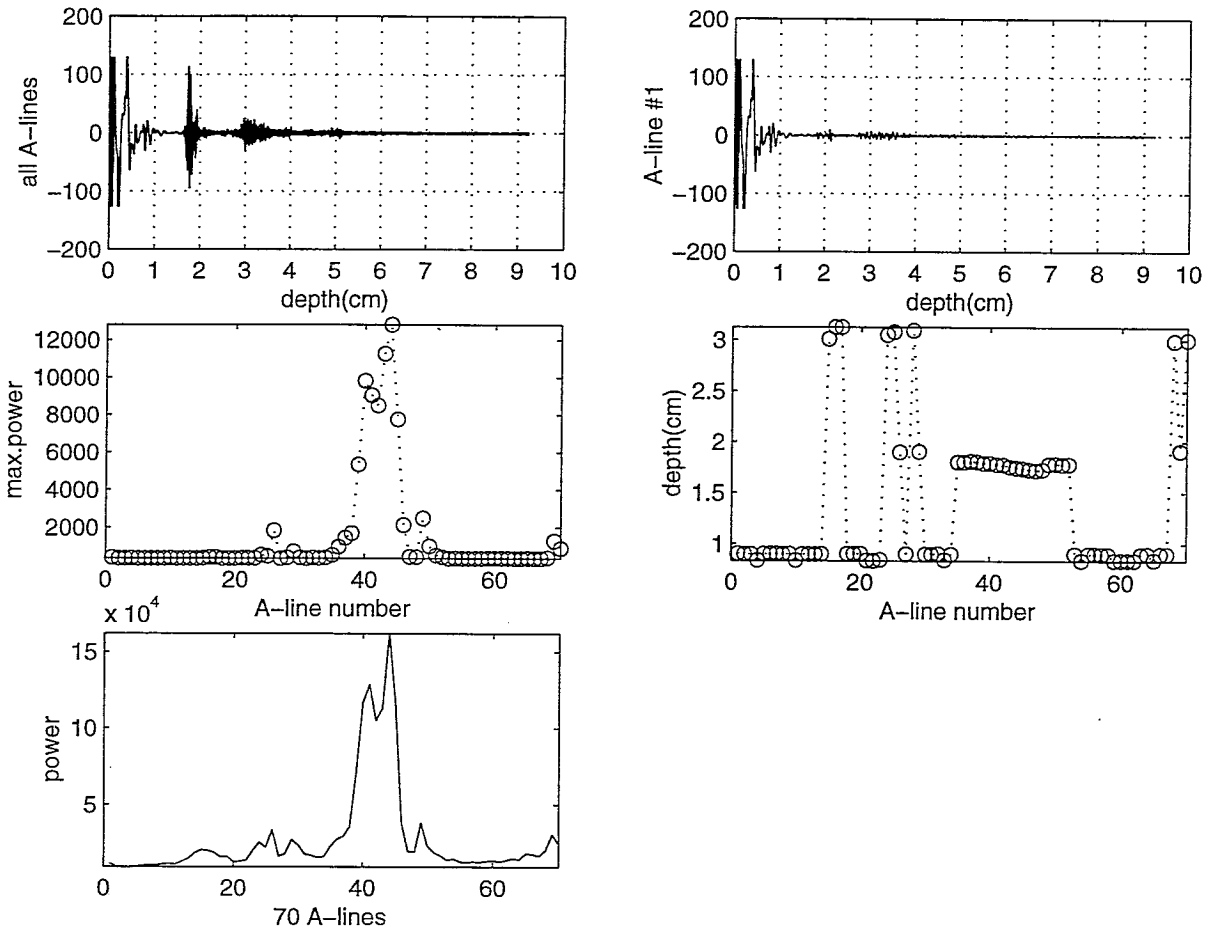
all A–lines
depth(cm)
A–line #1
depth(cm)
max.power
x 10^4
A–line number
depth(cm)
A–line number
power
70 A–lines

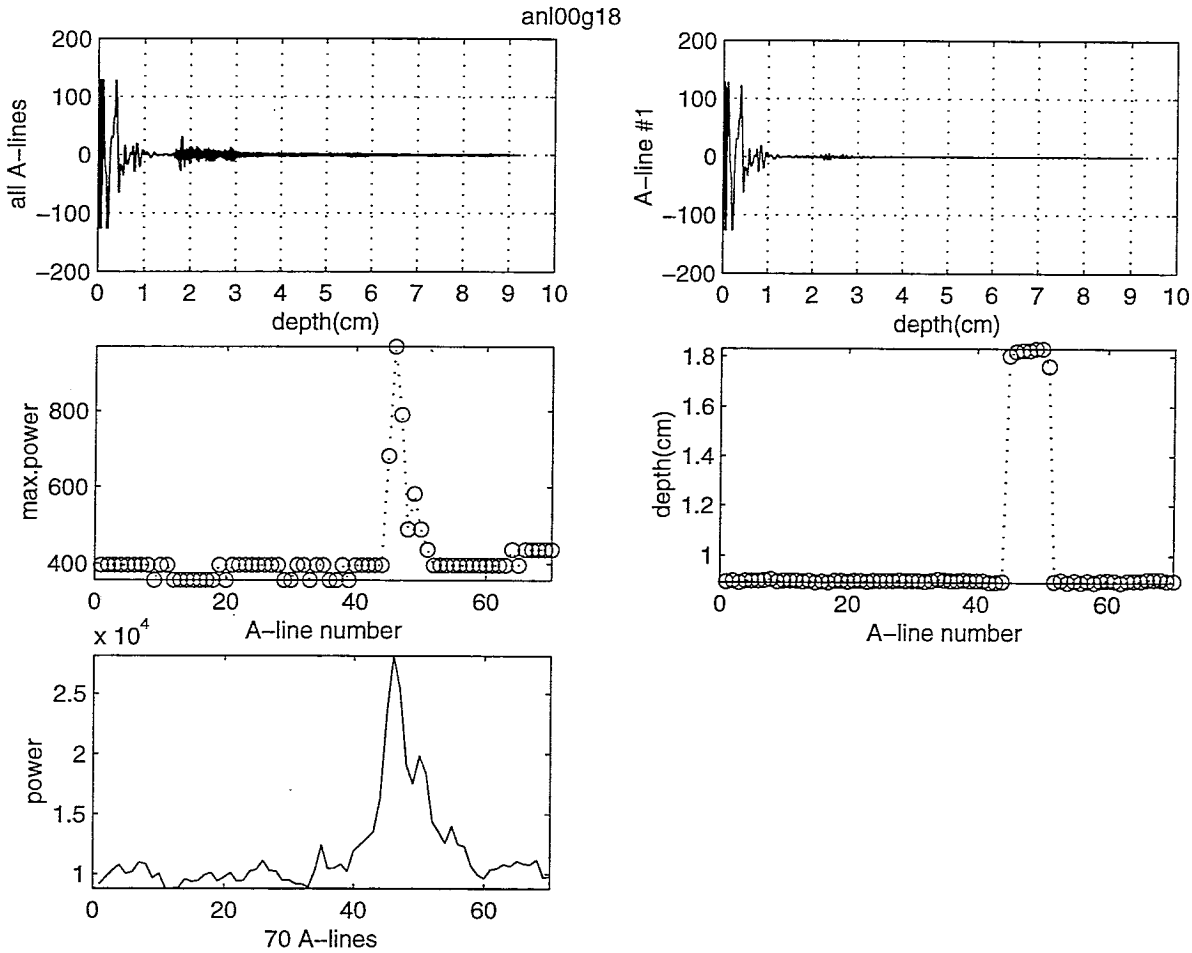
anl00g18
all A-lines
depth(cm)
A-line #1
depth(cm)
max.power
A-line number
depth(cm)
A-line number
x 10^4
power
70 A-lines

anl101g18

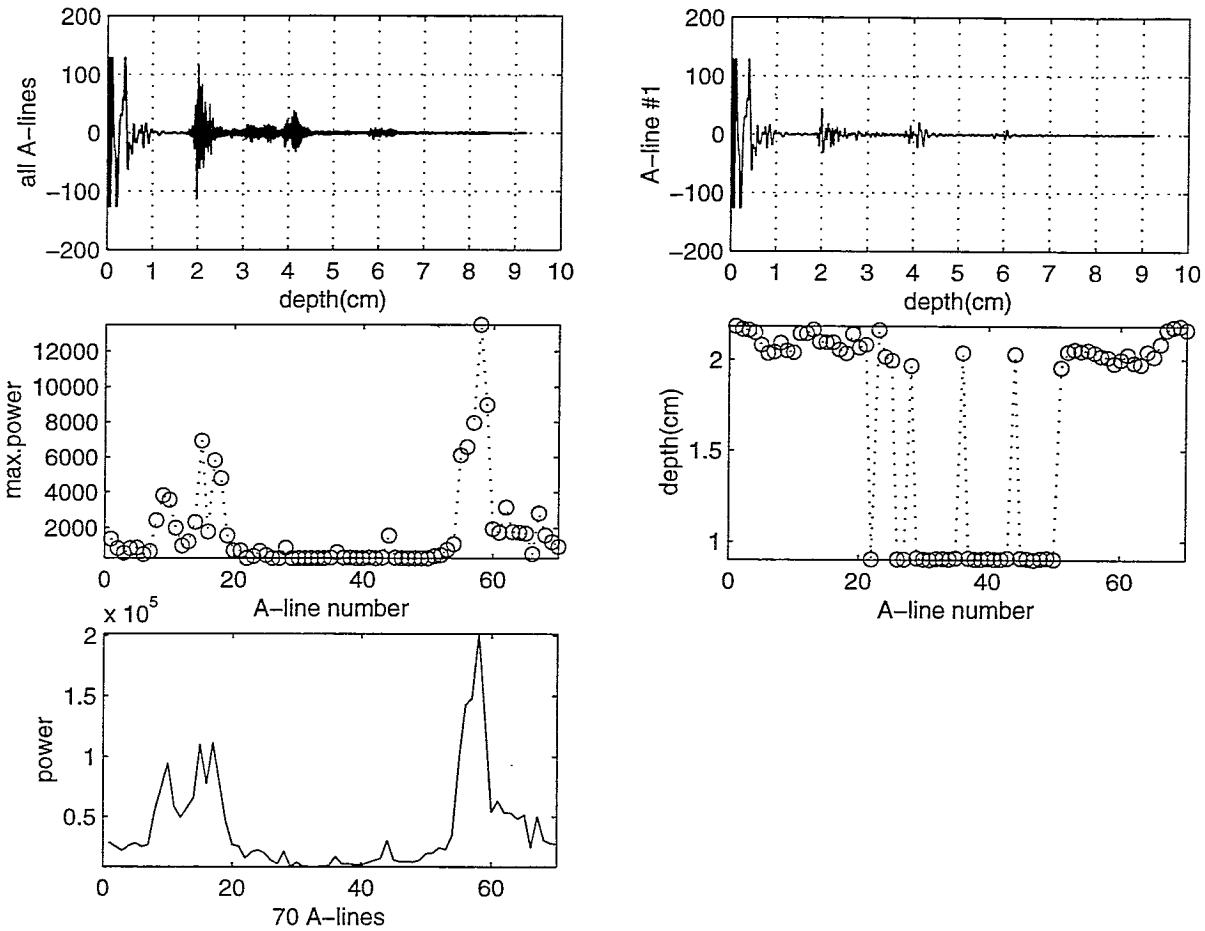
all A–lines
depth(cm)
A–line #1
depth(cm)
max.power
A–line number
depth(cm)
A–line number
x 10^5
power
70 A–lines

anl102g18

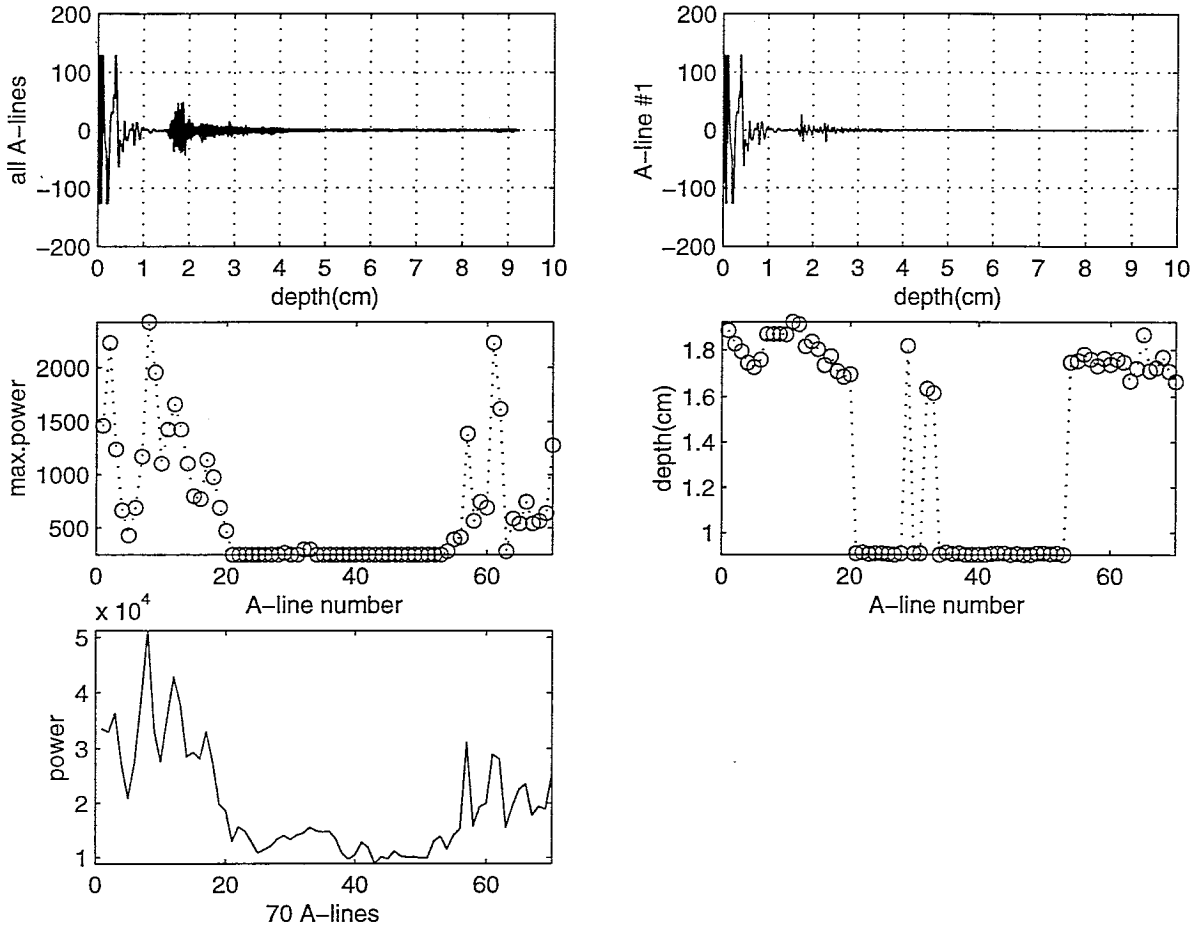
all A–lines
depth(cm)
A–line #1
depth(cm)
max.power
A–line number
depth(cm)
A–line number
x 10^4
power
70 A–lines

anl103g18

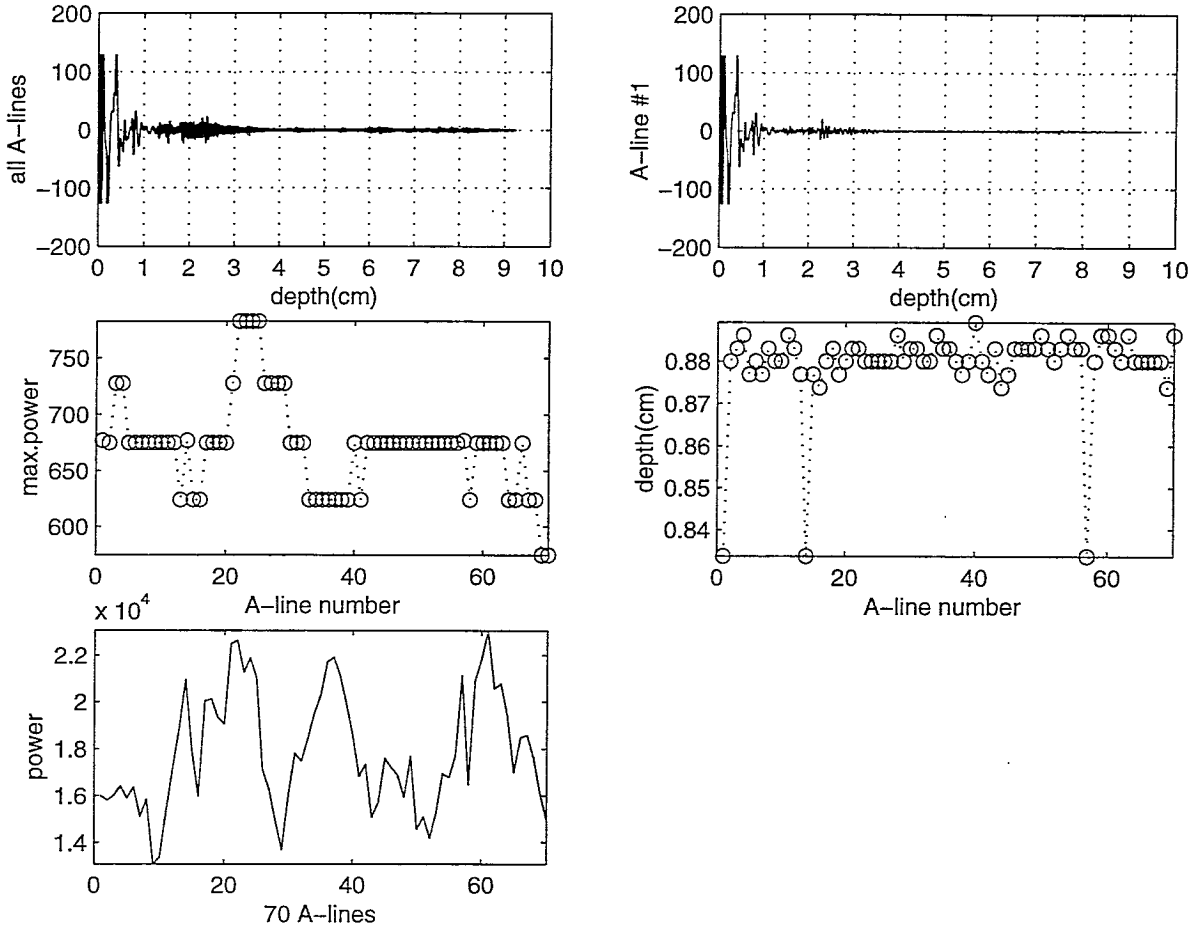
all A–lines
depth(cm)
A–line #1
depth(cm)
max.power
A–line number
depth(cm)
A–line number
x 10^4
power
70 A–lines

anl104g18

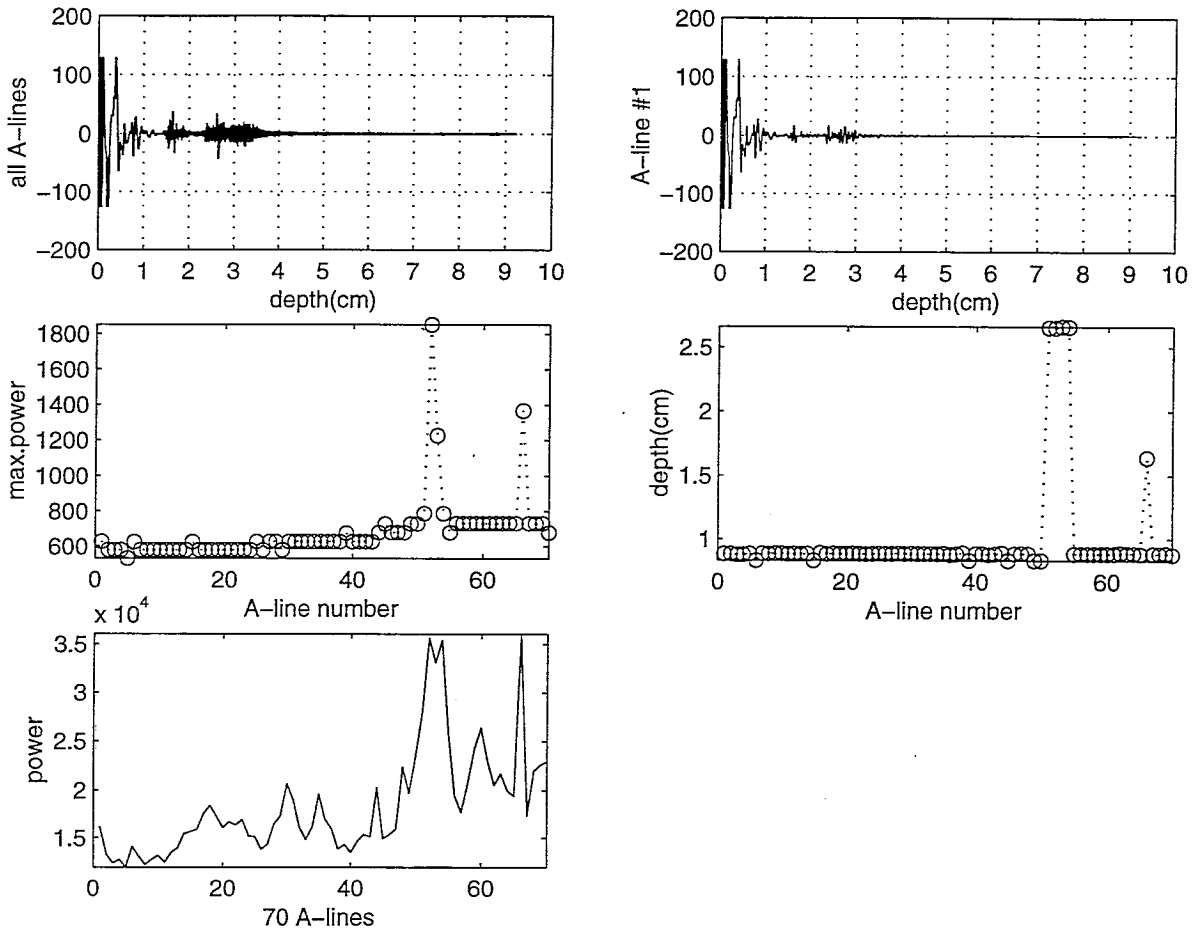
all A–lines
depth(cm)
A–line #1
depth(cm)
max.power
A–line number
depth(cm)
A–line number
x 10^4
power
70 A–lines

anl105g18

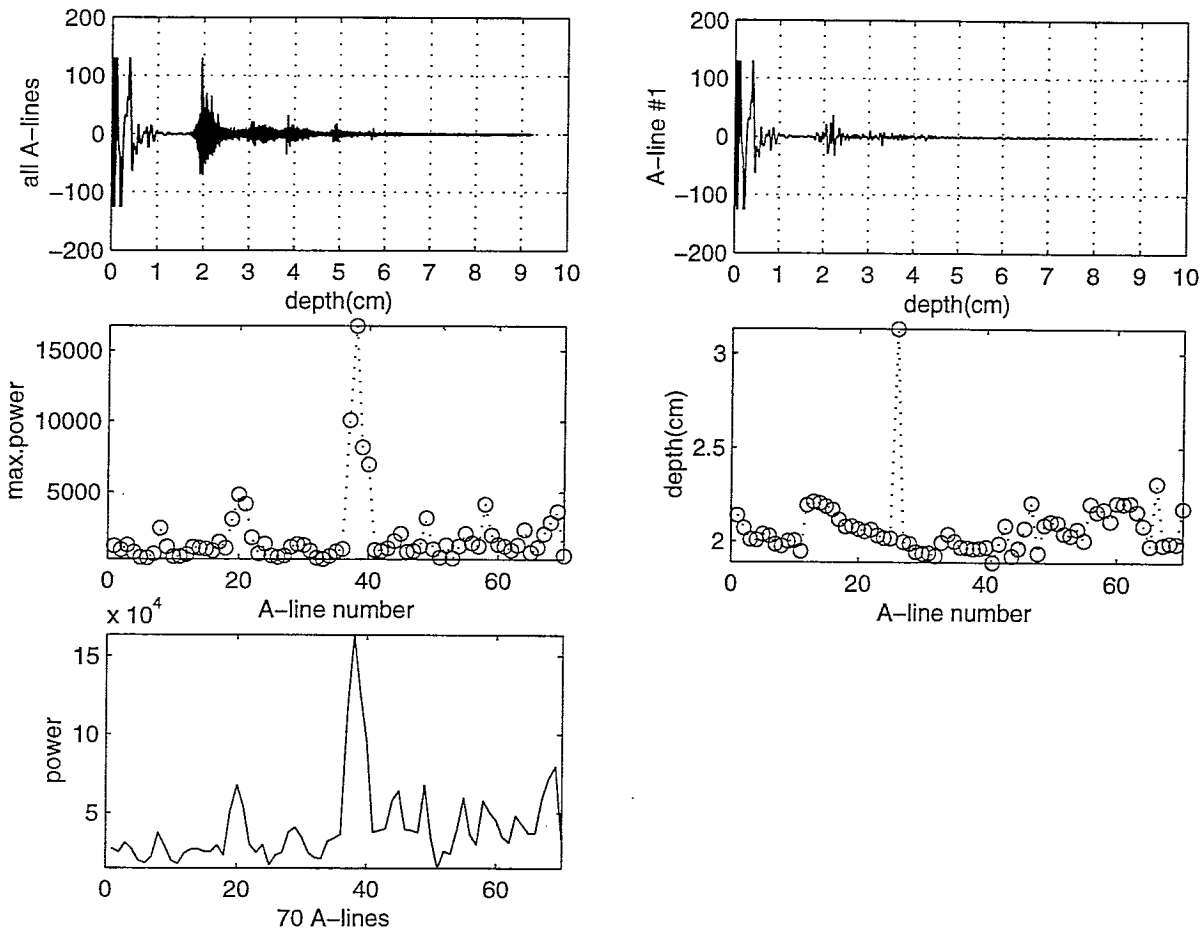
all A–lines
depth(cm)
A–line #1
depth(cm)
max.power
A–line number
depth(cm)
A–line number
x 10^4
power
70 A–lines

anl106g18

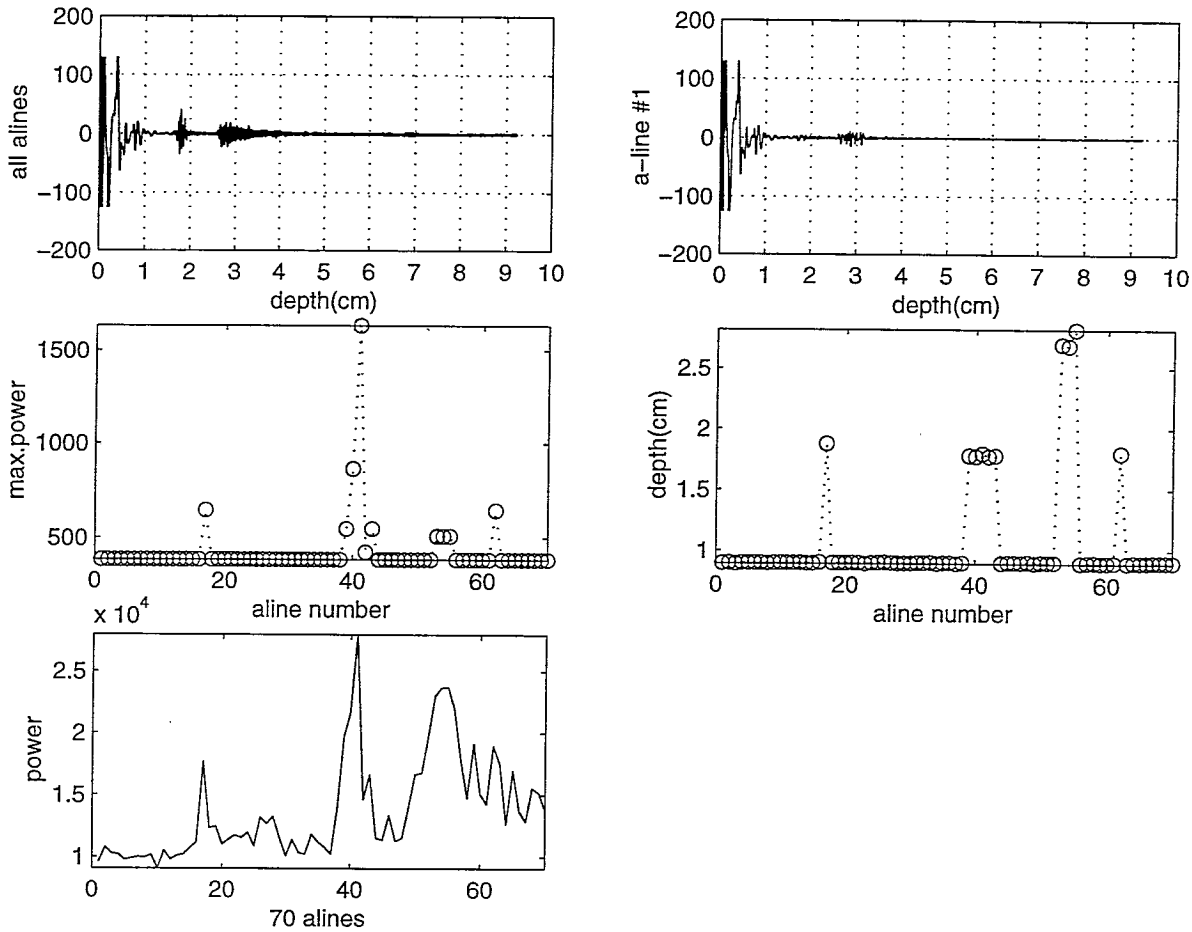
all alines
depth(cm)
a−line #1
depth(cm)
max.power
aline number
depth(cm)
aline number
x 10^4
power
70 alines

anl107g18

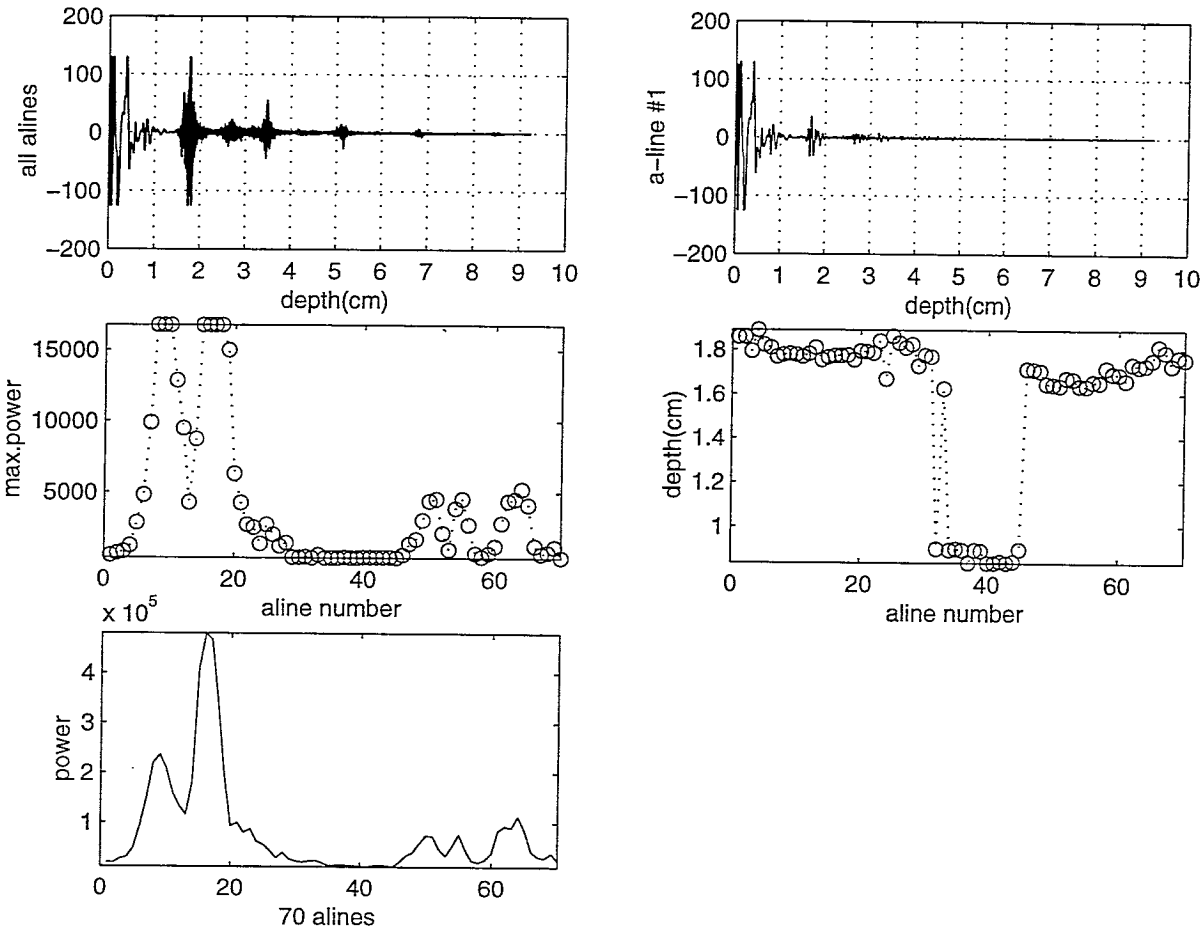
all alines
depth(cm)
a-line #1
depth(cm)
max.power
aline number
depth(cm)
aline number
x 10^5
power
70 alines

anl108g18

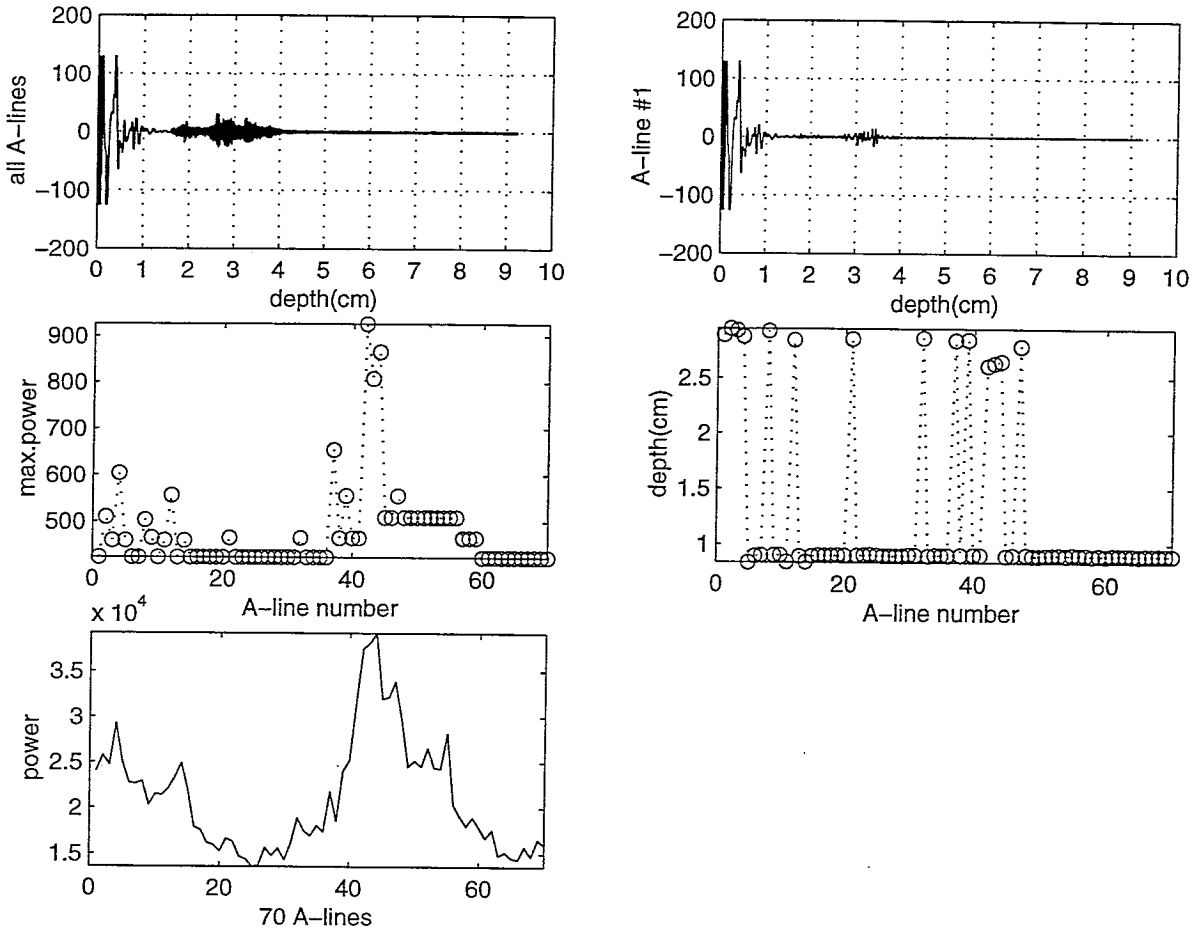
all A–lines
depth(cm)
A–line #1
depth(cm)
max.power
A–line number
depth(cm)
A–line number
x 10^4
power
70 A–lines

ani109g18

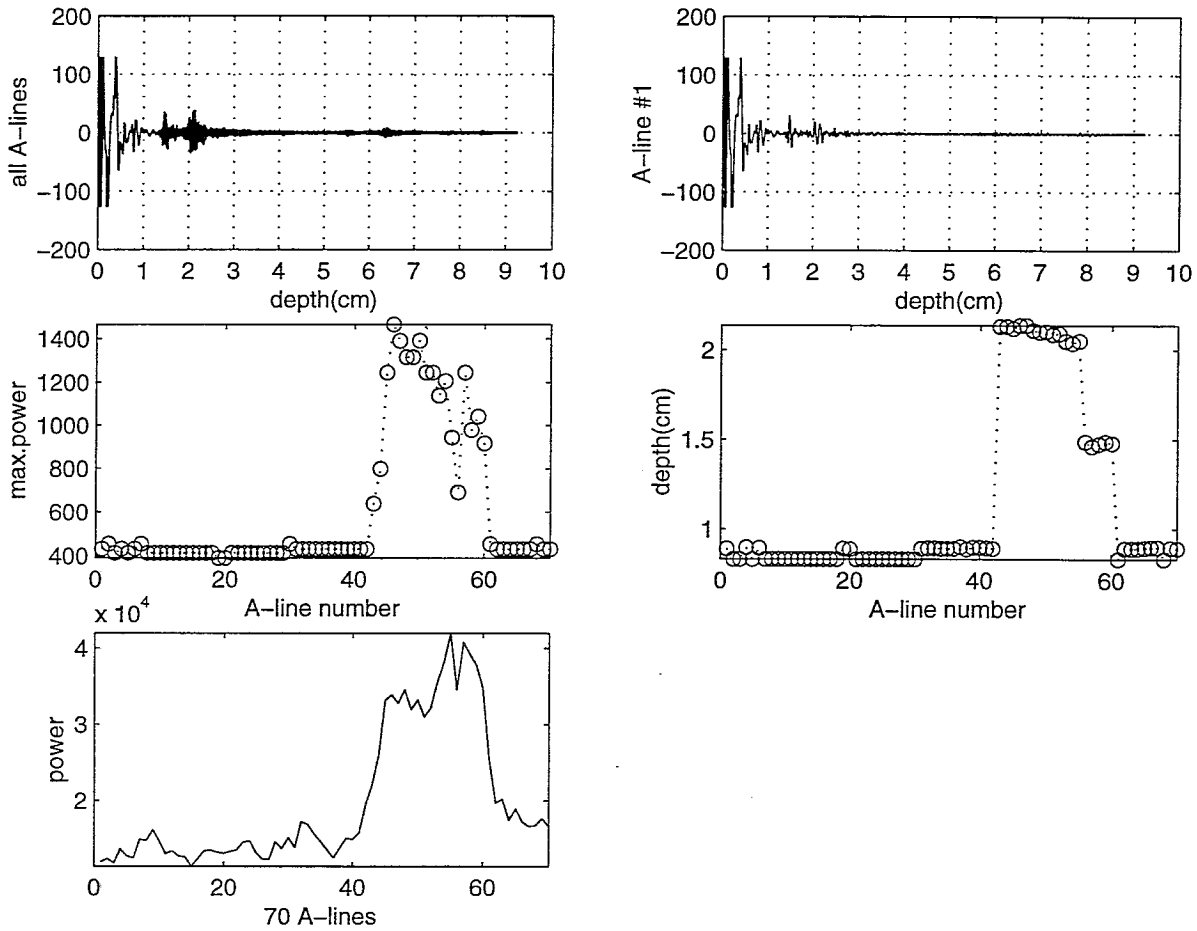
all A–lines
depth(cm)
A–line #1
depth(cm)
max.power
A–line number
depth(cm)
A–line number
x 10^4
power
70 A–lines

anl110g18

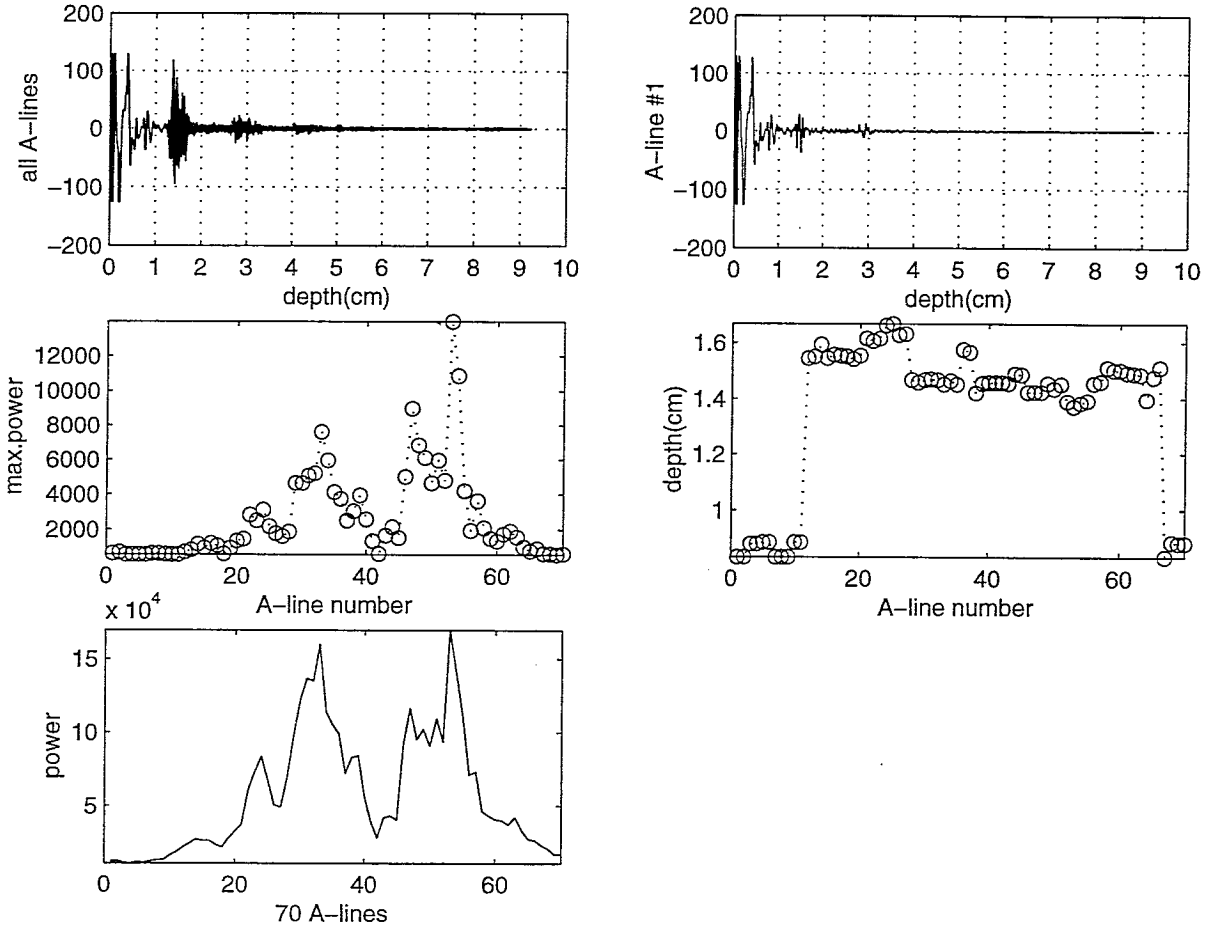
all A–lines
depth(cm)
A–line #1
depth(cm)
max.power
A–line number
depth(cm)
A–line number
x 10^4
power
70 A–lines

anl111g18

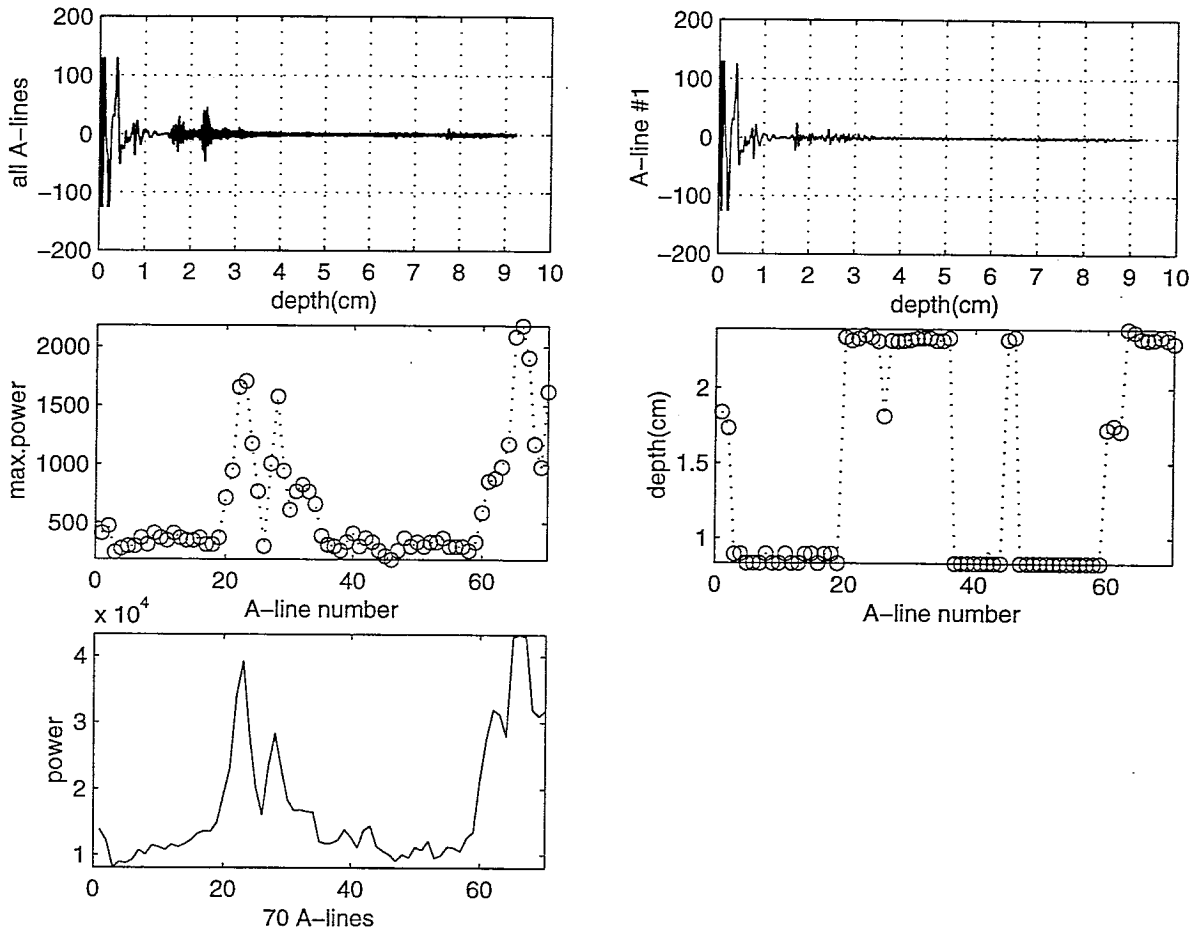
all A–lines
depth(cm)
A–line #1
depth(cm)
max.power
A–line number
depth(cm)
A–line number
x 10^4
power
70 A–lines

anl112g18

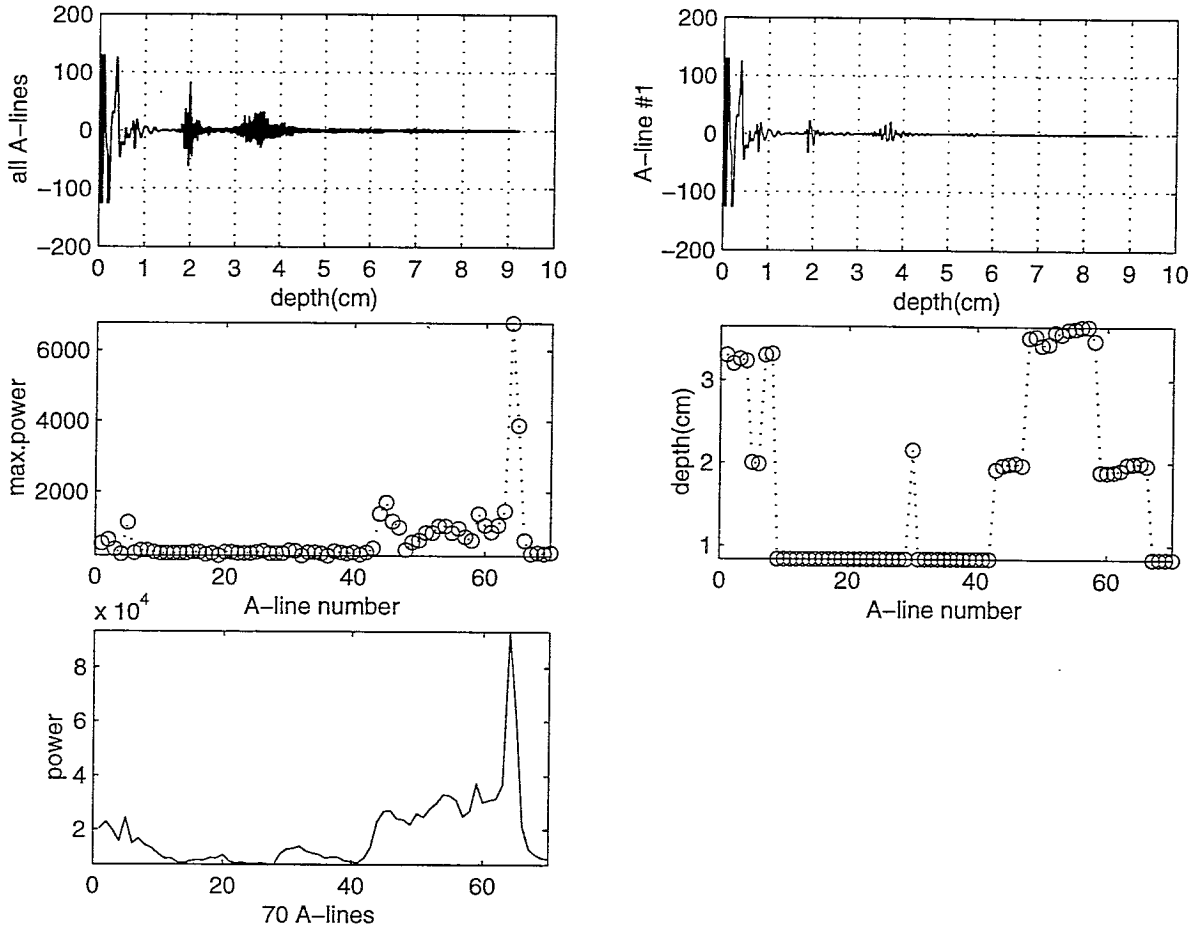
all A–lines
depth(cm)
A–line #1
depth(cm)
max.power
A–line number
depth(cm)
A–line number
x 10^4
power
70 A–lines

anl113g18

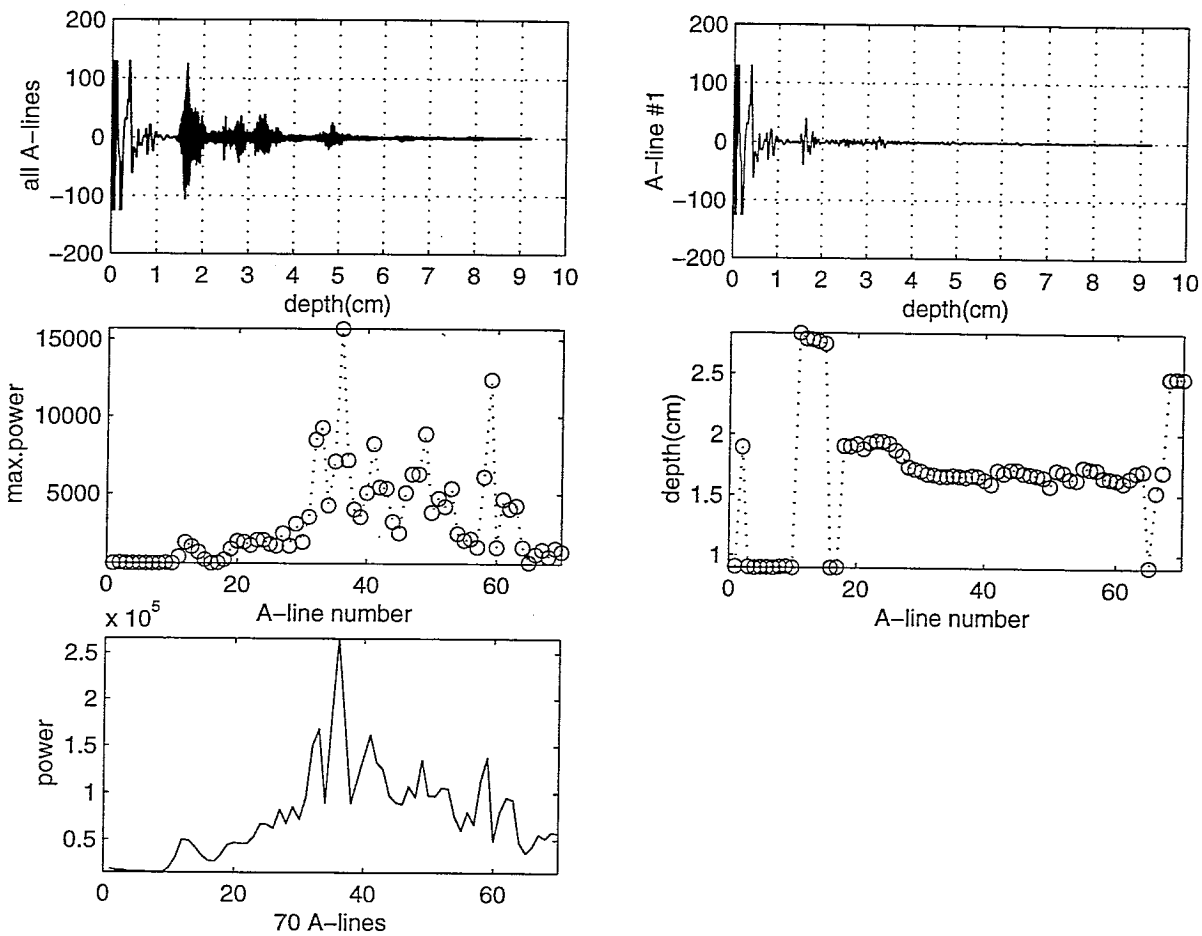
all A–lines
depth(cm)
A–line #1
depth(cm)
max.power
A–line number
depth(cm)
A–line number
x 10^5
power
70 A–lines

anl114g18

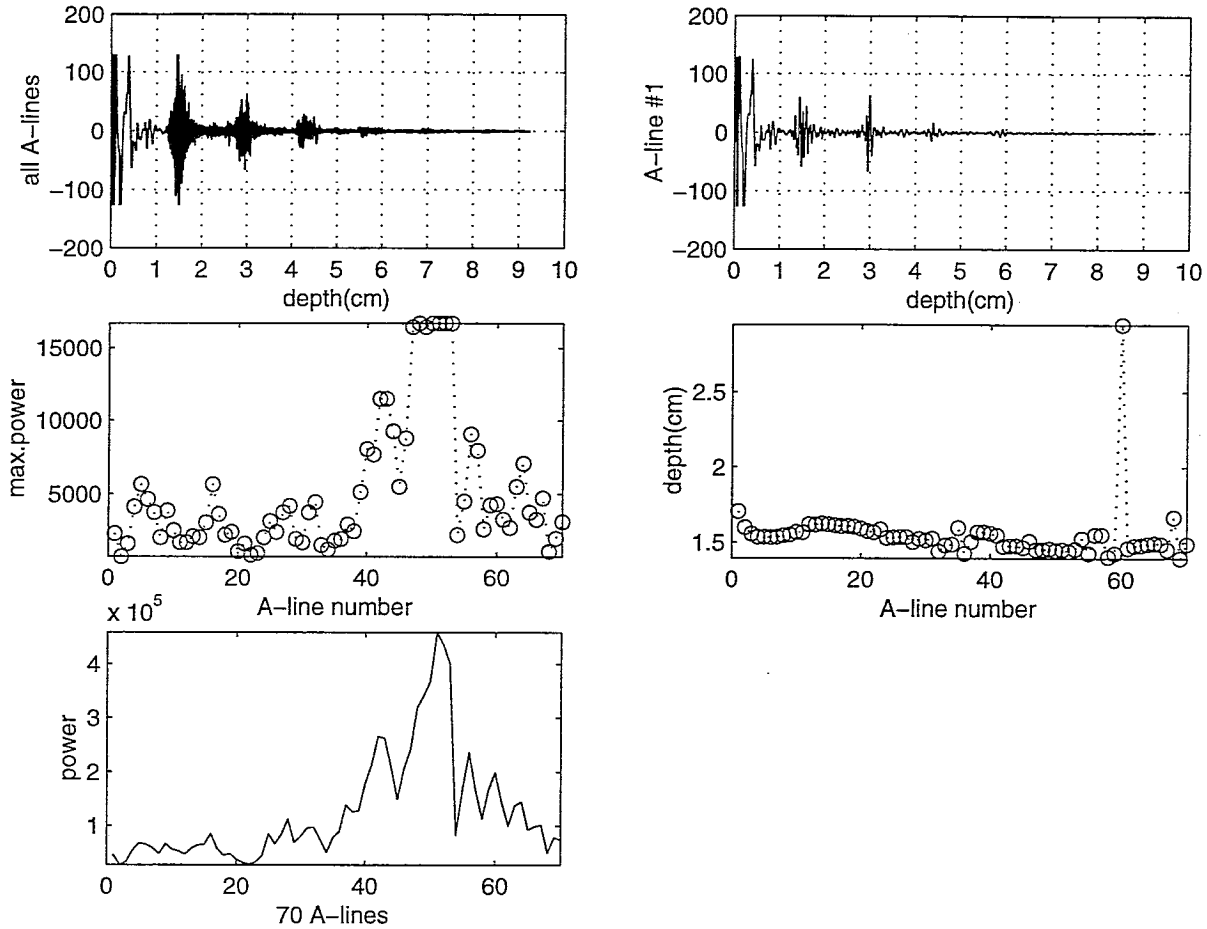
all A–lines
depth(cm)
A–line #1
depth(cm)
max.power
A–line number
depth(cm)
A–line number
x 10^5
power
70 A–lines

anl115g18

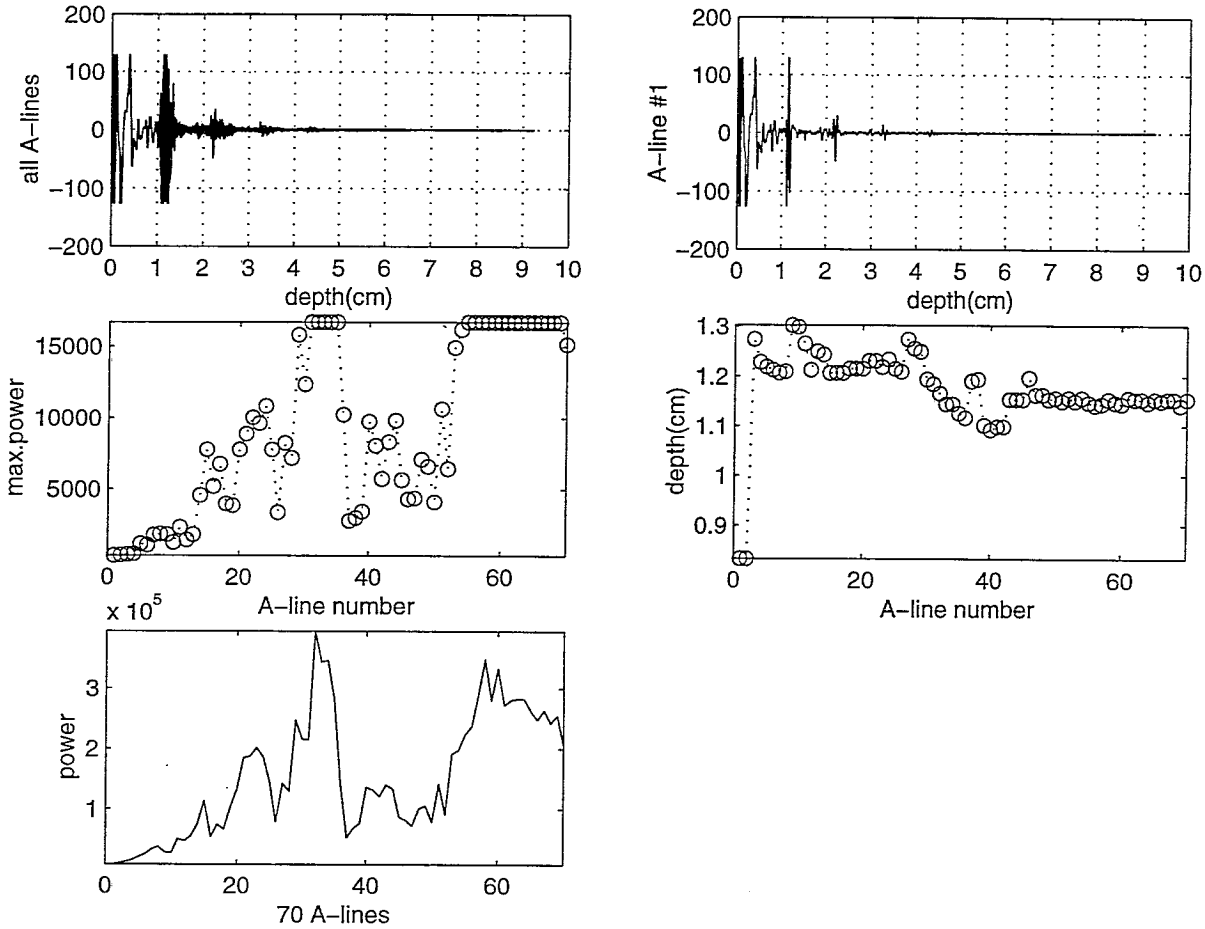
all A–lines
depth(cm)
A–line #1
depth(cm)
max.power
A–line number
depth(cm)
A–line number
x 10^5
power
70 A–lines

anl116g18

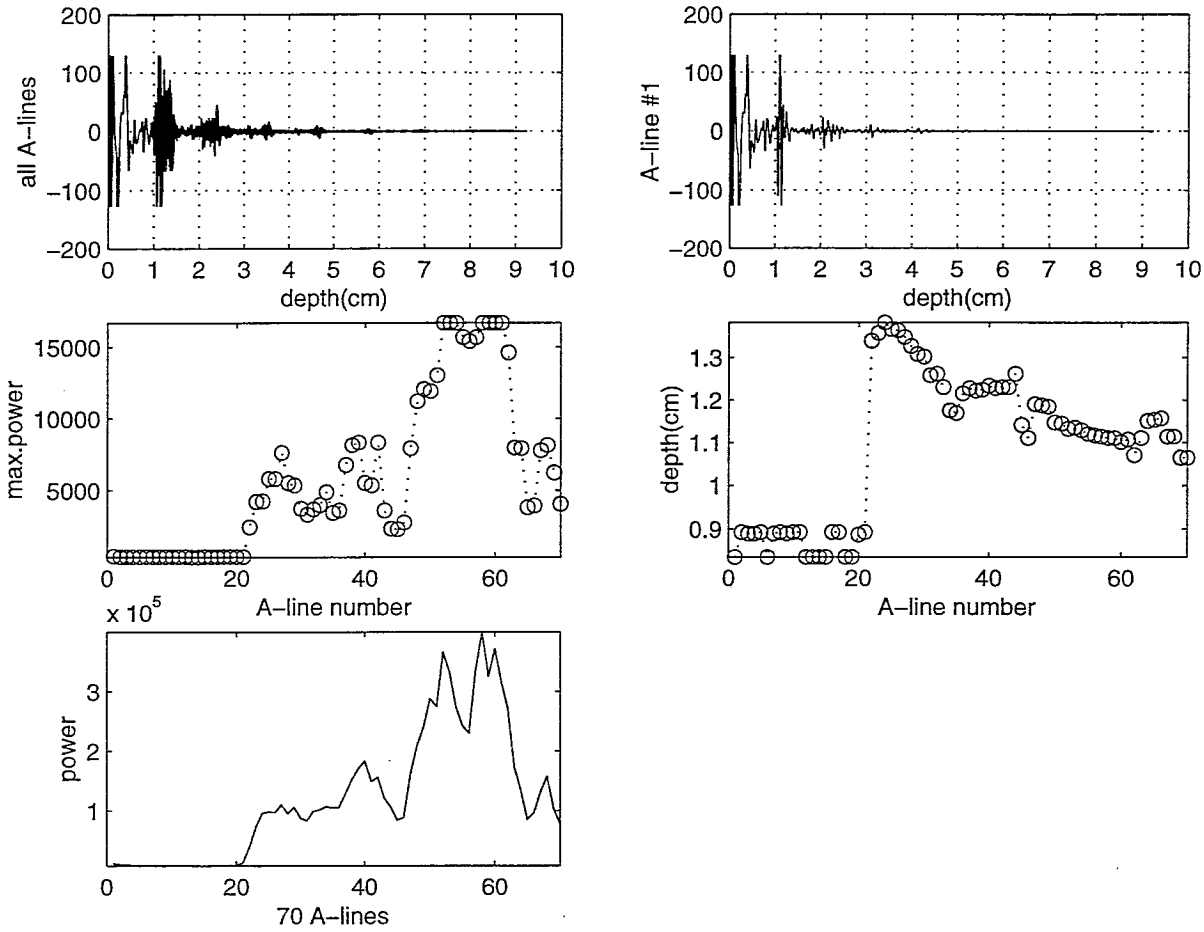
all A–lines
depth(cm)
A–line #1
depth(cm)
max.power
A–line number
depth(cm)
A–line number
x 10^5
power
70 A–lines

anl117g18

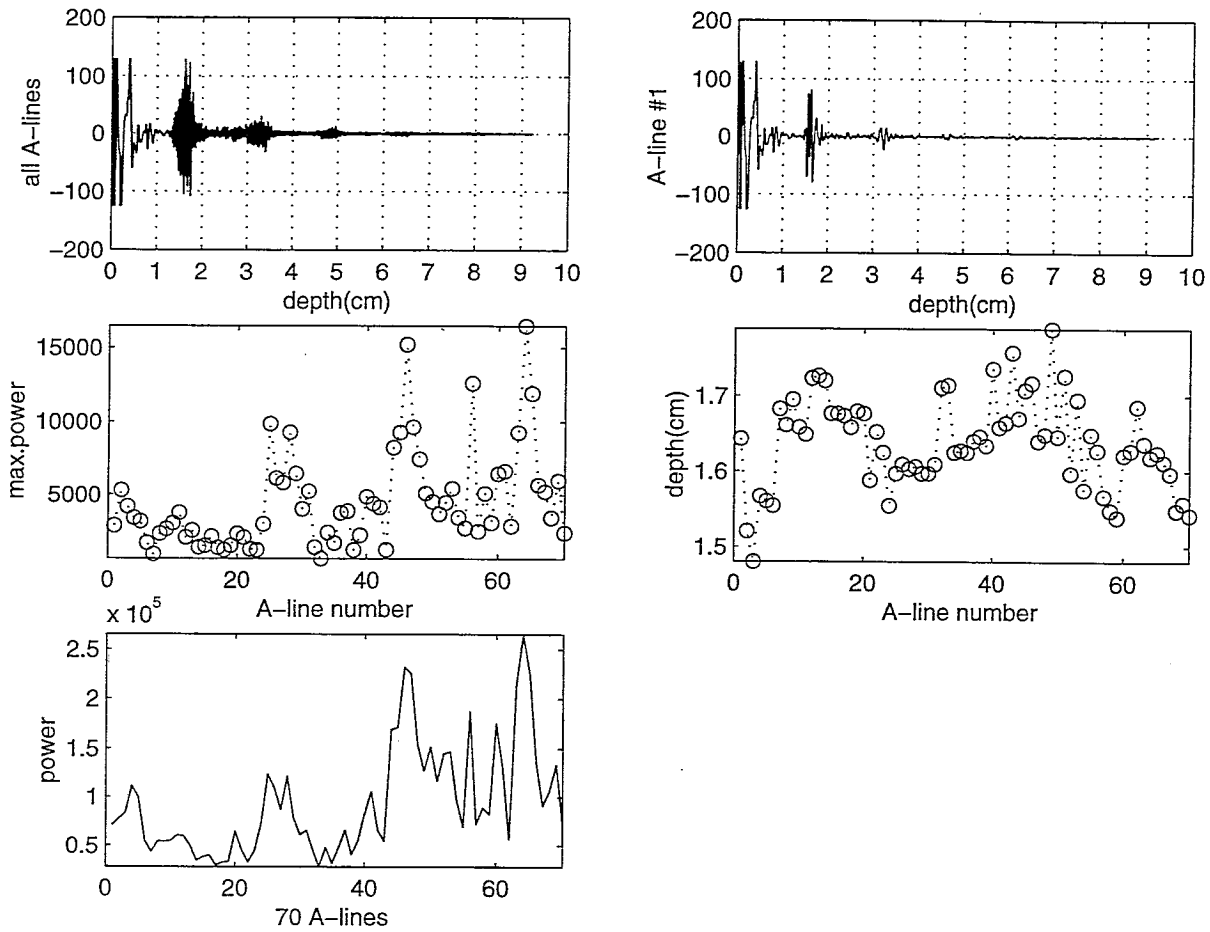
all A–lines
depth(cm)
A–line #1
depth(cm)
max.power
A–line number
depth(cm)
A–line number
x 10^5
power
70 A–lines

anl118g18

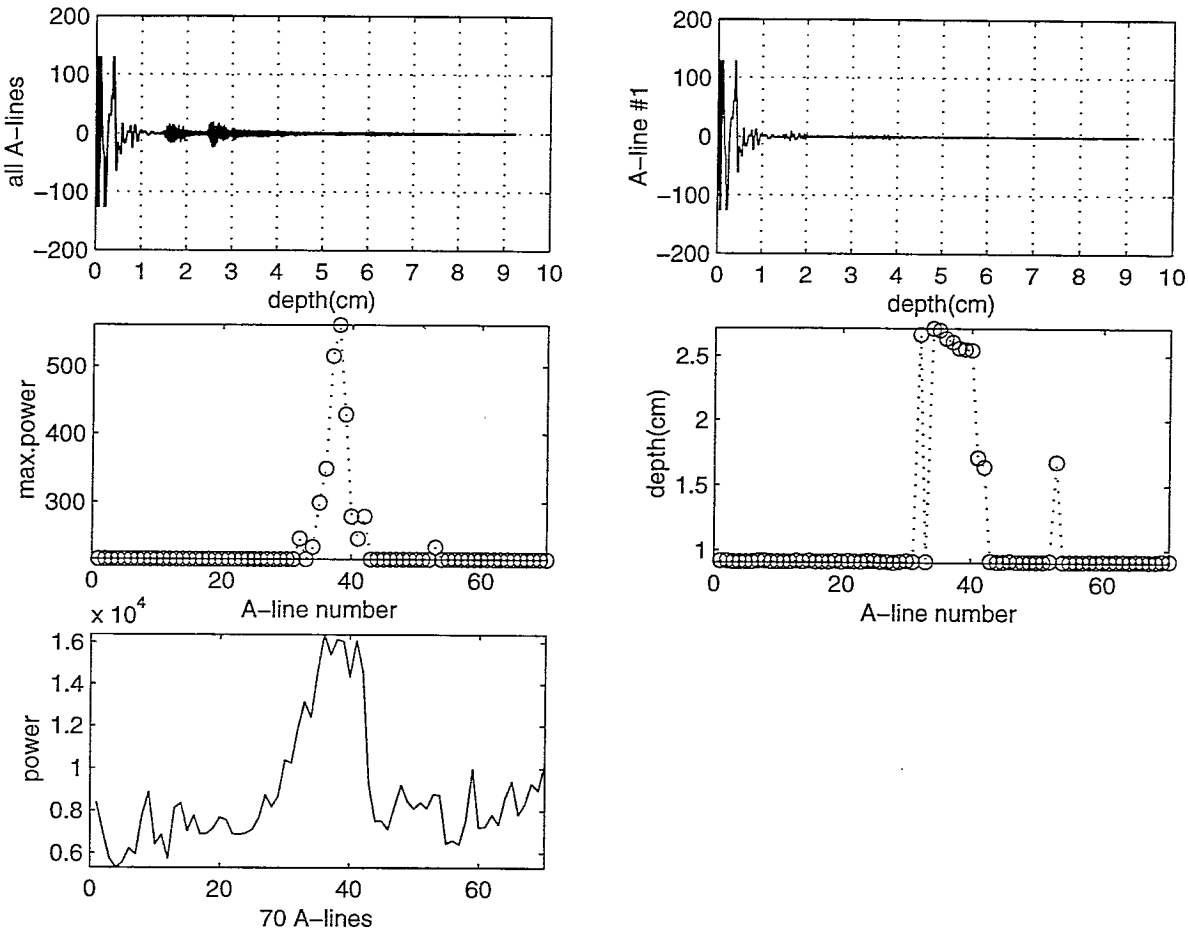
all A–lines
depth(cm)
A–line #1
depth(cm)
max.power
A–line number
depth(cm)
A–line number
x 10^4
power
70 A–lines

anl119g18

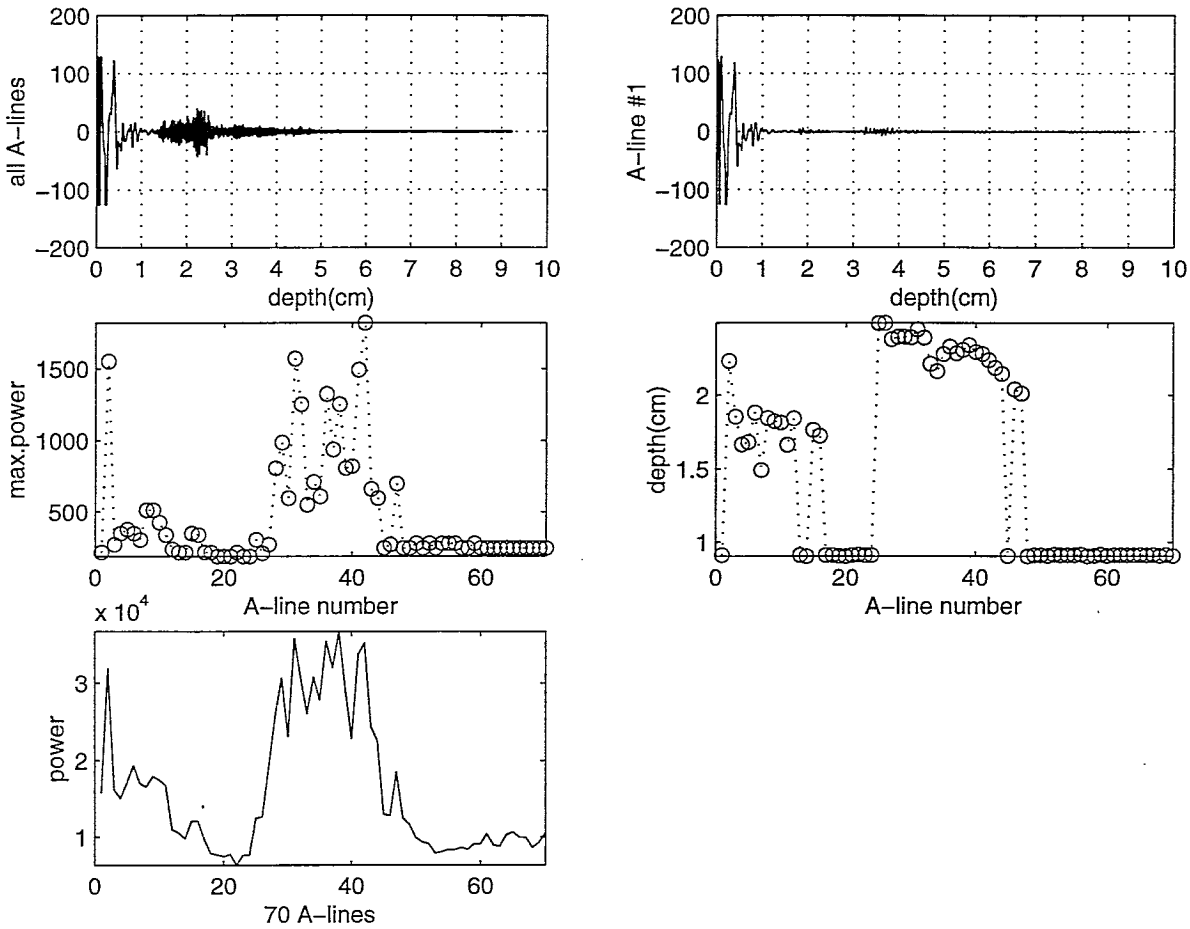
all A–lines
depth(cm)
A–line #1
depth(cm)
max.power
A–line number
depth(cm)
A–line number
x 10^4
power
70 A–lines

anl120g18

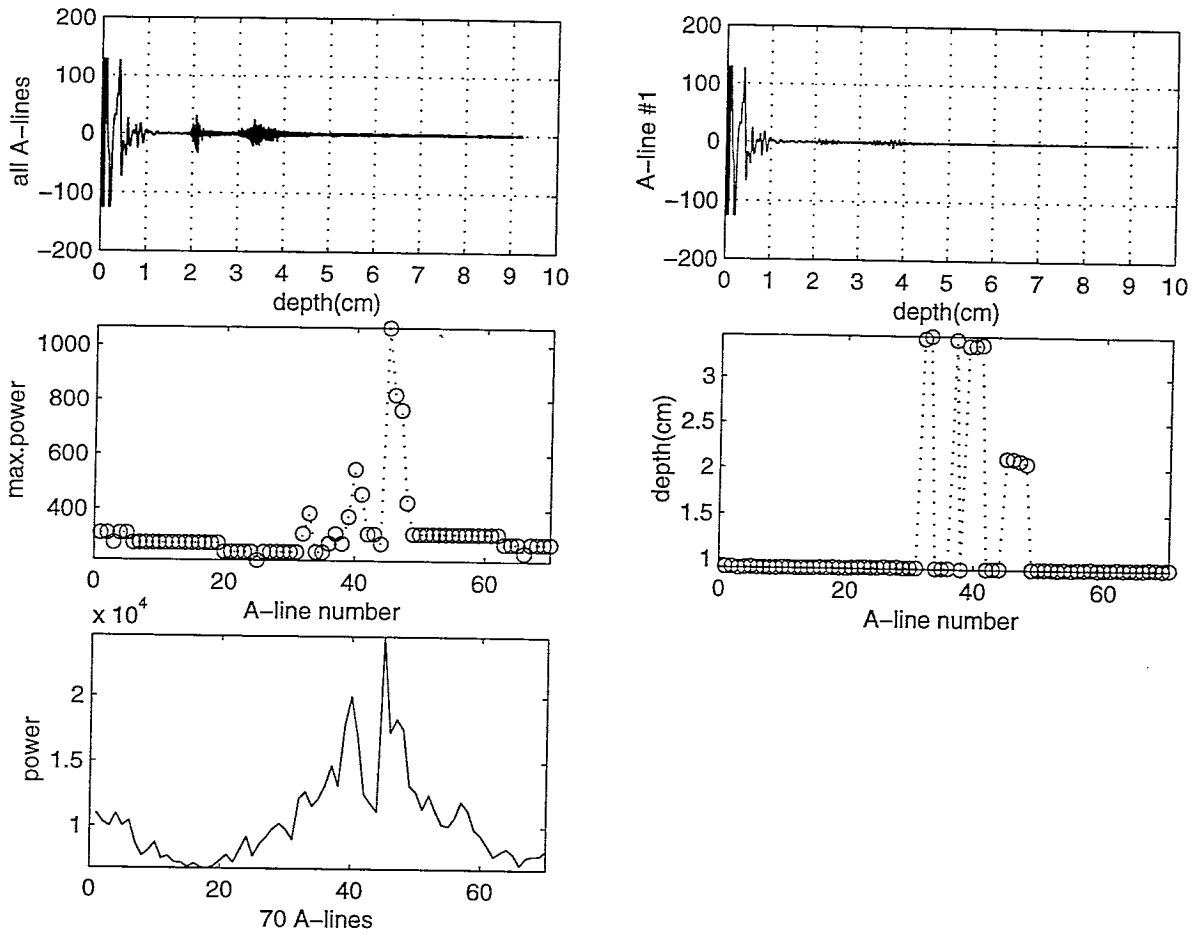
all A–lines
depth(cm)
A–line #1
depth(cm)
max.power
A–line number
depth(cm)
A–line number
x 10^4
power
70 A–lines

anl121g18

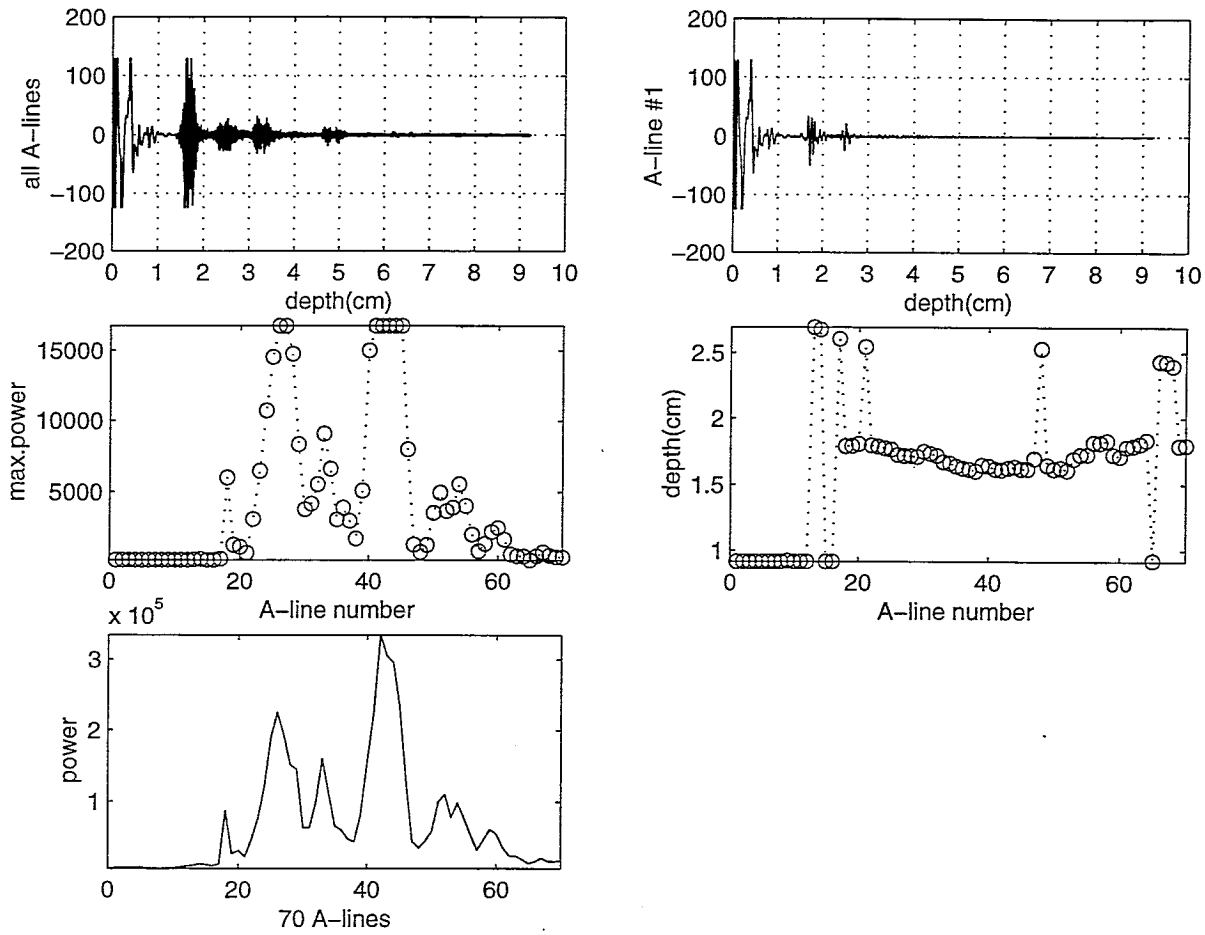
all A–lines
depth(cm)
A–line #1
depth(cm)
max.power
A–line number
depth(cm)
A–line number
x 10^5
power
70 A–lines

anl122g18

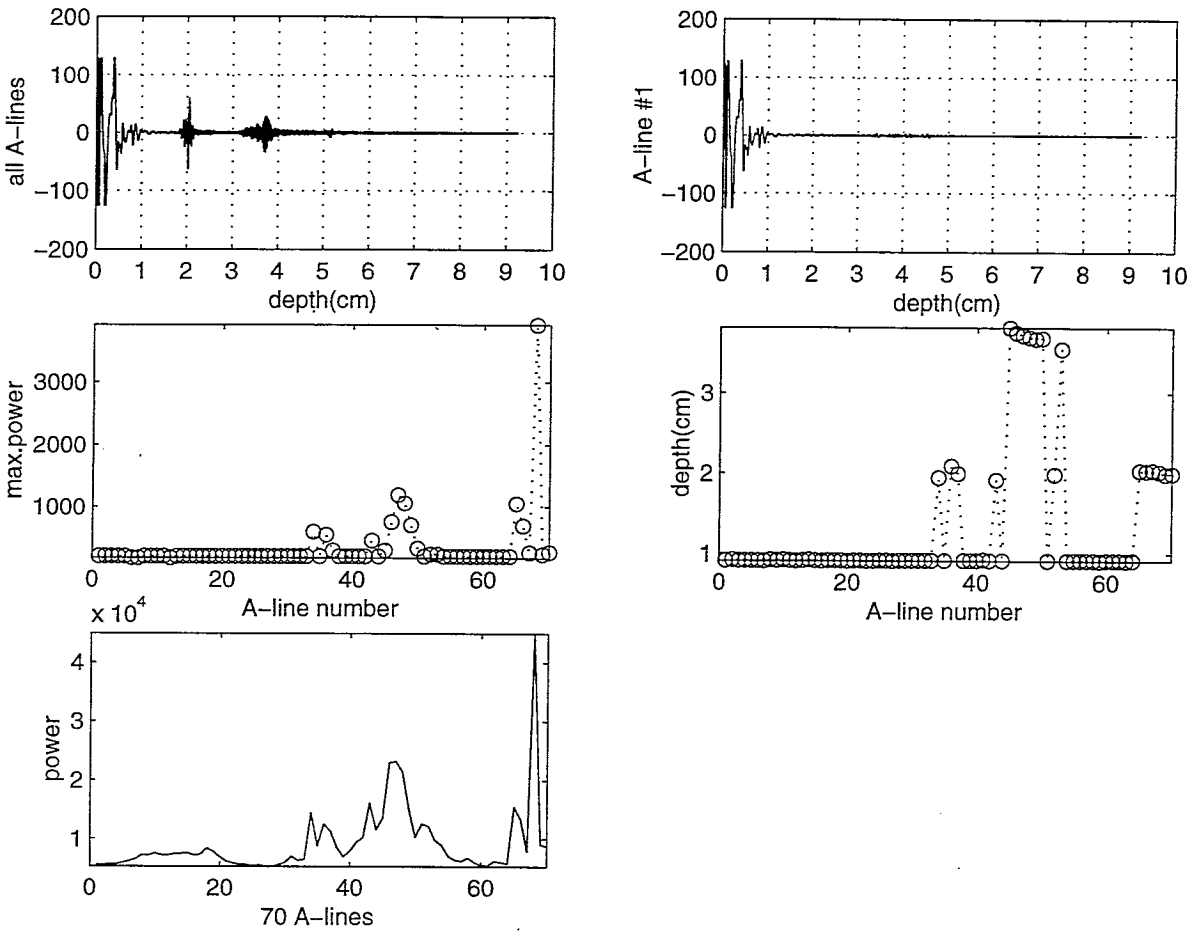
all A–lines
depth(cm)
A–line #1
depth(cm)
max.power
A–line number
depth(cm)
A–line number
x 10^4
power
70 A–lines

anl123g18

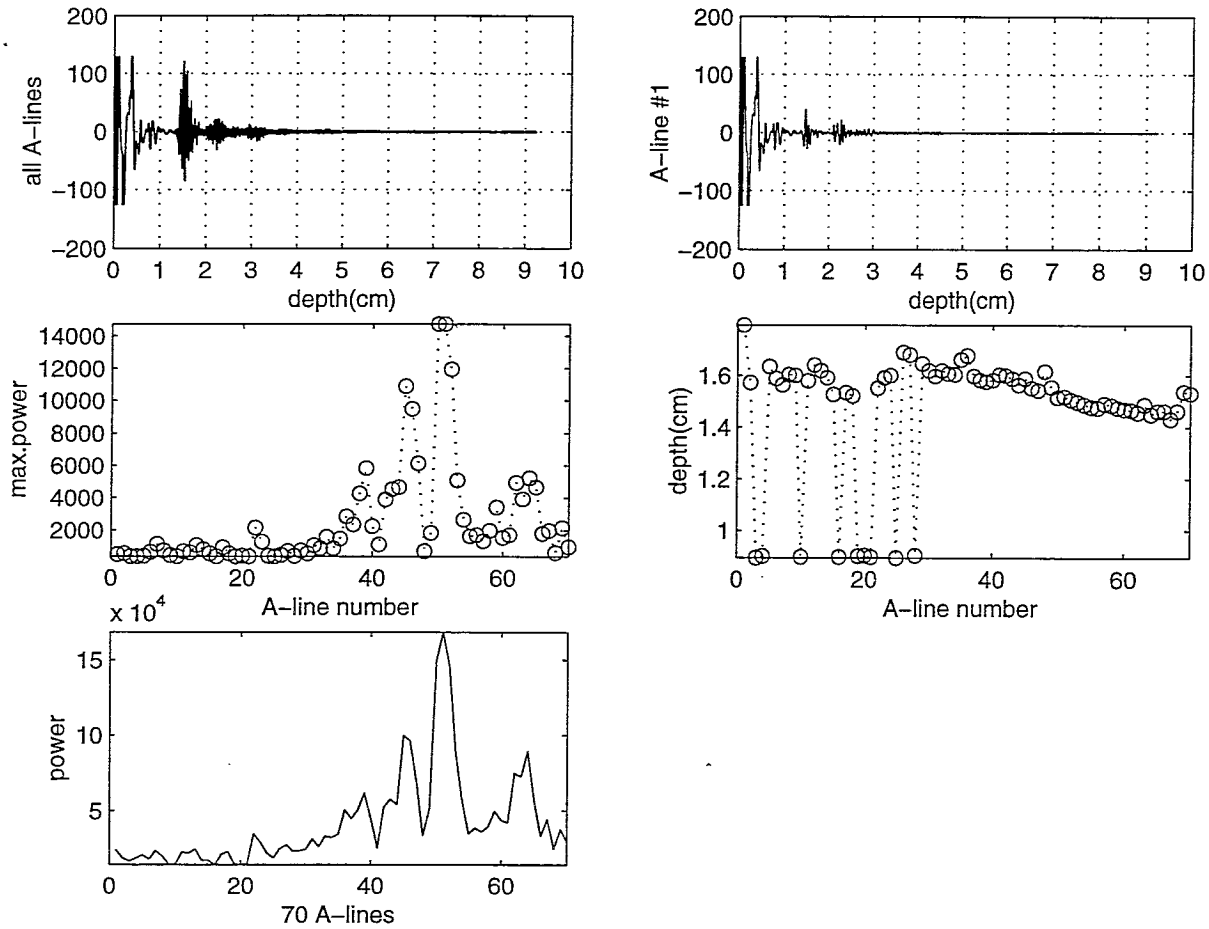
all A–lines
depth(cm)
A–line #1
depth(cm)
max.power
A–line number
depth(cm)
A–line number
x 10^4
power
70 A–lines

anl124g18

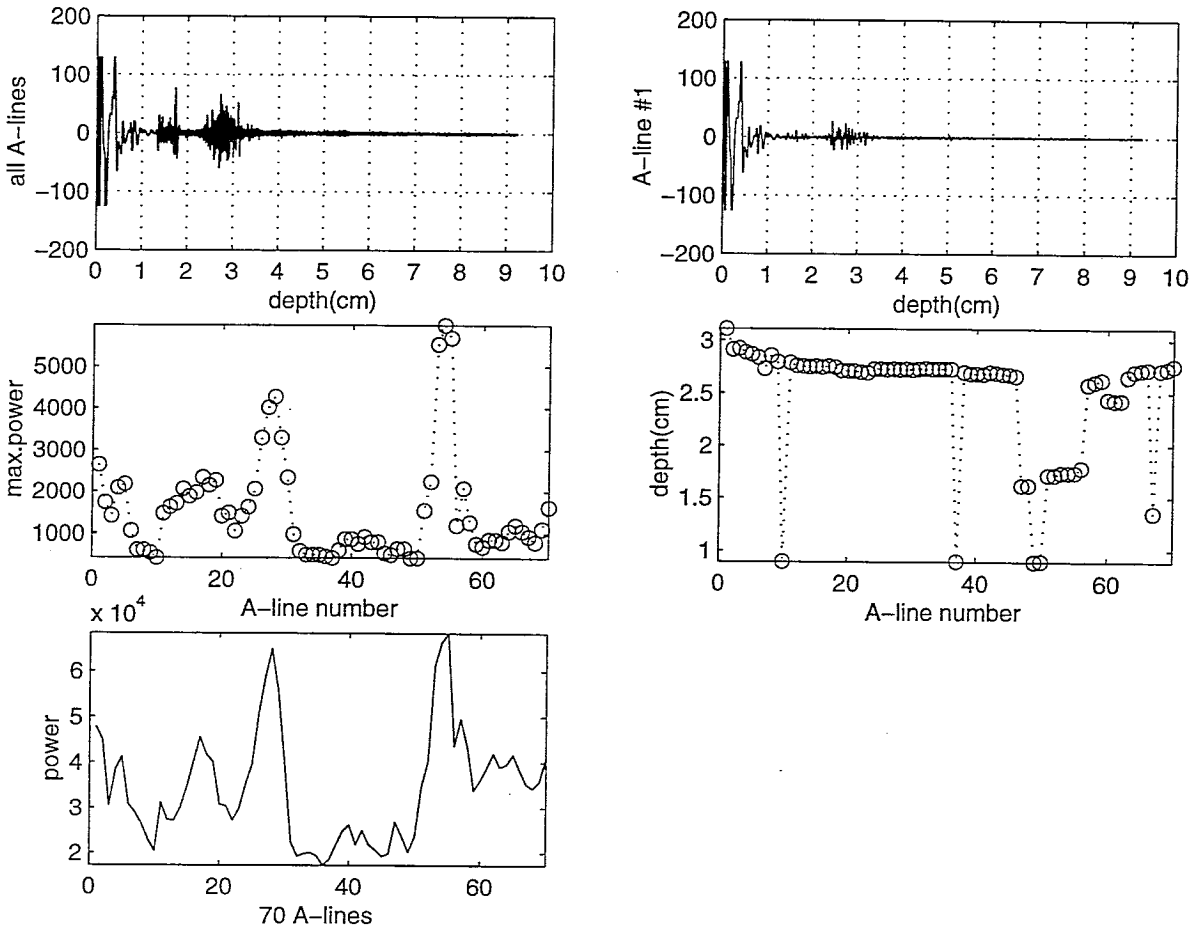
all A–lines
depth(cm)
A–line #1
depth(cm)
max.power
A–line number
depth(cm)
A–line number
x 10^4
power
70 A–lines